The Use of Metal Ions and Graphene-Based Compounds as Novel Antimicrobials Against Multidrug Resistant *Pseudomonas aeruginosa*, *Klebsiella pneumoniae* and *Staphylococcus aureus*

Nathalie Karaky

PhD 2020

The Use of Metal Ions and Graphene-Based Compounds as Novel Antimicrobials Against Multidrug Resistant *Pseudomonas aeruginosa*, *Klebsiella pneumoniae* and *Staphylococcus aureus*

A thesis submitted in partial fulfilment of the requirements of Manchester Metropolitan University for the degree of Doctor of Philosophy

Nathalie Karaky

Department of Life Sciences

Manchester Metropolitan University

2020

Table of contents

List of abbreviations

°C	Degrees Celsius
µg	Microgram
µL	Microlitres
Ag	Silver
Al	Aluminium
AMR	Antimicrobial resistance
ANOVA	Analysis of variance
ATCC	American type culture collection
ATP	Adenosine triphosphate
Au	Gold
CCCP	Carbonyl cyanide m-chlorophenyl hydrazone
CDC	Centre for Disease Prevention and Control
CFU	Colony Forming Unit
CHX	Chlorhexidine
Cu	Copper
CVBA	Crystal Violet Bioflim Assay
DNA	Deoxyribonucleic Acid
EARSS	European antimicrobial resistance surveillance system
ECDC	European centre for disease prevention and control
E. coli	*Escherichia coli*
EDTA	Ethyelenediaminetetraacetic acid
EUCAST	European Committee on Antimicrobial Susceptibility Testing
FBS	Foetal bovine serum
FIC	Fractional Inhibitory Concentration
Ga	Gallium
GO	Graphene
Gr	Graphene oxide
h	Hours
HCl	Hydrochloric Acid
HLMR	High level mupirocin resistance
HNO_3	Nitric Acid
In	Indium
ISA	Isopropyl alcohol
K. pneumoniae	*Klebsiella pneumoniae*
LDAO	Lauryldimethylamine oxide
L	Litres
LLMP	Low level mupirocin resistance
MBC	Minimal Bactericidal Concentration
MDR	Multidrug Resistant
mg	Milligrams
MH	Mueller-Hinton
MIC	Minimal Inhibitory Concentration
mL	Millilitres
mm	Millimetres
Mo	Molybdenum
mRNA	Messenger ribonucleic acid
MRSA	Methicillin resistant *S. aureus*

MTS	3-(4,5-dimethylthiazol-2-yl)-5-(3-carboxymethoxyphenyl)-2-(4-sulfophenyl)-2H-tetrazolium)
MTT	3-(4,5-dimethylthiazol-2-yl)-2,5-diphenyltetrazolium bromide
NaOH	Sodium hydroxide
Nb	Niobium
NCIMB	National Collection of Industrial Food and Marine Bacteria (UK)
NP	Nanoparticle
OD	Optical Density
PBS	Phosphate buffer saline
P. aeruginosa	*Pseudomonas aeruginosa*
Pd	Palladium
PEG7	Macrogol 7 glycerol cocoate
PEG400	Polyethylene glycol 400
PEG3350	Polyethylene glycol 3350
PEO	Polyethylene glycol
pH	Power of hydrogen
Pt	Platinum
Re	Rhenium
Rh	Rhodium
RNA	Ribonucleic acid
ROS	Reactive Oxygen Species
rpm	Revolutions per minute
Ru	Ruthenium
S. aureus	*Staphylococcus aureus*
SE	Standard error
SD	Standard deviation
SEM	Scanning Electron Microscopy
Sn	Tin
SPSS	Statistical Package for Social Sciences
Ta	Tantalum
tRNA	Transfer ribonucleic acid
TSA	Tryptone Soy Agar
TSB	Tryptone Soy Broth
TTC	Triphenyl Tetrazolium Chloride
WHO	World health organisation
XTT	2,3-bis (2-methoxy-4-nitro-5-sulfophenyl)-5-[(phenylamino) carbonyl] 2H-tetrazolium hydroxide
Y	Yttrium
Zn	Zinc
ZnO	Zinc oxide
ZoI	Zone of Inhibition
Zr	Zirconium
°C	Degrees Celsius
µg	Microgram
µL	Microlitres

List of Figures

List of Tables

Abstract

The burden of antimicrobial resistance is a daily challenge in clinical settings, especially in intensive care units. The escalating trends of multidrug-resistant (MDR) bacteria are reported on a global scale today, and the loss of effective antibiotics and disinfectants undermines the ability to fight infectious diseases. The development of novel antibacterial agents is urgently needed in healthcare settings to reduce bacterial resistance and potential nosocomial infections.

This study aimed at assessing the antimicrobial effect of metal ions and graphene-based compounds against multidrug resistant (MDR) isolates of *Pseudomonas aeruginosa*, *Staphylococcus aureus* and *Klebsiella pneumoniae*. It also aimed at incorporating the successful combinations of metal ions and graphene composites into novel formulations of skin cleansers and nasal sprays/ointments that are effective against MDR chlorhexidine-adapted *K. pneumoniae* and mupirocin-resistant *S. aureus* in clinical settings.

The antimicrobial efficacy of eighteen metal ion solutions, graphene and graphene oxide were tested, individually and in combination, against ten clinical isolates of *Pseudomonas aeruginosa*, *Staphylococcus aureus* and *Klebsiella pneumoniae* using minimal inhibitory concentration (MIC) and minimal bactericidal concentration (MBC). The antibiofilm activity of the compounds was tested using crystal violet biofilm assays (CVBA) and XTT assays. The synergistic effect between metal ions or combinations showing the best inhibitory activity against the three bacterial species and the excipients of the skin cleanser or nasal spray/ointment was assessed using fractional inhibitory concentration (FIC). Compounds that did not show any antagonistic effect were tested for their cytotoxicity using MTS assay against human skin fibroblast cell line, and were incorporated into different formulations of skin disinfectant, and nasal spray/ointment. The antimicrobial efficacy of the formulations was tested using the agar well diffusion method and CVBA assay. The organoleptic characteristics, uniformity, spreadability, thermal stability and other physical characteristics of each formulation were also evaluated. Morphological changes in bacterial

cells treated with the tested formulations were visualized using scanning electron microscopy (SEM).

Results showed that platinum, palladium, gold, tin and molybdenum ions exhibited the best inhibitory effect against the planktonic cells of *P. aeruginosa*, *S. aureus* and *K. pneumoniae*. Graphene oxide demonstrated no antimicrobial effect (>500 mg/L) against the 10 isolates, whilst graphene showed an excellent against *S. aureus* and *K. pneumoniae* only. It was evident, however, that the addition of graphene or graphene oxide enhanced the antimicrobial effect of metal ions against the three bacterial species. Cytotoxicity readings revealed that gallium, indium, platinum, palladium, gold, graphene and graphene oxide were not toxic to the tested skin fibroblasts.

Various formulations of skin disinfectants (14), topical ointments (9) and nasal sprays (9) containing metal ions and graphene composites were tested. The best inhibitory and antibiofilm activities were revealed by formulations containing gold/graphene, gold, platinum, platinum/graphene and palladium. The antibacterial effect of the different tested formulations was further confirmed by the clear morphological damages shown in bacterial cells characterized by the formation of deep grooves, pores, or cuts in their cell walls.

In the light of the inefficacy of the currently used antibiotics and disinfectants, this study highlighted specific metal ions, used alone or in combination with graphene composites, owing their antibacterial activity, as promising potential novel antibacterial agents in clinical settings.

Declaration and Copyright Statements

Declaration

No work referred to in this thesis has been submitted in support of an application for another degree or qualification of this university or any other academic institution.

Signed ……..... (candidate) Date ……

Statement 1

This thesis is being submitted in partial fulfilment of the requirements for the degree of PhD.

Signed ……..... (candidate) Date ……

Statement 2

This thesis is the result of my own independent work/investigation.

Signed ……..... (candidate) Date ……

Conferences and Publications Derived from this Thesis

Publications

- **Karaky Nathalie**, Kirby Andrew, McBain Andrew J, Butler, Jonathan A, El Mohtadi, Mohamed and Banks Craig E and Whitehead Kathryn A (2020) 'Metal ions and graphene-based compounds as alternative treatment options for burn wounds infected by antibiotic-resistant *Pseudomonas aeruginosa*', *Archives of microbiology*. doi.org/10.1007/s00203-019-01803-z.

- Slate Anthony J, **Karaky Nathalie** and Whitehead Kathryn (2018) 'Antimicrobial properties of Modified Graphene and other advanced 2D Material Coated Surfaces. 2D Materials: Characterization, Production and Applications' https://doi.org/10.1201/9781315152042.

Conferences

- Oral and Poster presentation and participant at the National PhD Training Programme in Antimicrobial Resistance Research, Medical Research Foundation
  Bristol, UK, Aug 12-16, 2019
- Oral and poster presentations at the ASM Microbe 2019 meeting
  San Francisco, USA, June 19-24, 2019
- Poster presentation at the Stevens Conference on Bacteria-Materials Interactions
  New Jersey, USA, June 12-13, 2019
- Poster presentation at the National PhD Training Programme in Antimicrobial Resistance Research, Medical Research Foundation
  Bristol, UK, Aug 16, 2018
- Poster presentation at the Eurobiofilm 2017, 5th European Conference on Microbial Biofilms
  Amsterdam, The Netherlands, September 19-22, 2017
- Oral presentation at The 17th International bio-deterioration & biodegradation symposium
  Manchester, UK, September 6-8, 2017
- Poster presentation at the Bacteria-material interactions 2017, The Stevens Institute of Technology
  New Jersey, USA, June 14-16, 2017

- Poster presentation at the BSAC Spring Conference: The Global Challenge of Multi-drug Resistant Gram Negative Bacterial Infections London, UK, March 14, 2017

Awards

- Award for the best poster presentation at the Stevens Conference on Bacteria-Material Interactions, The Stevens Institute of Technology, New Jersey, USA, June 2019
- Award for the best presentation in the 3MT presentation competition, Manchester CBS away day, Manchester Gallery, Manchester, UK, July 2018

Acknowledgments

First and foremost, I would like to thank my supervisor Prof Kathryn Whitehead for believing in me and granting me the opportunity to do this PhD. I am extremely privileged to have received your constant guidance, assistance and support. You were instrumental in defining the path of my scientific thinking and for that, you will always be inspiring my interest for any future research I will undertake. Thank you for teaching me much more than science.

I would like to extend my gratitude to my supervisory team namely Dr Andrew Kirby, Prof Andrew McBain, Dr Jonathan Butler, Dr Nina Dempsey and Prof Craig Banks.

I would also like to thank my lab team and all the microbiology staff members, especially Dr Paul Benson White for all the help.

Getting through my dissertation required more than academic support, and I have many, many people to thank for listening to me and, at times having to tolerate me over the past three years. I am foremost grateful for their friendship.

To Lauren, Helen, Becky, Laura, Xenia, Raya, and all my MMU friends thank you for the personal and professional support and the fun times during the long working hours.

To Mo, your support and encouragement was worth more than I can express on paper. Your friendship is one of the highlights of this PhD journey.

To my friends scattered around the globe, thank you for being an anchored support system. Joumana and Nivine, my rocks of support, Bob, Layal, Hoda, Nabil, Raafat, Sara, Nathalie and Anita, I am lucky to have you all.

Most importantly, the greatest deal of appreciation and gratitude goes to my family. To my mum and dad, the source of inspiration in my life. A simple thank you would be an understatement of what I want to express, but I hope this will slightly pay off for all your sacrifices. Most importantly, thank you for teaching me what grit is.

To my three brothers, Najwa and Diana, you knew it would be a long road, but still encouraged and supported me along the way. Thank you for being my steady compass that guided me to reach great heights and inspired me by the excellent examples you set.

This dissertation stands as a statement to your unconditional love and encouragement.

I would like to devote a last thank you to caffeine, sugar and F.R.I.E.N.D.S., my companions through long nights of writing.

Dedication

To everyone who believed in me…

To my mum and dad, to my three musketeers Ahmad, Mohamad and Ali and to my two beautiful sisters-in-law Najwa and Diana

This is for you …

Chapter 1 Introduction

1.1 Antimicrobial Resistance

Antimicrobial resistance (AMR) is the capability of a microorganism to resist the effect of one or multiple antimicrobial agents that once used to be successfully effective (ECDC, 2018).

1.1.1 History and Response to Antibiotic Resistance

The threat of antibiotic resistance dates back to 1940s, just a few years after the use of the first discovered antibiotic, penicillin (Demerec, 1948). In response to this, novel beta-lactams were developed and put into routine practice, restoring confidence in treating bacterial infections (Ventola, 2015). However, shortly after, the first case of methicillin resistant *Staphylococcus aureus* (*S. aureus*) was reported within less than a decade, particularly in 1962 in the United Kingdom (UK), and in 1968 in the United States of America (USA) (Sengupta *et al.*, 2013; Spellberg and Gilbert, 2014; Ventola, 2015). Since then, escalating trends of AMR have been reported globally, and new antibiotics have been released to the market, in a continuous cycle by pharmaceutical companies. However, following 75 years of continuous antibiotic use and spread of bacterial resistance (Figure 1.1), the antibacterial pipeline has started to abate, becoming insufficient to deal with the current risks (Spellberg and Gilbert, 2014). The intensity of concerns and actions taken regarding antibiotic resistance were postulated into five historical eras:

- Period between 1945 and 1963: known as the optimistic period since pharmaceutical industry was able to keep pace with the AMR race
- Period between 1963 and 1981: notable for the growing concerns and awareness following the discovery of the plasmid-mediated transmission of antibiotic resistance
- Period between 1981 and 1992: remarkable for the framing of AMR, for the first time, as a global concern
- Period between 1992 to 2013: where larger concerns of AMR have been demonstrated through an increase in attention for academic literature and funding

- Period between 2013 and present: acknowledging AMR as a “ticking time bomb” and “apocalyptic scenario” and understanding its linked health and economic consequences (Podolsky, 2018)

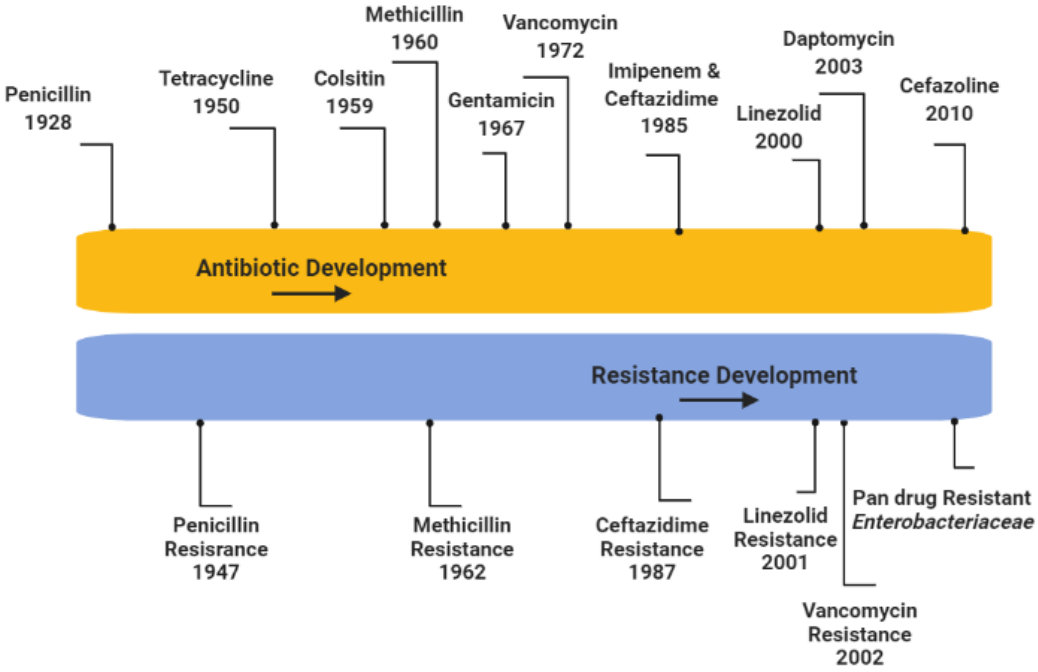

Figure 1.1 Timeline depicting the antibiotic development and antimicrobial resistance. Figure adapted and reproduced from Taneja *et al*. (2019).

1.1.2 Epidemiology of AMR

Decades after the first patients were treated with antibiotics, antibiotic resistant bacterial infections became noted by the European parliament and the commission implementing decision, as a serious health cross border threat (Spellberg and Gilbert, 2014; ECDC, 2018). The European Antimicrobial Resistance Surveillance System (EARSS) estimates that 670,000 infections occur every year due to antibiotic resistant bacteria in the European/European Economic Area (EU/EEA). Consequently, AMR contributes directly to the death of 33,000 people and a healthcare cost of EUR 1.1 billion (ECDC, 2018; Cassini *et al.*, 2019). AMR exhibits variable disparities within different countries in Europe depending on the dominant bacterial species, the antibiotic groups, and the geographical location. However, a north-to-south and west-to-east gradient can still be noted; whereby higher resistance rates were reported in the south and east of Europe, while lower rates were recorded in the north (WHO, 2014).

1.2 Main Causes of Antibiotic Resistance

The development of antibiotic resistance is a multifactorial process that is directly linked to the antibiotic's production, prescription, dispensing, and consumption (Ayukekbong *et al.*, 2017). Such issues have been exacerbated further due to human causes, clinical use, public behaviour, commercial pressure, and agricultural applications (Michael *et al.*, 2014). Inappropriate practice along this course will promote the development of resistance (Michael *et al.*, 2014).

1.2.1 Human Population

Following the exponential increase in human population (8 billion people in few years), the increase in urbanization and the ease of travel, global humanity is now considered as a single biological population (Michael *et al.*, 2014; WHO, 2014). Not only did this enhance the rapid transport of microbes and pathogens across the globe, but also exposed the population to a broader range for microbial predators (Michael *et al.*, 2014; WHO, 2014).

1.2.2 Overuse of Antimicrobials

Human use/misuse of antibiotics is still considered to be the principal risk factor contributing to AMR. Overconsumption of antibiotics has clearly put unnatural selective pressure on bacteria accelerating their evolutionary process (Fair and Tor, 2014). Virulence and pathogenicity also contribute in modulating the development of AMR. In fact, increased antibiotic exposure is associated with increased virulence, since virulent organisms exhibiting clinical symptoms are more frequently treated with antibiotics than nonvirulent ones (Martínez and Baquero, 2002). If eradication of the pathogen does not occur as a result of treatment, those strains will be subjected to increased antibiotic pressure (Martínez and Baquero, 2002). This can consequently lead to an acquired antibiotic resistance in which a minority of bacterial cells with resistant phenotype can find themselves in a less competitive and therefore more advantageous environment, as the phenotypically sensitive majority is killed (Fair and Tor, 2014). Furthermore, the treatment also alter the indigenous microflora who are challenged with

antibiotics only as an unwanted side effect of the therapy (Martínez and Baquero, 2002).

The misuse of antibiotics can be broadly attributed to the universal effectiveness of antibiotics that created the belief among the general public that these drugs can be implemented in the first instance of any disease (Lipsitch and Samore, 2002; Michael *et al.*, 2014). Another factor can be associated to the ease of purchase of antibiotics over the counter even without a medical prescription in some countries, especially the developing countries (Ayukekbong *et al.*, 2017). This situation has become even more aggravated with the online acquisition of antimicrobials facilitating self-medication (Taneja *et al.*, 2019).

1.2.3 Over/Inappropriate Prescription

The prescription practice of antibiotics is not unified and vary vastly among physicians in different countries. Healthcare professional may play a major role in promoting AMR by prescribing a wrong antibiotic, an unnecessary drug or an inappropriate dose (Usluer *et al.*, 2005; Ayukekbong *et al.*, 2017). In other cases especially in developing countries, overwhelmed doctors are treating patients with broad spectrum antibiotics without a definitive diagnosis due to the high patient-doctor ratio and lack of time to properly inform the patient on adherence guidelines (Ayukekbong *et al.*, 2017). For instance, Saleh *et al*. (2015) reported that 63.7% of cases treated were prescriptions with a wrong treatment duration, while 52% were dose-inappropriate in a Lebanese population. These practices can exert selective pressure not only on the pathogenic agent causing the disease, but also on a large proportion of the patient's microbiota (Calva, 1996).

1.2.4 Public Perception and Behaviour

The public practice of non-compliance with the physician's guidelines by skipping doses, deliberately or by mistake, has also been thought to be a major contributor to AMR (Michael *et al.*, 2014). The sub-therapeutic concentrations of the antibiotic used may not have an immediate clinical consequence on the patient. However, it may definitely increase the

chances for misapplication of the same drug to non-susceptible organisms in the near future (Michael *et al.*, 2014; Ayukekbong *et al.*, 2017).

1.2.5 Agricultural Applications of Antibiotics

The use of antibiotics in animals and crops to prevent and treat infections has significantly improved their yield, however, this gross application has profound effects upon spreading resistant bacteria from animals to humans through food consumption (Michael *et al.*, 2014). For instance, resistant bacteria have been isolated from meat, dairy products, and even humans in proximate contact with livestock (Kikuvi *et al.*, 2010; Fortini *et al.*, 2011).

1.2.6 Commercial Pressures and Low availability of Novel Antibiotics

During the last few years, an increase in advertising has been directed at the general public promoting the necessity to completely eradicate microbes from domestic surfaces and skin; which has led to the production and use of a vast range of household antimicrobial products (antibacterial soaps, hand gels, wipes, sanitizers and foams) (Round *et al.*, 2010; Michael *et al.*, 2014). The over-insistence on “clean environment” and the routine public use of these products (from floor cleansers to eye drops) may have enhanced cross resistance to bacteria against the effective disinfectants generally used in clinical settings (Michael *et al.*, 2014).

1.3 Overview and Modes of Action of Traditional Antibacterial Drugs

To better address AMR challenge and explore alternative therapies, it is crucial to first understand the different mechanisms by which antibiotics kill bacteria. Current antibiotics that cover a large array of infections are grouped into two main categories: bacteriostatic and bactericidal (Pankey and Sabath, 2004). Bacteriostatic agents inhibit the bacterial growth by keeping the organism in the stationary phase, whilst bactericidal agents kill the bacteria at an efficiency > 99.9 %. In reality, this classification is not accurate, since bacteriostatic drugs also possess a bactericidal efficiency of 90%-99% after 18 - 24h of a test, but does not exceed 99.9 % to be labelled as bactericidal (Pankey and Sabath, 2004). Antibacterial drugs are further

classified, according to their primary targets and modes of action, into subclasses including inhibitors of cell wall turnover, inhibitors of DNA replication and inhibitors of protein synthesis (Table 1.1) (Kohanski *et al.*, 2007). Despite the differences in their antibacterial mechanisms, a common-mechanism for antibiotic-mediated cell death has been demonstrated (Kohanski *et al.*, 2010). For instance, aminoglycoside, quinolone, and β-lactam were confirmed to promote the generation of lethal hydroxyl radicals in both Gram-negative and Gram-positive bacteria. This antibiotic-induced stress response was suggested to be mainly due to the stimulation of NADH oxidation through the electron transport chain (Kohanski *et al.*, 2007, 2010).

Table 1.1 Classification of the main classes of antibiotics according to their mode of action

Mode of Action	Antibiotic Class	Generic Name	Mechanism of Action	Reference
Inhibitors of Cell Wall Synthesis	β-lactams	Penicillin, piperacillin, ampicillin, cloxacillin, cephalosporins	Binds to penicillin-binding-protein to inhibit transpeptidation, leading to an increase in autolysins and cell death	Tipper and Strominger (1965)
	Lipopeptides	Polymyxin B, colistin	Bind to the bacterial outer membrane via its cationic peptide ring and displaces magnesium and calcium ions destabilizing the lipopolysaccharides	Zavascki *et al*. (2007)
	Glycopeptides	Vancomycin	Bind with peptidoglycan units and inhibit their synthesis reducing cellular mechanical strength	Kahne *et al*. (2005)
Inhibitors of DNA Synthesis	Fluoroquinolones	Ciprofloxacin, norfloxacin, nalidixic acid, levofloxacin	Creates double-stranded DNA breaks by binding to topoisomerases leading to cell death	Drlica *et al*. (2008)
	Sulfonamides	Sulfamthaxozole, sulfapyridine, sulfamethazine, sulfadiazine	Inhibit the synthesis of dihydrofolic acid essentially used for DNA replication and bacterial growth	Henry (1943)
Intercalators of DNA Replication	Anthracyclines	Doxorubicin	Have a chromophore moiety and inserts between adjacent DNA base pairs of DNA in the nucleus of the cell	Westman *et al*. (2012)
Inhibitors of RNA Synthesis	Rifamycins	Rifampicin, rifaximin, rifabutin	Sterically inhibit RNA strand initialization by binding with high-affinity to the DNA-bound subunit and inhibit DNA-dependent transcription	Campbell *et al*. (2001)
Inhibitors of Protein Synthesis	Aminoglycosides	Gentamicin, tobramycin, streptomycin, amikacin, spectinomycin	Bind to the 30 S of the ribosome to cause misincorporation of amino acids into peptides and incorporation of misfolded proteins in the cell wall, leading to increased drug uptake and cell death	Hancock (1981); Chopra and Roberts (2001)
	Tetracyclines	Tetracycline, minocycline, doxycycline		
	Macrolides	Erythromycin, clarithromycin, azithromycin, spiramycin	Bind to the 50 S ribosome to sterically inhibit the peptidyltransferse elongation reaction or block the initiation of protein translation	Tenson *et al*. (2003); Mukhtar and Wright (2005)
	Lincosamides	Clindamycin, lincomycin		
	Amphenicols	Chloramphenicol, thiamphenicol		

1.4 Mechanisms of Antibacterial Resistance

The bacterial response to an antimicrobial agent is the first example of bacterial adaptation (Munita *et al.*, 2016). Therefore, understanding the basis for intrinsic and acquired resistance is of utmost importance to reduce AMR.

1.4.1 Intrinsic Antimicrobial Resistance

Since most antibiotics are naturally produced compounds, over time, co-resident bacteria have developed mechanisms to overcome their mode of action (Munita *et al.*, 2016). Therefore, some bacterial species are naturally resistant to antibacterial agents. Perhaps, the most prominent example of intrinsic resistance is the ability of Gram-negative bacteria to exhibit resistance towards several classes of clinically efficacious Gram-positive antibiotics (Nikaido, 1994; Cox and Wright, 2013). This type of resistance is not a result of selective pressure of antibiotic use, but it is more of a complex network involving several genetic factors (Cox and Wright, 2013).

1.4.1.1 Outer-Membrane Permeability

The outer membrane of Gram-negative bacteria is composed of an unusual arrangement of lipid molecules covalently linked to units of polysaccharides in a tightly packed layout (Cox and Wright, 2013). The full saturation of fatty acids within lipopolysaccharides will render the membrane more fluid (Obst *et al.*, 1997). Consequently, Gram-negative bacteria are intrinsically tolerant to high doses of antibacterial agents due to the impermeability of the outer membrane serving as a self-sealing envelope (Vaara, 1992).

1.4.1.2 Efflux Pumps

Efflux pumps are normally present on the chromosomes of all eukaryotic and prokaryotic organisms. These proteins act as exporters of toxic substrates (including antibiotics) from within the cells to the external environment, allowing the bacterium to survive in a hostile milieu (Webber and Piddock, 2003). The first reported resistance mediated by efflux pumps was for tetracycline in 1970s (McMurry *et al.*, 1980).

1.4.2 Acquired Antimicrobial Resistance

Acquired resistance is a more complex phenomenon of greater concern in clinical settings (Munita *et al.*, 2016).

1.4.2.1 Genetic Basis of AMR

Bacteria use one of two genetic strategies to counteract the effect of an antibacterial agent. One genetic strategy through developing mutations in genes indispensable for the activity of the antibiotic, resulting in a resistant mutant bacteria (Santajit and Indrawattana, 2016). In general, genetic mutations leading to AMR are able to reverse the effect of the antibiotic via i) alteration or inactivation of the drug (β-lactamases), ii) modification of the drug binding site (mutation in gene encoding for penicillin binding protein), (iii) reduction in the uptake of the antibiotic, or (iv) alteration of metabolic pathways (Munita *et al.*, 2016). The second mechanism follows bacterial acquisition of foreign DNA through horizontal gene transfer. The bacterial genetic exchange takes place through transformation, transduction, or conjugation (Thomas and Nielsen, 2005). Transformation is the simplest type of horizontal gene transfer involving incorporation of naked DNA. However, conjugation is reported in hospital settings and involves the transfer of mobile genetic elements following cell-to-cell contact (Thomas and Nielsen, 2005; Manson *et al.*, 2010). The incorporation of vehicles carrying valuable genetic information play a crucial role in the dissemination of resistant cell structure or enzymes capable of bypassing toxic drugs (Munita *et al.*, 2016).

1.4.2.2 Mechanistic Basis of AMR

1.4.2.2.1 Modification of the Antibiotic Molecule

This occurs through the production of enzymes capable of introducing chemical alterations in the antibiotic molecule. The end result is steric hindrance of the drug decreasing its activity (requiring higher MICs) (Munita *et al.*, 2016). For instance, aminoglycoside modifying enzymes inhibit the aminoglycoside molecules by modifying the amino or hydroxyl groups

(Ramirez and Tolmasky, 2010). β-lactamases, on the other hand, deactivate the antimicrobial molecule by destroying the amide bond of the β-lactam ring (Schwarz *et al.*, 2004; Dcosta *et al.*, 2011).

1.4.2.2.2 Decreased Antibiotic Penetration

This is particularly significant in Gram-negative bacteria where the outer membrane acts as a first line of defence against the antibacterial drugs. The permeability change in the bacterial membrane will avert hydrophilic antibiotics (tetracycline, quinolones and β-lactams) that use water-filled diffusion channels from reaching the cytoplasmic milieu of *Pseudomonas* spp. and *Acinetobacter baumannii* (Hancock and Brinkman, 2002; Pages *et al.*, 2008). The reduced penetration of the drug is also linked to a porin-mediated resistance, that can be achieved through modification of (i) type, (ii) level or (iii) function of porins expressed. For instance, mutations in OrpD is a classic example of porin-mediated resistance towards imipenem in *P. aeruginosa*, and have been shown to increase among the clinical samples (Quinn *et al.*, 1986; Munita *et al.*, 2016).

1.4.2.2.3 Changes in Target Sites

To avoid being recognized by antibiotics, resistant bacteria can modify their target sites (Santajit and Indrawattana, 2016). This mechanism often results from a spontaneous mutation of a bacterial gene on the chromosome in light of the selective pressure exerted by an antibiotic. Examples include mutations in RNA polymerase and DNA gyrase, causing resistance to rifamycins and quinolones, respectively (Lambert, 2005). Other effective means of antibiotic resistance that does not require a mutational change in the genes encoding the target molecules involve enzymatic alterations of the binding sites or replacement of the original target (Blair *et al.*, 2015)(Floss and Yu, 2005; W. Li *et al.*, 2013; Munita *et al.*, 2016). For instance, the erythromycin ribosome methylase (*erm*) family of genes modify the drug-binding site by methylating 16S rRNA and prevent the binding of macrolides, lincosamines and streptogramins. Another example is the chloramphenicol–florfenicol resistance (cfr) methyltransferase, which

confers resistance to streptogramins, phenicols, oxazolidonones and pleuromutilins by methylating A2503 in the 23S rRNA (Blair *et al.*, 2015).

1.5 Terminology and Definition of Different Resistance Patterns

Synchronized and consistent definitions with which to classify multidrug resistant (MDR), extensive drug resistant (XDR), and pan-drug resistant (PDR) bacteria were needed. Therefore, a standardized international terminology was suggested during a meeting that was initiated by the Centre for Disease Prevention and Control (CDC) in Stockholm in 2008 (Magiorakos *et al.*, 2012). A bacterial isolate was designated as MDR if it exhibited resistance to at least one agent in three or more antimicrobial groups. XDR was defined as resistance to at least one agent in all antimicrobial categories, whilst PDR is the resistance to all agents in all antimicrobial classes (Magiorakos *et al.*, 2012).

1.6 Biofilm Formation and Antimicrobial Resistance

Biofilm formation represents an alternative microbial lifestyle in which microorganisms can survive in diverse environments, resist antimicrobial therapy, and persist in varied infections (Kostakioti *et al.*, 2013). Bacterial biofilms are immobile microbial communities that can colonize the host, or grow on biotic and abiotic surfaces in community and clinical settings, causing serious persistent infections (Kostakioti *et al.*, 2013). The National Institute of Health estimated that biofilm formation is responsible for around 65% and 80% of the total microbial infections and chronic infections, respectively (Jamal *et al.*, 2018).

The formation of a biofilm is a complex dynamic process occurring in response to environmental factors (Kostakioti *et al.*, 2013). The matrix of bacterial biofilms engulfing the cells accounts for almost 90% of the total biomass, and is composed of three stabilizing scaffolds including exopolysaccharides, extracellular DNA (eDNA) and proteins (Kostakioti *et al.*, 2013; Sharma *et al.*, 2019). Although nutrients and water are efficiently retained within the matrix, the polysacchrides' structure is being constantly modified by bacterial enzymes according to the nutrient access and availability (Sauer *et al.*, 2004; Kostakioti *et al.*, 2013). The developmental

process of biofilm formations involves a complex regulatory network and a series of steps including (1) adhesion of free floating bacterial cells to surfaces, (2) aggregation of bacterial cells to form small colonies and release of exopolysaccharide, (3) multi-layer biofilm formation, and (4) biofilm detachment and dispersion (Crouzet *et al.*, 2014). Mature biofilms provide protection to its bacterial inhabitants from altered pH, temperatures, nutrient deprivation, mechanical forces, and most importantly from immune-mediated clearance and antimicrobial action (Sharma *et al.*, 2019; Yamada and Kielian, 2019). The resistance mechanisms in biofilm communities are different from the ones employed by planktonic cells. The genetic and molecular basis of these mechanisms are not fully understood, however, biofilm resistance can be associated with four main factors:

1.6.1 Failure of Antimicrobial Penetration to the Biofilm

Studies have demonstrated that biofilm components can reduce the transport of the antimicrobial agents to the intracellular biofilm matrix (Figure 1.2.a) (Hoyle *et al.*, 1992; Stewart, 1996). Several hypotheses were postulated to explain this process since mathematical explanations proposed that antibiotics should be able to diffuse easily into the biofilm (Mah and O'Toole, 2001; Stewart, 2002). Nevertheless, Suci *et al*. (1994) demonstrated that a colonized bacterial surface was able to diminish the diffusion rate of ciprofloxacin compared to a sterile surface. Similar reaction-diffusion interactions were also able to sequester penicillin from entering bacterial biofilms (Anderl *et al.*, 2000). Evidence has suggested that the penetration of the positively charged penicillin was retarded by the negatively charged biofilm matrix (Nichols *et al.*, 1988; Stewart, 2002).

1.6.2 Slow Growth and Altered Environment

Slow bacterial growth, which is normally observed upon deprivation of certain nutrients, has been detected in mature biofilms and has been linked to biofilm antimicrobial resistance. This is associated with the fact that the biocidal action of many antibiotics is growth-dependent. For instance, penicillin's are known to act and kill bacteria in their growing phase only.

Furthermore, previous studies have demonstrated that the sensitivity of planktonic and biofilm cells of *P. aeruginosa*, *S. aureus* and *E. coli* towards ciprofloxacin and tobramycin have increased with increasing growth rate, proposing that slow growth is indirectly protecting biofilm cells from antibiotics (Mah and O'Toole, 2001).

The antibiofilm potency of the antibiotics can also be modified by chemical gradients such as oxygen and pH (Stewart, 2002). For instance, bacterial cells that inhabit an anaerobic region of a biofilm are distinctively protected from the action of aminoglycosides, which necessitate the presence of oxygen to be effective (Stewart, 2002). Another limiting factor is the heterogeneity of the cells within a biofilm ranging from metabolically inactive to rapidly growing cells. Therefore, bacterial cells within a dormant zone or far from the exposed zone of the biofilm can preferentially endure the antimicrobial attack (Korber *et al.*, 1994; Stewart, 2002) (Figure 1.2.b).

1.6.3 General Stress Adaptive Response

Recent studies associated the slow bacterial growth in biofilms to an adaptive stress response rather than nutrients deprivation. This stress response, initiated by regulator factors, is thought to protect the cells from damaging factors such as pH fluctuations, chemical attacks, and extreme temperatures (Figure 1.2.c) (Mah and O'Toole, 2001; Xu *et al.*, 2001). The central regulator of the stress adaptive response is the alternate ó factor, RpoS, which is induced by high cell density. Cochran *et al*. (2000) also showed that an additional ó factor, AlgT, acted in concert with RpoS to control this response (Mah and O'Toole, 2001).

1.6.4 Persisters

This small population of cells, called "persister cells", are a subset of metabolically inactive, phenotypic variants of regular bacteria that can tolerate toxic concentrations of antibiotics without undergoing genetic changes (Gebreyohannes *et al.*, 2019). This biofilm-specific phenotype was first reported in 1942 in one of the first studies on the mechanism of action

of penicillin by Hobby *et al*. (1942) who noted that 1% of *S. aureus* cells were not killed by penicillin and survived its effect.

Persister cells constitute 1% of the total bacterial population. These cells are formed in response to harsh environmental factors (nutrient and oxygen depletion), DNA damage and antimicrobials' action (Gebreyohannes *et al.*, 2019). Persister cells play a major role in highly recalcitrant infections, since they are able to repopulate in biofilms when the level of antibiotics drops, accounting for an increased biofilm tolerance to all known antimicrobials (Figure 1.2.d) (Lewis, 2007). The reason behind this tolerance is that persister cells do not undergo cellular activities that can be corrupted by antibiotics, instead, they produce multidrug resistance proteins to halt the antibiotic targets (Gebreyohannes *et al.*, 2019).

On the genetic basis, the formation of persister cells and their induction into a state of dormancy were associated with the toxin-antitoxin (TA) systems. TA systems mainly involve a stable toxin (a protein) which disrupts vital cellular processes such as translation via mRNA degradation, and a labile antitoxin (being RNA or a protein) that averts toxicity (Wood *et al.*, 2013, 2019). It seems evident that ceasing protein production visa ribosome activity and producing toxic proteins contribute to a significant increase in persistence (Wood *et al.*, 2019). Therefore, it is apparent that the increased dormancy in biofilms and the substantial reduction in growth rates of persister cells are the two major reasons for the reduced susceptibility of biofilms towards antibiotics, skin cleansers and chemical disinfectants including chlorhexidine and glutaraldehyde (Mah and O'Toole, 2001; Wood *et al.*, 2013). Mutants associated with high persistence were identified in different genera including *E. coli*, *P. aeruginosa*, *S. aureus*, *Lactobacillus acidophilus* and *Gardnerella vaginalis*. The well-known high persistence mutants comprise *hip*, *YafQ/DinJ*, *RelE/RelB* and *MazF/MazE* genes (Wood *et al.*, 2013, 2019).

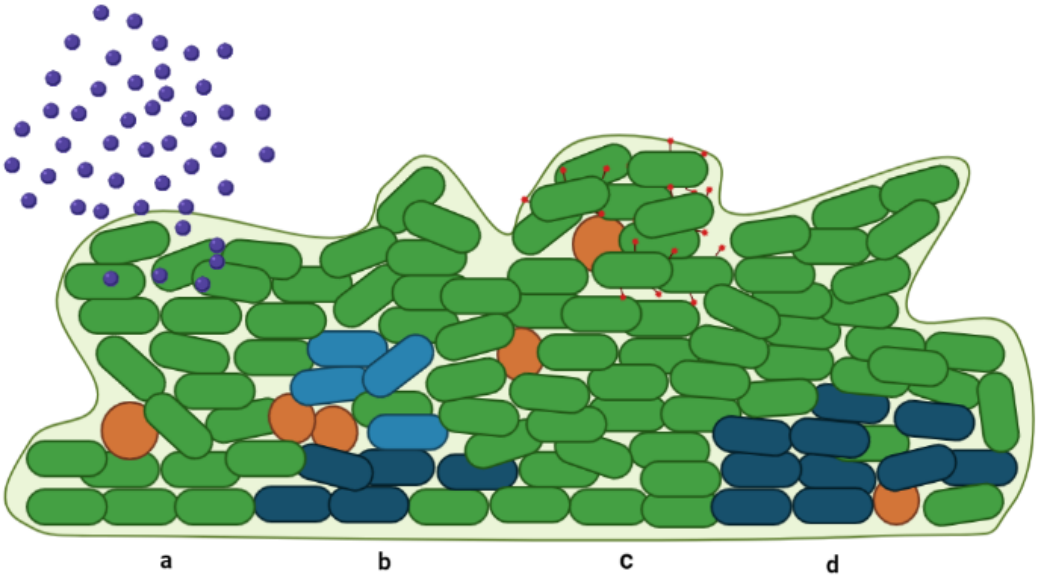

Figure 1.2 Suggested mechanisms for biofilm antimicrobial resistance (a) The slow or incomplete penetration of the biocide (purple dots) limits the cells' uptake of the agent (b) Adapted cells in altered or extreme microenvironments develop greater tolerance (shown as a gradient of green) to antibiotics (c) bacterial cells can trigger can adapt a stress response (cells marked in red) to endure environmental instabilities (d) Persister cells (dark cells at the bottom) can enter a highly protected state and exhibit multidrug resistance. Figure drawn based on information from Mah and O'Toole (2001).

1.7 Reduced Incentives to Develop New Antibiotics

The antibiotic revolution was distinctive for two main phases: the first phase (1930s – 1960s) that was remarkable for the continuous discovery of antibiotics and full control of bacterial infections, whilst the second one since 1965 where only one class of new antibiotics (oxazolidinone) has been introduced (Davies and Davies, 2010). Since then, the production of new antimicrobials has been reduced and development of new drugs has been mostly limited to synthetic tailoring of a few core scaffolds to generate second and third generation analogs of first generation compounds (Wong *et al.*, 2012).

The European Society of Clinical Microbiology and Infectious Diseases (ESCMID) reported, with great concern, that a new era has just began where very few new antibiotics are being developed (Cornaglia *et al.*, 2004; Norrby *et al.*, 2005). For instance, out of all the novel antibiotics introduced during the last 10 years, none showed a good efficacy against MDR Gram-negative

bacteria (Norrby *et al.*, 2005). Therefore, several major pharmaceutical companies, including Roche, Merck and Abbott, stated that they are substantially reducing/stopping the active research on the development of new antibiotics. Whilst other companies (GlaxoSmithKline) continued their antibiotic developmental progress, they have refocused their efforts into more profitable prospects (Norrby *et al.*, 2005).

The main reasons behind the "big pharma" decision to leave the antimicrobials market is that it is financially unattractive to developers. First, antibiotics are less profitable than other drug categories. Due to the high demands from regulatory authorities and strict pricing controls enforced by governments, antibiotics have a high cost of development and a poor return on investment (Norrby *et al.*, 2005). Second, the high sales figures achieved by industry from antibiotics are threatened by the rapid emergence of AMR, which would have a negative effect on future sales (Renwick *et al.*, 2016).

In addition, unlike other drugs, anti-infective agents are normally given for a short period of time, which limits the return per treatment, makes these drugs more susceptible to competition and increases marketing efforts (Norrby *et al.*, 2005). Other factors contributing to a cautious attitude towards developing new antibiotics are the uncertain and the continuously changing regulatory requirements for market approval in the United States and European Union (Projan, 2003; Renwick *et al.*, 2016). Third, many pharmaceutical firms have reallocated their scientific talent and capacity to more profitable opportunities, targeting long-term treatment for chronic diseases, in a way to diminish their antibiotic expertise and economies of scale (Renwick *et al.*, 2016; Towse *et al.*, 2017).

1.8 Call for Alternatives

The reluctance of pharmaceutical companies to invest in research for evolving new antibacterial drugs pushed researchers who are focused on medical therapeutics, to look beyond antibiotics (Wong *et al.*, 2012; Sengupta *et al.*, 2013).

Advancements within synthetic chemistry, genetic engineering and biotechnology have opened up new therapeutic avenues. Numerous

antimicrobial alternatives are being currently explored and investigated. These approaches can be grouped into three broad categories including naturally occurring alternatives (phage therapy, antimicrobial peptides, bacteriocins, probiotics and antibiodies), synthetically designed strategies (synthetic mimics of antimicrobial peptides (SMAMPs), antibacterial oligonucleotides, innate defence regulatory peptides) and biotechnology-based approaches (genetically modified bacteriophages, lysins, CRISPR-Cas 9 and antibiotic inactivators) (Ghosh *et al.*, 2019).

Some of these strategies have advanced offering significant promise to be used as alternatives, while others are still at the laboratory level (Ghosh *et al.*, 2019). For instance, bacteriophages have been approved for treatment of infections and use in food industry. Synthetic membrane-active agents also showed a great promise as topical agents. However, none of the new approaches have proven to be consistently efficient comparable to antibiotic treatment so far (Ghosh *et al.*, 2019). Most importantly, most of the alternative strategies are strain or species specific, as opposed to the broad-spectrum traditional antibiotics (Ghosh *et al.*, 2019). This constitutes a major disadvantage in their development due to their poor return on investment. Therefore, different therapeutic approaches or a combination of some might be needed for the treatment of different infections (Wong *et al.*, 2012; Ghosh *et al.*, 2019).

The following section will present an overview of the use of metal ions and graphene-based compounds as alternative antimicrobials with broad-spectrum activity against Gram-positive and Gram-negative bacteria. The focus on metal ions relies on the fact that these molecules have access to modes of action that are difficult or even impossible to achieve with traditional organic molecules (Frei, 2020). They also have a unique 3D character that has repeatedly been associated with higher clinical success rates (Galloway *et al.*, 2010).

1.8.1 History of Use of Metals as Antimicrobials

Historical evidence indicates that ancient civilizations prompted the use of heavy metals such as arsenic, bismuth and mercury to treat infections

(Gould, 2016). The antimicrobial effect of metals and metalloids have been investigated and applied since the Persian Kings, and later on the Phoenicians, Greeks, Romans and Egyptians used silver and copper vessels for water decontamination and food preservation (Alexander, 2009). Silver coins were also dropped in water, milk and wine containers by North Americans and Japanese soldiers during World War II as a strategy to prevent the spread of dysentery (Borkow and Gabbay, 2009; Lemire *et al.*, 2013). Antimicrobial metals have been prized for their use in agriculture and medicine. For instance, copper salts is the first astringent known in history, dating back to 1500 BP, that was used as a fungistatic to manage plant diseases, whilst silver was used to repair vaginal tears and treat gonorrhoeal eye infections (Sims, 1998; Ayres, 2004).

1.8.2 Chemical Properties and Microbial Toxicology of Metal Ions

The reactivity of metals in living cells and their extent of microbial toxicity is governed by three main factors: donor atom selectivity, reduction potential and, speciation (Lemire *et al.*, 2013).

1.8.2.1 Donor Atom Selectivity

The electronic arrangement of metal ions enables them to bind to atoms (O, N and S) of donor ligands in a selective manner resulting in distinct geometrical bonding interactions (Lemire *et al.*, 2013). Therefore, proteins of the donor ligand have a preference of a bias selection for the proper metal needed for protein folding. The reactivity of metal ions can be also attributed to the Hard-Soft acid base theory (HSAB; or Pearson's acid base theory). HSAB categorizes metal ions into soft, hard and borderline acids (Table 1.2) (Pearson, 1963). Soft acids (such as mercury (II), cadmium (II), silver (I), copper (I), nickel (II)) being large and very polarizable, tend to establish a firm association with the soft bases (R-SH) found in proteins (Workentine *et al.*, 2008). Consequently, the antimicrobial activity of metal ions is proportional to a big extent to its affinity for sulphur (Lemire *et al.*, 2013).

Table 1.2 Properties and classification of metal ions

Metals	Abbreviation	Atomic number	Electronegat-ivity	Polarizability
Copper	Cu	29	1.90	Soft
Silver	Ag	47	1.93	Soft
Molybdenum	Mo	42	2.16	Soft
Palladium	Pd	46	2.20	Soft
Platinum	Pt	78	2.28	Soft
Gold	Au	79	2.54	Soft
Tantalum	Ta	73	1.50	Borderline/ Hard
Zinc	Zn	30	1.65	Borderline
Rhenium	Re	75	1.90	Borderline
Ruthenium	Ru	44	2.20	Borderline
Rhodium	Rh	45	2.28	Borderline
Tin	Sn	50	1.96	Borderline/ Hard
Yttrium	Y	39	1.22	Hard
Zirconium	Zr	40	1.33	Hard
Niobium	Nb	41	1.60	Hard
Aluminium	Al	13	1.61	Hard
Indium	In	49	1.78	Hard
Gallium	Ga	31	1.81	Hard

Hard metal ions are electron acceptors of small size and low polarizability that can form ionic bonds with oxygen-containing ligands. Soft metal ions are electron acceptors of large size and high polarizability that can form covalent bonds molecules with nitrogen or Sulphur centres (Nieboer and Richardson, 1980; Duffus, 2002). If a metal is neither hard nor soft, it is labelled as Borderline (intermediate) metal ion. These are transition metals and can behave as a hard or soft acid depending on their valence and local bonding environment (Ho, 1975).

1.8.2.2 Reduction Potential

Reduction potential is a thermodynamic criterion that defines the tendency of metals to gain electrons and become reduced (Lemire *et al.*, 2013). Therefore, two redox reactions take place (reduction of metal ions and oxidation of donor ligand) at different kinetics, with the most physiologically relevant dictated by the reaction rate (Finney and Halloran, 2003; Harrison *et al.*, 2007; Lemire *et al.*, 2013).

1.8.2.3 Speciation

Metal ions can exist in more than one species depending on several parameters including pH value, ionic strength, and temperature (Finney and Halloran, 2003). The oxidation state of the metals is also affected by other factors in the subcellular milieu. As such, the fact that the cytoplasm of Gram-negative bacteria is a strong reducing environment compared to the periplasm has a great impact on the oxidation state of the metal, and hence its activity (Stewart *et al.*, 1998; Lemire *et al.*, 2013).

1.8.3 Mechanisms of Action of Metals

The toxicity of metal ions to bacterial cells and inhibition of cellular growth are complex processes that result from one or a combination of mechanisms (Figures 1.3 and 1.4).

1.8.3.1 Reactive Oxygen Species (ROS) Production

Certain metals (Cu, Ag, chromium (Cr), vanadium (V), nickel (Ni), and cobalt (Co)) are known for their ability to disrupt the protein clusters that control iron (Fe) by targeting their cellular donor ligands (Anjem and Imlay, 2012). The damage of the clusters will therefore lead to the release and accumulation of Fe in the cytoplasm, which consequently triggers an Fe-mediated Fenton reaction (Touati, 2000).

$$Fe^{2+} + H_2O_2 \rightarrow Fe^{3+} + OH^- + OH^\bullet$$

$$Fe^{3+} + O_2^{\bullet-} \rightarrow Fe^{2+} + O_2$$

The $OH^{\bullet}$ generated reacts with other biomolecules and provokes the formation of additional free radicals, leading to cell injury and eventual death (Anjem and Imlay, 2012).

Another aspect involved in oxidative stress is the depletion of antioxidants through oxidation of cellular thiols (Lemire *et al.*, 2013). This feature is associated with the ability of soft and borderline metals, having high electron-sharing affinity, to bond with sulphur, enhancing the formation of protein disulphides, and therefore the depletion of antioxidant reserves (Helbig *et al.*, 2008). For instance, reports have indicated depleted levels of thiols for *Escherichia coli* (*E. coli*) exposed to doses of Ag, Zn, Co, Cr and tellurium (Te) (Harrison *et al.*, 2009).

1.8.3.2 Protein Dysfunction

A few amino acid residues (lysine, proline, arginine and histidine) found in proteins are adjacent to metal-binding sites, and hence are prone to oxidation by metal ions to form carbonyl derivatives (Stadtman and Levine, 2003). The oxidation reaction leads to protein degradation and loss of enzymatic activity, which partly accounts for the metals' antimicrobial activity (Stadtman and Levine, 2003). For instance high carbonyl levels were detected in *Saccharomyces cerevisiae* following high doses of Cr (VI) (Sumner *et al.*, 2005).

1.8.3.3 Impaired Membrane Function

It is proposed that metal ions act on the highly electronegative chemical groups found in bacterial membrane which may compromise its structural integrity (Zhang and Rock, 2008). Previous studies have visualized the clear morphological damages of the cytoplasmic membrane of *E. coli* and *S. aureus* caused by Ag and Al (Yaganza *et al.*, 2004; Yamanaka *et al.*, 2005). Ag, for instance, was shown to weaken the membrane by disrupting the electron transport chain and causing proton leakage (Lok *et al.*, 2006). However, Cu has been associated with an increased production of thiobarbiutiric acid reactive substances (TBARS) and lipid peroxidation (Hong *et al.*, 2012). Bacterial membrane impairment due to bacterial toxicity

is still a controversial mechanism since it is hard to decide if this is a cause or a consequence of cell death.

1.8.3.4 Interference With Nutrient Assimilation

Starvation-induced growth inhibition is another mechanism that some metal ions (Cr and Ga) may incur on bacterial cells. Kaneko *et al*. (2007) reported the ability of Ga to decrease the expression of genes encoding for the selective uptake for Fe (III), leading to Fe starvation and cell death. Pereira *et al*. (2008) also showed that the antimicrobial toxicity of Cr (VI) was related to its ability to inhibit sulphur uptake due to the competitive inhibition of the sulphur transporters.

1.8.3.5 Genotoxicity

With the lack of the *in-vivo* evidence, *in-vitro* studies indicate that few metals can promote DNA damage. Those metals disrupt Fe homeostasis and increase the rate of spontaneous mutagenesis causing irreversible DNA break and cell death (Desroches *et al.*, 2013). Mn, Co, Mo and Cr are renowned as mutagenic metals against bacteria (Asakura *et al.*, 2009).

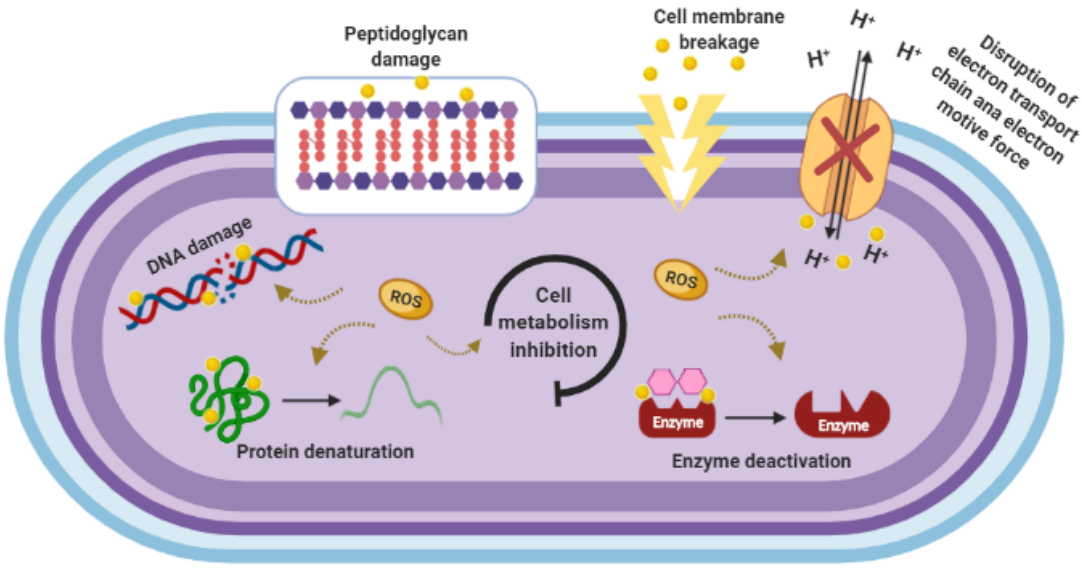

Figure 1.3 General mechanisms for antimicrobial activity of metals. Different metal ions exhibit different modes of action towards bacterial pathogens. Metals can lead to inactivation of enzymes and proteins that are necessary for cellular metabolism. They can also trigger an ROS-dependent oxidative stress response and antioxidants depletion. Some metals can be genotoxic accelerating DNA damage and cell death, whilst others act through disruption of cell wall and plasma membrane leading to a massive leakage of cellular contents. Figure drawn based on information from Lemire *et al*. (2013) Wyszogrodzka *et al*. (2016) and Roy *et al*. (2019).

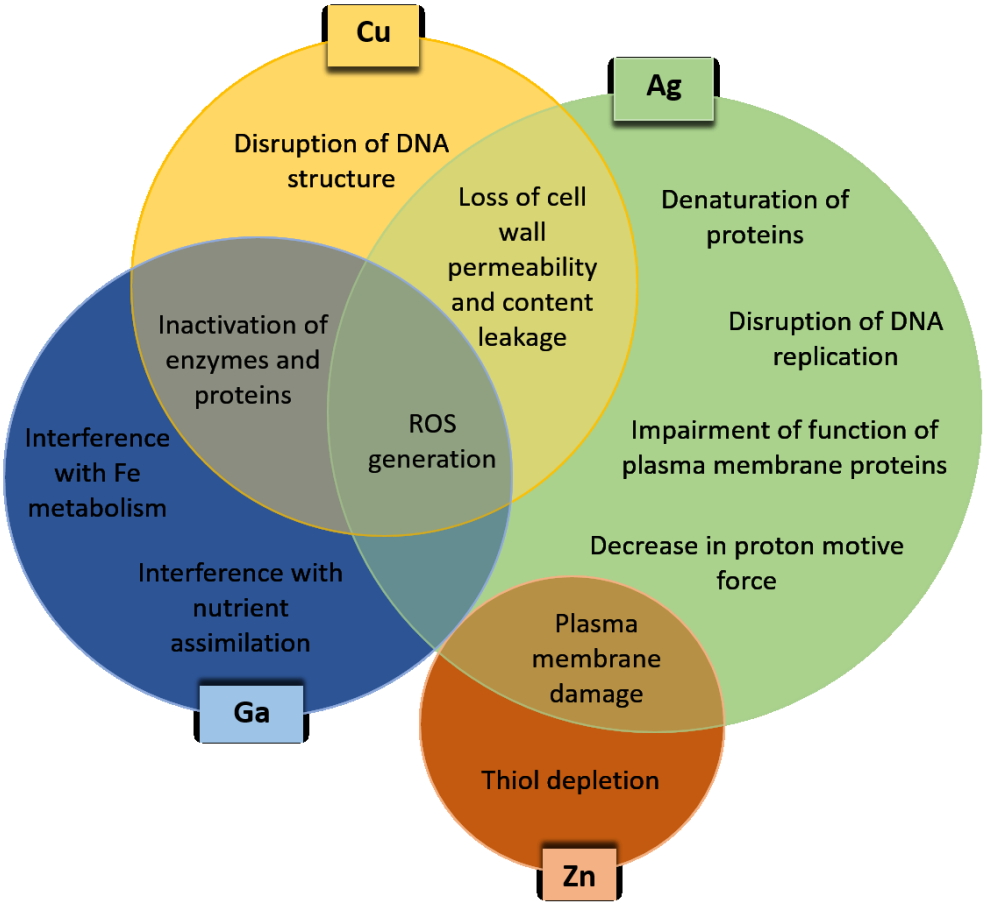

Figure 1.4 Schematic of specific antibacterial mechanisms of action associated with particular metal ions. Figure drawn based on information from Ciriolo *et al*. (1994), Feng *et al*. (2000), Kaneko *et al*. (2007) and Wyszogrodzka *et al*. (2016).

1.9 Metal-Based Antimicrobials (MBA)

Following the increasing knowledge regarding the mode of action of metals, a wide range of metal-based antimicrobials have been designed and incorporated in a variety of commercial products during the last few years (Turner, 2017). Although the use of MBA is not very new, recent and continuous additions are being made to the MBA depository making it highly effective. Below are a few examples of the main MBA commercial practices (Table 1.3).

Ag has demonstrated a 99% efficacy in reducing bacterial cell viability when incorporated in wound dressings (Boonkaew *et al.*, 2014). A better antimicrobial performance was noted for Ag-coated urinary catheters compared to the conventional alloy-coated catheters (Rupp *et al.*, 2004). Furthermore, an enhanced activity was recorded against *S. aureus* and

Klebsiella pneumoniae (*K. pneumoniae*) for catheters coated with a combination of Ag and titanium (Ti), while exhibiting, at the same time, no cytotoxic effects to osteoblasts and epithelial cells (Ewald *et al.*, 2006).

Meanwhile, Cu coatings have gained substantial attention lately due to its ability to inhibit a variety of pathogenic bacteria including verocytotoxigenic *E. coli*, vancomycin-resistant *Enterococci*, *Mycobacterium tuberculosis*, *Salmonella enterica* (*S. enterica*), *Campylobacter jejuni*, *Listeria monocytogenes* and methicillin-resistant *S. aureus* (Faúndez *et al.*, 2004; Wilks *et al.*, 2005; Noyce *et al.*, 2006; Mehtar *et al.*, 2008). Bacterial isolates were able to survive for few minutes to hours on Cu coatings compared to other surfaces coated with polyvinyl chloride (PVC), stainless steel, aluminium and silicon (Borkow *et al.*, 2010). Socks impregnated with Cu have been suggested by Borkow and Gabbay (2009) to improve wound healing in diabetic people (athlete's foot).

The use of Au have been thoroughly investigated, and showed promising results for biomedical applications in imaging, detection, and therapy, especially for gold nanoparticles (AuNPs) that displayed higher stability than silver nanoparticles, are inert, non-toxic and size-controllable (Katas *et al.*, 2019; Yougbare *et al.*, 2019). Similar to Au, Pd has demonstrated a high compatibility for use in the oral environment and can be used for dental fillings. Pt is an exceptionally valuable metal that possesses antimicrobial properties against *K. pneumoniae*, *Enterobacter faecium*, and *Acinetobacter baumannii* (Vaidya *et al.*, 2017). It presents a high potential to be incorporated in an array of biomedical applications (including permanent implants, orthopaedic, and surgical instruments), but this is limited by its high cost and low abundance (Cowley and Woodward, 2011).

Due to their additive effects when combined together or with other compounds, metals are being used in different combinations in numerous applications. For instance, a combination of desferrioxamine-Ga (DFO-Ga) and gentamicin has been reported to kill *P. aeruginosa* biofilms (Banin *et al.*, 2008). Cu and quaternary ammonium have also been used in combination to create an industrial wood-preservative fungicide that is currently used in

North American, Australia and Europe (Harrison *et al.*, 2008). Following the promising antimicrobial potential, research into MBA therapy has now progressed towards clinical studies (Lemire *et al.*, 2013).

Table 1.3 Overview of the use of metals as antimicrobials in different biomedical and cosmetic applications

Metal ion	Target Bacterium	Medical/Clinical Use	Reference
Ag	*S. aureus, K. pneumoniae, P. aeruginosa*	• Urinary catheters • Implants • Wound dressings	Dizaj *et al*. (2015) Mittapally *et al*. (2018)
Sn	*S. aureus, E. coli, Shigella flexineri*	• Used to decontaminate circulating water • Antifouling	John *et al*. (2018) Mittapally *et al*. (2018)
Au	MDR *E. coli,* MDR *S. typhimurium,* MDR *S. aureus*	• Dental fillings • Biosensors • Water remediation	Dasari *et al*. (2015) Lopez *et al*. (2019)
Cu	*Legionella, E. coli,* MRSA, *Enterococci, S. enterica*	• Cu/Ag to decontaminate drinking water in hospitals • Wound/ulcer dressing	Lin *et al*. (2011) Vincent *et al*. (2016)
Zn	*S. aureus*, *E. coli*, *P. aeruginosa*, *Bacillus subtilis*, *E. faecalis*	• Ointments, lotions, and mouthwashes	Jiang *et al*. (2018)
Pt	*E. coli, S. aureus, B. cereus, P. aeruginosa*	• Hip and knee implants • Cardiovascular defibrillator • Catheters	Cowley *et al*. (2011) Koller *et al.* (2017)
Pd	*Bacillus, E. coli, K. pneumoniae*	• Dental fillings • Medical implants	Rimbu *et al*. (2014) Koller *et al*. (2017)
Ga	*A. baumannii*, *P. aeruginosa*, Enterobacteriaceae	• Antineoplastic agent	Bonchi *et al*. (2014) Hijazi *et al*. (2018)

1.10 Graphene and Graphene Oxide

The interest in research of the applications of carbon-based nanotechnologies has been expanding for the last few years in light of its promising potential applications in various fields, including sensor development, biomedicine, drug delivery, molecular imaging, energy conversion, water treatment, and storage devices (Gurunathan *et al.*, 2012). Although the increase in graphene use has boomed after its isolation by Geim and Novoselov, graphite has been known as a mineral for almost 500 years (Geim and Novoselov, 2007). Owing its weak dispersion forces, graphite was even used as a marking instrument in the middle ages, which is equivalent to using a pencil today (Allen *et al.*, 2010).

1.10.1 Chemical Perspectives of Graphene-Based Compounds

The valence of the carbon element enables it to form different allotropes of distinct shapes, structures and properties including graphite, graphene, fullerene and carbon nanotubes (Szunerits and Boukherroub, 2016). Graphene (Gr) is an ultrathin 2D nanomaterial which is composed of a single layer of sp^2-bonded carbon atoms packed in a honeycomb crystal lattice (Figure 1.5.a) (Zhu *et al.*, 2017). Graphene oxide (GO) is a chemically modified form of graphene having multiple oxygen containing functionalities (epoxides, alcohol or carboxylic acids) (Figure 1.5.b). These functional groups allows GO to react with many chemical groups (Lu *et al.*, 2012). There is no general consensus over the exact structure of GO due to its complicated non-stoichiometric nature, however several models have been proposed (Dreyer *et al.*, 2010).

Figure 1.5 Chemical structures of (a) graphene and (b) GO. Figures reproduced from Ilbay *et al*. (2017) and Azman *et al*. (2018).

The two carbon-based structures possess unique characteristics such as thermal and electrical conductivity, chemical stability, high specific surface area, and mobility of charge carriers (Lu *et al.*, 2012; Slate *et al.*, 2019). Graphene-derivatives are preferentially used over other carbon-based materials. This is related to that fact that, unlike fullerenes and carbon-nanotubes that are synthesized from carbon-containing gases in the presence of catalytic nanoparticles, graphene composites are free from metallic impurities (Szunerits and Boukherroub, 2016).

1.10.2 Antibacterial Mechanism of Action of Graphene and GO

Graphene and GO have previously been shown to exhibit an inhibitory and bactericidal effect against Gram-positive (*S. aureus*) and Gram-negative (*E.coli*, *P. aeruginosa*) bacteria (Table 1.4) (Tu *et al.*, 2013; Pham *et al.*, 2015). Graphene and GO have risen to the spotlight of antibacterial agents due to their remarkable properties, low cytotoxicity to mammalian cells, and their synergistic activity with other biocides (Liao *et al.*, 2011; Zhu *et al.*, 2017). The exact mechanism of antibacterial activity of the carbon nanosheets is not fully elaborated. However, several scenarios have been proposed and examined. Experimental approaches to understand the mechanism of action of the graphene nanocomposites revealed a physical damage to the bacterial membrane (Akhavan and Ghaderi, 2010). Bacterial membrane stress has been associated with a physical interaction between the bacterial cell and the sharp nanosheets of graphene or GO, via two possible mechanisms (1) self-insertion and cutting of the phospholipid membrane by the graphene composites, and (2) detrimental extraction of

the phospholipids (Figure 1.6) (Zhou and Gao, 2014; Al-Jumaili *et al.*, 2017). Tu *et al*. (2013) used transmission electron microscopy and molecular dynamic simulations to explain the details of the antibacterial action. They proposed three stages through which a graphene sheet could cross the outer and inner membranes including the swing mode, the insertion mode, and the extraction mode. The process starts with a vibrational movement (10-100 nanoseconds) of the graphene sheet that is swinging back and forth with its tail end touching the cell membrane several times. The insertion mode is initiated when the graphene tail becomes trapped in the membrane due to the powerful van der Waals interactions from membrane lipids and hydrophobic interactions. Once the tail is inserted, the graphene nanosheets punctures and cut through the lipid membrane within nanoseconds. The nanosheets start then a vigorous extraction of the phospholipid molecules from the lipid membrane onto its own surfaces, leading to an irreversible distortion of the membrane due to the sparse lipid content and strong protracted forces (Tu *et al.*, 2013; Al-Jumaili *et al.*, 2017).

The antibacterial action of graphene is not only confined to the structural damage of the bacterial membrane and cell wall. It also depends on the chemical interactions between carbon nanosheets and cells resulting in an electron transfer phenomenon (Li *et al.*, 2014). The electron drainage from the outer bacterial membrane triggers an oxidative stress response and cell death (Al-Jumaili *et al.*, 2017). Graphene is also able to trigger an oxidative stress response through ROS generation that causes extensive damage to the lipids and proteins found in bacterial cells (Sanchez *et al.*, 2012). Previous studies have investigated the interaction of graphene and graphene oxide with glutathione and reported a catalytic activity mediating an oxidative damage (X. Liu *et al.*, 2011; Sanchez *et al.*, 2012) due to a series of direct oxidation reactions on graphene/GO planes or due to an indirect trigger for cellular oxidants' production (Sanchez *et al.*, 2012).

The activity of graphene is dependent on a complex interplay of several parameters including shape, size, surface area, synthesis methods and exposure time. Dallavalle *et al*. (2015) reported that small sheets (<5.2 nm) could pierce through the membrane and pass through it without affecting the

order of phospholipids. Larger graphene sheets (< 11.2 nm), on the other hand, exhibited a higher bactericidal effect against bacteria, due to the increase in the cutting effect and the improved ability to displace phospholipids in the membrane (Dallavalle *et al.*, 2015; Al-Jumaili *et al.*, 2017; Neto, 2019). Larger sheets were also able to entrap bacterial cells in a "wrapping" process, isolating them from their surrounding and depriving them from nutrients and oxygen (Dallavalle *et al.*, 2015; Neto, 2019).

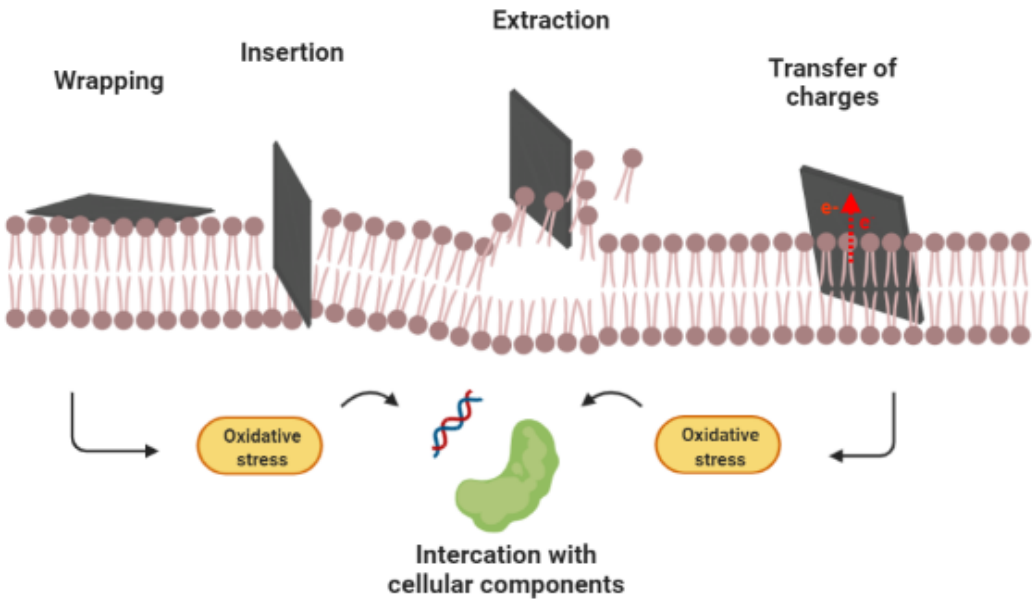

Figure 1.6 Schematic for graphene-related different antimicrobial mechanisms. The proposed mechanisms of antibacterial action of graphene include bacterial wrapping, cutting through the inner and outer bacterial membrane causing extraction of phospholipids and irreversible membrane damage, and electron transfer triggering an ROS response. Figure adapted and modified from Jia *et al*. (2016) and Al-Jumaili *et al*. (2017).

1.10.3 Combinations of Graphene Composites and Metal Ions

Once the antimicrobial properties of the graphene nanocomposites were well established, their alteration into several application-driven purposes was necessary. Promising results were reported by incorporating metal nanoparticles into graphene-based scaffolds (Table 1.4) (Al-Jumaili *et al.*, 2017).

1.10.3.1 Graphene/Silver Nanoparticles

Silver is recognized as one of the oldest most efficacious antimicrobials used for the last 40 years (Roy *et al.*, 2019). Nonetheless, the efficient

antibacterial use of silver is limited by the oxidation and aggregation of Ag nanoparticle (AgNPs). The addition of GO was able to diminish the nanoparticles' oxidation process enhancing the antimicrobial efficacy. Gao *et al*. (2013) associated this finding with the high number of oxygenated groups found on the GO-AgNPs planes that increases the ability of the compound to bind to surfaces and materials.

1.10.3.2 Graphene/Gold Nanoparticles

Recent studies have demonstrated that the addition of gold nanostructures into reduced GO (rGO) sheets results in a bactericidal effect (Hussain *et al.*, 2014). Furthermore, graphene sheets encased with gold are currently used for bacterial photothermal ablation, which might be a new possibility to treat Urinary tract infections (UTIs) (Szunerits and Boukherroub, 2016).

1.10.3.3 Graphene/Copper Nanoparticles

Aiming to control the release of Cu ions, Ouyang *et al*. (2013) integrated CuNPs into modified poly-L-lysine rGO, which exhibited remarkable properties of antimicrobial activity, high stability, long endurance and water solubility.

1.10.3.4 Graphene/Zinc Oxide Nanoparticles

Much like AgNPs, the long-lasting antimicrobial activity of zinc oxide nanoparticles (ZnO NPs) is compromised by their aggregation. Therefore, several groups have investigated the incorporation of ZnO NPs into graphene. The outcome indicated that GO sheets helped the dispersion of ZnO NPs and brought them closer to bacterial cells, facilitating bacterial lysis (Wang *et al.*, 2014).

Table 1.4 Properties and antibacterial activity of graphene, GO and graphene/GO loaded with nanoparticles

Gr/GO/metal	size	Bacteria	concentration	Reference
GO	~ 205 nm	*E. coli* (90.9% viability loss)	< 100 µg/mL	Tu *et al.* (2013)
GO	0.31 µm	*S. aureus* *E. faecalis* *P. aeruginosa*	10 µg/mL 10 µg/mL 150 µg/mL	Liu *et al.* (2011)
GO	10 nm to 20 µm	*E. coli*	40 µg/mL	Liu *et al.* (2012)
GO	0.525 -3.40 µm	*P. aeruginosa* (87% viability loss)	0.1 mg/mL	Guruntham *et al.* (2012)
GO nanosheets	1.4 nm	*E. coli*	50 - 200 µg/mL	Perreault *et al.* (2015)
Graphene nanosheets	----	*B. subtilis* *S. typhimurium* *E. faecalis*	4.0 µg/mL 1 .0 µg/mL 8.0 µg/mL	Krishnamoorthy *et al*. (2012)
Graphene films	----	*S. aureus*	60 µL/mL	Li *et al.* (2014)
GO-AgNPs	9.4 nm	MRSA	15 µg/mL	De Moraes *et al.* (2015)
rGO-AuNPs	8-15 nm	*P. aeruginosa* *K. pneumoniae* *B. cereus*	5-50 µg/mL	Saikia *et al.* (2016)
Gr-ZnO	22 nm	*E. coli* 100% inhibition	0.003 µg/mL	Kavitha *et al*. (2012)
GO-ZnO	4 nm	*E. coli*	10 µg/mL	Wang *et al*. (2014)

1.11 Negative Aspects of Using Metal-Based And Graphene-Based Antimicrobials

1.11.1 Bacterial Resistance

The loss of effectiveness and the development of bacterial resistance towards metal ions must be considered as a consequence of common uses of metal-based antimicrobials (Turner, 2017).

Bacterial metal-ion resistance is a common mechanism that stretches back to 1960s, when the first mercury resistant *S. aureus* isolated from an infected wound was reported (Barber, 1961). Some of the well-characterized examples of bacterial metal resistance include copper and silver resistance among *E. coli*, *K. pneumoniae* and *Staphylococcus pseudointermedius* (Delmar *et al.*, 2014; Hobman and Crossman, 2015). Arsenic resistance has been detected in *Staphylococcus haemolyticus* and *Yersinia pestis*, whilst cadmium, lead, cobalt, zinc and uranium resistance were detected in *Stenotrophomoas maltophila* (Crossman *et al.*, 2008; Yu *et al.*, 2014).

Bacterial metal-ion resistance was first discovered in the second half of the twentieth century (Hobman and Crossman, 2015). The natural exposure of microorganisms to bioavailable metals, over billions of years, has been the driving factor for bacterial innate immunity towards metal ions, at least at their “environmental concentrations” (Monych *et al.*, 2019). Bacteria has developed the ability to control the intracellular levels of these metals, by evolving mechanisms to acquire the essential metals and eliminate the deleterious excess levels or toxic metals (Hobman and Crossman, 2015).

The resistance mechanisms employed by the bacteria to nullify the effects of metal toxicity are conceptually similar to the antibiotic resistance mechanisms (Lemire *et al.*, 2013). Most of these mechanisms have been well characterized at the bacterial genetic level and were linked predominantly to efflux of metal ions from the cell. The genes that are responsible for efflux transporters’ are plasmid-mediated, hence, are easily transferable through horizontal gene transfer (Hobman, 2017). These genes are often part of an operon coding for metal chelator molecules or proteins

including multiple transporters that account for a full efflux system extending from the cytoplasm to the outside of the cell (Delmar *et al.*, 2014; Hobman and Crossman, 2015). Other mechanisms of general metal resistance in bacteria can include methylation/demethylation of metals, stress response mechanisms, intracellular/extracellular sequestration and reduction of metal ions (Ianeva, 2009). However, specific metal ion resistance mechanisms are often characterized by a group of structural resistance genes that are encoded by a metal ion specific response regulator (Delmar *et al.*, 2014; Hobman and Crossman, 2015). The products of these genes produce a metal ion-specific efflux protein or enzyme that can modify the metal ion into a less toxic form (Silver and Phung, 1996). The chemistry of the metal ion itself can notably dictate the bacterial resistance mechanism towards it. For instance, certain metals are more prone to chemical modification, making them either insoluble or less toxic (Tchounwou *et al.*, 2012). Mercuric ion resistance in Gram-negative bacteria is a very good example where Hg^{2+} are imported across the cytoplasmic membrane via MerT to the cytoplasm where they are reduced to the non-toxic form (Hg^0) by mercuric reductase (MeRA) (Hobman and Crossman, 2015). Furthermore, metallic mercury (Hg^0) is volatile at room temperature and pressure; therefore, it is capable of leaving the bacterial cell by passive diffusion (Hobman and Crossman, 2015).

Bacterial resistance towards graphene composites is less likely to happen since the antimicrobial mechanism of these composites rely on the destruction of the bacterial memnrane through insertion of the carbon sheets. There are no reports, to date, reporting bacterial resistance towards graphene or graphene oxide.

1.11.2 Potential Toxicity towards to Human Cells

While research to date on MBAs has considerable promise, it is evident that very little is known when investigating their antimicrobial potential (Turner, 2017). A common misconception among non-inorganic chemists is the notion that metals, metalloids and their complexes are mostly toxic (Frei, 2020). The concept of toxicity stems from the different modes of action

employed by metal ions to kill bacteria including ROS production, generation of free radicals, protein dysfunction or impaired membrane function (Lemire *et al.*, 2013). These general mechanisms are not specific to bacteria and can be detrimental to human cells. To address this issue, Frei *et al*. (2020) analysed the antimicrobial profile of more than 1000 metal complexes using the Community for Open Antimicrobial Drug Discovery (CO-ADD) – a global antimicrobial platform that screens user-submitted compounds against ESKAPE pathogens and two fungal species. They also assessed the haemolytic activity of the compounds against human red blood cells and their toxicity by measuring mammalian cell viability using HEK293 human embryonic kidney cells. The results indicated that 88 out of 246 metal compounds exhibited a broad-spectrum antimicrobial activity with no indication of any toxicity or haemolytic properties at the highest tested concentrations (Frei, 2020; Frei *et al.*, 2020). Amongst the metal complexes, ruthenium, silver, palladium and iridium were the most frequent element found in active 'non-toxic' compounds (Frei *et al.*, 2020). For instance, ruthenium showed a remarkable antimicrobial activity against *E. coli*, *S. aureus* and *B. subtilis* and normal activity against human lung fibroblasts (Le Gall *et al.*, 2018). In fact, Feng *et al*. (2019) demonstrated the preferential killing of ruthenium of bacterial over mammalian cells in vitro. Bismuth, which has been lately used for the treatment of colitis wound infection and gastrointestinal disorders, also showed a low cytotoxicity against human cells while being potent against *Helicobacter pylori* (Fock *et al.*, 2013). Furthermore, metal-based FDA-approved drugs have been in the market for several decades, such as Auranofin (gold-based antirheumatic drug). Auranofin was found to be safe with no traces of toxicity observed in patients following a 5 year treatment (Blodgett and Pietrusko, 1986; Frei, 2020). While further studies and investigations are required to assess the safety of metal ions, preliminary studies highlight the future promising directions for the development of metal-based antibacterial agents (Frei, 2020).

The toxicity of graphene is dependent on so many factors including the graphene chemical structure, the nature of the functionalized coatings, the size, the cell type, the number of layers (Gurunathan *et al.*, 2012; Seabra *et*

al., 2014). The administration route, dose, time of exposure, and synthesis methods are also critical for *in-vivo* experiments (Gurunathan *et al.*, 2012). Therefore, generalized conclusions regarding the potential toxicity of graphene-based compounds can be inaccurate and misleading, since it is case-specific (Seabra *et al.*, 2014). Hence, contradictory results regarding the toxicity of graphene have been reported since 2004. To evaluate their potential toxicity, a zebrafish embryo has been established as a model due to its close homology with the human genome. Gollavelli *et al*. found no significant abnormalities in the survival rate of zebrafish embryos, following their injection with multifunctionalized graphene (Gollavelli and Ling, 2012; Seabra *et al.*, 2014). In general, the toxicity of GO was observed to be dose-dependent in both human and animal cells, displaying little to no effect for low and medium doses in mice (Ruiz *et al.*, 2011; Wang *et al.*, 2011). Although the mechanisms responsible for graphene and GO toxicity have been discussed previously, no conclusions have been drawn that are sufficient to establish risk assessments or regulations (Seabra *et al.*, 2014).

1.12 Bacterial Pathogens Selected for this Study

To tackle the AMR crisis, a global action plan was published by WHO in 2015, with the prospects that individual countries will develop their own national action plans on AMR in keeping with the global strategy (Zhen *et al.*, 2019). The WHO plan encompasses a global priority list of resistant organisms including *Enterococcus spp*., *S. aureus*, *K. pneumoniae*, *A. baumannii*, *P. aeruginosa* and *E. coli* – collectively known as ESKAPE pathogens - to guide the research, discovery and development of new antibiotics (Pogue *et al.*, 2015; Zhen *et al.*, 2019). ESKAPE pathogens are the leading cause of health-care-associated infections worldwide; therefore, directing attention towards these organisms is essential since MDR ESKAPE bacteria are associated with higher morbidity and mortality rates, opportunities for spreading to other patients, as well as economic burden (Pogue *et al.*, 2015; Karlowsky *et al.*, 2017; Zhen *et al.*, 2019).

1.12.1 ESKAPE Pathogens

ESKAPE, by definition, is an acronym designating six bacterial pathogens of high virulence, including *Enterobacter* spp., *S. aureus*, *K. pneumoniae*, *A. baumannii*, *P. aeruginosa* and *Enterococcus faecium*. There is a new designation to include *E. coli* as a member of the ESKAPE family, since *E. coli* and ESKAPE pathogens together, cause the majority of life-threatening bacterial infections in health care facilities among critically ill and immunocompromised patients worldwide (Savin *et al.*, 2020). As their name indicates, ESKAPE pathogens, together with E. coli, are able to “escape” the biocidal action of antibiotics, presenting novel prototypes in pathogenesis and resistance, and new challenges for treatment (El-mahallawy *et al.*, 2016). ESKAPE pathogens are grouped according to their necessity for developing new effective antibacterial agents into three main priority tiers: medium, high, and critical priority (Figure 1.7) (WHO, 2017; Zhen *et al.*, 2019). In particular, carbapenem-resistant *K. pneumoniae* and *P. aeruginosa* are classified as critical-priority pathogens, whilst MRSA and vancomycin resistant *S. aureus* are on the high-priority list (WHO, 2017). The number of antibiotics that are still effective against ESKAPE organisms has diminished to a point where many antibiotics have been deleted since 2010, whilst only few were added. This study focused on three ESKAPE pathogens, which were *P. aeruginosa*, *K. pneumoniae* and *S. aureus*.

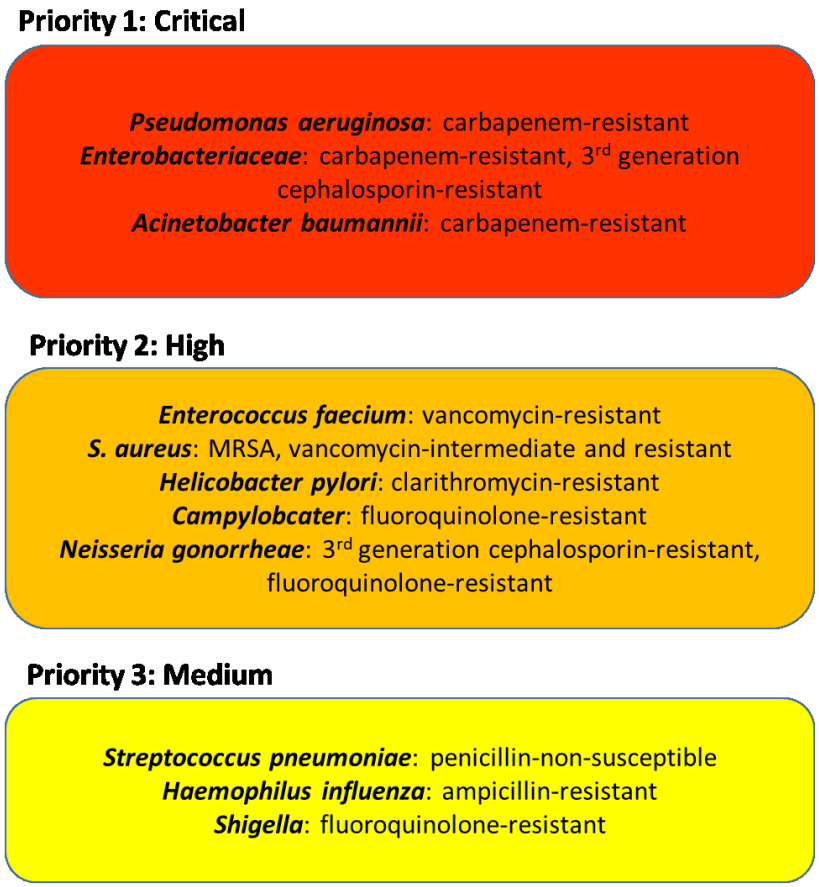

Figure 1.7 WHO priority pathogens list for research and development of new antibiotics. Figure adapted from WHO (2017).

1.12.1.1 *P. aeruginosa*

P. aeruginosa is a Gram-negative rod, facultative anaerobe belonging to the family Pseudomonadaceae. It is an opportunistic pathogen that is responsible for 11-22.6% of nosocomial infections (particularly in immunocompromised and burn patients) (Driscoll *et al.*, 2007). Infections can range from dermatitis, soft tissue infections, urinary tract infections, gastrointestinal infections, respiratory infections to bacteraemia. *P. aeruginosa* is a pathogen of a specific concern in burn patients, being the second most frequent bacteria (14.29% - 27%) isolated from burn infections (Othman *et al.*, 2014; Latifi and Karimi, 2017). Furthermore, the isolation of *P. aeruginosa* can increase up to 55% in burn patients hospitalized for more than 2-3 weeks (Lachiewicz *et al.*, 2017). Due to its outer membrane, *P. aeruginosa* can be intrinsically resistant to various antimicrobial agents. *P. aeruginosa* infections can be treated with one of the following antimicrobial groups: polymyxins, aminoglycosides (amikacin, gentamicin and

tobramycin), fluoroquinolones (levofloxacin and ciprofloxacin), or ß-lactams (Driscoll *et al.*, 2007; ECDC, 2018). Resistance, however, can develop through modification of the structure of the antibiotic target, degradation of the enzymes or efflux and permeability reduction (Driscoll *et al.*, 2007). EARS-Net reports indicated that, in 2018, 32.1% and 19.2% of *P. aeruginosa* isolates were resistant to at least one antimicrobial group, and two or more antimicrobial groups, respectively (ECDC, 2018).

1.12.1.2 *K. pneumoniae*

K. pneumoniae is a Gram-negative, rod-shaped member of the Enterobacteriaceae family. *K. pneumoniae* is known to be the causative agent of major healthcare associated infections including intra-abdominal infections, bloodstream infections, lower respiratory tract infections, pneumonia, and septicaemia (Keynan and Rubinstein, 2007). *K. pneumoniae* has developed resistance towards several classes of antibiotics during the last few years, most importantly it acquired a variety of ß-lactamase enzymes (Santajit and Indrawattana, 2016). Beta-lactamases (ESBL) producing *K. pneumoniae* are able to inactivate the effect of ß-lactam antibiotics (cephalosporin and penicillin) by opening up their rings. Carbapenem can frequently endure the action of ESBLs, and therefore it is conventionally used as one of the few options for treating *K. pneumoniae* persistent infections (Navon-Venezia *et al.*, 2017). The problematic situation of *K. pneumoniae* resistance to carbapenem has the potential to confer resistance to all ß-lactams. Furthermore, carbapenemase genes are encoded on plasmids that can be easily exchanged between *K. pneumoniae* and other Gram-negative bacteria (Navon-Venezia *et al.*, 2017). Healthcare professionals confirm that cases of outbreaks of carbapenemase-mediated MDR resistant *K. pneumoniae* strains can only be reduced and not completely eliminated, even with severe precautionary practices (Santajit and Indrawattana, 2016). The six WHO regions (American region, African region, European, Eastern Mediterranean, West-east Asia and South Pacific) were reported to have more than 50% resistance of *K. pneumoniae* towards third generation cephalosporin, whilst two regions exhibited more

than 50% to carbapenems (Zhen *et al.*, 2019). Surveillance reports also indicated that there was a 6-fold increase in the in *K. pneumoniae* attributed-deaths between 2007 and 2015 (ECDC, 2018).

1.12.1.3 *S. aureus*

S. aureus is a Gram-positive cocci-shaped bacterium that is normally found in the environment and can persistently colonize the anterior nares of 15% of the population (Wertheim *et al.*, 2005). *S. aureus* is the leading cause of a wide range of infections in the community and clinical settings, including device related infections, skin ad soft tissue infections, bacteraemia and endocarditis (Tong *et al.*, 2015). Penicillin remained the treatment of choice for *S. aureus* infections until the emergence of ß-lactamase producing *S. aureus* in 1948, that accounts for 65%-85% resistance to penicillin G among *S. aureus* today (Santajit and Indrawattana, 2016). *S. aureus* can acquire resistance to ß-lactams (including methicillin) through the expression of a foreign penicillin binding protein (PBP) that shows low affinity for methicillin, precluding the inhibition of cell wall synthesis (Stapleton and Taylor, 2002). Glycopeptide antibiotics such as teicoplanin and vancomycin are currently used to treat MRSA, however, their extensive use has induced some clinical strains to display intermediate and full resistance towards vancomycin (Chambers and Deleo, 2009). Combined resistance to more than one antimicrobial agent was very common among MRSA, with MRSA-fluoroquinolone being the most frequent resistance combination (ECDC, 2018). The incidence of MRSA exceeded 20% in the six WHO regions, among which three regions exceeded 80% (Zhen *et al.*, 2019).

The high levels of AMR for several combinations of important bacterial species to antimicrobial group as reported by ECDC for 2018 demonstrate that AMR is still a serious challenge in the UK (Figure 1.8) (Santajit and Indrawattana, 2016).

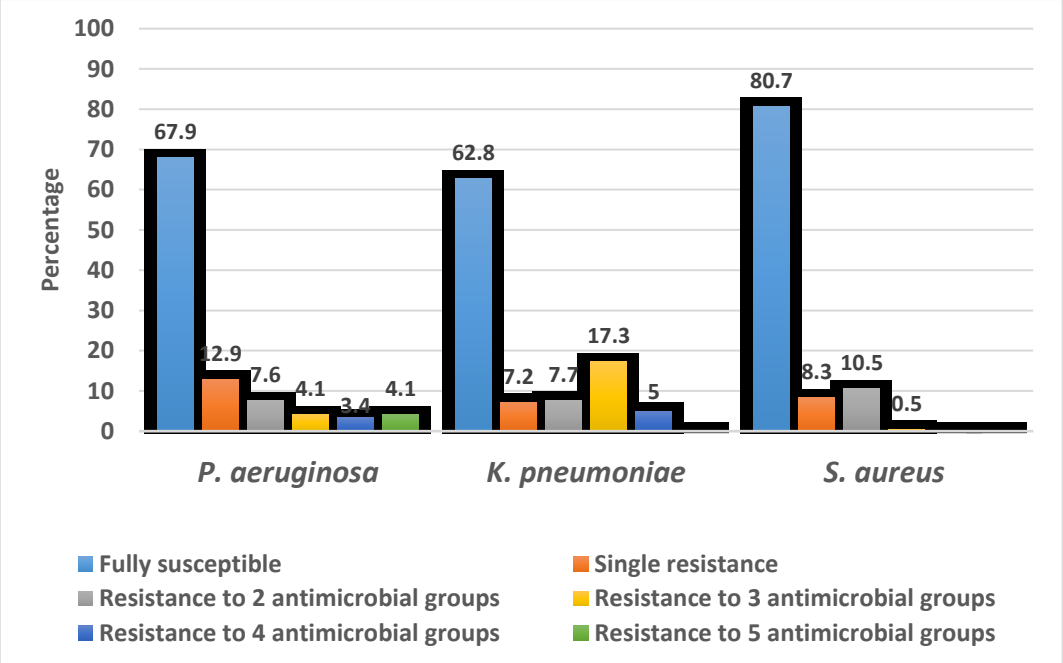

Figure 1.8 Representation of the percentage of *P. aeruginosa*, *S. aureus* and *K. pneumoniae* isolates, collected within UK during 2018, into fully susceptible and resistant to one, two, three, four or five antimicrobial groups. Data represents invasive bacterial isolates from blood and cerebrospinal fluid only. AMR data for 2018 was reported to EARS-Nat before August 2019. Histogram plotted based on data from ECDC (2018).

1.13 Aim and Objectives of the Study

The use/misuse of antibiotics during the past 60 years has exerted a selective pressure on susceptible bacteria, favouring the survival of resistant strains and endangering the efficacy of antibiotics.

In the light of the global increase in AMR threatening the management of infections and the decrease in antibiotic development, there is a compelling need to address AMR with novel agents.

The main interest of this thesis was to assess the antimicrobial efficacy of metal ions and graphene composites against ten MDR ESKAPE pathogens. It also aimed at developing new antimicrobial formulations (for skin cleansers and nasal topicals) containing the most effective combinations of metal ions, graphene or graphene oxide.

Objectives:

- Test the antimicrobial efficacy of eighteen metal ion solutions, graphene and graphene oxide, individually and in combinations, against ten clinical MDR isolates of *P. aeruginosa*, *K. pneumoniae* and *S. aureus* in their planktonic and biofilm forms
- Test the cytotoxic effects of the metal ions showing the greatest inhibitory effect against the ten pathogens
- Incorporating the most antimicrobially effective metal ions or metal ions/graphene composites into the formulations of skin cleansers and test their efficacy against chlorhexidine-sensitive and adapted *K. pneumoniae* isolates
- Incorporating the most effective metal ions or metal ions/graphene composites into nasal spray formulations and nasal ointments and test their efficacy against mupirocin-sensitive, intermediate and resistant *S. aureus* isolates

Chapter 2 Materials and Methods

2.1 Materials

Acetic acid (Fischer Scientific, UK)

Acetone (Sigma-Aldrich, UK)

Aluminium (Sigma-Aldrich, UK)

Amikacin (30 µg) (Oxoid, UK)

Amoxicllin/Clavulanic acid (20/10 µg) (Oxoid, UK)

Ampicillin (10 µg) (Oxoid, UK)

Aztreonam (30 µg) (Oxoid, UK)

Cephalotin (30 µg) (Oxoid, UK)

Cefepime (30 µg) (AB Biodisk, UK)

Cefotaxime (30 µg) (Sigma-Aldrich, UK)

Cefoxitin (30 µg) (Oxoid, UK)

Ceftazidime (30 µg) (Oxoid, UK)

Cefuroxime (30 µg) (Sigma-Aldrich, UK)

Cefuroxime/Axetilssssss (30 µg) (Oxoid, UK)

CellTiter 96 Aqueous solution (Promega, USA)

Chlorhexidine gluconate (Sigma-Aldrich, UK)

Ciprofloxacin (5 µg) (AB Biodisk, UK)

Clindamycin (2 µg) (Oxoid, UK)

Colistin (Sigma-Aldrich, UK)

Copper (Sigma-Aldrich, UK)

Crystal violet (0.1 % w/v) (Oxoid, UK)

D-glutamine (Sigma-Aldrich, UK)

Diethyl ether (Sigma-Aldrich, UK)

Ethanol (Fisher Scientific, UK)

Erythromycin (15 µg) (Oxoid, UK)

Ertapenem (10 µg) (Oxoid, UK)

Foetal Bovine serum (FBS) (Lonza, UK)

Fosfomycin (AB Biodisk, UK)

Gallium (Sigma-Aldrich, UK)

Gentamicin (10 µg) (Oxoid, UK)

Gluconolactone (Fischer scientific, UK)

Glutaraldehyde (Sigma-Aldrich, UK)

Glycerol (Fischer scientific, UK)

Gold (Sigma-Aldrich, UK)

Graphene (Manchester Metropolitan University, UK)

Graphene oxide (Graphene Supermarket, USA)

Graphene oxide (Manchester Metropolitan University, UK)

Hydrochloric acid (Sigma-Aldrich, UK)

Human skin fibroblasts WS1 (ATCC PCS-201-012)

Imipenem (10 µg) (AB Biodisk, UK)

Indium (Sigma-Aldrich, UK)

Isopropyl alcohol (70 %) (Fisher Chemicals, UK)

Linezolid (30 µg) (Oxoid, UK)

Menadione solution (Sigma-Aldrich, UK)

Meropenem (10 µg) (Oxoid, UK)

Methanol (BDH, UK)

Methicillin (5 µg) (Oxoid, UK)

Molybdenum (Sigma-Aldrich, UK)

Mupirocin (5 µg and 200 µg) (Applichem Gmbh, USA)

Mupirocin 2 % ointment (Advanz Pharma, UK)

Niobium (Sigma-Aldrich, UK)

Nitric acid (Fisher Chemicals, UK)

Oxacillin (1 µg) (Sigma-Aldrich, UK)

Palladium (Sigma-Aldrich, UK)

Penicillin – streptomycin (Lonza, UK)

Phosphate buffer Saline (Fisher Chemicals, UK)

Piperacillin (100 µg) (AB Biodisk, UK)

Piperacillin/ tazobactam (100/10 µg) (Oxoid, UK)

Platinum (Sigma-Aldrich, UK)

Polished 304 grade stainless steele coupons (10 mm × 10 mm)

Polyethylene glycol 7 (Sigma-Aldrich, UK)

Polyethylene glycol 400 (Sigma-Aldrich, UK)

Polyethylene glycol 3350 (Sigma-Aldrich, UK)

Rhenium (Sigma-Aldrich, UK)

Rhodium (Sigma-Aldrich, UK)

Rifampicin (5 µg) (Oxoid, UK)

Roswell Park Memorial Institute - RPMI 1640 Medium (Sigma-Aldrich, UK)

Ruthenium (Sigma-Aldrich, UK)

Silicon Wafers (Montco Technologies, USA)

Silver (Sigma-Aldrich, UK)

Soft white paraffin (Sigma-Aldrich, UK)

Softisan 649 (IOI Oleo GmbH, Germany)

Tantalum (Sigma-Aldrich, UK)

Tetracycline (30 µg) (Oxoid, UK)

Tigecycline (15 µg) (Oxoid, UK)

Tin (Sigma-Aldrich, UK)

Tobramycin (10 µg) (AB Biodisk, UK)

Trimethoprim (1.25 µg) (Oxoid, UK)

Triphenyl Tetrazolium Chloride (Sigma-Aldrich, UK)

Trypan blue solution (Lonza, UK)

Trypsin EDTA (Lonza, Belgium)

Tryptone Soy Agar (Oxoid, UK)

Tryptone Soy Broth (Oxoid, UK)

Yttrium (Sigma-Aldrich, UK)

Zinc (Sigma-Aldrich, UK)

Zirconium (Sigma-Aldrich, UK)

2,3-Bis(2-methoxy-4-nitro-5-sulfophenyl)-2H-tetrazolium-5-XTT sodium salt (Sigma-Aldrich, UK)

12-well plates (Thermo Scientific, UK)

96-well plates (Thermo Scientific, UK)

2.2 Methods

2.2.1 Bacterial Strains and Culture Media

Three different types of bacteria including *P. aeruginosa* (2 isolates), *K. pneumoniae* (4 isolates) and *S. aureus* (4 isolates) were evaluated in this study. The ten isolates were selected from a large sample of clinical isolates based on their antibiotic susceptibility profiles. The bacterial isolates showing the most resistant profiles were used in this study.

The two clinical isolates of *P. aeruginosa* were collected from The Royal Bolton Hospital and were designated as *P. aeruginosa*-NK1 and *P. aeruginosa*-NK2. The four clinical isolates of *K. pneumoniae* were collected from Leeds Institute of Medical Research and were designated as *K. pneumoniae*-NK1, *K. pneumoniae*-NK2, *K. pneumoniae*-NK3 and *K. pneumoniae*-NK4, and the four clinical isolates of *S. aureus* were collected from The Withington Hospital and were designated as *S. aureus*-SA1, *S. aureus*-SA2, *S. aureus*-SA3 and *S. aureus*-SA4.

Staphylococcus epidermidis (ATCC 35984), *S. epidermidis* (ATCC 12228), *K. pneumoniae* (ATCC 13883) and *S. aureus* (ATCC 25923) (LGC Standards-UK) were used as control strains throughout the assays.

All clinical and control bacterial strains were cultured on tryptone soy agar (TSA) (Oxoid, UK) or tryptone soy broth (TSB) (Oxoid, UK), previously prepared per manufacturer's instructions, and incubated for 24 h at 37°C in aerobic conditions. Identification of bacterial isolates was based on culture, colony morphology, Gram staining and biochemical identification. Typical biochemical tests included catalase, coagulase and mannitol for *S. aureus*, and oxidase and citrate for *K. pneumoniae* and *P. aeruginosa*.

2.2.2 Antibiotic Susceptibility Testing

The antimicrobial susceptibility testing of the three different pathogens investigated in this study was performed according to the European Committee on Antimicrobial Susceptibility Testing (EUCAST) guidelines (EUCAST, 2019). A bacterial suspension of each tested organism was prepared in saline and adjusted to 0.5 McFarland turbidity standard. One

hundred microliters of the bacterial suspension were swabbed in three different directions on Muller-Hinton agar plates (Sigma-Aldrich, UK). Within 15 min of inoculation, antibiotic discs listed below (except for colistin and fosfomycin) were applied to the inoculated agar using aseptic conditions. A maximum of four discs were applied per plate to avoid interference and overlapping of the zones of the different agents. The plates were incubated in an inverted position at 35 °C ± 1 °C for 18 ± 2 h. The zones of inhibition were measured the next day, and interpreted into susceptibility categories according to the EUCAST breakpoints (EUCAST: European Committee on Antimicrobial Susceptibility Testing, 2019).

The antimicrobial susceptibility of the isolates towards colistin was carried out using the broth microdilution method following the EUCAST guidelines in 96-well polystyrene microplates. Dilutions of colistin ranging from 0.12 to 128 mg/L were prepared in separate tubes contacting Mueller-Hinton broth. Fifty microliters of each intermediate concentration and 50 µL of the bacterial suspension adjusted to 5×10^5 CFU/mL were dispensed into the wells. Microplates were incubated in an incubator at 35°C ± 2°C for 16 to 20 h. The minimal inhibitory concentration (MIC) of colistin was recorded as the lowest concentration (mg/L) inhibiting visible growth of the microorganism. The agar dilution method was performed to assess the antimicrobial susceptibility towards fosfomycin. Mueller-Hinton agar plates containing fosfomycin in concentrations ranging from 0.25 mg/L to 1,024 mg/L were prepared. Bacterial inoculum was placed onto the agar plate and allowed to dry. The plates were incubated for 16 to 20 h at 35°C, and the lowest concentration of antimicrobial agent at which complete inhibition of bacteria occurs is the MIC.

Bacterial isolates were classified as multi-drug resistant (MDR) if they showed resistance to multiple (three or more) antimicrobial agents, classes or subclasses of antibiotics (Magiorakos *et al.*, 2012). A complete list of the different antibiotics tested against the three types of bacteria were listed (Table 2.1). All assays were performed in triplicate (n=3). *S. aureus* NCTC 6571 and *Enterococcus faecalis* ATCC 29212 were used as control strains.

Table 2.1 List of all the antibiotics tested against the four bacterial pathogens

P. aeruginosa	Cefepime (30 µg) Ciprofloxacin (5 µg) Colistin Imipenem (10 µg) Piperacillin (100 µg) Tobramycin (10 µg)
K. pneumoniae	Amikacin (30 µg) Amoxicillin/Clavulanic acid (20/10 µg) Ampicillin (10 µg) Aztreonam (30 µg) Cephalotin (30 µg) Cefepime (30 µg) Cefotaxime (30 µg) Cefoxitin (30 µg) Ceftazidime (30 µg) Cefuroxime (30 µg) Cefuroxime Axetil (30 µg) Ciprofloxacin (5 µg) Colistin Ertapenem (10 µg) Gentamicin (10 µg) Meropenem (10 µg) Piperacillin/Tazobactam (100/10 µg) Tigecycline (15 µg) Tobramycin (10 µg) Trimethoprim (1.25 µg)
S. aureus	Cefoxitin (30 µg) Cefuroxime (30 µg) Ciprofloxacin (5 µg) Clindamycin (2 µg) Erythromycin (15 µg) Gentamycin (10 µg) Imipenem (10 µg) Linezolid (30 µg) Methicillin (5 µg) Mupirocin (5 µg and 200 µg) Oxacillin (1 µg) Rifampin (5 µg) Tetracycline (30 µg) trimethoprim-sulfamethoxazole (25 µg)

2.2.3 Test Compounds

The eighteen metal ions evaluated in this study were solutions in hydrochloric acid (HCl) or nitric acid (HNO_3) at a concentration of 1,000 mg/L (Table 2.2). The metal ions evaluated in this study included aluminium, copper, gallium, gold, indium, molybdenum, niobium, palladium, platinum, rhenium, rhodium, ruthenium, silver, tantalum, tin, yttrium, zinc, and zirconium (Table 2.2). The Graphene compounds were kindly provided by the laboratories of Prof Banks at Manchester Metropolitan University. Graphene was mechanically broken down into small particles raging between 200 nm to 1 µm. The particles were re-suspended in water to a final concentration of 500 mg/L. Two types of graphene oxide were assessed in this study. The first type was an aqueous dispersion of single layer graphene oxide (500 mg/L) was purchased from Graphene-Supermarket (USA). The graphene oxide solution had a flake size of 300 nm to 700 nm and a thickness of 1 atomic layer. The second type was graphene oxide particles, generously prepared by Prof Banks laboratories, and suspended in water for a final concentration of 500 mg/L.

Table 2.2 List of the 18 metal ions tested and their respective acid controls.

	Metals		Acid control
Soft metal ions	Copper	Cu	2% HNO_3
	Silver	Ag	2% HNO_3
	Molybdenum	Mo	10% HCl
	Palladium	Pd	5% HCl
	Platinum	Pt	5% HCl
	Gold	Au	5% HCl
Borderline metal ions	Tantalum	Ta	2% HNO_3
	Zinc	Zn	2% HNO_3
	Rhenium	Re	2% HNO_3
	Ruthenium	Ru	5% HCl
	Rhodium	Rh	5% HCl
	Tin	Sn	10% HCl
Hard metal ions	Yttrium	Y	2% HNO_3
	Zirconium	Zr	2% HNO_3
	Niobium	Nb	2% HNO_3
	Aluminium	Al	2% HNO_3
	Indium	In	2% HNO_3
	Gallium	Ga	5% HNO_3

2.2.4 Bacterial Culture Preparation

Using a sterile loop, one bacterial colony was removed from the agar plate and inoculated into tryptone soy broth (TSB). Bacterial culture were grown overnight (18h - 24 h) in a shaker incubator at 37 °C in aerobic conditions. The cultures were centrifuged (Sigma 3-16L, UK) at 1721 g for 10 min. The supernatant was discarded and the pellet was re-suspended in distilled water and vortexed until complete dissolution. The suspension was centrifuged again at 1721 g for 10 min. The water supernatant was dispensed, replaced by 10 mL of fresh TSB and vortexed. The bacterial density was calibrated using a spectrophotometer (Jenway 6305) at 540 nm and diluted in TSB to attain an optical density equivalent to 1.5×10^8 cells/mL.

2.2.5 Minimal Inhibitory Concentration (MIC)

Using a multichannel pipette, 100 µL of fresh TSB were added to all the wells of a 96 well microplate (Thermo Scientific, UK). One hundred microliters of the tested compound (metal ions, graphene or graphene oxide) were added to the first column. After pipetting the components up and down several times to ensure proper mixing, 100 µL was transferred from column 1 to column 2. Again, the solution was mixed thoroughly using a pipette and 100 µL was transferred to column 3. This step was repeated until column 10 where the 10^{th} 100 µL was discarded. Meanwhile, 10 mL of triphenyl tetrazolium chloride (TTC) solution was prepared by mixing 150 mg of TTC into 10 mL of sterile distilled water. The solution was wrapped in aluminium foil and kept on ice ensuring a cold dark environment. Nine millilitres of the previously adjusted bacterial solution (section 2.2.4) was mixed with 1 mL of tetrazolium chloride (0.15 % w/v); and 100 µL of the resulting mixture was added to all the wells of the first 10 columns. Acid controls of hydrochloric acid (%w/v) (5 % and 10 %), nitric acid (2 % and 5 %) were also evaluated. The last two columns served as controls where 100 µL of double strength TSB mixed with 0.15 % TTC and 100 µL of distilled water were added respectively to columns 11 and 12. The microplates were covered with lids and were wrapped with Parafilm® to prevent any evaporation or contamination and were incubated at 37 ºC for 24 h. The MIC

was defined as the lowest concentration of the tested compound that inhibited the bacterial growth and was allocated by the last well showing no change of colour (no blue colour) indicating the lack of viability detection. All MIC assays were performed in triplicate (n=3).

2.2.6 Minimal Bactericidal Concentration (MBC)

Following the MIC readings, the MBC was defined as the lowest concentration of the tested compound that was able to kill the bacteria. The bactericidal effect was determined by plating 20 µL from each of the wells with no visible blue colouration onto TSA plates. Following an overnight incubation at 37 °C for 24 h, the MBC was defined as the lowest concentration (well) showing no bacterial growth on the agar plate. All MBC assays were performed in triplicate (n=3). For the purpose of this study, the correlation between MIC and MBC values and the scope of the antimicrobial activity was designated as follows; very good antimicrobial activity (≤ 30 mg/L), good antimicrobial activity (≥31 mg/L ≤60 mg/L), moderate antimicrobial activity (≥61 mg/L ≤90 mg/L) and no efficacy (≥91 mg/L).

2.2.7 Fractional Inhibitory Concentration Index (FIC)

The interaction between two or more compounds being metal ions or graphene-based composites was estimated by synergy testing using the fractional inhibitory concentration index (FIC). Bacterial cultures were prepared as previously described (section 2.2.4). To determine the MIC of the compounds in combinations, the same microdilution procedure (section 2.2.5) was performed. The compounds tested were added in a 1:1 ratio (50 µL of metal ion, Gr or GO). Synergy is defined as a 4-fold decrease or more in the MIC value of the agents in combination when compared with the same agents tested alone (Saiman, 2007).

The FIC index of two compounds A and B was calculated and interpreted as follows (Jenkins and Schuetz, 2012):

$$\text{FIC of compound A} = \frac{\text{MIC of compound A in combination}}{\text{MIC of compound A alone}}$$

$$\text{FIC of compound B} = \frac{\text{MIC of compound B in combination}}{\text{MIC of compound B alone}}$$

$$\sum\text{FIC} = \text{FIC (A)} + \text{FIC (B)} \qquad [1]$$

Accordingly, a synergistic effect was defined if ∑FIC ≤ 0.5, an additive effect if 0.5 < ∑FIC ≤ 1, an indifferent effect if 1 < ∑FIC < 4 and an antagonistic effect if ∑FIC > 4. The FIC values guidelines were previously reported and published by the American Society of Microbiology to determine the nature of interaction between different agents (Eliopoulos and Eliopoulos, 1988; Botelho, 2000; EUCAST, 2000; Barapatre *et al.*, 2016). All synergy testing carried out in this study were repeated in triplicate (n=3).

2.2.8 Bacterial Biofilm Assessment

2.2.8.1 Crystal Violet Biofilm Assay (CVBA) for Biofilm Forming Ability

The ability of the tested clinical strains to form biofilms was evaluated using the CVBA assay. This assay was first defined by Christensen *et al*. in 1985, and has been developed since then to be suitable for all bacterial biofilms (Christensen *et al.*, 1985; Xu *et al.*, 2016). The evaluation of biofilm formation in this study was conducted according to the method described by Merritt *et al*. in 2015 with some modifications (Meritt *et al.*, 2015). Polished 304 grade stainless steel coupons of 10 mm × 10 mm dimensions were used to assess biofilm formation in this study. The coupons were soaked for 10 min in undiluted acetone, methanol and ethanol, respectively, and were rinsed with sterile water after each step. The coupons were dried at room temperature, and were placed in the centre of the wells of the twelve well culture plates. One millilitre of adjusted bacterial suspension (O.D. 1.0) (section 2.2.4) of each strain was added into the respective wells. The plate was sealed with parafilm and incubated for 7 days at 37 °C under static conditions. Wells supplemented with sterile TSB only served as negative controls. After incubation, the coupons were carefully washed with 1 mL of sterile distilled water to eliminate free planktonic cells, and then air-dried for

2 h at room temperature. The adherent biofilm cells were stained with 0.1 % crystal violet for 30 min at room temperature. The stained coupons were washed three times with sterile distilled water, and dried at room temperature, for 1 h. One millilitre of 33 % glacial acetic acid (Fisher Scientific, UK) in water was added to each well. After 20-30 min, the supernatant mixture of crystal violet/acetic acid solution was mixed, collected and transferred into a cuvette. The absorbance of each sample was measured at a wavelength of 590 nm. The 33 % acetic acid was used to blank the spectrophotometer before reading. All biofilm growth conditions were done in triplicate (n=3), the data was averaged and the standard error was calculated. The adhesion ability of the biofilm of each strain was assessed and classified by calculating the resource unit (Xu *et al.*, 2016).

$$\mathrm{RU} = \frac{\mathrm{OD\ sample}}{\mathrm{OD\ control}} \qquad [2]$$

Accordingly, a strain was classified as a strong biofilm producer if RU>4, a moderate biofilm producer if 2<RU≤4 and a weak biofilm producer if 0<RU≤2. *Staphylococcus epidermidis* ATCC 35984 and *S. epidermidis* ATCC 12228 were used as biofilm positive and negative control strains, respectively.

2.2.8.2 Antibiofilm Potential of Metal Ions and Graphene Composites using CVBA

The antibiofilm activity of metal ions and graphene-based compounds was assessed following the same procedure outlined (section 2.2.8.1). Following the 7 days incubation, the coupons were washed with 1 mL of sterile distilled water to eliminate free planktonic cells, and then air-dried for 2 h at room temperature. One millilitre of the desired compound (metal ions, graphene, graphene oxide, acid controls) 0x (untreated/negative controls), 1x, 2x and 4x MICs to be tested was added into the respective well, while wells supplemented with TSB only served as negative controls. Following an incubation for 18 h - 24 h at 37 °C, the compounds were discarded using a pipette. The coupons were washed with distilled water again to remove non-adherent cells. The adherent biofilm cells were stained with 0.1 % crystal violet for 30 min at room temperature. Subsequently, the stained coupons

were washed three times with sterile distilled water, and dried at room temperature for 1 h. One millilitre of 33 % glacial acetic acid in water was added to each well. After 20 - 30 min, the supernatant mixture of crystal violet/acetic acid solution was mixed, collected and transferred into an optically clear cuvette. The absorbance of each sample was measured at a wavelength of 590 nm. The 33 % acetic acid was used to blank the spectrophotometer before reading. For synergy testing of different compounds of metal ions and graphene-based compounds on biofilm models, 500 µL of each compound were added following the same procedure (2.2.7).

2.2.8.3 XTT Reduction Assay

The XTT reduction assay is as a routine tool used to quantify the viability of bacterial and fungal biofilms because it specifically measures the cell vitality and metabolic activity (da Silva *et al.*, 2008). XTT (2,3-bis (2-methoxy-4-nitro-5-sulfophenyl)-5-[(phenylamino) carbonyl] 2H-tetrazolium hydroxide) is one type of tetrazolium salt that can be reduced by enzymes of the respiratory chain within the cells (mitochondrial dehydrogenases) into formazan (Xu *et al.*, 2016). The reduction of the tetrazolium salt can be traced by a change in colour from pale yellow (XTT) to bright orange (water-soluble formazan). Unlike crystal violet that stains the viable and dead cells equally, the XTT dye stains the viable cells only and depends on cell activity instead of cell mass (da Silva *et al.*, 2008). Prior to performing each assay, fresh XTT solution was prepared by dissolving 4 mg of XTT into 10 mL of sterile pre-warmed (37 °C) phosphate buffer saline (PBS, including 130 mM NaCl, 2.7 mM KCl, 7 mM Na_2HPO_4 and 3 mM $Na_2H_2PO_4$ at pH 7.4), and stored at -20 °C. The XTT-menadione solution was prepared at a 5:1 ratio by adding 1.5 mL of XTT (1 mg/mL) to 300 µL menadione solution (0.4 mM in acetone) supplemented with D-glutamine (50mM). After biofilm formation for 7 days (as previously described in 2.2.7.1), the supernatant of each well was removed and the biofilms were washed gently with sterile water three times. The test compounds (metal ions and graphene composites, or combinations) were added to the appropriate wells at concentrations of 2x

MICs and incubated for 1 h at 37 °C in static conditions. Post-treated biofilms were washed thrice in sterile PBS. After drying, 750 µL of XTT-menadione solution was added to each well and incubated in the dark for 3 h at 37 °C. The supernatant was removed and the absorbance read at 490 nm using a spectrophotometer. Wells with sterile medium and XTT/menadione solution were used as blank controls. To reduce false results due to background interference, the OD values of the blank controls were subtracted from the values of the tested wells. The percentage of reduction in biofilm metabolic activity was calculated using the equation:

$$[(OD_{\text{growth control}} - OD_{\text{sample}})/OD_{\text{growth control}}] \times 100 \qquad [3]$$

Wells without tested samples were considered untreated and served as negative controls. The positive controls were bacterial cells treated with 100 µL of isopropyl alcohol (50 %). The experiments were performed in triplicate per strain.

2.2.9 Scanning Electron Microscopy (SEM)

The bacterial solution was prepared according to section 2.2.4.The bacterial density was calibrated using a spectrophotometer at 600 nm and diluted in sterile distilled water to attain an optical density of an OD of 1.0. One millilitre of the adjusted bacterial solution was mixed with 30 mL of fresh TSB in a sterile universal. One millilitre of 0.5 × MIC of the tested compound (metal ion of graphene-based compound) was added to the solution. The whole mixture was incubated at 37 °C for 18 h. Following incubation, 5 mL was transferred into a new sterile universal and centrifuged at 1721 g for 10 min. The supernatant was carefully discarded, and 100 µL of sterile distilled water was added to the bacterial pellet and vortexed to obtain a homogenous mixture. Twenty microliters from each sample of the resulting suspension was taken and pipetted onto individual silicon wafers (previously cut into 1 mm × 1 mm dimensions using diamond scribes). This was followed by the fixation step where the samples were soaked overnight in 4 % glutaraldehyde in phosphate buffer saline (PBS) at 4 °C. The wafers were washed three times with PBS buffer and one time with sterile distilled water, then dehydrated by an ethanol gradient of 30 % absolute ethanol for 10 min,

50 % absolute ethanol for 10 min, 70 % absolute ethanol for 10 min, 90 % absolute ethanol for 10 min, and 100 % absolute ethanol for 30 min. After drying the samples, they were mounted on SEM stubs and were sputter-coated with gold/palladium (10 nm) alloys for clear observation and future preservation in a vacuum-assisted desiccator (Sigma-Aldrich, UK). SEM images were captured using the SmartSEM software (Carl Zeiss Ltd, Germany) and the Supra 40VP scanning electron microscope (Zeiss, Germany).

2.2.10 Cell Cytotoxicity Testing

2.2.10.1 Culture Media (RPMI-1640) Preparation

The foetal bovine serum (FBS) (Lonza, UK) was incubated in a water bath at 56 °C for 30 min to ensure a proper heat inactivation of complement. Afterwards, the Rosewell Park Memorial Institute (RPMI-1640) (L-Glutamine, 25 mM HEPES) medium was mixed with 10 % foetal bovine serum (FBS), and 2 % penicillin-streptomycin under aseptic conditions. The new supplemented medium was denoted as RPMI-1640 complete medium and was kept at 4 °C until needed.

2.2.10.2 Cell Culture

Human skin fibroblasts WS-1 (ATCC PCS-201-012) were purchased from ATCC, USA. The cells were cultured aseptically using RPMI-1640 complete medium (Sigma-Aldrich, UK) and were incubated at 37 °C and 5 % CO_2. The cells were centrifuged and re-suspended in fresh medium every 2-3 days.

2.2.10.3 Assessment of Cell Viability

The cell viability assay was performed to determine the effect of the tested metal ions and graphene-based compounds on cell proliferation and cytotoxicity using Trypan blue solution (0.4 %). This dye determined the cell viability based on the dye exclusion test, since the dye will be exclusively taken up by dead cells but will not affect the viable cells having an intact membrane. Hence, the non-viable cells were stained dark blue while viable

cells stayed colourless. WS1 cells were first harvested by removing the media and adding 3 mL of trypsin to detach the adherent cells. Three millilitres of fresh media pre-warmed to 37 °C were added to neutralize the trypsin effect, and the whole volume was transferred into a 15 mL centrifuge tube. Cells were collected by centrifugation for 5 min at 1200 rpm. After dispensing the supernatant, the pellet was re-suspended in fresh media. Twenty microliters of the cell suspension were diluted with an equal volume of trypan blue, and 10 µL of the resulting solution was loaded into a haemocytometer where cells were counted using a TC10 automated cell counter (Bio-Rad, USA). Following the readings, the cells were adjusted to a concentration of 2×10^6 cells/mL. The viability of the cells was maintained above 80% for the following experiments.

2.2.10.4 Assessment of Cell Proliferation (MTS assay)

Following manufacturer's instructions, MTS assays were carried out by adding 100 µL of previously adjusted fibroblast cells into all the wells of the 96 well plate. This was followed by adding 100 µL of each tested compound into three respective wells. Negative control wells included 100 µL of cells and 100 µL of media, while the positive controls wells included 100 µL of cells and 100 µL of ethanol. The plate was incubated at 37 °C and 5 % CO_2 for 24 h. Following incubation, the supernatant was discarded and all the wells were re-suspended in 100 µL of fresh media, followed by 20 µL of CellTitre 96 Aqueous MTS Reagent solution. The plate was incubated again for 4 h at 37 °C and 5 % CO_2 in the dark. The absorbance was measured at 490 nm every single hour using a Synergy HT microplate reader (Vermont, USA). The viability assay of each sample tested was replicated three times (n=3).

2.2.11 Statistical Analysis

Statistical analysis in this study was performed using IBM SPSS Statistics Software (version 25). The one-way analysis of variance test (ANOVA) with Tukey Kramer Multiple Comparison Test was performed to assess the significance level of the different treatments. The distribution of the data from

mean values of antimicrobial efficacies was analysed using standard deviation and error with 95 % confidence intervals.

Chapter 3 Antimicrobial Activity of Metal Ions and Graphene-Based compounds against ESKAPE Pathogens

3.1 Introduction

As the efficiency of antibiotics is compromised by increasing trends of AMR, efforts must be shifted towards finding alternative therapies for treating resistant bacterial infections. Metal ions have a long empirical history of medical use as first line antimicrobials, biocides and chemotherapeutics. For instance, silver, mercury, and copper have been used to treat burns, to cure from syphilis and to control bacterial and fungal diseases (Mittapally *et al.*, 2018). However, recently, there has been an explosion in the development of metal-based nano-antimicrobials (Turner, 2017). Due to their unique properties, the metallic-based nano-structured materials have created a new interesting field in all sciences for continuous investigations (Dastjerdi and Montazer, 2010).

Additionally, graphene-based materials have shown low bacterial resistance and cytotoxic effect on mammalian cells, hence, they have emerged as novel antibacterials with a broad-spectrum activity (Ji *et al.*, 2016). These carbon-based applications have contributed to the expansion of new practical productions in biotechnology, biomedicine and even drug delivery (Li *et al.*, 2014).

This study provides an introduction to promising approaches of using metal ions and graphene-based compounds in clinical settings, and to contribute towards developing antimicrobials that might improve the management of resistant bacteria. For this, the antimicrobial efficacy of yttrium, zirconium, niobium, silver, tantalum, indium, copper, zinc, rhenium, gallium, ruthenium, rhodium, platinum, gold, palladium, molybdenum, tin, graphene and graphene oxide was assessed in this study.

3.2 Aim

To investigate the antimicrobial efficacy of eighteen single metal ion solutions, graphene and graphene oxide, individually and in combination, against clinical isolates of *P. aeruginosa*, *K. pneumoniae* and *S. aureus* in their planktonic and biofilm forms.

3.3 Methods

The antimicrobial activity of the tested compounds (metal ions and graphene-based compounds) against each bacterium was evaluated using the minimal inhibitory concentration (section 2.2.5) and the minimal bactericidal concentration (section 2.2.6).

The synergy testing between metal ion solutions and graphene or graphene oxide was assessed by calculating the fractional inhibitory concentration (section 2.2.7).

The effect of the tested compound on the biofilm forms of each bacterium and their metabolic activity was evaluated using crystal violet biofilm assay (section 2.2.8.2) and XTT assay (section 2.2.8.3).

3.4 Results

3.4.1 Antibiotic Susceptibility Testing

The antibiotic resistance patterns for the ten tested bacterial strains were determined. Organisms were classified accordingly into susceptible, intermediate and resistant, where “susceptible” (S) denoted that the organism was inhibited *in-vitro* by the designated concentration of the antibiotic (high probability of therapeutic success). “Intermediate” (I) signified that the organism was inhibited *in-vitro* but the actual therapeutic effect will be uncertain, whilst “resistant” (R) (highlighted in blue) means that this concentration of the drug was highly associated with therapeutic failure (Rodloff *et al.*, 2008).

3.4.1.1 *P. aeruginosa*

The two *P. aeruginosa* isolates displayed different antibiotic susceptibility patterns. *P. aeruginosa*-NK1 was found to be susceptible to cefepime, colistin, tobramycin, and resistant to piperacillin, imipenem and ciprofloxacin. The *P. aeruginosa*-NK2 isolate was susceptible to colistin, piperacillin and tobramycin, intermediate to imipenem and resistant to cefepime and ciprofloxacin(Table 3.1).

Table 3.1 Phenotypic antimicrobial resistance pattern of *P. aeruginosa* isolates.

	***P. aeruginosa*-NK1**	***P. aeruginosa*-NK2**
Ciprofloxacin	R	R
Piperacillin	R	S
Imipenem	R	I
Cefepime	S	R
Tobramycin	S	S
Colistin	S	S

S = susceptible, R = resistant (highlighted in blue) and I = intermediate.

3.4.1.2 *K. pneumoniae*

All *K. pneumoniae* isolates were resistant to ampicillin. *K. pneumoniae*-NK1 also showed resistance to amoxicillin/clavulanic acid, aztreonam, piperacillin-tazobactam, cefalotin, amikacin and trimethoprim. *K. pneumoniae*-NK2 was resistant to ampicillin, cefotaxime and ertapenem, whilst the *K. pneumoniae*-NK3 strain was resistant to ampicillin, cefuroxime-axetil, tigecyclines. *K. pneumoniae*-NK4 was resistant to ampicillin, ciprofloxacin and tigecyclines. The four isolates exhibited an intermediate susceptibility towards aztreonam and ceftazidime. *K. pneumoniae*-NK1, -NK2 and -NK3 were intermediate to ciprofloxacin and *K. pneumoniae*-NK1, -NK3 and –NK4 were intermediate to cefotaxime. *K. pneumoniae*-NK2 also showed an intermediate susceptibility to five other agents (amoxicillin, aztreonam, ceftazidime, cefalotin and piperacillin) (Table 3.2).

Table 3.2 Phenotypic antimicrobial resistance pattern of *K. pneumoniae* isolates.

	***K. pneumoniae*-NK1**	***K. pneumoniae*-NK2**	***K. pneumoniae*-NK3**	***K. pneumoniae*-NK4**
Ampicillin	R	R	R	R
Amoxicillin/ Clavulanic acid	R	I	S	S
Aztreonam	R	I	I	I
Cefotaxime	I	R	I	I
Piperacillin/ Tazobactam	R	I	S	S
Amikacin	R	S	S	S
Gentamicin	S	S	S	S
Tobramycin	S	S	S	S
Ceftazidime	I	I	I	I
Cefalotin	R	I	S	S
Cefuroxime	S	S	S	S
Cefuroxime Axetil	S	S	R	S
Cefepime	S	S	S	S
Cefoxitin	S	S	S	S
Ertapenem	S	R	S	S
Meropenem	S	S	S	S
Ciprofloxacin	I	I	I	R
Colistin	S	S	S	S
Tigecylcine	S	S	R	R
Trimethoprim	R	S	S	S

S = susceptible, R = resistant (highlighted in blue) and I = intermediate.

3.4.1.3 *S. aureus*

While the four *S. aureus* isolates investigated in this study exhibited different susceptibility patterns, all of them were Methicillin resistant *S. aureus* (MRSA). The four isolates showed resistance to ampicillin, methicillin and cefuroxime. *S. aureus*-SA1 exhibited resistance towards cefoxitin, clindamycin, erythromycin, oxacillin, gentamicin, and imipenem, whilst remaining susceptible to ciprofloxacin, linezolid, tetracycline and trimethoprim-sulfamethoxazole (Table 3.3). *S. aureus*-SA2 showed resistance to 10 out of the 14 tested antibiotics, and it was only susceptible to trimethoprim-sulfamethoxazole and gentamicin, and intermediate to clindamycin. *S. aureus*-SA3 exhibited a profile relatively comparable to *S. aureus*-SA1, but it was susceptible to oxacillin, gentamicin, and resistant to trimethoprim-sulfamethoxazole. *S. aureus*-SA4 showed the least resistance among the four isolates. It was found to be resistant to ampicillin, methicillin, oxacillin, ciprofloxacin and cefuroxime, while being intermediate to cefoxitin and imipenem.

Table 3.3 Phenotypic antimicrobial resistance pattern of *S. aureus* isolates.

	***S. aureus*-SA1**	***S. aureus*-SA2**	***S. aureus*-SA3**	***S. aureus*-SA4**
Ampicillin	R	R	R	R
Methicillin	R	R	R	R
Oxacillin	R	R	S	R
Cefuroxime	R	R	R	R
Cefoxitin	R	R	R	I
Erythromycin	R	R	R	S
Imipenem	R	R	R	I
Ciprofloxacin	S	R	S	R
Clindamycin	R	I	R	S
Gentamicin	R	S	S	S
Rifampin	S	R	S	S
Tetracycline	S	R	S	S
Trimethoprim/ sulfamethoxazole	S	S	R	S
Linezolid	S	S	S	S

S = susceptible, R = resistant (highlighted in blue) and I = intermediate.

Since all bacterial strains were shown to be resistant to three or more agents belonging to different classes or subclasses of antibiotics, they were designated as MDR strains.

3.4.2 Antimicrobial Activity of Single Metal Ions, Graphene and Graphene Oxide Against *P. aeruginosa*, *K. pneumoniae* And *S. aureus*

MIC and MBC assays were performed to assess the antibacterial activity of eighteen metal ions and graphene-based compounds towards *P. aeruginosa*, *K. pneumoniae* and *S. aureus*. Lower MIC and MBC values are associated with higher antimicrobial activity. The MIC and MBC results were grouped, for the purpose of this study, according to their antimicrobial efficacies as very good (≤ 30 mg/L), good (≥31 mg/L ≤60 mg/L), moderate (≥61 mg/L ≤90 mg/L) and no efficacy (≥91 mg/L). Molar concentrations of each compound were also calculated and compared to their mass concentrations. When comparing mass to molar concentrations for the compounds, no discrepancy was found in the classification of metal ions according to their antimicrobial efficacy. The compounds showing a “very good” antimicrobial effect (MIC≤30 mg/L or ≤0.2 mM) were highlighted in yellow. Since the molecular weight of graphene or GO is not clearly defined and depends mainly on the average size of the sheets, the average number of C atoms and their degree of oxidation, the concentrations of graphene composites could not be expressed in mM.

3.4.2.1 Minimal Inhibitory Concentrations

3.4.2.1.1 *P. aeruginosa*

Five out of the eighteen metal ions tested showed a very good inhibitory antimicrobial activity against the two bacterial strains (Table 3.4.). Pt (7.8 mg/L – 0.04 mM), Pd and Sn (13.0 mg/L – 0.11 mM) ions demonstrated the best inhibitory antimicrobial activity against both *P. aeruginosa* isolates followed by the Mo (15.6 mg/L – 0.16 mM) and Au (26.0 mg/L – 0.13 mM) ions. The metal ions that showed good antimicrobial efficacy included Re and Ga (31.3 mg/L), Rh (41.7- 52.1 mg/L), Al (41.7 mg/L), and Ru (52.1

mg/L). Y (62.5 mg/L), Ta (62.5 mg/L), In (62.5 mg/L), Zn (62.5 mg/L), Zr (83.3 mg/L) and Nb (83.3 mg/L) demonstrated moderate antimicrobial inhibitory effects, while no antimicrobial efficacy was demonstrated for Ag (104 mg/L) or Cu ions (125 mg/L) against the bacterial isolates. Graphene (125 mg/L) and GO (> 500 mg/L) showed no antimicrobial activity. Among the 18 tested metal ions, only rhodium exhibited different MIC values against the two different *P. aeruginosa* isolates.

Table 3.4 MIC (mg/L) ± SE and molar concentrations (mM) of the metal ions, graphene and graphene oxide against the tested *P. aeruginosa* isolates.

	MIC (mg/L)		Molar concentration (mM)	
Metal / Compound	***P. aeruginosa*-NK1**	***P. aeruginosa*-NK2**	***P. aeruginosa*-NK1**	***P. aeruginosa*-NK2**
Cu	125.0 ± 0.00	125.0 ± 0.00	1.967	1.967
Ag	104 ± 20.8	104 ± 20.8	0.964	0.964
Pd	13.0 ± 2.60	13.0 ± 2.60	0.122	0.122
Mo	15.6 ± 0.00	15.6 ± 0.00	0.163	0.163
Pt	7.8 ± 0.00	7.8 ± 0.00	0.040	0.040
Au	26.0 ± 5.20	26.0 ± 5.20	0.132	0.132
Ta	62.5 ± 0.00	62.5 ± 0.00	0.363	0.363
Zn	62.5 ± 0.00	62.5 ± 0.00	0.956	0.956
Re	31.3 ± 0.00	31.3 ± 0.00	0.167	0.167
Ru	52.1 ± 10.4	52.1 ± 10.4	0.515	0.515
Rh	41.7 ± 10.4	52.1 ± 10.4	0.405	0.405
Sn	13.0 ± 2.60	13.0 ± 2.60	0.110	0.110
Y	62.5 ± 0.00	62.5 ± 0.00	0.728	0.728
Zr	83.3 ± 20.8	83.3 ± 20.8	0.916	0.916
Nb	83.3 ± 20.8	83.3 ± 20.8	0.897	0.897
Al	41.7 ± 10.4	41.7 ± 10.4	1.545	1.545
In	62.5 ± 0.00	62.5 ± 0.00	0.544	0.544
Ga	31.3 ± 0.00	31.3 ± 0.00	0.441	0.441
2% HNO_3	1250 ± 0.00	1250 ± 0.00	20.15	20.15
5% HNO_3	2343 ± 0.00	2343 ± 0.00	37.10	37.10
5% HCl	2343 ± 0.00	2343 ± 0.00	64.26	64.26
10% HCl	3125 ± 0.00	3125 ± 0.00	85.71	85.71
Graphene	125 ± 0.00	125 ± 0.00	---	---
Graphene oxide	>500	>500	---	---

3.4.2.1.2 *K. pneumoniae*

The best antimicrobial activity against the four isolates was exhibited by Au (6.5 - 7.8 mg/L) (0.033-0.039 mM), Ga (6.5 - 7.8 mg/L) (0.091-0.109 mM), Mo (7.8-13.02 mg/L) (0.081-0.135 mM), Sn (7.8-13.02 mg/L) (0.109 mM), Pt (13.02-15.63 mg/L) (0.066-0.08 Mm), Pd (13.02- 20.83 mg/L) (0.122-0.195 Mm) and In (26.04 mg/L) (0.226 mM) (Table 3.5). The six metal ions displayed similar or comparable efficacies against the four distinct isolates. Silver, however, exerted different antimicrobial efficacies against *K. pneumoniae*-NK1 (104.17 mg/L – 0.965 mM) compared to *K. pneumoniae*-NK2, -NK3 and –NK4 (15.63 mg/L – 0.144 mM). A good antimicrobial activity was revealed by Ru, Rh, Ta (31.25-41.67 mg/L), Y and Re (41.67-52.08 mg/L). The same antimicrobial activity pattern was exerted by the five metal ions against the four isolates. Zr, Nb, Al and Zn (>91 mg/L) showed no antimicrobial activity against any of the four isolates. No antimicrobial effect was recorded for GO against the four isolates while graphene (26 mg/L) showed the same good activity against the four isolates.

Table 3.5 MIC values (mg/L) ± SE of the metal ions, graphene and graphene oxide against the tested *K. pneumoniae* isolates.

	MIC (mg/L)			
Metal / Compound	***K. pneumoniae* -NK1**	***K. pneumoniae* -NK2**	***K. pneumoniae* -NK3**	***K. pneumoniae* -NK4**
Cu	125.00 ± 00.00	125.00 ± 00.00	125.00 ± 00.00	125.00 ± 00.00
Ag	104.17 ± 20.83	15.63 ± 0.00	15.63 ± 0.00	15.63 ± 0.00
Pd	20.83 ± 5.21	15.63 ± 0.00	13.02 ± 2.61	20.83 ± 5.21
Mo	13.02 ± 2.61	7.80 ± 0.00	13.02 ± 2.61	7.80 ± 0.00
Pt	15.62 ± 0.00	13.02 ± 2.61	15.62 ± 0.00	13.02 ± 2.61
Au	7.80 ± 0.00	6.50 ± 1.30	6.50 ± 0.00	7.80 ± 1.30
Ta	31.25 ± 0.00	41.67 ± 10.42	41.67 ± 10.42	41.67 ± 10.42
Zn	125.00 ± 62.50	104.17 ± 20.83	125.00 ± 62.50	104.17 ± 20.83
Re	52.08 ± 10.42	52.08 ± 10.42	41.67 ± 10.42	52.08 ± 10.42
Ru	41.67 ± 10.42	31.25 ± 0.00	41.67 ± 10.42	41.67 ± 10.42
Rh	41.67 ± 10.42	41.67 ± 10.42	41.67 ± 10.42	31.25 ± 0.00
Sn	13.02 ± 2.61	13.02 ± 2.61	13.02 ± 2.61	7.80 ± 0.00
Y	41.67 ± 10.42	52.08 ± 10.42	41.67 ± 10.42	41.67 ± 10.42
Zr	93.75 ± 31.25	93.75 ± 31.25	104.17 ± 20.83	93.75 ± 31.25
Nb	104.17 ± 20.83	104.17 ± 20.83	104.17 ± 20.83	104.17 ± 20.83
Al	125.00 ± 62.50	104.17 ± 20.83	125.00 ± 62.50	104.17 ± 20.83
In	26.04 ± 5.21	26.04 ± 5.21	26.04 ± 5.21	26.04 ± 5.21
Ga	7.80 ± 0.00	7.80 ± 0.00	7.80 ± 0.00	6.50 ± 1.30
HNO_3 (2 %)	1250 ± 0.00	1250 ± 0.00	1250 ± 0.00	1250 ± 0.00
HNO_3 (5 %)	2343 ± 0.00	2343 ± 0.00	2343 ± 0.00	2343 ± 0.00
HCl (5 %)	2343 ± 0.00	2343 ± 0.00	2343 ± 0.00	2343 ± 0.00
HCl (10 %)	3125 ± 0.00	3125 ± 0.00	3125 ± 0.00	3125 ± 0.00
Graphene	26.00 ± 5.21	26.00 ± 5.21	26.00 ± 5.21	26.00 ± 5.21
Graphene oxide	>500	>500	>500	>500

Table 3.6 Molar inhibitory concentrations (mM) of the metal ions, graphene and graphene oxide against the tested *K. pneumoniae* isolates.

	Molar inhibitory concentration (mM)			
Metal / Compound	***K. pneumoniae* -NK1**	***K. pneumoniae* -NK2**	***K. pneumoniae* -NK3**	***K. pneumoniae* -NK4**
Cu	1.967	1.967	1.967	1.967
Ag	0.965	0.144	0.144	0.144
Pd	0.195	0.146	0.122	0.195
Mo	0.135	0.081	0.135	0.081
Pt	0.080	0.066	0.080	0.066
Au	0.039	0.033	0.033	0.039
Ta	0.181	0.242	0.242	0.242
Zn	1.911	1.593	1.911	1.593
Re	0.278	0.278	0.222	0.278
Ru	0.412	0.309	0.412	0.412
Rh	0.404	0.404	0.404	0.303
Sn	0.109	0.109	0.109	0.065
Y	0.485	0.606	0.485	0.485
Zr	1.031	1.031	1.146	1.031
Nb	1.121	1.121	1.121	1.121
Al	4.632	3.860	4.632	3.860
In	0.226	0.226	0.226	0.226
Ga	0.109	0.109	0.109	0.091
HNO_3 (2 %)	20.15	20.15	20.15	20.15
HNO_3 (5 %)	37.18	37.18	37.18	37.18
HCl (5 %)	64.26	64.26	64.26	64.26
HCl (10 %)	85.71	85.71	85.71	85.71

3.4.2.1.3 *S. aureus*

The best antimicrobial efficacy against the four *S. aureus* isolates was revealed by Pt at 0.49 mg/L (0.003 Mm), followed by Au (10.42 mg/L - 0.053 Mm), Sn (15.62 mg/L – 0.132 Mm), Ga (10.42 mg/L – 0.147 mM), Mo (15.62 mg/L – 0.163 Mm), and Pd (20.83 mg/L – 0.196 Mm)). Rh exhibited a good antimicrobial efficacy (31.25 mg/L), while Ru, Re 62.5 mg/L) and Cu (83.33 mg/L) exhibited a moderate effect. Y, Zr, Nb, Ta, In, and Al demonstrated no antimicrobial effect with MIC exceeding 91 mg/L (Table 3.7). Silver was the only metal ion displaying different activity against the four distinct isolates, where it inhibited *S. aureus*-SA2, -SA3 and –SA4 at 10.74 mg/L but had no effect against *S. aureus*-SA1. GO did not show any activity against *S. aureus* isolates in contrast to graphene that inhibited the four isolates at 20 mg/L.

Table 3.7 MIC values (mg/L) ± SE of the metal ions, graphene and graphene oxide against the tested *S. aureus* isolates.

MIC (mg/L)				
Metal / Compound	***S. aureus* -SA1**	***S. aureus* -SA2**	***S. aureus* -SA3**	***S. aureus* -SA4**
Cu	83.33 ± 0.00	83.33 ± 0.00	83.33 ± 0.00	83.33 ± 0.00
Ag	104.17 ± 20.83	10.74 ± 2.61	10.74 ± 2.61	10.74 ± 2.61
Pd	20.83 ± 5.21	20.83 ± 5.21	20.83 ± 5.21	20.83 ± 5.21
Mo	15.62 ± 0.00	15.62 ± 0.00	15.62 ± 0.00	15.62 ± 0.00
Pt	0.49 ± 0.00	0.49 ± 0.00	0.49 ± 0.00	0.49 ± 0.00
Au	10.42 ± 2.61	10.42 ± 2.61	10.42 ± 2.61	10.42 ± 2.61
Ta	125.00 ± 0.00	125.00 ± 0.00	125.00 ± 0.00	125.00 ± 0.00
Zn	104.17 ± 20.83	104.17 ± 20.83	104.17 ± 20.83	104.17 ± 20.83
Re	62.50 ± 0.00	62.50 ± 0.00	62.50 ± 0.00	62.50 ± 0.00
Ru	62.50 ± 0.00	62.50 ± 0.00	62.50 ± 0.00	62.50 ± 0.00
Rh	31.25 ± 0.00	31.25 ± 0.00	31.25 ± 0.00	31.25 ± 0.00
Sn	15.62 ± 0.00	15.62 ± 0.00	15.62 ± 0.00	15.62 ± 0.00
Y	166.67 ± 41.67	166.67 ± 41.67	166.67 ± 41.67	166.67 ± 41.67
Zr	104.17 ± 20.83	104.17 ± 20.83	104.17 ± 20.83	104.17 ± 20.83
Nb	125.00 ± 0.00	125.00 ± 0.00	125.00 ± 0.00	125.00 ± 0.00
Al	333.33 ± 83.33	250.00 ± 0.00	250.00 ± 0.00	250.00 ± 0.00
In	104.17 ± 20.83	104.17 ± 20.83	104.17 ± 20.83	104.17 ± 20.83
Ga	10.42 ± 2.61	10.42 ± 2.61	10.42 ± 2.61	10.42 ± 2.61
HNO_3 (2 %)	625 ± 6.00	625 ± 0.00	625 ± 0.00	625 ± 0.00
HNO_3 (5 %)	1562 ± 0.00	1562 ± 0.00	1562 ± 0.00	1562 ± 0.00
HCl (5 %)	3125 ± 0.00	3125 ± 1.20	3125 ± 1.20	3125 ± 0.00
HCl (10 %)	3125 ± 0.00	3125 ± 0.00	3125 ± 0.00	3125 ± 0.00
Graphene	20.80 ± 6.70	20.80 ± 6.70	20.80 ± 6.70	20.80 ± 6.70
Graphene oxide	>500	>500	>500	>500

Table 3.8 Molar inhibitory concentrations (mM) of the metal ions, graphene and graphene oxide against the tested *S. aureus* isolates.

Molar inhibitory concentration (mM)				
Metal / Compound	***S. aureus* -SA1**	***S. aureus* -SA2**	***S. aureus* -SA3**	***S. aureus* -SA4**
Cu	1.311	1.311	1.311	1.311
Ag	0.965	0.100	0.100	0.100
Pd	0.196	0.196	0.196	0.196
Mo	0.163	0.163	0.163	0.163
Pt	0.003	0.003	0.003	0.003
Au	0.053	0.053	0.053	0.053
Ta	0.727	0.727	0.727	0.727
Zn	1.593	1.593	1.593	1.593
Re	0.334	0.334	0.334	0.334
Ru	0.618	0.618	0.618	0.618
Rh	0.304	0.304	0.304	0.304
Sn	0.132	0.132	0.132	0.132
Y	1.940	1.940	1.940	1.940
Zr	1.146	1.146	1.146	1.146
Nb	1.346	1.346	1.346	1.346
Al	12.354	9.265	9.265	9.265
In	0.907	0.907	0.907	0.907
Ga	0.147	0.147	0.147	0.147
HNO_3 (2 %)	9.9	9.9	9.9	9.9
HNO_3 (5 %)	24.78	24.78	24.78	24.78
HCl (5 %)	85.70	85.70	85.70	85.70
HCl (10 %)	85.70	85.70	85.70	85.70

3.4.2.2 Minimal Bactericidal Concentration

3.4.2.2.1 *P. aeruginosa*

Pt (7.8 mg/L – 0.04 mM), Sn (13.0 mg/L – 0.110 mM) and Re (31 mg/L – 0.167 mM) demonstrated a very good bactericidal activity against the bacterial strains, whilst Re and Mo (31.1 mg/L – 0.326 mM), Au (41.7 mg/L – 0.212 mM) and Pd (41.7 mg/L – 0.392 mM) showed a good bactericidal activity (Table 3.9). A moderate antimicrobial activity was exhibited by Ru, Rh (62.5 mg/L), Ta and Ga (83.3 mg/L). Y, Ag, Zn (125 mg/L), Zr (333 mg/L), Cu (125 mg/L against *P. aeruginosa* NK-1 and 250 mg/L against *P. aeruginosa* NK-2) and Nb (333 mg/L against *P. aeruginosa* NK-1 and 250 mg/L against *P. aeruginosa* NK-2) showed no antimicrobial effect. The MBCs of GO (> 500 mg/L), and graphene (250 mg/L) also indicated no bactericidal activity. Despite the differences shown in their antibiotic profiles, both *P. aeruginosa* strains exhibited the same MBC values for graphene, graphene oxide and each metal ion with the exception of Nb and Cu.

Table 3.9 MBC values (mg/L) ± SE and molar concentration (mM) of the metal ions, graphene and graphene oxide against the tested *P. aeruginosa* isolates.

	MBC (mg/L)		Molar concentration (mM)	
Metal / Compound	***P. aeruginosa*-NK1**	***P. aeruginosa*-NK2**	***P. aeruginosa*-NK1**	***P. aeruginosa*-NK2**
Cu	125.00 ± 0.00	250.00 ± 0.00	1.967	1.967
Ag	125.00 ± 0.00	125.00 ± 0.00	1.159	1.159
Pd	41.70 ± 10.4	41.70 ± 10.4	0.392	0.392
Mo	31.30 ± 0.00	31.30 ± 0.00	0.326	0.326
Pt	7.81 ± 0.00	7.81 ± 0.00	0.040	0.040
Au	41.70 ± 10.4	41.70 ± 10.4	0.212	0.212
Ta	83.33 ± 20.8	83.33 ± 20.8	0.485	0.485
Zn	125.00 ± 0.00	125.00 ± 0.00	1.912	1.912
Re	31.30 ± 0.00	31.30 ± 0.00	0.167	0.167
Ru	62.5 ± 0.00	62.5 ± 0.00	0.618	0.618
Rh	62.5 ± 0.00	62.5 ± 0.00	0.607	0.607
Sn	13.00 ± 2.60	13.00 ± 2.60	0.110	0.110
Y	125.00 ± 0.00	125.00 ± 0.00	1.406	1.406
Zr	333.33 ± 83.3	333 .33 ± 83.3	3.708	3.708
Nb	333.33 ± 83.3	250.00 ± 0.00	3.588	3.588
Al	41.70 ± 10.4	41.70 ± 10.4	1.546	1.546
In	125.00 ± 0.00	125.00 ± 0.00	1.089	1.089
Ga	83.30 ± 20.8	83.30 ± 20.8	1.175	1.175
HNO_3 (2 %)	1250 ± 0.00	1250 ± 0.00	20.15	20.15
HNO_3 (5 %)	2343 ± 0.00	2343 ± 0.00	37.10	37.10
HCl (5 %)	2343 ± 0.00	2343 ± 0.00	64.26	64.26
HCl (10 %)	3125 ± 0.00	3125 ± 0.00	85.71	85.71
Graphene	125 ± 0.00	125.00 ± 0.00	---	---
Graphene oxide	>500	>500	---	---

3.4.2.2.2 *K. pneumoniae*

The same metal ions (excluding indium) that exhibited the best inhibitory effect against the *K. pneumoniae* isolates also showed the best bactericidal effect against the same isolates. The best bactericidal activity was displayed by Au (10.41 mg/L – 0.053 mM), Pt (15.62 mg/L – 0.08 mM), Ga (10.41 mg/L – 0.147 mM), Sn (15.63 mg/L – 0.132 mM), Pd (20.83 mg/L – 0.196 mM) and Mo (20.83 mg/L - 0.210 mM). In (52.08 mg/L) showed a good bactericidal effect while Ta (62.4 mg/L), Re (62.5-83.3 mg/L), Rh and Ru (83.33 mg/L) showed a moderate effect. No bactericidal activity was noted against any of the *K. pneumoniae* isolates when treated with Y, Zr, Nb, Al, Cu or Zn (Table 3.10). Graphene demonstrated an inhibitory and bactericidal effect against *K. pneumoniae* isolates at 26 mg/L. GO showed no effect (>500 mg/L).

Table 3.10 MBC values (mg/L) ± SE of the metal ions, graphene and graphene oxide against the tested *K. pneumoniae* isolates.

	MBC (mg/L)			
Metal / Compound	***K. pneumoniae* -NK1**	***K. pneumoniae* -NK2**	***K. pneumoniae* -NK3**	***K. pneumoniae* -NK4**
Cu	125.00 ± 0.00	125.00 ± 0.00	125.00 ± 0.00	125.00 ± 0.00
Ag	125.00 ± 0.00	31.25 ± 0.00	31.25 ± 0.00	31.25 ± 0.00
Pd	20.83 ± 5.21	20.83 ± 5.21	20.83 ± 5.21	20.83 ± 5.21
Mo	20.83 ± 5.21	20.83 ± 5.21	20.83 ± 5.21	20.83 ± 5.21
Pt	15.62 ± 0.00	15.62 ± 0.00	15.62 ± 0.00	15.62 ± 0.00
Au	10.41 ± 2.61	10.41 ± 2.61	10.41 ± 2.61	10.41 ± 2.61
Ta	62.50 ± 0.00	62.50 ± 0.00	62.50 ± 0.00	62.50 ± 0.00
Zn	125.00 ± 0.00	125.00 ± 0.00	125.00 ± 0.00	166.67 ± 41.67
Re	62.50 ± 0.00	62.50 ± 0.00	62.50 ± 0.00	62.50 ± 0.00
Ru	83.33 ± 20.83	83.33 ± 20.83	83.33 ± 20.83	83.33 ± 20.83
Rh	83.33 ± 20.83	83.33 ± 20.83	83.33 ± 20.83	83.33 ± 20.83
Sn	15.63 ± 0.00	15.63 ± 0.00	15.63 ± 0.00	15.63 ± 0.00
Y	125.00 ± 0.00	125.00 ± 0.00	104.17 ± 20.83	125.00 ± 0.00
Zr	104.17 ± 20.83	104.17 ± 20.83	104.17 ± 20.83	104.17 ± 20.83
Nb	125.00 ± 0.00	104.17 ± 20.83	104.17 ± 20.83	104.17 ± 20.83
Al	208.33 ± 41.67	125.00 ± 0.00	104.17 ± 20.83	125.00 ± 0.00
In	52.08 ± 10.42	52.08 ± 10.42	52.08 ± 10.42	52.08 ± 10.42
Ga	10.41 ± 2.60	10.41 ± 2.60	10.41 ± 2.60	10.41 ± 2.60
HNO_3 (2 %)	1250 ± 0.00	1250 ± 0.00	1250 ± 0.00	1250 ± 0.00
HNO_3 (5 %)	2343 ± 0.00	2343 ± 0.00	2343 ± 0.00	2343 ± 0.00
HCl (5 %)	2343 ± 0.00	2343 ± 0.00	2343 ± 0.00	2343 ± 0.00
HCl (10 %)	3125 ± 0.00	3125 ± 0.00	3125 ± 0.00	3125 ± 0.00
Graphene	26.00 ± 5.21	26.00 ± 5.21	26.00 ± 5.21	26.00 ± 5.21
Graphene oxide	>500	>500	>500	>500

Table 3.11 Molar bactericidal concentrations (mM) of the metal ions, graphene and graphene oxide against the tested *K. pneumoniae* isolates.

	Molar concentration (mM)			
Metal / Compound	***K. pneumoniae* -NK1**	***K. pneumoniae* -NK2**	***K. pneumoniae* -NK3**	***K. pneumoniae* -NK4**
Cu	1.967	1.967	1.967	1.967
Ag	1.159	0.290	0.290	0.290
Pd	0.196	0.196	0.196	0.196
Mo	0.217	0.217	0.217	0.217
Pt	0.080	0.080	0.080	0.080
Au	0.053	0.053	0.053	0.053
Ta	0.363	0.363	0.363	0.363
Zn	1.912	1.912	1.912	2.549
Re	0.334	0.334	0.334	0.334
Ru	0.824	0.824	0.824	0.824
Rh	0.810	0.810	0.810	0.810
Sn	0.132	0.132	0.132	0.132
Y	1.406	1.406	1.172	1.406
Zr	1.159	1.159	1.159	1.159
Nb	1.346	1.121	1.121	1.121
Al	7.722	4.633	3.861	4.633
In	0.454	0.454	0.454	0.454
Ga	0.147	0.147	0.147	0.147
HNO_3 (2 %)	20.15	20.15	20.15	20.15
HNO_3 (5 %)	33.58	33.58	33.58	33.58
HCl (5 %)	57.13	57.13	57.13	57.13
HCl (10 %)	85.71	85.71	85.71	85.71

3.4.2.2.3 *S. aureus*

The greatest bactericidal effect against the four *S. aureus* isolates was revealed by the same metal ions exhibiting the lowest MICs. Pt (7.0 mg/L – 0.04 mM)), Au (7.0 mg/L – 0.052 mM), Ga (10.41 mg/L – 0.147 mM), Sn (15.62 mg/L – 0.132 mM) and Mo (15.62 mg/L – 0.163 mM) were the most effective in killing the *S. aureus* cells (Table 3.12). Pd (31.25 mg/L – 0.29 mM) and Rh (31.25 mg/L – 0.30 mM) showed a good bactericidal effect, while Ru and Re (62.5 mg/L) showed a moderate one. The rest of the metal ions did not have any effect on the tested isolates. No discrepancy was observed in the MBC values of the same metal ion against the four isolates, except for the Ag ions. The bactericidal effect of Ag was only shown against three isolates *S. aureus*-SA2, -SA3 and –SA4 at 31.25 mg/L (Table 3.12). The bactericidal effect of Gr against the four strains of *S. aureus* was exhibited at 20.8 mg/L, meanwhile, no effect was shown for GO.

Table 3.12 MBC values (mg/L) ± SE of the metal ions, graphene and graphene oxide against the tested *S. aureus* isolates.

	MBC (mg/L)			
Metal / Compound	***S. aureus* -SA1**	***S. aureus* -SA2**	***S. aureus* -SA3**	***S. aureus* -SA4**
Cu	125.00 ± 0.00	125.00 ± 0.00	125.00 ± 0.00	125.00 ± 0.00
Ag	104.17 ± 20.83	31.25 ± 0.00	31.25 ± 0.00	31.25 ± 0.00
Pd	31.25 ± 0.00	31.25 ± 0.00	31.25 ± 0.00	31.25 ± 0.00
Mo	15.62 ± 0.00	15.62 ± 0.00	15.62 ± 0.00	15.62 ± 0.00
Pt	7.80 ± 2.61	7.80 ± 2.61	7.80 ± 2.61	7.80 ± 2.61
Au	10.41 ± 2.61	10.41 ± 2.61	10.41 ± 2.61	10.41 ± 2.61
Ta	125.00 ± 0.00	125.00 ± 0.00	125.00 ± 0.00	125.00 ± 0.00
Zn	125.00 ± 0.00	125.00 ± 0.00	125.00 ± 0.00	125.00 ± 0.00
Re	62.50 ± 0.00	62.50 ± 0.00	62.50 ± 0.00	62.50 ± 0.00
Ru	62.50 ± 0.00	62.50 ± 0.00	62.50 ± 0.00	62.50 ± 0.00
Rh	31.25 ± 0.00	31.25 ± 0.00	31.25 ± 0.00	31.25 ± 0.00
Sn	15.62 ± 0.00	15.62 ± 0.00	15.62 ± 0.00	15.62 ± 0.00
Y	166.67 ± 41.67	166.67 ± 41.67	166.67 ± 41.67	166.67 ± 41.67
Zr	104.17 ± 20.83	104.17 ± 20.83	104.17 ± 20.83	104.17 ± 20.83
Nb	125.00 ± 0.00	125.00 ± 0.00	125.00 ± 0.00	125.00 ± 0.00
Al	333.33 ± 83.33	333.33 ± 83.33	333.33 ± 83.33	333.33 ± 83.33
In	125.00 ± 0.00	125.00 ± 0.00	125.00 ± 0.00	125.00 ± 0.00
Ga	10.41 ± 2.61	10.41 ± 2.61	10.41 ± 2.61	10.41 ± 2.61
HNO_3 (2 %)	625 ± 6.00	625 ± 0.00	625 ± 0.00	625 ± 0.00
HNO_3 (5 %)	1562 ± 0.00	1562 ± 0.00	1562 ± 0.00	1562 ± 0.00
HCl (5 %)	3125 ± 0.00	3125 ± 1.20	3125 ± 1.20	3125 ± 0.00
HCl (10 %)	3125 ± 0.00	3125 ± 0.00	3125 ± 0.00	3125 ± 0.00
Graphene	20.80 ± 6.70	20.80 ± 6.70	20.80 ± 6.70	20.80 ± 6.70
Graphene oxide	>500	>500	>500	>500

Table 3.13 Molar bactericidal concentrations (mM) of the metal ions, graphene and graphene oxide against the tested *S. aureus* isolates.

Molar concentration (mM)				
Metal / Compound	***S. aureus* -SA1**	***S. aureus* -SA2**	***S. aureus* -SA3**	***S. aureus* -SA4**
Cu	1.967	1.967	1.967	1.967
Ag	0.966	0.290	0.290	0.290
Pd	0.294	0.294	0.294	0.294
Mo	0.163	0.163	0.163	0.163
Pt	0.040	0.040	0.040	0.040
Au	0.053	0.053	0.053	0.053
Ta	0.727	0.727	0.727	0.727
Zn	1.912	1.912	1.912	1.912
Re	0.334	0.334	0.334	0.334
Ru	0.618	0.618	0.618	0.618
Rh	0.304	0.304	0.304	0.304
Sn	0.132	0.132	0.132	0.132
Y	1.875	1.875	1.875	1.875
Zr	1.159	1.159	1.159	1.159
Nb	1.346	1.346	1.346	1.346
Al	12.355	12.355	12.355	12.355
In	1.089	1.089	1.089	1.089
Ga	0.147	0.147	0.147	0.147
HNO_3 (2 %)	9.9	9.9	9.9	9.9
HNO_3 (5 %)	24.78	24.78	24.78	24.78
HCl (5 %)	85.70	85.70	85.70	85.70
HCl (10 %)	85.70	85.70	85.70	85.70

3.4.3 Synergy Testing Between Metal Ions and Graphene-Based Compounds

The fractional inhibitory concentration (FIC) was carried out to quantify any synergistic activity between the metal ions exhibiting the best antimicrobial activity with the graphene-based compounds in a 1:1 ratio against any of the bacterial pathogens. A combination was deemed synergistic if ∑FIC≤0.5, additive if 0.5 <∑FIC≤1, indifferent if 1 <∑FIC<41and antagonistic if ∑FIC≥4. The FIC values of the different combinations against the four pathogens were listed in Tables 3.14. and 3.15. The synergistic results were highlighted with yellow, while additive FICs were highlighted in grey.

3.4.3.1 *P. aeruginosa*

Silver, yttrium, gallium and indium ions showed an enhanced antimicrobial effect against both *P. aeruginosa* isolates when combined with graphene oxide (∑FIC ≤ 0.5). Graphene, on the other hand, exhibited a synergistic effect when combined with Mo, Ag, Y, Ga, I and Pd ions against the two *P. aeruginosa* strains (∑FIC ≤ 0.5) (Table 3.14). An additive effect was detected against both isolates when treated with the following combinations Mo-GO, Au-GO, Au-Gr, Sn-GO, Sn-Gr, Pd-GO, Ru-GO, Ru-Gr, Re-Gr, Re-GO, Rh-GO and Rh-Gr (∑FIC = 0.88 – 1.00) (Table 3.14 and 3.15). While Pt-GO (∑FIC = 3.00) was the only combination showing an indifferent effect against both isolates, three combinations including Pt-Gr, Ta-GO and Ta-Gr demonstrated an antagonistic effect against the bacterial isolates (∑FIC =3.00 - 4.00) (Table 3.14 and 3.15).

3.4.3.2 *K. pneumoniae*

All FIC values exhibited by the different combinations against the four bacterial isolates were determined (Tables 3.14. and 3.15). A synergistic antimicrobial effect was shown against the four *S. aureus* isolates treated with the following combinations: Ru-Gr, Pt-Gr, Au-Gr, Ga-Gr, I-Gr, Sn-Gr, Pd-Gr, Ru-GO, Pt-GO, Au-GO, Ga-GO, I-GO, Sn-GO, Pd-GO (∑FIC= 0.26-

0.5). Y-Gr, Re-Gr, Y-GO, Re-GO, Ag-GO and Ag-Gr (0.50 <∑FIC ≤1.00) exhibited an additive antimicrobial effect, while Mo-Gr, Mo-GO, Rh-Gr and Rh-GO (∑FIC = 0.83-1.00) showed an indifferent effect. Ta-Gr and Ta-GO (∑FIC = 4.50-5.00) were the only two combinations that indicated an antagonistic effect against the bacterial isolates.

3.4.3.3 *S. aureus*

When combined with different metal ions, graphene and graphene oxide displayed the same patterns against *K. pneumoniae* isolates. An enhanced antimicrobial activity was observed when gold, tin, platinum, palladium, ruthenium, gallium and indium were added to either graphene or graphene oxide. An additive effect was noted for Mo-Gr, Mo-GO, Y-Gr, Y-GO, Rh-Gr, Rh-GO, Re-Gr and Rh-GO. Silver and tantalum were the only two metals demonstarting an antagonistic activity when added to either of the graphene-based compounds. The same effect was seen for all metals against the four isolates.

Table 3.14 FIC values (±SD) of the combinations of metal ions with graphene oxide in 1:1 ratio against the four bacterial pathogens.

	***P. aeruginosa* -NK1**	***P. aeruginosa* -NK2**	***K. pneumoniae* -NK1**	***K. pneumoniae* -NK2**	***K. pneumoniae* -NK3**	***K. pneumoniae* -NK4**	***S. aureus* -SA1**	***S. aureus* -SA2**	***S. aureus* -SA3**	***S. aureus* -SA4**
Mo	0.99 ± 0.00	1.00 ± 0.00	2.05 ± 1.1	3.39 ± 0.31	2.05 ± 0.66	3.39 ± 0.31	1.00 ± 0.00	1.00 ± 0.00	1.00 ± 0.00	1.00 ± 0.00
Au	0.88 ± 0.06	1.00 ± 0.00	0.50 ± 0.05	0.50 ± 0.00	0.50 ± 0.00	0.50 ± 0.00	0.40 ± 0.04	0.32 ± 0.10	0.32 ± 0.10	0.40 ± 0.04
Ag	0.50 ± 0.00	0.50 ± 0.05	0.88 ± 0.06	0.88 ± 0.06	1.00 ± 0.00	1.00 ± 0.00	4.40 ± 1.00	5.00 ± 0.00	8.03 ± 2.54	11.00 ± 2.50
Sn	1.00 ± 0.00	1.00 ± 0.00	0.31 ± 0.04	0.31 ± 0.04	0.31 ± 0.04	0.50 ± 0.00	0.40 ± 0.03	0.31 ± 0.01	0.22 ± 0.02	0.30 ±
Y	0.37 ± 0.06	0.50 ± 0.05	0.89 ±0.22	0.94 ± 0.22	0.89 ± 0.88	0.89 ± 0.88	1.00 ± 0.00	1.00 ± 0.00	1.00 ± 0.00	0.88 ±
Pt	3.00 ± 0.28	2.00 ± 0.15	0.26 ± 0.03	0.31 ± 0.04	0.26 ± 0.02	0.31 ± 0.00	0.50 ± 0.00	0.50 ± 0.00	0.31 ± 0.00	0.40 ± 0.00
Pd	1.00 ± 0.00	1.00 ± 0.00	0.39 ± 0.4	0.50 ± 0.00	0.31 ± 0.04	0.39 ± 0.12	0.31 ± 0.06	0.22 ± 0.12	0.31 ± 0.06	0.40 ± 0.00
Ru	1.00 ± 0.05	1.00 ± 0.05	0.50 ± 0.00	0.50 ± 0.00	0.50 ± 0.00	0.50 ± 0.00	0.41 ± 0.00	0.50 ± 0.00	0.41 ± 0/00	0.50 ± 0.00
Rh	0.88 ± 0.05	0.88 ± 0.05	1.63 ± 0.22	1.63 ± 0.31	1.63 ±0.22	2.13 ± 1.03	1.00 ± 0.00	1.00 ± 0.00	1.00 ± 0.00	1.00 ± 0.00
Ta	4.10 ± 0.55	4.10 ± 0.55	4.25 ± 0.88	6.50 ± 0.22	6.50 ± 0.22	6.50 ± 0.22	4.00 ± 1.00	3.00 ± 0.31	3.00 ± 0.31	4.00 ± 1.00
Ga	0.50 ± 0.00	0.50 ± 0.00	0.50 ± 0.00	0.50 ± 0.00	0.50 ± 0.00	0.50 ± 0.00	0.14 ± 0.01	0.22 ± 0.14	0.45 ± 0.21	0.33 ± 0.00
In	0.50 ± 0.00	0.50 ± 0.00	0.32 ± 0.00	0.50 ± 0.00	0.32 ± 0.00	0.50 ± 0.00	0.32 ± 0.06	0.41 ± 0.00	0.32 ± 0.12	0.41 ± 0.30
Re	1.00 ± 0.00	1.00 ± 0.00	0.88 ± 0.00	0.88 ± 0.00	0.81 ± 0.00	0.88 ± 0.00	1.00 ± 0.00	1.00 ± 0.00	1.00 ± 0.00	1.00 ± 0.00

Table 3.15 FIC values (±SD) of the combinations of metal ions with graphene in 1:1 ratio against the four bacterial pathogens.

	***P. aeruginosa* -NK1**	***P. aeruginosa* -NK2**	***K. pneumoniae* -NK1**	***K. pneumoniae* -NK2**	***K. pneumoniae* -NK3**	***K. pneumoniae* -NK4**	***S. aureus* -SA1**	***S. aureus* -SA2**	***S. aureus* -SA3**	***S. aureus* -SA4**
Mo	0.44 ± 0.03	0.50 ± 0.00	2.42 ± 0.71	3.96 ± 0.22	2.63 ± 0.31	3.76 ± 1.22	1.00 ± 0.00	1.00 ± 0.00	1.00 ± 0.00	1.00 ± 0.00
Au	0.99 ± 0.11	1.00 ± 0.00	0.43 ± 0.03	0.50 ± 0.00	0.50 ± 0.00	0.50 ± 0.00	0.40 ± 0.05	0.33 ± 0.00	0.40 ± 0.05	0.33 ± 0.00
Ag	0.50 ± 0.05	0.24 ± 0.02	0.88 ± 0.06	1.00 ± 0.27	0.88 ± 0.06	1.00 ± 0.00	4.01 ± 1.04	5.25 ± 1.22	5.25 ± 0.5	4.01 ± 0.66
Sn	1.00 ± 0.00	1.00 ± 0.00	0.34 ± 0.03	0.37 ± 0.06	0.37 ± 0.05	0.53 ± 0.05	0.41 ± 0.06	0.31 ± 0.04	0.22 ± 0.09	0.33 ± 1.1
Y	0.24 ± 0.08	0.24 ± 0.08	1.00 ± 0.00	0.83 ± 0.11	1.00 ± 0.00	1.00 ± 0.00	1.00 ±0.00	1.00 ± 0.00	1.00 ± 0.00	1.00 ± 0.00
Pt	4.00 ± 1.22	4.00 ± 0.13	0.31 ± 0.04	0.39 ± 0.06	0.50 ± 0.00	0.50 ± 0.00	0.50 ± 0.05	0.5 ± 0.00	0.33 ± 0.00	0.40 ± 0.11
Pd	0.50 ± 0.05	0.50 ± 0.05	0.50 ± 0.00	0.50 ± 0.00	0.50 ± 0.00	0.50 ± 0.00	0.33 ± 0.00	0.22 ± 0.00	0.33 ± 0.07	0.40 ± 0.05
Ru	0.99 ± 0.00	1.00 ± 0.00	0.31 ± 0.00	0.44 ± 0.08	0.37 ± 0.15	0.31 ± 0.22	0.41 ± 0.03	0.50 ± 0.000	0.41 ± 0.03	0.50 ± 0.00
Rh	0.88 ± 0.05	0.88 ± 0.05	1.25 ± 0.13	1.50 ± 0.11	1.50 ± 0.36	1.50 ± 0.41	1.00 ± 0.01	1.00 ± 0.05	1.00 ± 0.01	1.00 ± 0.16
Ta	4.10 ± 0.55	4.10 ± 0.66	4.50 ± 0.55	4.50 ± 1.04	4.50 ± 0.66	5.00 ± 0.00	4.02 ± 0.42	3.22 ± 0.55	4.01 ± 0.88	4.02 ± 1.01
Ga	0.50 ±0.05	0.50 ± 0.00	0.50 ± 0.05	0.50 ± 0.05	0.50 ± 0.05	0.50 ± 0.05	0.14 ± 0.03	0.22 ± 0.11	0.44 ± 0.10	0.33 ± 0.05
In	0.50 ± 0.00	0.50 ± 0.00	0.50 ± 0.00	0.50 ± 0.00	0.50 ± 0.00	0.50 ± 0.00	0.50 ± 0.00	0.50 ± 0.00	0.50 ± 0.00	0.50 ± 0.00
Re	1.00 ± 0.00	1.00 ± 0.10	0.92 ± 0.18	0.90 ± 0.11	1.00 ± 0.00	0.92 ± 0.05	1.00 ± 0.00	1.00 ± 0.12	1.00 ± 0.17	1.00 ± 0.12

3.4.4 Anti-biofilm Activity of Metal Ions and Graphene-Based Compounds

3.4.4.1 Testing the Adhesion Ability of the Bacterial Biofilms

The mean of the resource unit (RU ± SD) for each bacterial biofilm was calculated to assess its adhesion ability, and to classify it into a strong biofilm producer (RU>4) a moderate biofilm producer (2<RU≤4) and a weak biofilm producer (0<RU≤2). It was demonstrated that *P. aeruginosa*-NK1 (RU = 5.17 ± 0.33) and *P. aerginosa*-NK-2 (RU = 4.20 ± 0.44) were strong biofilm formers (Figure 3.1). *K. pneumoniae*-NK1 (RU = 5.72 ± 0.42), *K. pneumoniae*-NK2 (RU = 4.51 ± 0.22) and *K. pneumoniae*-NK4 (RU= 4.29 ± 0.42) exhibited a strong biofilm formation ability while *K. pneumoniae*-NK3 (RU = 3.48 ± 0.42) had a moderate ability (Figure 3.1). The three *S. aureus* isolates (-SA1, -SA3 and –SA4) (RU>4) were strong biofilm formers while only *S. aureus*-SA2 showed a moderate ability for biofilm formation (Figure 3.1).

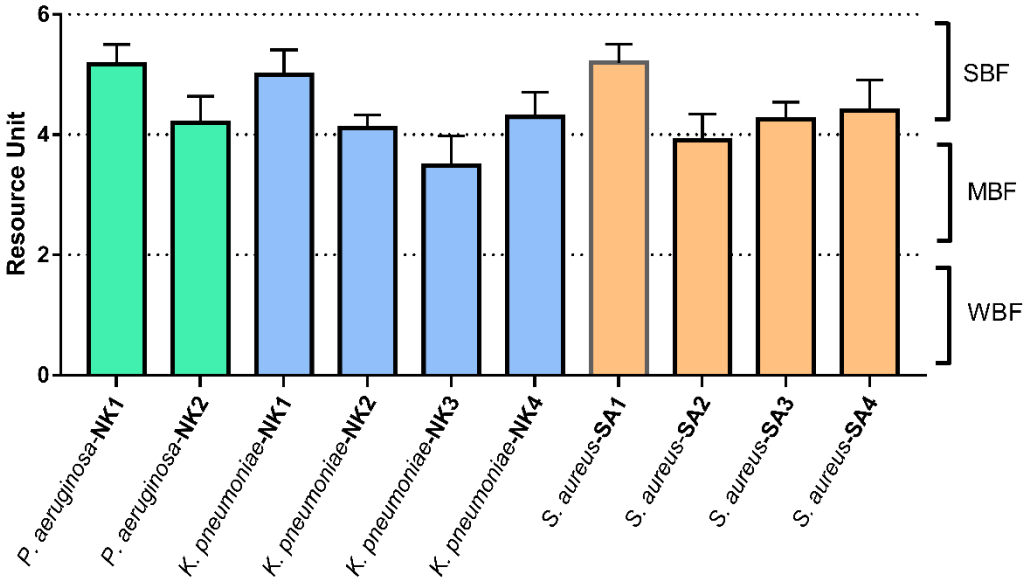

Figure 3.1 Assessment of biofilm formation for the ten strains of *P. aeruginosa*, *K. pneumoniae* and *S. aureus* through the resource unit.

3.4.4.2 Crystal Violet Biofilm Assay

The effect of the tested compounds on preformed biofilms of *P. aeruginosa*, *K. pneumoniae* and *S. aureus* in microplates was evaluated using the crystal violet method. The metal ions showing the best inhibitory effect against the planktonic cells were tested for their antimicrobial efficacy at three different concentrations (1×MIC, 2×MIC and 4×MIC) against the biofilm forms of the same bacterial isolates (Appendix A-F). When compared to the untreated biofilm (0×MIC), the antibiofilm activity against *P. aeruginosa*, *K. pneumoniae* and *S. aureus* isolates was optimal at 2×MIC of the tested compounds. Metal ions and graphene-based compounds tested at 1×MIC were not able to display any activity against the bacterial biofilms of the three pathogens. However, when tested at 4×MIC, they showed an activity similar to the 2×MIC. Hence, the following CVBA tests were performed at 2×MIC.

3.4.4.2.1 *P. aeruginosa*

Out of the eight metal ions tested, Ag, Zn, Sn (p= 0.0001) and Pd (p= 0.0005) were able to inhibit further growth of the preformed biofilms of *P. aeruginosa*-NK1 and -NK2 (Figure 3.2). The inhibitory effect of graphene (p= 0.0001) against the biofilm forms of both isolates was much greater than the planktonic *P. aeruginosa* cells. Combinations of Mo-Gr, Mo-GO, Au-GO, Pt-GO, Ga-GO and Ga-Gr (p<0.0001) and Ag-Gr (p=0.0037) revealed the optimal antibiofilm effect (Figure 3.2). A lower absorbance was detected upon addition of Gr or GO to Mo, Au and Ga, or GO to Pt; which signified that these compounds exhibited a better antimicrobial activity against the biofilms compared to the metal ions alone. No discrepancy in the antibiofilm effect of the tested compounds was noted between the distinct *P. aeruginosa* isolates exhibiting different antibiotic profiles (Figure 3.2 A-B).

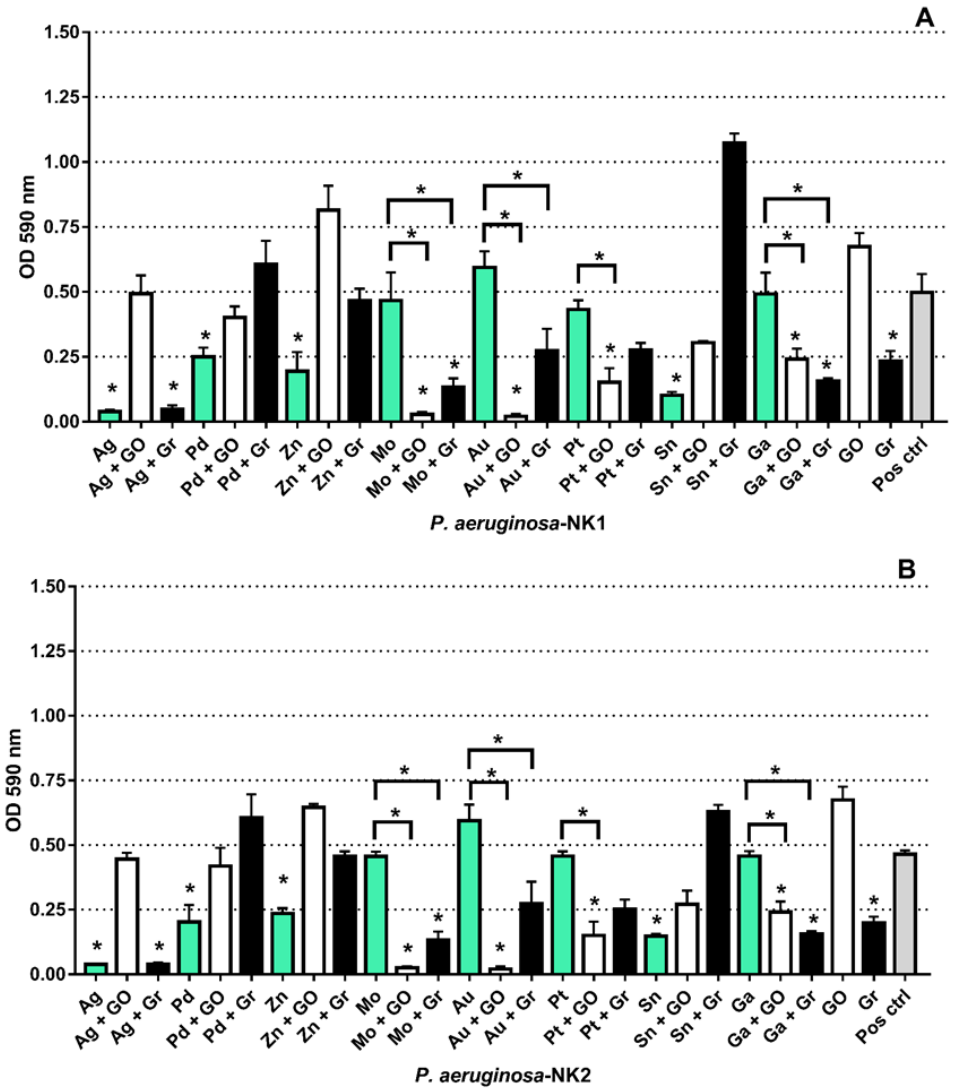

Figure 3.2 The antimicrobial effect of metal ions and graphene-based compounds as determined by CVBA (at 2 × MIC) on pre-formed biofilms of (A) *P. aeruginosa*-NK1 and (B) *P. aeruginosa*-NK2 after 24 h treatment. The absorbance values (±SD) are directly proportional to the amount of biofilm that remained intact post exposure. * represents $p \leq 0.05$ when compared to the control.

3.4.4.2.2 *K. pneumoniae*

Biofilm assessment of *K. pneumoniae* isolates showed that six out of the nine metal ions tested inhibited preformed *K. pneumoniae* biofilms at 2×MIC of each tested compound. The best antimicrobial activity against the four *Klebsiella* isolates was revealed by Ga, Au, Sn, Pt, Pd and Mo (p= 0.0001) (Figure 3.3). It was evident that the addition of Gr or GO to Mo, Pt, Au and Pd, previously proven to inhibit *K. pneumoniae* biofilm formation, resulted in lower ODs (Figure 3.3). This reflected an enhanced antibiofilm activity for Mo-GO (p= 0.0001), Mo-Gr (p= 0.0001), Pt-GO (p= 0.009), Pt-Gr (p= 0.008), Au-GO (p= 0.019), Au-Gr (p= 0.018), Pd-GO (p= 0.009) and Pd-Gr (p= 0.008) compared to their respective metal ions alone. The OD values for the different treatments were similar for the four distinct isolates (Figure 3.3 A-D).

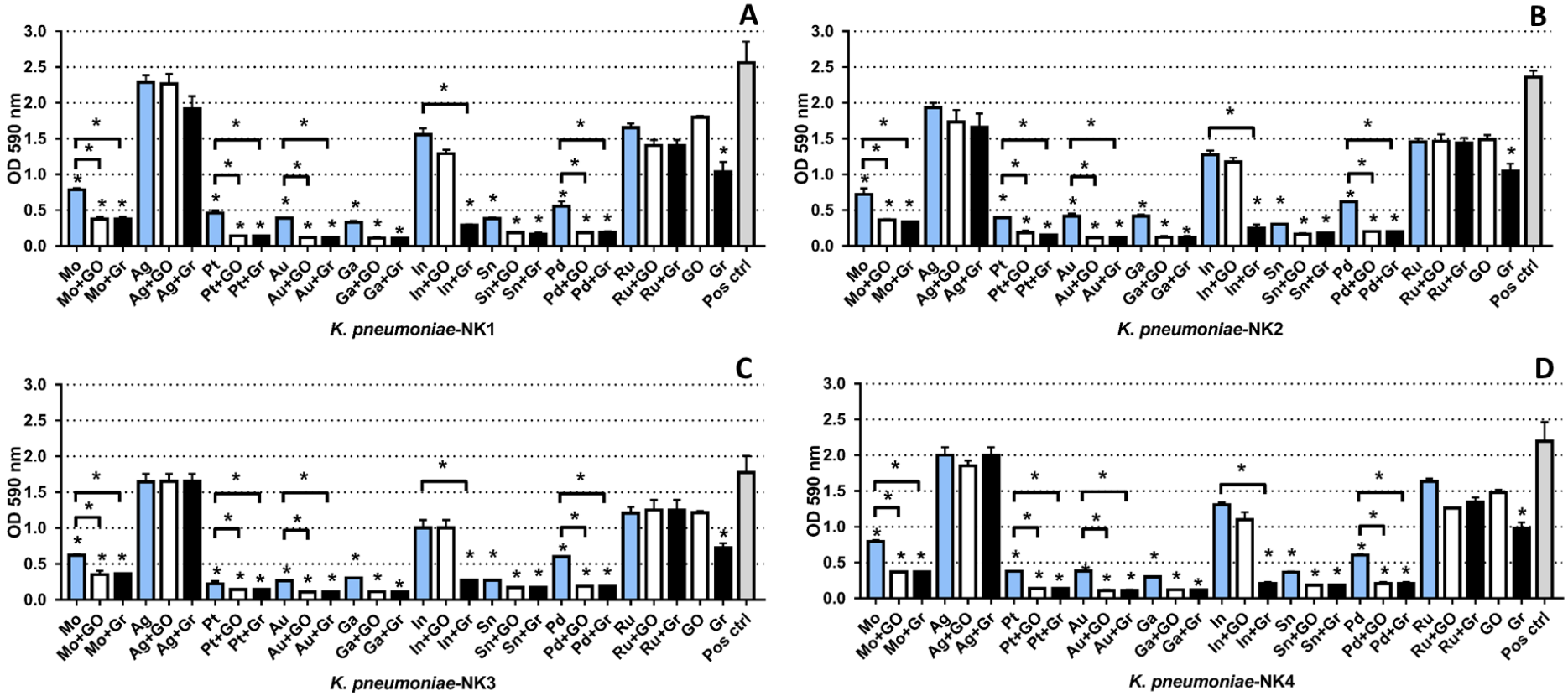

Figure 3.3 The antimicrobial effect of metal ions and graphene-based compounds as determined by CVBA (at 2 × MIC) on pre-formed biofilms of (A) *K. pneumoniae*-NK1, (B) *K. pneumoniae*-NK2, (C) *K. pneumoniae*-NK3 and (D) *K. pneumoniae*-NK4 after 24 h treatment. The absorbance values (±SD) are directly proportional to the amount of biofilm that remained intact post exposure. * represents $p \leq 0.05$ when compared to the control.

3.4.4.2.3 *S. aureus*

Crystal violet biofilm assay of *S. aureus* isolates revealed that Mo, Pt, Au, Sn, Ga and Pd inhibited the bacterial biofilms following an overnight treatment. Combinations of Mo-GO, Pt-GO, Pt-Gr, Au-GO, Au-Gr, Sn-GO, Sn-Gr, Ga-GO, Ga-Gr, Pd-GO and Pd-Gr also exerted an antibiofilm efficacy. Addition of Gr or GO to metal ions enhanced their disruptive efficacy against the biofilms, as in the case of Pt-GO, Pt-Gr, Au-GO, Au-Gr, Ga-GO, Ga-Gr, Sn-GO, Sn-Gr, Pd-GO, Pd-Gr. It was noted that the four *S. aureus* isolates showed no variation in their biofilm assessment when treated with the same tested compound (Figure 3.4 A-D).

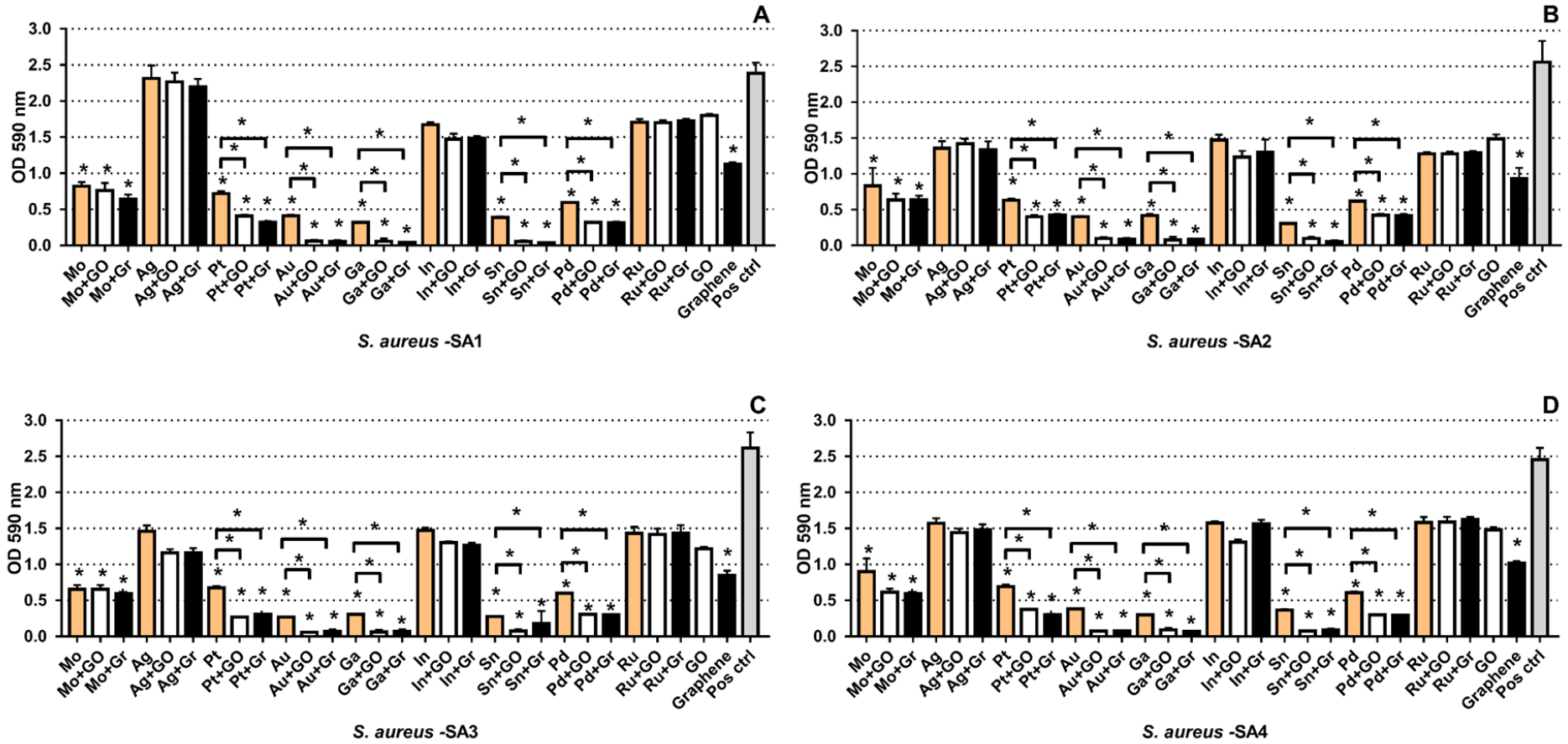

Figure 3.4 The antimicrobial effect of metal ions and graphene-based compounds as determined by CVBA (at 2 × MIC) on pre-formed biofilms of (A) *S. aureus*-SA1, (B) *S. aureus*-SA2, (C) *S. aureus*-SA3 and (D) *S. aureus*-SA4 after 24 h treatment. The absorbance values (±SD) are directly proportional to the amount of biofilm that remained intact post exposure. * represents $p \leq 0.05$ when compared to the control.

3.4.4.3 XTT Reduction Assay

The changes in metabolic activity of the active bacterial cells following their treatment with metal ions or graphene-based compounds was quantified using an XTT reduction assay. Consequently, the tested compounds were classified as having an antimicrobial effect when they resulted in a mean ≥ 50% reduction in the XTT colorimetric assay (threshold level for antimicrobial activity). Little or no antimicrobial activity was assigned to an XTT reduction <50%.

3.4.4.3.1 *P. aeruginosa*

The metabolic activity of the biofilms of *P. aeruginosa* –NK1 and –NK2 treated with Ag, Ag/Gr, Mo/GO and Au/GO was mostly reduced to an extent of 90%. Biofilms treated with Mo/Gr, Pt/GO, Sn, Ga/GO showed an 80% activity reduction, while those treated with Zn, Pt/Gr, Sn/GO, Ga/GO and Gr had a reduction of 50-60%. Little inhibition of the metabolic activity was assigned to Ag/GO, Pd, Pd/GO and Au/Gr (<50% reduction). The combinations of Pd/Gr, Zn/GO, Zn/Gr, Mo, Au, Pt, Sn/Gr, Ga and GO, showed negative values, and thus had no effect on the biofilms' metabolic activity (Figure 3.5). Both isolates of *P. aeruginosa* exhibited the same patterns for metabolic activity following their treatment with the tested combinations (Figure 3.5 A-B).

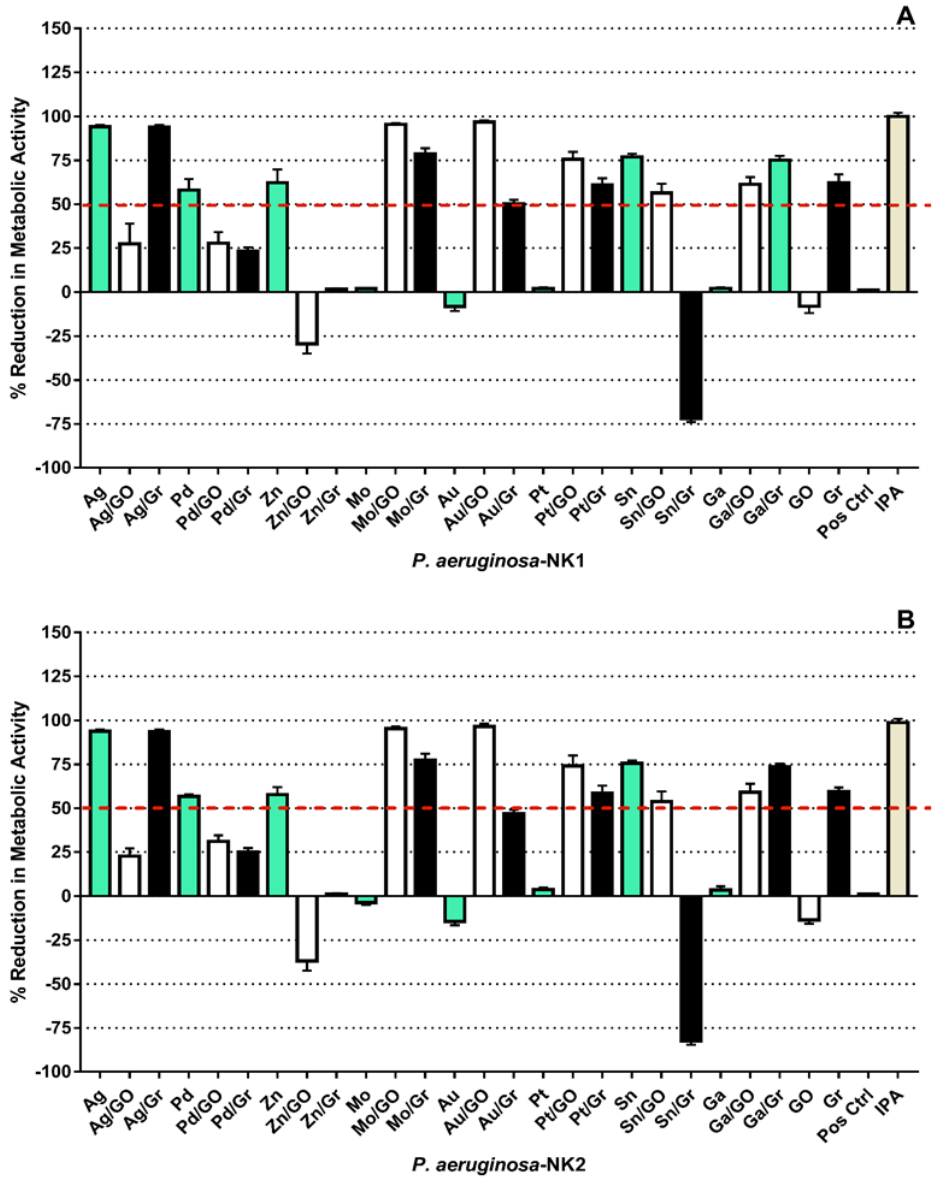

Figure 3.5 The antimicrobial effect of experimental compounds against the clinical *P. aeruginosa* (A) –NK1, (B) –NK2 isolates as assessed by percentage reduction in XTT colorimetry. Data shown as mean (± SD). The dotted red line (----) represents the threshold for minimum antibacterial activity.

3.4.4.3.2 *K. pneumoniae*

The XTT assay showed a decrease by 80% in metabolic activity when biofilms of *K. pneumoniae* were treated with Au, Ga or Sn, and by 60-65% when treated with Mo, Pt or Pd. The cellular activity was even more reduced when Gr or GO was added to any of the following metal ions: Au, Ga, Sn, Mo, Pt or Pd (Figure 3.6). In, Ru, GO and their combinations had less than 50% effect on the vitality of the four *Klebsiella* biofilms, while Ag, Ag-GO and Ag-Gr had no effect at all (5% reduction) (Figure 3.6 A-D).

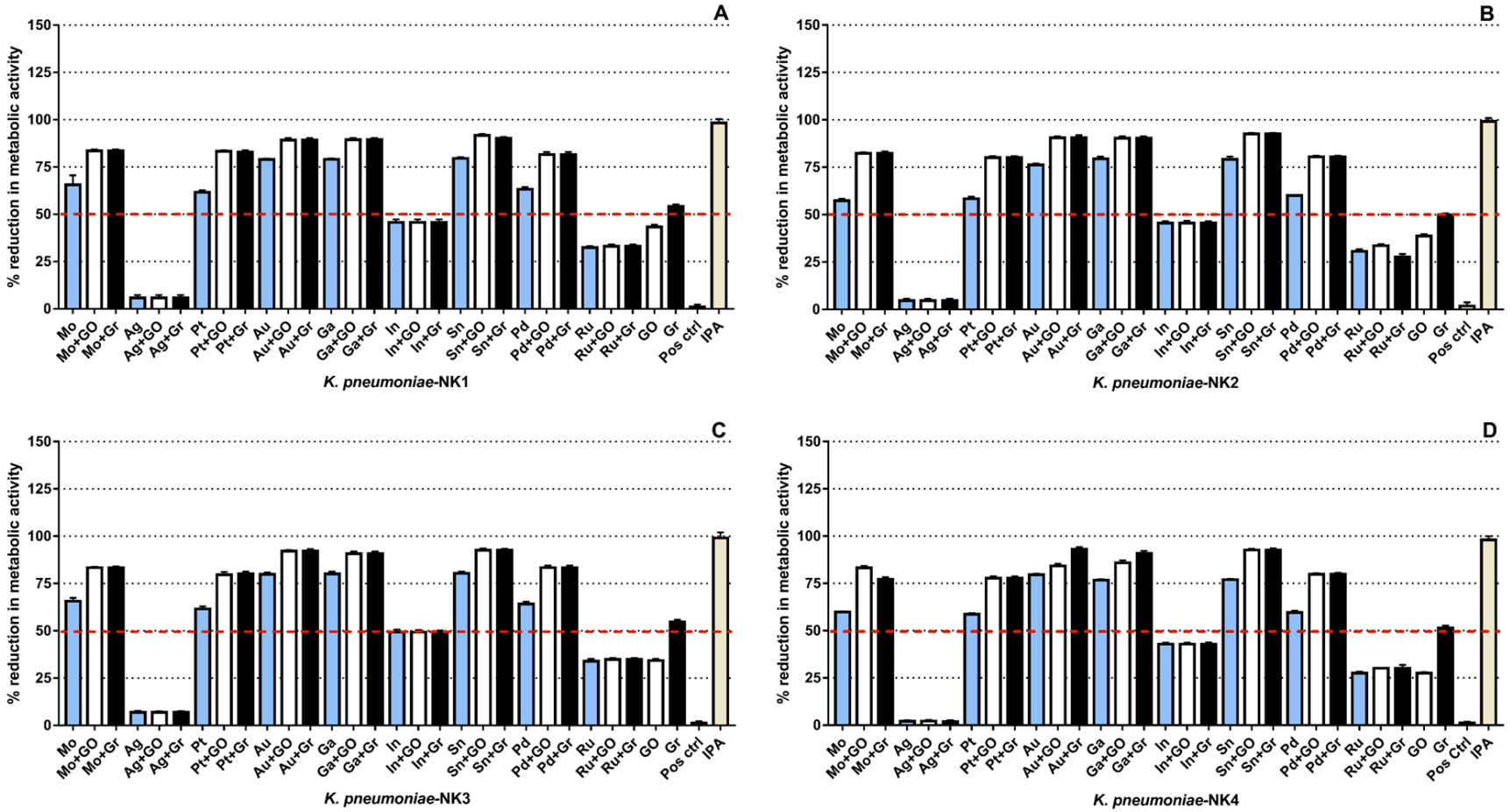

Figure 3.6 The antimicrobial effect of experimental compounds against the clinical *K. pneumoniae* (A) -NK1, (B) -NK2, (C) –NK3, (D) –NK4 isolates as assessed by percentage reduction in XTT colorimetry. Data shown as mean (± SD). The dotted red line (----) represents the threshold for minimum antibacterial activity.

3.4.4.3.3 *S. aureus*

A reduced XTT conversion was observed in bacterial biofilms exposed to treatments with single metal ions of Au (83.5%), Ga, Sn, Pd or Gr (80%). The best combinations that demonstrated a decrease in metabolic activity exceeding 92% in all tested isolates were Ga-Go, Ga-Gr, Sn-GO, Sn-Gr, Au-GO and Au-Gr (Figure 3.7). Pt-GO (84%), Mo-Gr (83%), Pd-GO (83%), Pd-Gr (79.3%), Pt-Gr (78.22%) and Mo-GO (73%) showed a good difference in XTT conversion. There was no difference in the XTT conversion following the different treatments among the four isolates (Figure 3.7 A - D).

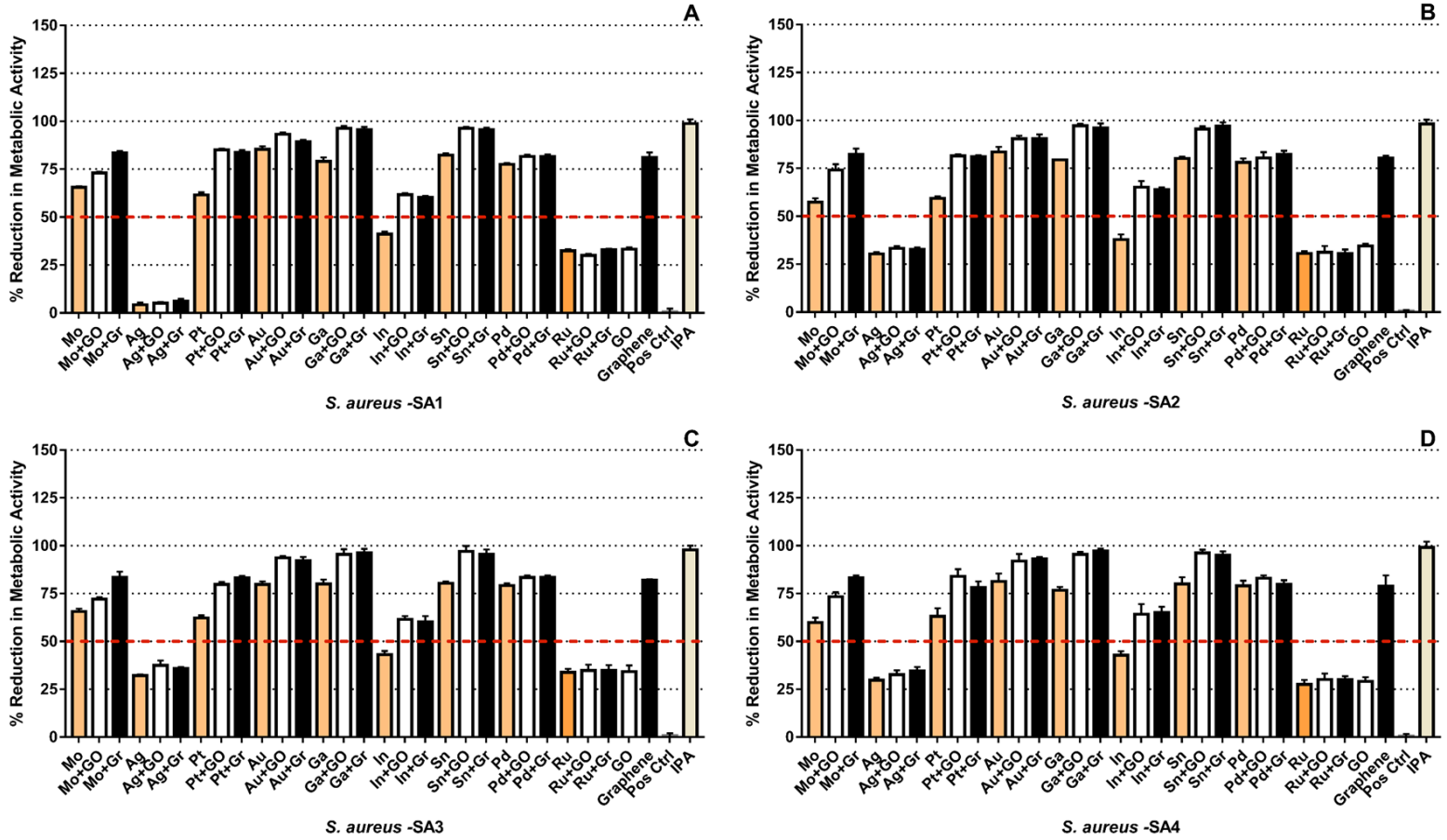

Figure 3.7 The antimicrobial effect of experimental compounds against the clinical *S. aureus* (A) -SA1, (B) -SA2, (C) -SA3, (D) -SA4 isolates as assessed by percentage reduction in XTT colorimetry. Data shown as mean (± SD). The dotted red line (----) represents the threshold for minimum antibacterial activity.

3.5 Discussion

Following the emergence of multidrug resistant bacteria, infection control and treatments have risen as a serious concern. Thus, research into the assessment of novel, effective antibacterial agents as alternatives to antibiotics is necessary.

3.5.1 Antibiotic Susceptibility Testing

This study investigated only clinical strains collected from different hospitals within UK without testing any laboratory reference strains. Clinical strains seem to have a more adequate representation of 'real-world' pathogenesis compared to reference strains that have shown to lose their pathophysiological characteristics following serial *in-vitro* passages (Fux *et al.*, 2005).

The susceptibility testing for the pathogens revealed that isolates belonging to the same genus showed different resistance profiles. All ten tested strains showed resistance to three or more agents belonging to different classes of antibiotics; hence, they were classified as MDR pathogens. For instance, while both *P. aeruginosa* strains were resistant to ciprofloxacin, *P. aeruginosa*-NK1 was also resistant to piperacillin, and imipenem and *P. aeruginosa*-NK2 was resistant to fosfomycin and cefepime. This means that each isolate was resistant to, at least, two out of the eight classes of antibiotics generally incorporated in the treatment of *P. aeruginosa* infections. These include cephalosporins, monobactams, aminoglycosides, carabapenems, quinolones, ß-lactams, fosfomycins and polymyxins and can be given as a mono- or combination therapy (Bassetti *et al.*, 2018). In light of this resistance diversity, it should be pointed out that the treatment of burns, infected with *P. aeruginosa,* is not standardised among hospitals, and still depends on the individual preparation of the topical agent in burn units in each hospital (Rowan *et al.*, 2015).

One of the four *K. pneumoniae* strains was resistant to all β-lactams tested. The four isolates also showed different levels of resistance to other agents of different categories such as quinolones, cephalosporin, carbapenem, tetracycline and sulphonamides. Similar results of high prevalence of *K.*

pneumoniae resistance was reported from previous studies indicating that UK and Ireland encompass a highly diverse resistant population of *K. pneumoniae* isolates (Moradigaravand *et al.*, 2017).

The results also showed that the antibiotic susceptibility profiles of the MRSA isolates tested were found to be variable. It should be noted that the multiple antibiotic resistance profiles of *S. aureus*, similar to our isolates, was reported earlier in London, UK by The Royal Brompton Hospital and The Royal Marsden Hospital (Gould *et al.*, 2010).

3.5.2 Antimicrobial Efficacy of Single Metal Ions

Testing for the antimicrobial effect of the single metal ions revealed that Pt, Pd, Sn, Mo and Au exhibited the best inhibitory effect (by mass and molar concentrations), at different rates, against all ten tested bacterial isolates. The antibacterial efficacy of metal ions can be first attributed to Pearson's (hard and soft acid and base) concept that classifies metals into soft and hard ions depending on their polarizability. In theory, hard ions have a high charge density (charge/radius ratio), hence they are not easily polarized compared to the soft ions that have a lower charge density and higher polarizability (Mittapally *et al.*, 2018). Soft ions have the ability to promote their antibacterial activity by forming bonds with sulphur found in proteins of bacteria, a property known as "thiophilicity" (Mittapally *et al.*, 2018). Accordingly, this makes the antimicrobial effect of these metal ions relatively proportional to their affinity for sulphur (Harrison *et al.*, 2007). This can provide a possible explanation for the observation that Pt, Pd, Sn and Mo, being part of the soft metals (Table 1.2), exhibited a better antimicrobial efficacy compared to other metals belonging to the hard group such as Al, Y and Zn.

The difference in the antimicrobial extent of metal ions against the three pathogens can also be linked to the difference in the membrane structure between the Gram positive and Gram-negative bacteria. The outer membrane of Gram-negative bacteria can act as a barrier preventing charged macromolecules (such as metal ions) from penetrating the hydrophobic bilayer (Clifton *et al.*, 2015). For instance, higher

concentrations of Pt were needed to inhibit Gram-negative *P. aeruginosa* (7.8 mg/L – 0.04 mM) and *K. pneumoniae* (13.00 -15.62 mg/L) (0.066-0.08 mM) compared to Gram-positive *S. aureus* (0.49 mg/L – 0.003 mM). Furthermore, 83 mg/L or 1.31 mM of Cu ions was enough to inhibit *S. aureus* compared to 125 mg/L (1.967 mM) for *P. aeruginosa* and *K. pneumoniae*. Increased tolerance to copper among Gram-negative bacteria was reported by several studies (Pontel and Soncini, 2009; Santo *et al.*, 2010; Altimira *et al.*, 2012). Polysaccharides found in a number of bacterial strains, including *Klebsiella* and *Pseudomonas*, were shown to be able to bind to toxic metal cations outside the cell as a survival mechanism (Bridge *et al.*, 1999; Gutnick and Bach, 2000). Kazy *et al.* (2002) reported that the presence of Cu ions in the medium causes a 4-fold stimulation in the synthesis of extracellular polysaccharides in *P. aeruginosa*. The enhanced extracellular polysaccharides composition acts as a protective barrier against the environmental stress.

Surprisingly, despite its high electronegativity (1.93), Ag was not very efficacious in this study. Silver did not exhibit any antimicrobial effect against both isolates of *P. aeruginosa*, *S. aureus*-SA1 and *K. pneumoniae*-NK1. Silver was known for years for to be bactericidal (Mittapally *et al.*, 2018), however, concerns have been raised regarding bacterial resistance to silver following its extensive use mainly in the clinical settings (Percival *et al.*, 2005). Although the incidence of silver resistance has been shown to be variable, silver resistant bacteria of *P. aeruginosa* and *K. pneumoniae* have been previously reported (Haefeli *et al.*, 1984; Percival *et al.*, 2005).

It should be noted that most of the research onto the antimicrobial activity of Ag or Cu focuses on the surface, alloys or nanoparticles forms of Cu and Ag rather than the ionic forms (Noyce *et al.*, 2006; Santo *et al.*, 2010; Qasim *et al.*, 2018). Nevertheless, it was demonstrated that the surface-released free silver and copper ions play an important role in contact killing, which proceeds by successive membrane damage, oxidative damage, and DNA degradation (Souli *et al.*, 2013).

With the exception of Ag ions, no clear discrepancy was noted for the MIC values recorded for the distinct isolates of the same bacterial type being *S.*

aureus, *K. pneumoniae* or *P. aeruginosa*. Hence, the antimicrobial effect of metal ions was independent of the antibiotic profile of each isolate.

3.5.3 Antimicrobial Efficacy of Graphene-Based Compounds

Graphene and its derivatives have been the focus of research for the last decade with the aim of developing novel diverse biomedical applications (Pham *et al.*, 2015). Results in this study showed that graphene oxide had no antimicrobial activity against the ten tested isolates with MIC and MBC values exceeding 500 mg/L. This was inconsistent with several studies that demonstrated the ability of GO to inhibit the growth of *P. aeruginosa* and *S. aureus* and induce cell lysis (Akhavan and Ghaderi, 2010; S. Liu *et al.*, 2011). The exact mechanism by which the graphene-based compounds act against different bacteria continue to be controversial. However, it has been proposed that the extent of their antibacterial effect depends largely on the sample preparation and concentration, the time of exposure, their physio-chemical properties, as well as on the method of the microbiological analysis (Akhavan and Ghaderi, 2010; Hu *et al.*, 2010). Therefore, it may be proposed that the negative effect for GO towards the planktonic form of the three organisms might be due to the highly purified type of GO used. This observation was validated by Barbolina *et al*. (2016) who demonstrated that GO of high purity did not exhibit any bacteriostatic or bactericidal effect against *E. coli* and *S. aureus* cells at concentrations up to 1000 mg/L. Barbolina *et al*. (2016) also suggested that the bactericidal activity of GO was referred to the chemical contaminants (sulphur and nitrogen impurities) present during sample preparation, rather than the sample itself.

Graphene showed a good antimicrobial activity against the distinct isolates of *S. aureus* (20.8 mg/L), and *K. pneumoniae* (26.0 mg/L). A slightly higher concentration of graphene was required to inhibit the *K. pneumoniae* isolates compared to the *S. aureus* ones, and this might be associated again with the difference in the outer membrane of the Gram-negative *Klebsiella* that can delay the mechano-bactericidal effect of the thin layer of graphene, acting as a blade cutting the cell membrane (Linklater *et al.*, 2018). Several mechanisms were suggested for the mode of action of graphene, most

importantly the direct contact of the sharp edges with the bacterial cell wall. In particular, the precise orientation (orthogonal or perpendicular) of the graphene edges can determine the extent of their insertion into the cell wall and hence, the bacterial damage it caused (Gurunathan *et al.*, 2012; Tu *et al.*, 2013). For instance, Pham *et al*. (2015) has demonstrated the ability of graphene sheets to induce pores in the membranes of *P. aeruginosa* and *S. aureus,* and suggested that the density of the graphene edges was a main parameter governing the antibacterial behavior of the graphene compounds. Tu *et al*. (2013) also confirmed the degradation of inner and outer membrane of *E. coli* cells by graphene through the extraction of phospholipids.

3.5.4 Synergy Testing Between Metal Ions and Graphene Composites

Despite the fact that GO was ineffective against any of the bacterial strains, the combination of GO with Ag, Y, In and Ga enhanced their antimicrobial activity against *P. aeruginosa* isolates. The addition of GO to Au, Sn, Pt, Pd, Ru, Ga and In also enhanced their activity against the four isolates of *K. pneumoniae* and *S. aureus*. The same metal ions stated above resulted in a synergistic relationship when added to graphene against the same isolates. Different combinations including Ag-GO, Y-GO, I-GO, Ga-GO, Ag-Gr, Y-Gr, I-Gr, Ga-Gr, Mo-Gr and Pd-Gr were synergistically effective against *P. aeruginosa* isolates. Several hypotheses have been formulated to explain the complimentary mode of action resulting from the combination of metal ions and graphene composites. One of which is that metal ions are found in a solution and are evenly dispersed around the bacterial cell with no specific orientation. The addition of graphene components will depolarize the cell wall making it more vulnerable, hence, assisting metal ions to enter to the cytoplasm (Pal *et al.*, 2007; McQuillan *et al.*, 2012). The fact that graphene and graphene oxide and their combinations exerted the same bactericidal effect against the bacterial isolates having diverse antibiograms, suggested that metal ions have a more generalized mode of action compared to the targeted mode of antibiotics (Kohanski *et al.*, 2010).

3.5.5 Antibiofilm Activity of Metal Ions and Graphene-Based Compounds

Evidence suggests that biofilms are responsible for the chronicity of persistent bacterial infections in 60-80% of hospital acquired cases (Bjarnsholt, 2013). The biofilm testing in this study was performed on stainless steel coupons. The majority of hospital equipment (such as the uterine aspiration set, the catheter tray, the anaesthesia trolley, the glass operation room cabinet, overshoe bonnet cabinet, the hospital elevators) are made of stainless steel (Weitzul and Taylor, 2005). Some surgical and medical implants are also constructed of a large percentage of stainless steel metal including the surgical stainless steel staples that are used as suturing closing material (Weitzul and Taylor, 2005). Both the hospital installations and surgical tools constitute a potential reservoir for bacterial biofilms, therefore, testing on stainless steel might provide a close imitation of the actual biofilms encountered in clinical settings. The biofilm assays showed that eight out of the ten tested isolates were strong biofilm formers and two were moderate ones. This indicated that this study investigated clinically challenging strains. It also showed that the metal ions (Ag, Zn, Pd) that inhibited the biofilms of both isolates of *P. aeruginosa* were different from those (Pt, Sn) inhibiting the planktonic *P. aeruginosa* cells. In contrast, the same metal ions (Au, Sn, Pt, Pd, Mo) were able to inhibit the planktonic and biofilm forms of *K. pneumoniae* and *S. aureus*. However, three combinations (Au-GO, Ga-GO and Ga-Gr) proved to be effective against *P. aeruginosa*, *K. pneumoniae* and *S. aureus* in their planktonic and biofilm forms.

The controversial antimicrobial efficacy of Ag was raised again in the biofilm testing. Silver did not show any effect against the planktonic *P. aeruginosa* cells but inhibited biofilms of *P. aeruginosa*-NK1 and *P. aeruginosa*-NK2. However, Ag that did not inhibit the planktonic cells of *S. aureus*-SA1 and *K. pneumoniae*-NK1, did not affect their biofilms. Similar to the planktonic testing, the biofilm assays showed that the addition of graphene or GO to metal ions enhanced their inhibitory effect.

The difference in the efficacy of metal ions towards the planktonic and the biofilm forms is mainly due to the unique biofilm architecture and formation, which is dictated by several factors including strain specificity, internal genes and external conditions (quorum sensing) (Xu *et al.*, 2016).

Despite the fact that Ru is classified as "borderline" metal ion according to HSAB, and is known to exhibit an antimicrobial activity that is approximately proportional to their affinity for thiols, Ru ions did not show any antimicrobial activity against biofilms of *K. pneumoniae* and *S. aureus* in this study (Lemire *et al.*, 2013). It has been suggested that Ru ions mediate their antimicrobial activity through the carbon monoxide-releasing molecules (CORMs) (Southam *et al.*, 2017). Ru-CORMs, also known as carrier antimicrobial complex, act as carbon monoxide releasers and induce a bactericidal action through an inhibition of aerobic respiration, a decrease in viability of biofilms, an increase in ROS production or DNA damage (Southam *et al.*, 2017). However, recent studies investigating the antimicrobial activities of Ru ions have demonstrated that CORMs within Ru had a low activity against *S. aureus* and were even inactive against MRSA and *P. aeruginosa* (Li *et al.*, 2011; Páez *et al.*, 2013). Furthermore, Li *et al*. (2013) confirmed that Ru ions caused membrane depolarization in *E. coli* cells, but was not able to permeabilise the membrane of *S. aureus*. Therefore, the low antimicrobial effect shown by Ru in this study might be dependent on the extent of intracellular accumulation of Ru-CPRMs and consequential reversible binding to targets within bacterial cells (F. Li *et al.*, 2015).

While the CVBA derived data resulted from the dye staining of live and dead cells and exopolysaccharides, the XTT assay was used to specifically track the metabolic activity of live cells of all the biofilms post treatment. The percentage of agreement between the two tests was compared and showed that the metal ions and combinations inhibiting the biofilms were the same compounds showing the highest percentage of inhibition (>50%) of the metabolic activity for the ten isolates. It was clear that the two assays complemented each other in terms of the analysis of biofilm formation in response to treatment. XTT staining for cell viability and CV assay for biofilm mass determination, showed that combinations of metal ions and graphene

or GO, had a better inhibitory effect against the bacterial isolates, compared to metal ions alone or graphene or GO alone. In view of the vigorous complex process of biofilm formation, it was previously revealed that the metabolic activity of each biofilm is very specific to the bacterial strain itself (Xu *et al.*, 2016). The tested combinations of Au, Ga, Sn, Mo, Pt or Pd with Gr/GO were able to reduce the metabolic activity of all biofilms of the ten isolates by more than 80%, irrespective of the antibiotic profiles of the isolates or the strain specificity.

3.6 Conclusion

Findings from this study revealed that Pt, Au, Sn, Pd and Mo ion solutions were able to inhibit ten MDR isolates of *P. aeruginosa*, *S. aureus,* and *K. pneumoniae* in their planktonic forms, regardless of their antibiotic susceptibility profiles. It was also demonstrated that Pd, Sn and combinations of Mo-Gr, Mo-GO, Au-GO, Pt-GO, Ga-GO and Ga-Gr inhibited the biofilm formation and reduced the metabolic activity of the same isolates. The previously stated metal ions and successful combinations can open the door for possible incorporation in applied or biomedical applications.

Chapter 4 Novel Antiseptic Alternatives for Chlorhexidine-Adapted *K. pneumoniae*

4.1 Introduction

The escalating concerns regarding antimicrobial resistance has pushed scientists and clinicians to pay more attention to problems of resistance toward commonly used antiseptics and disinfectants, including chlorhexidine (CHX) (Kampf, 2016; Cieplik *et al.*, 2019). Although several publications reported a high incidence of clinical bacterial isolates with reduced CHX susceptibility and high virulence, the focus on CHX resistance is still limited (Higgins *et al.*, 2001; Horner *et al.*, 2012; Suwantarat *et al.*, 2014; Cieplik *et al.*, 2019).

4.1.1 History of CHX

CHX dates back to the 1950s where it was first synthesized in Manchester (UK) by Imperial Chemical Industries and was primarily used as a potent anti-malarial agent (Cieplik *et al.*, 2019). CHX, found today as hydrochloride diacetate or gluconate salts, is used in a broad range of applications including catheter site preparation, bladder irrigation, oropharyngeal decontamination and endodontic treatment (Karpiński and Szkaradkiewicz, 2015). Most importantly, CHX has been used as an antimicrobial skin cleanser for sterilization of healthcare providers and patients pre- and post-surgery. Due to its safety and effectiveness, CHX was listed on the World Health Organization's List of Essential Medicines and be obtained over the counter with an NHS cost of £4.80 for 500 mL in UK (WHO, 2015).

4.1.2 Chemical Features

CHX is a bisbiguanide compound ($C_{22}H_{30}Cl_2N_{10}$) also known as 1,1'-hexamethylene bis (5-[4-chlorophenyl] biguanide). Its symmetrical structure comprises two chloroguanide chains linked by a hexamethylene bridge (Figure 4.1.) (EMBL-EBI, 2019). At physiological pH, CHX is a cationic molecule carrying two positive charges and it acts as a strong alkali that is practically insoluble in water (Cieplik *et al.*, 2019). Conversely, salts of CHX such as CHX diacetate, CHX dihydrochloride and CHX digluconate exhibit water solubility and therefore are mixed with water and alcohol for disinfectant formulations (Karpiński and Szkaradkiewicz, 2015).

Figure 4.1 The chemical structural formula of CHX. Figure adapted and reproduced from National Center for Biotechnology Information (2019a)**.**

4.1.3 Surgical Skin Cleansers

Surgical site infections constitute annually 5% of the “clean contaminated operations” in hospitals and create complex clinical scenarios (Hemani and Lepor, 2009). Whole-body bathing or showering with commercial skin antiseptics is a routine pre-operative practice to reduce these infections, as recommended by WHO surgical site infection prevention guidelines (WHO, 2016). The use of antiseptics dates back to the mid-1800s when the Hungarian scientist and physician Dr. Semmelwies observed a substantial decrease in sepsis, infections, and hence in surgical morbidity, with proper handwashing techniques (Bednarek *et al.*, 2020). A variety of commercial surgical scrubs is currently available in the market. Commonly used antiseptic agents in dermatologic surgery can include benzalkonium chloride, iodine, chloroxylenol, hydrogen peroxide, or isopropyl alcohol. However, chlorhexidine-based skin cleansers remain the most extensively used in clinical settings (Hemani and Lepor, 2009; Bednarek *et al.*, 2020). The main purposes of using antiseptic skin cleansers are mainly for healthcare personnel hand-wash, patient pre-surgical skin preparation and wound cleansing. The choice of which specific agent to use is mainly related to the target site of operation and approaches in surgery (Hemani and Lepor, 2009). The main active ingredient of the CHX-based antimicrobial skin scrub is CHX gluconate (4% W/V), but the mixture also contains other ingredients including poloxamer 237, isopropyl alcohol, lauryl dimethyl amine oxide, glycerol, macrogol 7 glycerol cocoate, gluconolactone, perfume (Herbacol), ponceau 4R (E124), sodium hydroxide and purified water. The details of all

the ingredients including the nature, the chemical formula, and the role of each compound are listed (Table 4.1).

Table 4.1 **Complete list of all the excipients included in the surgical skin cleanser, their chemical features and main function.**

Excipient	Chemical name	Function/ Use	References
Poloxamer 237	Poly(ethylene glycol)-block-poly(propylene glycol)-block-poly(ethylene glycol) 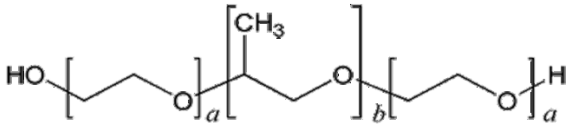	• Surfactant • Emulsifying agent • Solubilizing and dispersing agent	Patel *et al*. (2009)
Isopropyl alcohol (ISA)	Propan-2-ol - C_3H_8O 	• Emulsifier • Viscosity decreasing agent • Cosmetic astringent	National Centre for Biotechnology (2019)
Lauryl dimethyl amine oxide (LDAO)	$C_{14}H_{31}NO$ 	• Strong hydrophilic surfactant • Antimicrobial agent	Birnie and Malamud (2000) National Centre for Biotechnology Information (2019b)
Glycerol	Glycerin - $C_3H_8O_3$ 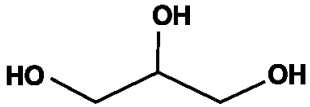	• Denaturant • Skin protectant • Skin-conditioning agent • Humectant • Viscosity decreasing agent • Antimicrobial agent	Becker *et al.* (2014) Singh (2014) Stout and Mckessor (2012)
Macrogol 7 glycerol cocoate (PEG-7)	Caprylic/capric glyceride Polyethylene glycol derivative	• Excellent emulsifying agent • Emollient	The CIR Expert Panel (2014)

		• Very useful as surfactant and foam booster • Skin conditioning agent • Can be added to formulas as is, usual concentration 1 - 10% (2% in skin cleansers)	
Gluconolactone	D-gluconic acid - $C_6H_{10}O_6$ 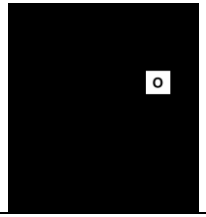	• Preservative • Humectant • Solvent • Free-radical scavenger protecting skin from UV radiation and exfoliation	Kantikosum *et al*. (2019)
Ponceau 4R (E124)	Trisodium salt of 1-(4-sulpho-1-napthylazo)- 2-napthol-6,8-disulphonic acid $C_{20}H_{11}N_2Na_3O_{10}S_3$ 	• Red color inducer	National Centre for Biotechnology Information (2019c)
Herbacol 015393 TD		• Perfume	
Sodium hydroxide	NaOH	• pH adjustor	Burnett (2015)

4.1.4 Mode of Action of CHX

The wide spectrum of antimicrobial activity of CHX covers a variety of bacteria such as methicillin sensitive *S. aureus* (MSSA), MRSA, *P. aeruginosa*, *K. pneumoniae*, *Enterococcus faecalis*, *Streptococcus mutans*, *Lactobacillus* and *E. coli* (Karpiński and Szkaradkiewicz, 2015). At low concentrations (0.02%-0.06%), CHX exhibits a bacteriostatic activity against Gram-negative and Gram-positive bacteria and a bactericidal one at higher concentrations (>0.12%) (Jones, 1997). The antimicrobial effect of the bisbiguanide compound is mainly due to the binding of the cationic CHX molecule to the negatively charged phospholipid bacterial membrane. The hydrophobic regions of the CHX molecule are not flexible and long enough to interlink themsleves in the bacterial cell membrane (Spellberg and Gilbert, 2014). Therefore, CHX creates bridges between adjacent head groups of phospholipids and displaces the Mg^{2+} and Ca^{2+} cations (Figure 4.2.B) (Wand *et al.*, 2017). Interestingly, the distance between the phospholipid groups compares closely to the length of the hexamethylene chain of the CHX molecule, which facilitates the binding of each biguanide moiety to a phospholipid headgroup (Gilbert and Moore, 2005). The damage caused to the bacterial membrane affects its osmoregulation and fluidity and leads to cytoplasmic leakage (Figure 4.2.C). The low concentration of CHX can force more than 50% of potassium and phosphorous ions and other low weight molecules to be released out of the cytoplasm, but this process is still reversible (McDonnell and Russell, 1999). However, lethal concentrations of CHX causes precipitation of intracellular components including proteins and nucleic and congealing of the cytoplasm (Gilbert and Moore, 2005; Karpiński and Szkaradkiewicz, 2015). Since the first target of the CHX is the cytoplasmic membrane, it might be occasionally trapped by the outer membrane of the Gram-negative bacteria that acts as a permeability block (Cheung *et al.*, 2012; Cieplik *et al.*, 2019).

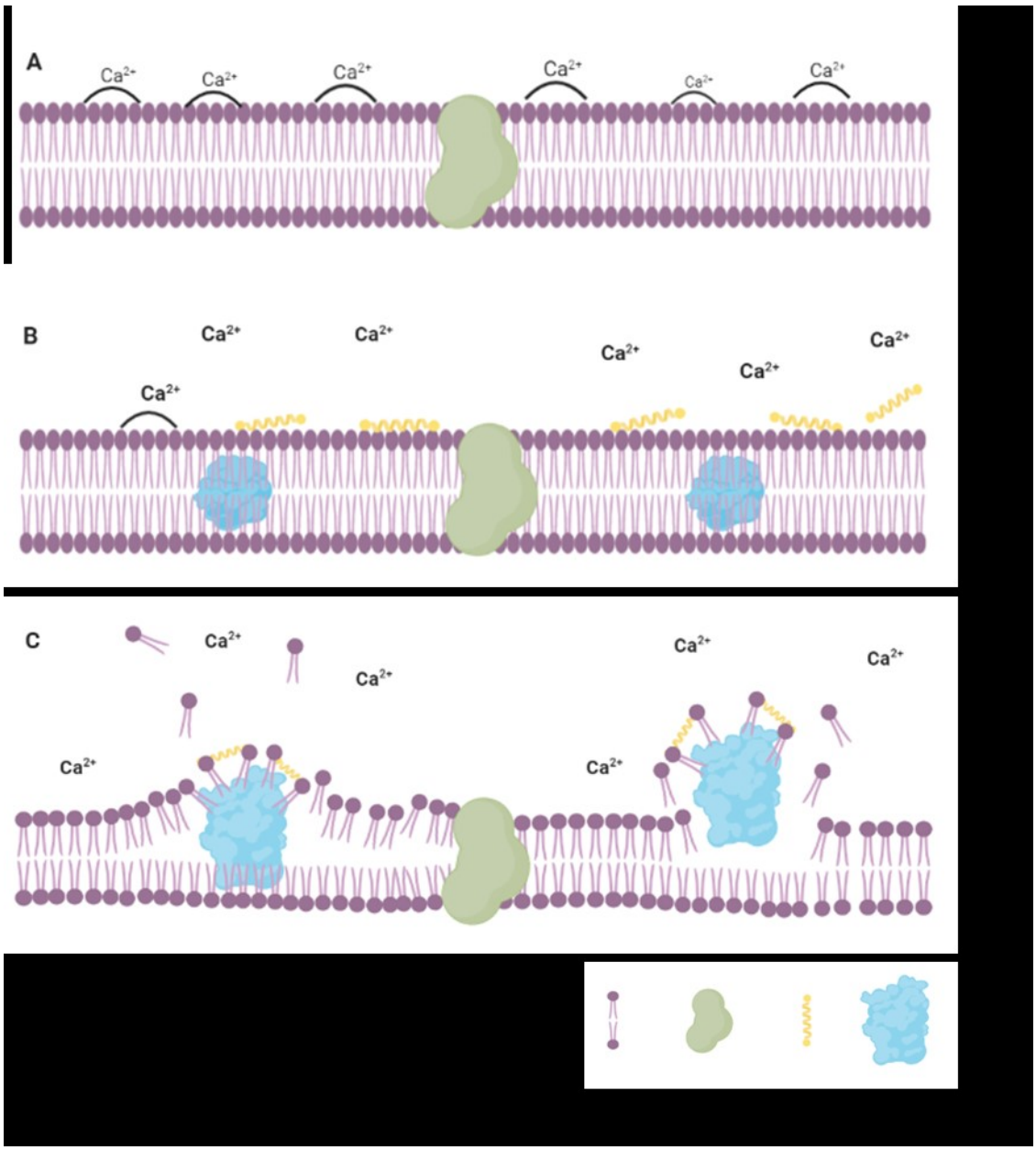

Figure 4.2 Schematic representation of the interaction of CHX with the negatively charged cytoplasmic membrane. (A) The divalent cations (Ca^{2+}) stabilize the structure of the negatively charged phospholipid bilayer that forms a hydrophobic environment protecting the integrity of the implanted proteins (B) The positively charged CHX molecules interact with the cytoplasmic membrane by linking different pairs of phospholipid and replacing the divalent cations (C) The gradual reduction in fluidity and the creation of hydrophilic domains will alter the osmoregulation and metabolic activity of cytoplasmic membrane Figure adopted and modified from Gilbert and Moore (2005) and Cieplik *et al*. (2019).

4.1.5 Resistance Towards CHX

Following the use of CHX as an antiseptic for several decades, a reduced susceptibility has increasingly emerged in clinical isolates (Saleem *et al.*, 2016). Nevertheless, little attention has been given to bacterial resistance

towards CHX and the cross-resistance between this agent and clinically important antibiotics. The definition of resistance towards antiseptics remains ambiguous. Unlike antibiotic susceptibility testing, there is a lack of standardized susceptibility methods with clear cut-off values for biocides (Vijayakumar and Sandle, 2019). In 1973, a disinfectant failure was reported describing Gram-negative *K. pneumoniae* being able to endure CHX-containing disinfectants (Kampf, 2016). Resistance of *K. pneumoniae* towards CHX is mainly acquired genetically through mechanisms conferring efflux pumps, changes in the structure of the cell wall or inactivation of the active ingredients (Levy, 2002; Kampf, 2016). Two of the five major multidrug efflux pumps are the Small Multidrug Resistance (SMR) and the Major Facilitator Superfamily (MFS) which is the largest family of secondary transporters (Wassenaar *et al.*, 2015). MFS comprises by itself no less than 74 protein families including qacA and qacB, also known as antiseptic resistance genes (Smith *et al.*, 2008; Wassenaar *et al.*, 2015). qacA/B and qacE were previously detected in *K. pneumoniae* isolates and were correlated to CHX resistance, and it was claimed that the introduction of the resistance gene was a mere reflection of the introduction of biocides (Guo *et al.*, 2015). The association between the exposure of Gram-negative bacteria to small doses of biocides and the cross resistance to antibiotics is still controversial (Kampf, 2018). For instance, no cross-resistance was reported between CHX and antibiotics among 130 *Salmonella* isolates and 101 *Burkholderia* isolates (Rose *et al.*, 2009; Beier *et al.*, 2011). However, a positive link between resistance towards antibiotics and antiseptics (including CHX) was established among 701 Gram-negative isolates belonging to 16 different genera of *Serratia marcescens* and *Alcaligenes* spp (Maris, 1991). Furthermore, it was found that the highest MIC value for CHX was reported for XDR *K. pneumoniae* in a study involving 126 resistant *K. pneumoniae* clinical isolates (Naparstek *et al.*, 2012).

4.2 Aim

The aim of this chapter was to determine the possibility of implementing metal ions or combinations of metal ions and graphene-based compounds into the skin cleanser formulation, as a potential substitution to CHX gluconate. Hence, a commercial antimicrobial skin cleanser that is commonly used in UK hospitals as a standard pre-operative hand disinfection and skin antisepsis was selected for further study.

4.3 Materials and Methods

4.3.1 Cell Cytotoxicity Testing of the Tested Compounds

The cell viability assay was performed to determine the cytotoxic effect of the metal ions and graphene-based compounds on cell viability and proliferation *in-vitro* using MTS assay as previously described (section 2.2.11). The compounds tested here were the ones exhibiting the best antimicrobial effect against *K. pneumoniae* and *S. aureus* at the following concentrations (In (26.04 mg/L), Au (10.42 mg/L), Ga (10.42 mg/L), Pt (15.62 mg/L), Pd (20.83 mg/L), Mo (15,62 mg/L), Sn (15.62 mg/L), Gr (26.00 mg/L) and GO (26.0 mg/L)).

4.3.2 Susceptibility Testing of *K. pneumoniae* Isolates Towards CHX

The broth microdilution method was used to determine the susceptibility of *K. pneumoniae* isolates to CHX as previously described (section 2.2.5) with some modifications. MICs were performed by adding 100 µL of fresh TSB in all the wells (column 1 to 9) in a polystyrene 96 well plate. Next, 100 µL of the CHX gluconate solution (1024 mg/L in sterile distilled water) was added to the first column only. After pipetting the components up and down several times to ensure proper mixing, 100 µL was transferred from column 1 to column 2. Again, the solution was mixed thoroughly using a pipette and 100 µL was transferred to column 3. This step was repeated until column 9 where the 9^{th} 100 µL was discarded. One hundred microliters of fresh bacterial culture, previously prepared (section 2.2.4) and adjusted to 5×10^5 CFU/mL, was added to all the wells (columns 1 to 9). The plate was incubated overnight at 37°C. The last three wells served as controls containing the uninoculated medium only (column 10), CHX only (column 11), and bacterial culture only (column 12). The results were read after 18 h - 24 h, and the MICs were recorded as the lowest CHX concentration inhibiting visible growth of bacteria in broth wells. Bacterial growth was viewed as “turbidity” compared to that of an uninoculated well (column 10 - negative control). For MBC analysis, 10 µL of the MIC well and the preceding wells were inoculated onto TSA plates and incubated at 37°C for 18 h. MBC

was defined as the lowest concentration showing no bacterial colonies. *K. pneumoniae* ATCC 13883 (MIC = 16 mg/L) was included in the experiment as a control strain. The testing was repeated for each strain in triplicate from three separate cultures.

4.3.3 Adaptation of *K. pneumoniae* Isolate to CHX

K. pneumoniae was adapted to CHX as described by Wand *et al*. (2017) and Bock *et al*. (2016) with modifications. *K. pneumoniae*-NK1 isolate was grown in 3 mL of TSB containing a quarter of the MIC of CHX of the corresponding isolate (previously tested in section 4.3.2) in a shaking incubator (250 rpm) at 37°C. The culture was passaged on alternate days into fresh TSB containing the same concentration of CHX. The concentration of CHX was doubled on alternate passages and the procedure was repeated to reach a final concentration of 256 mg/L. For subsequent analysis, the *K. pneumoniae* adapted strain was passaged 8-10 times grown on TSA plate at 37 °C in the absence of the selective pressure. Any subsequent assays were performed on the passaged strains that were designated as *K. pneumoniae*-NA.

4.3.4 Assessment of the Susceptibility of CHX-Adapted *K. pneumoniae* Isolate Towards Antibiotics, Metal Ions and Graphene Composites

K. pneumoniae-NA was tested to determine whether adaptation to CHX led to any changes in bacterial susceptibility/resistance toward the tested antibiotics, metal ions or graphene-based compounds. The antibiotic susceptibility testing of *K. pneumoniae*-NA was tested against the previously tested antibiotics (section 2.2.2) according to EUCAST guidelines. Additionally, the antimicrobial activity of the previously tested compounds (metal ions, graphene and graphene oxide) against *K. pneumoniae*-NA were determined using MIC method (section 2.2.5).

4.3.5 Evaluation of the Antimicrobial Activity of CHX in the Presence of an Efflux Pump Inhibitor

Carbonyl cyanide 3-chlorophenyl hydrazine (CCCP) (Sigma Aldrich, UK) was dissolved in 1 mL of distilled water (10 mg/L). The susceptibility of *K. pneumoniae*-NA towards CHX in the presence of CCCP was assessed using the broth microdilution (section 4.3.2). The outcome of adding CCCP on the antimicrobial activity of CHX against the bacterial isolate was defined as effective by at least a 4-fold reduction in MIC.

4.3.6 Fractional Inhibitory Concentration

The interaction between the excipients of the skin cleanser (Table 4.1) with metal ions and graphene composites in different combinations was assessed by calculating the FIC (section 2.2.7). Each metal ion (In (26.04 mg/L), Ga (7.8 mg/L), Au (7.8 mg/L), Pt (15.62 mg/L), Pd (20.83 mg/L), Mo (13.02 mg/L), and Sn (13.02 mg/L)) was tested at its previously determined MIC. The components of the skin cleanser including LDAO (0.1 mg/mL), gluconolactone (0.2 mg/mL), isopropyl alcohol (70%), herbacol (0.05%), NaOH (25%), poloxamer 237 (5%), glycerol (60%) and PEG7 (2%) were dissolved in water. The tested components were classified as having a synergistic effect if $\sum FIC \leq 0.5$, an additive effect if $0.5 < \sum FIC \leq 1$, an indifferent effect if $1 < \sum FIC \leq 4$ and an antagonistic effect if $\sum FIC > 4$.

4.3.7 Preparation of the Skin Cleanser Formulations

Various formulations were developed containing the excipients previously listed (Table 4.1) and different combinations of metal ions and graphene composites. The different compositions of all formulations were prepared according to (Table 4.2).

Table 4.2 Composition of the skin cleanser

Composition (100 mL)														
	F1	**F2**	**F3**	**F4**	**F5**	**F6**	**F7**	**F8**	**F9**	**F10**	**F11**	**F12**	**F13**	**F14**
Poloxamer 237	5 mL	5 mL	5 mL	5 mL	5 mL	5 mL	5 mL	5 mL	5 mL	5 mL	5 mL	5 mL	5 mL	5 mL
ISA (70%)	4 mL	4 mL	4 mL	4 mL	4 mL	4 mL	4 mL	4 mL	4 mL	4 mL	4 mL	4 mL	4 mL	4 mL
LDAO	10 mg	10 mg	10 mg	10 mg	10 mg	10 mg	10 mg	10 mg	10 mg	10 mg	10 mg	10 mg	10 mg	10 mg
Glycerol	60 mL	60 mL	60 mL	60 mL	60 mL	60 mL	60 mL	60 mL	60 mL	60 mL	60 mL	60 mL	60 mL	60 mL
PEG-7	2 mL	2 mL	2 mL	2 mL	2 mL	2 mL	2 mL	2 mL	2 mL	2 mL	2 mL	2 mL	2 mL	2 mL
Gluconolactone	2 mg	2 mg	2 mg	2 mg	2 mg	2 mg	2 mg	2 mg	2 mg	2 mg	2 mg	2 mg	2 mg	2 mg
Ponceau 4R (80%)	0.05 mL	0.05 mL	0.05 mL	0.05 mL	0.05 mL	0.05 mL	0.05 mL	0.05 mL	0.05 mL	0.05 mL	0.05 mL	0.05 mL	0.05 mL	0.05 mL
Herbacol	0.05 mL	0.05 mL	0.05 mL	0.05 mL	0.05 mL	0.05 mL	0.05 mL	0.05 mL	0.05 mL	0.05 mL	0.05 mL	0.05 mL	0.05 mL	0.05 mL
NaOH (25%)	0.05 mL	0.05 mL	0.05 mL	0.05 mL	0.05 mL	0.05 mL	0.05 mL	0.05 mL	0.05 mL	0.05 mL	0.05 mL	0.05 mL	0.05 mL	0.05 mL
Metal ion	In 2.6 mg	Ga 0.8 mg	Au 0.8 mg	Pt 1.6 mg	Pd 2.08 mg	In 3.25 mg	Ga 1.5 mg	Ga 2 mg	Au 1.5 mg	Au 2 mg	Pt 2.5 mg	Pt 3.75 mg	Pd 3 mg	Pd 5 mg
Gr/GO	---	---	---	---	---	Gr 3.25 mg	Gr 1.5 mg	GO 2 mg	Gr 1.5 mg	GO 2 mg	Gr 2.5 mg	GO 3.75 mg	Gr 3 mg	GO 5 mg
Water	qs 100	qs 100	qs 100	qs 100	qs 100	qs 100	qs 100	qs 100	qs 100	qs 100	qs 100	qs 100	qs 100	qs 100

4.3.8 Assessment of Antimicrobial Activity of Formulations Against Bacterial Cells

The *in-vitro* antibacterial activity of the different tested formulations was assessed by measuring the zones of inhibition. TSA agar plates were prepared following the manufacturer's instructions and stored at 4°C until needed. Bacterial cultures of *K. pneumoniae*-NK1 and *K. pneumoniae*-NA were subcultured overnight. One to two colonies of each isolate were suspended in sterile saline and adjusted to 0.5 McFarland standard. Hundred microliters of the suspension was then inoculated on the TSA plates and streaked in three different directions (by rotating the plates around 60 degrees) to ensure proper distribution. The plates were dried for 5 min. Using a cork borer, holes of 5 mm diameters were punched in the inoculated agar. Each formulation (100 µL) was mixed with 50 µL of water and were pipetted slowly in each well to prevent foaming. Following an overnight incubation at 37°C, the diameters of the zones of inhibition were measured and recorded in millimetre (mm). Each formulation was tested in triplicate and results were presented as mean value ± SD.

4.3.9 Assessment of Antibiofilm Activity of the Formulations

The antimicrobial efficacy of the tested formulations (1 mL) against the bacterial biofilms was investigated using CVBA assay (section 2.2.8.2). Each formulation was added to each biofilm well. Results were presented as absorbance at 590 nm, and the samples were blanked with acetic acid solutions containing the corresponding formulations.

4.3.10 Scanning Electron Microscopy

Deformations and morphological changes in the bacterial cells following treatment with CHX or metal ions and/or graphene-based compounds were visualized using SEM (section 2.2.2.10).

4.4 Results

4.4.1 Cell Viability

Metal ions exhibiting the best inhibitory effect against *K. pneumoniae* isolates were tested for their cytotoxicity levels against a commercial human skin fibroblast cell line (WS-1). Cytotoxicity was quantified by spectrophotometric measurements of the formazan production under exposure to different treatments for 24 h (Figure 4.3). Indium, gallium, gold, platinum, palladium, graphene and graphene oxide had little to no cytotoxic effect ($p>0.05$) (Figure 4.3.A). The negative control (untreated cells) showed the highest viability percentage (99.24%), followed by palladium (94%), gold (93%), platinum (92%) and graphene oxide (90%). Gallium, indium and graphene were able to retain the cell viability above 80%. Tin (43%) and molybdenum (39%) were toxic to the fibroblasts ($p<0.05$). The respective acids in which the metal ions were dispersed were tested and showed that 5% HCl and 10% HCl had a detrimental effect on skin cells. When combined with graphene composites, In-Gr, Ga-Gr, Ga-GO, Pt-Gr, Pt-GO, Au-Gr, Au-GO, Pd-Gr, Pd-GO and Ru-Gr did not significantly affect the vitality of the cells ($p>0.05$) (Figure 4.3.B).

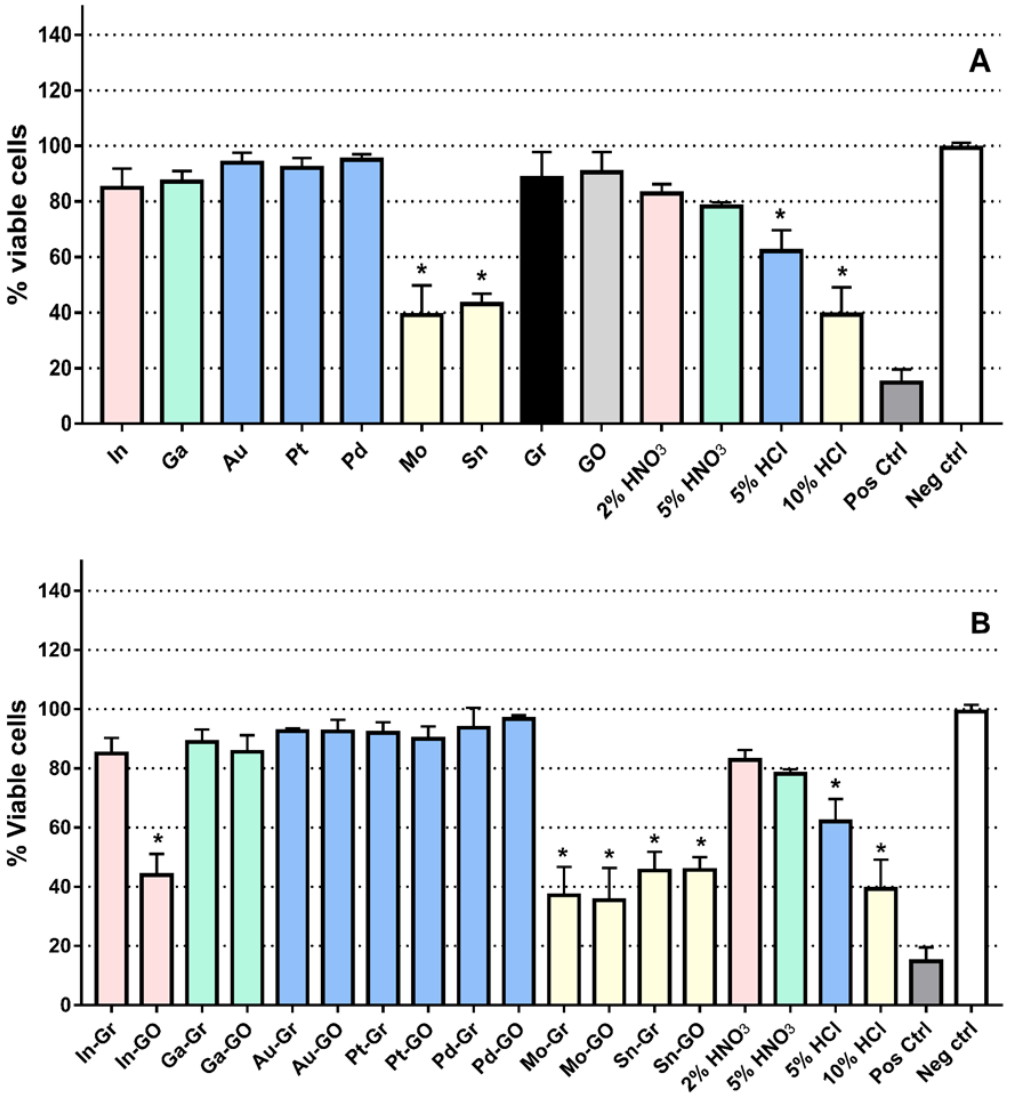

Figure 4.3 Percentage viability of skin fibroblast cells incubated with different treatment of (A) metal ions and (B) metal ions combined with graphene-based compounds. * denotes $p \leq 0.05$ compared to negative control.

4.4.2 Susceptibility Testing of CHX Toward *K. pneumoniae* Isolates

Although there are no clinical standard cut-off values for CHX, the three *K. pneumoniae* isolates showed a high susceptibility to CHX solution with low MIC values ranging between 8-16 mg/L. *K. pneumoniae*-NK1 and *K. pneumoniae*-NK3 were inhibited at 8 mg/L while *K. pneumoniae*-NK2 at 16 mg/L. The *K. pneumoniae*-NK1 isolate was exposed to increasing concentrations of CHX until full adaptation and was designated as *K. pneumoniae*-NA. Serial exposure to CHX led to a 16-fold increase in MIC

from 8 mg/L to 128 mg/L showing a reduced susceptibility of *K. pneumoniae*-NA toward CHX.

4.4.3 Susceptibility Testing of *K. pneumonia*-NA towards Antibiotics

To track changes in the antibiotic susceptibility following CHX adaptation, *K. pneumoniae*-NA was screened against all antibiotics (Table 2.1) previously tested against the *K. pneumoniae* isolates. Out of the 20 antibiotics tested (Table 4.2), no change in antimicrobial susceptibility for *K. pneumoniae*-NA was detected except for colistin and cefepime. The CHX adapted isolate showed decreased susceptibility to colistin. The zone of inhibition of colistin disc was reduced from 24 mm to 8 mm. *K. pneumoniae*-NA also showed resistance towards cefepime with a reduction in ZoI from 31 mm to 16 mm. The resistant profiles were highlighted in blue.

Table 4. 3 Phenotypic antimicrobial resistance pattern of *K. pneumoniae* isolates.

	***K. pneumoniae*-NK1**	***K. pneumoniae*-NKA**
Ampicillin	R	R
Amoxicillin/ Clavulanic acid	R	R
Aztreonam	R	R
Cefotaxime	I	I
Piperacillin/ Tazobactam	R	R
Amikacin	R	R
Gentamicin	S	S
Tobramycin	S	S
Ceftazidime	I	I
Cefalotin	R	R
Cefuroxime	S	S
Cefuroxime Axetil	S	S
Cefepime	S	R
Cefoxitin	S	S
Ertapenem	S	S
Meropenem	S	S
Ciprofloxacin	I	I
Colistin	S	R
Tigecylcine	S	S
Trimethoprim	R	R

S = susceptible, R = resistant (highlighted in blue) and I = intermediate.

4.4.4 Susceptibility Testing of *K. pneumonia*-NA towards Metal Ions, Graphene and Graphene Oxide

The antimicrobial susceptibility of the 18 metal ions, graphene and graphene oxide was tested against *K. pneumoniae*-NA. The MIC and MBC alues of both isolates *K. pneumoniae*-NK1 and -NA were listed and compared (Table 4.4 – 4.5). The results showed that the effect of metal ions remained unchanged after CHX adaptation.

Table 4. 4 MIC values (mg/L) of metal ions, graphene and graphene oxide of *K. pneumoniae*-NK1 (pre-CHX adaptation) and *K. pneumoniae*-NA (post-CHX adaptation).

	MIC (mg/L)		Molarity (mM)	
Metal / Compound	***K. pneumoniae*-NK1**	***K. pneumoniae*-NKA**	***K. pneumoniae*-NK1**	***K. pneumoniae*-NKA**
Cu	125.00 ± 00.00	125.00 ± 00.00	1.967	1.967
Ag	104.17 ± 20.83	104.17 ± 20.83	0.965	0.965
Mo	13.02 ± 2.61	13.02 ± 2.61	0.195	0.195
Pd	20.83 ± 5.21	20.83 ± 5.21	0.135	0.135
Pt	15.62 ± 0.00	15.62 ± 0.00	0.080	0.080
Au	7.80 ± 0.00	7.80 ± 0.00	0.039	0.039
Ta	31.25 ± 0.00	31.25 ± 0.00	0.181	0.181
Zn	125.00 ± 62.50	125.00 ± 62.50	1.911	1.911
Re	52.08 ± 10.42	52.08 ± 10.42	0.278	0.278
Ru	41.67 ± 10.42	41.67 ± 10.42	0.412	0.412
Rh	41.67 ± 10.42	41.67 ± 10.42	0.404	0.404
Sn	13.02 ± 2.61	13.02 ± 2.61	0.109	0.109
Y	41.67 ± 10.42	41.67 ± 10.42	0.485	0.485
Zr	93.75 ± 31.25	93.75 ± 31.25	1.031	1.031
Nb	104.17 ± 20.83	104.17 ± 20.83	1.121	1.121
Al	125.00 ± 62.50	125.00 ± 62.50	4.632	4.632
In	26.04 ± 5.21	26.04 ± 5.21	0.226	0.226
Ga	7.80 ± 0.00	7.80 ± 0.00	0.109	0.109
Graphene	26.00 ± 5.21	26.00 ± 5.21	---	---
Graphene oxide	>500	>500	---	---

Table 4. 5 MBC values (mg/L) of metal ions, graphene and graphene oxide of *K. pneumoniae*-NK1 (pre-CHX adaptation) and *K. pneumoniae*-NA (post-CHX adaptation).

	MIC (mg/L)		Molarity (mM)	
Metal / Compound	***K. pneumoniae*-NK1**	***K. pneumoniae*-NKA**	***K. pneumoniae*-NK1**	***K. pneumoniae*-NKA**
Cu	125.00 ± 00.00	125.00 ± 00.00	1.967	1.967
Ag	125.00 ± 00.00	125.00 ± 00.00	1.159	1.159
Mo	20.83 ± 5.21	20.83 ± 5.21	0.196	0.196
Pd	20.83 ± 5.21	20.83 ± 5.21	0.217	0.217
Pt	15.62 ± 0.00	15.62 ± 0.00	0.080	0.080
Au	10.41 ± 2.61	10.41 ± 2.61	0.053	0.053
Ta	62.50 ± 0.00	62.50 ± 0.00	0.363	0.363
Zn	125.00 ± 62.50	125.00 ± 62.50	1.912	1.912
Re	62.50 ± 0.00	62.50 ± 0.00	0.334	0.334
Ru	83.33 ± 20.83	83.33 ± 20.83	0.824	0.824
Rh	83.33 ± 20.83	83.33 ± 20.83	0.810	0.810
Sn	15.63 ± 0.00	15.63 ± 0.00	0.132	0.132
Y	125.00 ± 00.00	125.00 ± 00.00	1.406	1.406
Zr	104.17 ± 20.83	104.17 ± 20.83	1.159	1.159
Nb	125.00 ± 00.00	125.00 ± 00.00	1.346	1.346
Al	208.33 ± 41.67	208.33 ± 41.67	7.722	7.722
In	52.08 ± 10.42	52.08 ± 10.42	0.454	0.454
Ga	10.41 ± 2.60	10.41 ± 2.60	0.147	0.147
Graphene	26.00 ± 5.21	26.00 ± 5.21	---	---
Graphene oxide	>500	>500	---	---

4.4.5 Susceptibility Testing of *K. pneumoniae*-NA towards CHX in the Presence of CCCP

The susceptibility of *K. pneumoniae*-NA isolate toward CHX was assessed in the absence and presence of CCCP. The results showed that the addition of CCCP had reduced the MIC of CHX from 128 mg/L to 16 mg/L, resulting in an 8-fold reduction.

4.4.6 Synergy Testing Between Excipients of the Skin Cleanser and Metal Ions

Synergy testing between the different excipients of the surgical scrub and metal ions and graphene composites was investigated to rule out antagonistic effects between any two or more factors. A total of 252 different combinations were tested against each of *K. pneumonie*-NK1 and *K. pneumoniae*-NA, and the FICs were calculated. The results indicated that no antagonistic effect was revealed between the metal ions and any of the cleanser's components tested singularly or in different combinations. When each excipient was tested individually with metal ions, a synergistic effect was noted for poloxamer 237 with In (FIC = 0.50), Ga (FIC = 0.44), Pt (FIC = 0.5), Pd (FIC = 0.31), and Au (FIC = 0.39) against both isolates (Tables 4.6 and 4.7). PEG-7 also exhibited an additive effect when combined with each metal ion In (FIC = 1.00, FIC = 0.88), Ga (FIC = 0.68, FIC = 0.75), Pt (FIC = 0.88, FIC = 0.75), Pd (FIC = 1.00, FIC = 0.88), and Au (FIC = 0.96, FIC = 0.88) against *K. pneumoniae*-NK1 and *K. pneumoniae*-NA, respectively (Tables 4.6 and 4.7). Furthermore, glycerol displayed a synergistic effect with graphene (FIC= 0.5; FIC= 0.03).

When various combinations of different components were tested, poloxamer 237-ISA combination showed a synergistic effect with the five metal ions (In (FIC = 0.33, FIC = 0.25), Ga (FIC = 0.31), Pt (FIC = 0.33), Pd (FIC = 0.39), Au (FIC = 0.5)). Additionally, an additive effect with each of poloxamer 237-glycerol, PEG-7-glycerol and poloxamer 237-PEG-7 combinations (FIC≤1) against both isolates (Tables 4.8 and 4.9). Graphene showed a synergistic effect with poloxamer 237 (FIC = 0.21, FIC = 0.50) and glycerol (FIC = 0.50,

FIC = 0.33) only, while showing an additive effect toward glycerol-ISA (FIC = 0.73), poloxamer 237-glycerol (FIC = 0.88, FIC = 0.77) and PEG-7-glycerol (FIC = 0.66), and an indifferent effect with the rest of the tested components FICs (1.11 – 3.33). Graphene oxide, on the other hand, revealed an indifferent effect against all tested combinations. No discrepancy in the results was noted between the two isolates *K. pneumoniae*-NK1 and *K. pneumoniae*-NA. All the FIC values of the various tested combinations against both bacterial isolates were listed (Tables 4.6-4.9). The synergistic interactions were highlighted in yellow, while the additive interactions in blue.

Table 4.6 FIC values of excipients of the skin cleanser, tested individually, with metal ions, graphene and graphene oxide against *K. pneumoniae*-NK1.

	In	Ga	Pt	Pd	Au	GO	Gr
Poloxamer 237	0.50	0.44	0.50	0.31	0.39	1.11	0.21
ISA	1.44	1.03	1.45	1.50	1.36	1.96	1.68
LDAO	3.00	3.67	2.12	1.46	1.75	1.50	2.68
Glycerol	1.21	1.10	1.30	2.06	1.06	1.11	0.50
PEG - 7	1.00	0.68	0.88	1.00	0.96	2.30	1.21
Gluconolactone	2.33	2.00	3.00	2.67	1.80	2.09	2.21
Ponceau 4R	2.40	3.67	2.00	2.00	2.70	2.25	2.25
NaOH	3.67	3.00	1.80	3.00	1.17	3.00	3.00

Table 4.7 FIC values of excipients of the skin cleanser, tested individually, with metal ions, graphene and graphene oxide against K. pneumoniae-NA.

	In	Ga	Pt	Pd	Au	GO	Gr
Poloxamer 237	0.31	0.44	0.50	0.31	0.39	1.11	0.25
ISA	1.44	1.03	1.45	1.50	1.36	1.96	1.68
LDAO	3.00	3.67	2.12	1.46	1.75	1.50	2.68
Glycerol	1.21	1.22	1.30	2.06	1.75	1.11	0.33
PEG-7	0.88	0.75	0.75	0.88	0.88	1.75	1.11
Gluconolactone	2.33	2.00	3.00	2.67	1.80	2.09	2.21
Ponceau 4R	2.40	3.67	2.00	2.00	2.70	2.25	2.25
NaOH	3.67	3.00	1.80	3.00	1.17	3.00	3.00

Table 4.8 FIC values of excipients of the skin cleanser, tested in combination, with metal ions, graphene and graphene oxide against *K. pneumoniae*-NK1

	In	Ga	Pt	Pd	Au	GO	Gr
Poloxamer 237 - ISA	0.34	0.31	0.33	0.39	0.50	1.30	1.11
LDAO - ISA	1.33	2.46	2.36	1.71	2.71	1.12	1.25
Glycerol - ISA	1.46	1.20	1.68	2.31	1.11	1.88	0.73
PEG - 7 - ISA	1.87	2.68	1.11	1.75	1.66	1.25	2.09
Gluconolactone - ISA	2.50	2.21	1.46	1.96	3.15	2.46	2.15
Ponceau 4R - ISA	1.15	2.21	2.25	2.12	3.21	3.09	2.96
NaOH - ISA	2.33	2.25	1.25	2.25	1.50	2.31	3.03
Poloxamer 237 - LDAO	1.96	1.11	2.68	2.11	1.75	1.96	1.11
Glycerol - LDAO	1.88	1.33	1.25	1.11	1.50	1.11	1.33
PEG-7 - LDAO	1.33	1.50	1.50	1.67	2.00	1.17	1.80
Gluconolactone - LDAO	2.12	1.46	2.09	3.12	2.03	2.21	2.12
Ponceau 4R - LDAO	2.68	1.46	3.25	2.09	2.06	3.03	2.96
NaOH - LDAO	2.00	2.25	2.25	2.40	3.00	3.67	3.33
Poloxamer 237 - Glycerol	0.65	0.73	0.75	0.68	0.69	1.11	0.88
PEG - 7 - Glycerol	0.75	1.00	1.00	0.96	0.83	1.31	0.66
Gluconolactone - Glycerol	1.75	2.15	2.11	1.75	1.06	2.46	1.27
Ponceau 4R - Glycerol	2.27	3.21	1.46	1.31	2.11	1.12	2.30
NaOH - Glycerol	3.12	3.31	2.68	3.40	2.50	2.68	1.31
Poloxamer 237 - PEG - 7	0.68	0.96	1.00	0.87	0.99	1.11	1.11
Gluconolactone - PEG - 7	1.34	2.13	1.25	3.12	2.06	1.12	2.30
Ponceau 4R - PEG - 7	2.75	2.30	3.25	2.75	3.06	2.96	1.46
NaOH – PEG - 7	1.75	3.06	2.22	2.15	3.40	1.30	1.75
Poloxamer 237- Gluconolacone	1.75	2.50	1.88	1.11	1.67	1.88	2.75
Ponceau 4R - Gluconolacone	1.21	2.68	1.75	2.37	2.13	2.46	3.15
NaOH - Gluconolacone	2.12	2.06	3.09	1.98	3.31	1.46	1.21
Poloxamer 237 - Ponceau 4R	1.09	1.46	2.15	1.96	1.21	1.30	1.31
NaOH - Ponceau 4R	2.21	1.30	2.68	3.13	2.96	2.11	2.25

Table 4.9 FIC values of excipients of the skin cleanser, tested in combination, with metal ions, graphene and graphene oxide against *K. pneumoniae*-NA

	In	Ga	Pt	Pd	Au	GO	Gr
Poloxamer 237-ISA	0.25	0.31	0.33	0.39	0.50	1.30	1.11
LDAO-ISA	1.33	2.46	2.36	1.71	2.71	1.12	1.25
Glycerol - ISA	1.46	1.20	1.68	2.31	1.11	1.88	0.73
PEG-7 - ISA	1.33	2.11	1.06	2.00	1.66	1.11	2.50
Gluconolactone - ISA	2.50	2.21	1.46	1.96	3.15	2.46	2.15
Ponceau 4R - ISA	1.15	2.21	2.25	2.12	3.21	3.09	2.96
NaOH - ISA	2.33	2.25	1.25	2.25	1.50	2.31	3.03
Poloxamer 237-LDAO	1.75	1.11	2.68	2.11	1.75	1.96	1.11
Glycerol - LDAO	1.88	1.33	1.25	1.11	1.50	1.11	1.33
PEG-7 - LDAO	1.33	1.50	1.50	1.67	2.00	1.17	1.80
Gluconolactone-LDAO	2.12	1.46	2.09	3.12	2.03	2.21	2.12
Ponceau 4R - LDAO	2.68	1.46	3.25	2.09	2.06	3.03	2.96
NaOH - LDAO	2.00	2.25	2.25	2.40	3.00	3.67	3.33
Poloxamer 237 - Glycerol	0.75	0.75	0.83	0.69	1.00	1.11	0.77
PEG-7 - Glycerol	1.00	0.86	1.00	0.96	0.83	1.31	0.66
Gluconolactone - Glycerol	1.75	2.15	2.11	1.75	1.06	2.46	1.27
Ponceau 4R - Glycerol	2.27	3.21	1.46	1.31	2.11	1.12	2.30
NaOH -Glycerol	3.12	3.31	2.68	3.40	2.50	2.68	1.31
Poloxamer 237-PEG7	0.75	1.00	0.88	1.00	1.00	2.33	1.11
Gluconolactone -PEG-7	1.75	2.00	2.13	3.12	1.25	1.33	2.00
Ponceau 4R - PEG-7	1.86	2.00	3.33	2.15	3.11	1.75	1.46
NaOH - PEG-7	1.46	3.11	2.06	3.15	3.40	1.75	1.75
Poloxamer 237 - Gluconolacone	2.15	2.50	1.88	1.11	1.67	1.88	2.75
Ponceau 4R - Gluconolacone	1.21	2.68	1.75	2.37	2.13	2.46	3.15
NaOH - Gluconolacone	2.12	2.06	3.09	1.98	3.31	1.46	1.21
Poloxamer 237 - Ponceau 4R	1.68	1.46	2.15	1.96	1.21	1.30	1.31
NaOH - Ponceau 4R	2.21	1.30	2.68	3.13	2.96	2.11	2.25

4.4.7 Testing of the Antimicrobial Activity of the 14 Formulations

4.4.7.1 Testing of The antimicrobial Activity of the 14 Formulations against the Planktonic Forms of *K. pneumoniae*-NK1 and *K. pneumoniae*-NA

The *in-vitro* antibacterial activity of the tested formulations against the two bacterial isolates was assessed by measuring and comparing their zones of inhibition. ZoI is defined as the clear region surrounding the well and reflects the efficiency of the tested antimicrobial. Formulations (F1 to F14) were diluted (1:1) in water before testing. The results indicated that the ZoIs recorded for each formulation (F1 to F14) demonstrated a similar trend for both *K. pneumoniae*-NK1 and *K. pneumoniae*-NA. However, the inhibitory effect of the CHX gluconate towards *K. pneumoniae*-NK1 (9 mm) was larger than that of *K. pneumoniae*-NKA (6 mm). Among the 14 tested combinations, F9 (Au-Gr) (25 mm, 23.75 mm) showed the largest ZoI, followed by F3 (Au) (23 mm, 21.5 mm), F4 (Pt) (21mm, 19.75mm), F11 (Pt-Gr) (20 mm, 21.5 mm) and F5 (Pd) (20 mm, 20 mm), F13 (20 mm, 20 mm) and F10 (19.55 mm, 20 mm) against *K. pneumoniae*-NK1 and *K. pneumoniae*-NA, respectively. The diameters of zones (ZoI ± SD) of inhibition of all formulations are listed in appendix G.

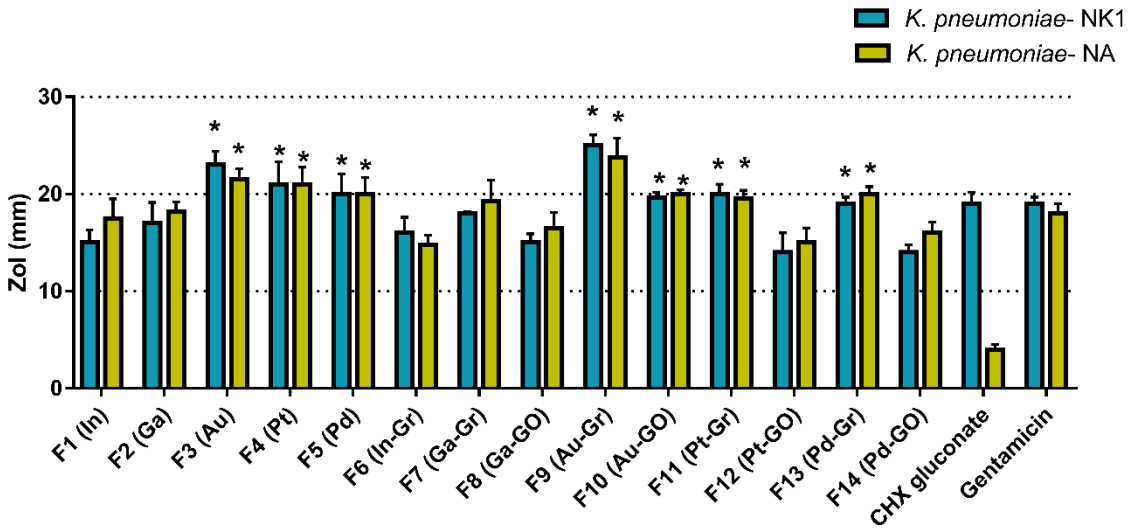

Figure 4.4 Antimicrobial activity (ZoI) of various skin cleansers formulations (F1 to F14) containing different metal ions and graphene composites against (A) *K. pneumoniae*-NK1 and (B) *K. pneumoniae*-NA (n=3, results shown as mean ± SD).* denotes $p \leq 0.05$ when compared to CHX gluconate and gentamicin.

4.4.7.2 Testing of The Antimicrobial Activity of the 14 Formulations against the Biofilm Forms of *K. pneumoniae*-NK1 and *K. pneumoniae*-NA

The fourteen formulations were tested against 7 day-biofilms of the same bacterial isolates. The CVBA assays indicated that, except for F10 (Au-GO), the same formulations that inhibited the planktonic forms of *K. pneumoniae*-NK1 and –NA were able to disrupt their biofilms preventing further growth. The best antibiofilm activity against both isolates was noted for F9 (Au-Gr) followed by F3 (Au), F4 (Pt), F11 (Pt-Gr), F5 (Pd), F2 (Ga) and F13 (Pd-Gr) (p= 0.001) against both isolates (Figure 4.5). Additionally, the antimicrobial activity of five of these formulations (F9 (Au-Gr), F3 (Au), F4 (Pt), F11 (Pt-Gr) and F2 (Ga)) was significantly greater than the antimicrobial activity of CHX alone, even against the CHX susceptible isolate (*K. pneumoniae*-NK1). The 14 formulations showed no difference in their antimicrobial activity against the biofilms of CHX-susceptible (-NK1) and adapted strains (-NA) (Figure 4.5). The diameters of zones (ZoI ± SD) of inhibition of all formulations are listed in appendix H.

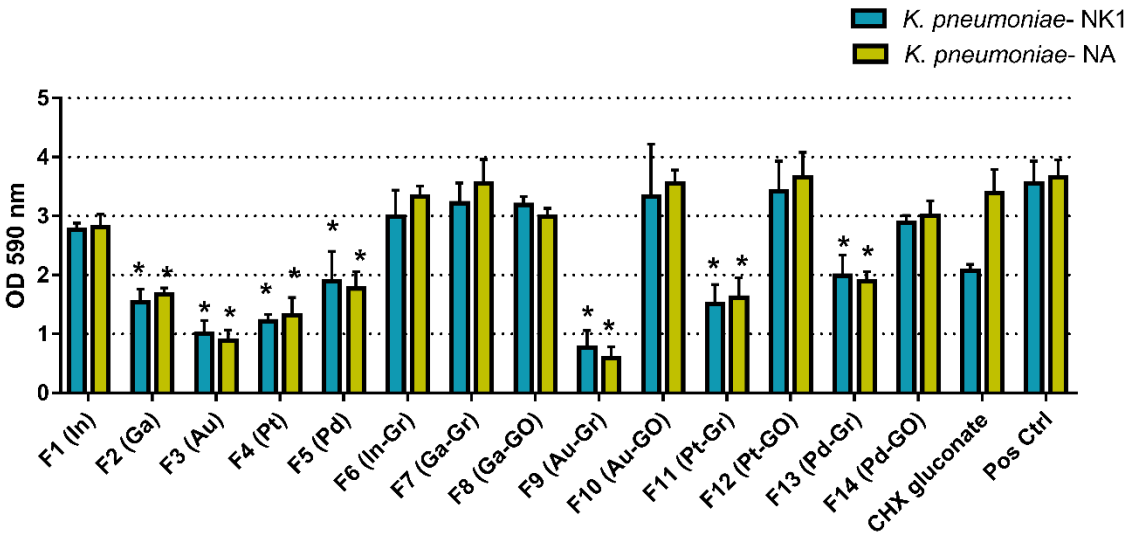

Figure 4.5 Antibiofilm activity as determined by CVBA of various skin cleansers formulations (F1 to F14) containing different metal ions and graphene composites against (A) *K. pneumoniae*-NK1 and (B) *K. pneumoniae*-NA (n = 3, results shown as mean ± SD). * denotes p≤0.01 compared to the control.

4.4.7.3 Testing of the Efficacy of the Formulations In the Presence of CHX.

To investigate any synergistic activity between CHX gluconate with the metal ions and graphene composites**,** CHX gluconate (3%) was added to formulations F1-F14 and tested against *K. pneumonia*-NA. The addition of CHX gluconate to F2 (Ga) (*p*= 0.01), F3 (Au), F4 (Pt) , F7 (Ga-Gr), F9 (Au-Gr) (*p*= 0.001) led to a expansion in their ZoIs, reflecting an enhanced antimicrobial activity (Figure 4.6). The diameters of zones of inhibition (ZoI ± SD) are listed in appendix H.

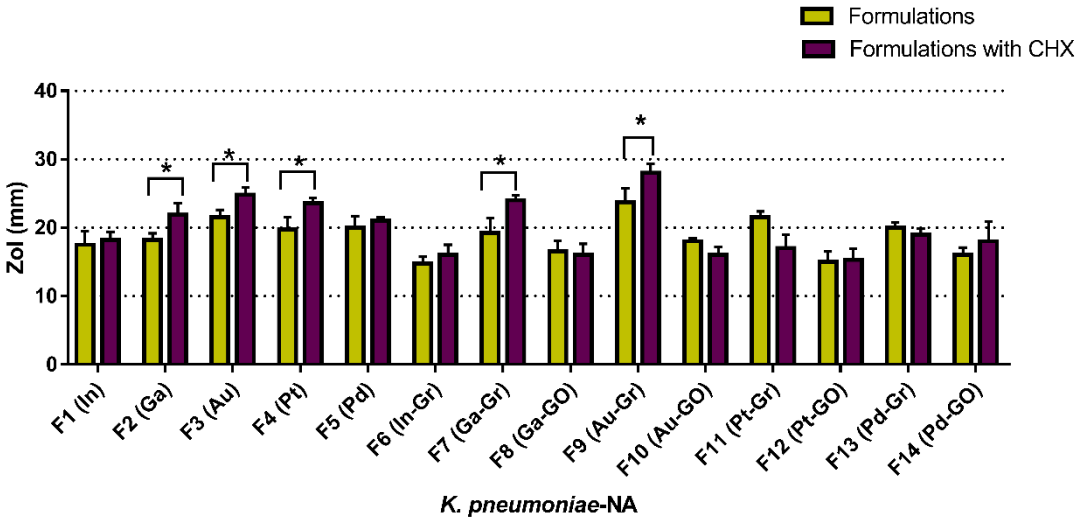

Figure 4.6 Antimicrobial activity (ZoI) of various skin cleansers formulations (F1 to F14) containing different metal ions, graphene composites and CHX gluconate against *K. pneumoniae*-NA (n = 3, results shown as mean ZoI ± SD). * denotes *p*≤0.05.

4.4.8 Scanning Electron Microscopy

Scanning electron microscopy was used to visualize the effects of metal ions, metal ions/graphene combinations, and the tested formulations on the *K. pneumoniae* cells. The untreated control cells of *K. pneumoniae*-NK1 (1680 ± 20 nm) (Figure 4.7a) and –NA (2060 ± 43 nm) (Figure 4.7b) showed intact plump rod shaped cells.

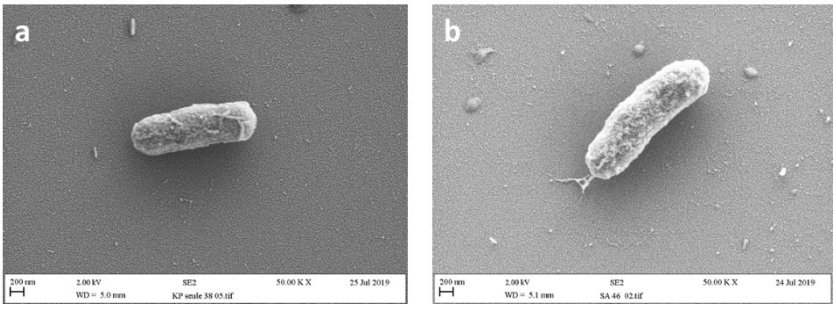

Figure 4.7 SEM images illustrating *K. pneumoniae*-NK1 (a) and *K. pneumoniae*-NA (b) in untreated media.

The morphological changes in bacterial cells treated with metal ions were prominent. Flattened surfaces with curved centres were detected in the presence of In (Figure 4.8a) or Pd (Figure 4.8j). Grooves and pits in the cellular membranes were visualized in bacterial membranes treated with every metal ion tested (Figure 4.8 a-j). *K. pneumoniae*-NA showed an elongated shape with rough surface membrane when treated Pt (Figure 4.8h).

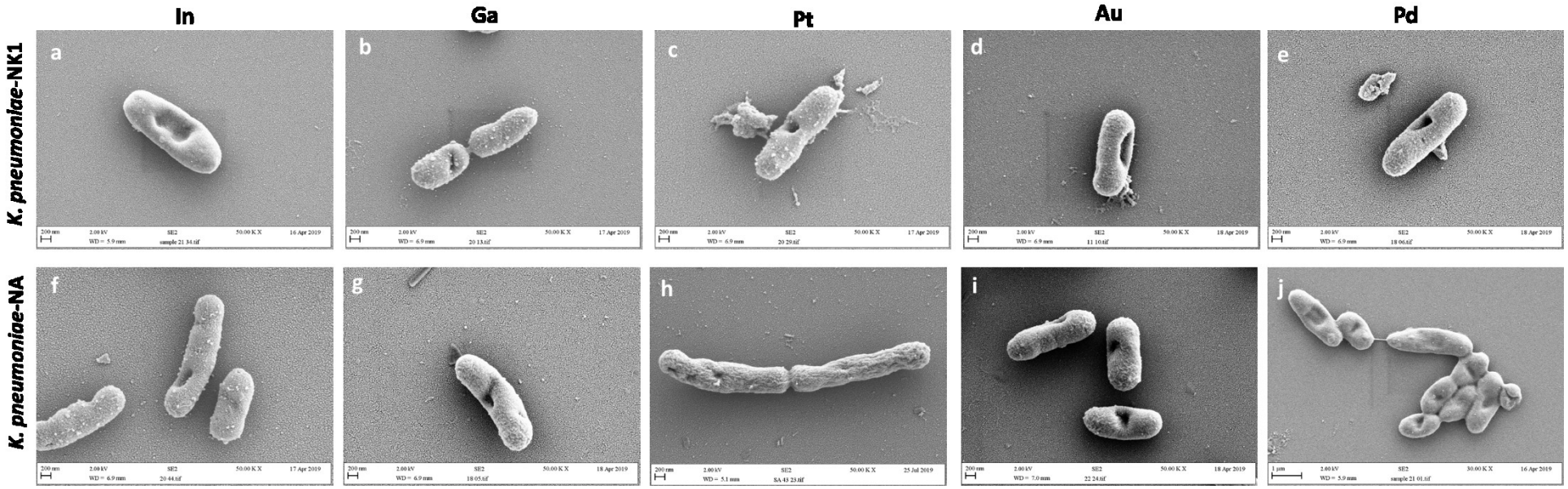

Figure 4.8 SEM images illustrating morphological changes in cell membrane in *K. pneumoniae*-NK1 (a-e) and *K. pneumoniae*-NA (f-j) following their treatment with (a,f) In, (b,g) Ga, (c,h) Pt, (d,i) Au and (e,j) Pd.

The antimicrobial activity of the combinations Au-Gr (Figure 4.9a), Ga-Gr (Figure 4.9b), In-Gr (Figure 4.9c) and Pt-Gr (Figure 4.9d and 4.9i) was revealed by deep grooves in the cell walls. Following the addition of graphene to metal ions, the bacterial membrane of *K. pneumoniae* appeared rough, with deep folding and swollen edges (Figure 4.9 d-j). A complete distortion of the bacterial membrane was detected following the Pt-Gr treatment (Figure 4.9d).

Formulations (F3 (Au), F4 (Pt), F5 (Pd), F9 (Au-Gr) and F11(Pt-Gr) tested revealed complete deformations in the bacterial morphology, including elongation of cells (4500 ± 100 nm) (Figures 4.10j), deep grooves and pits (Figures 4.10 c-j), rough folded surfaces (Figures 2.10 a-b).

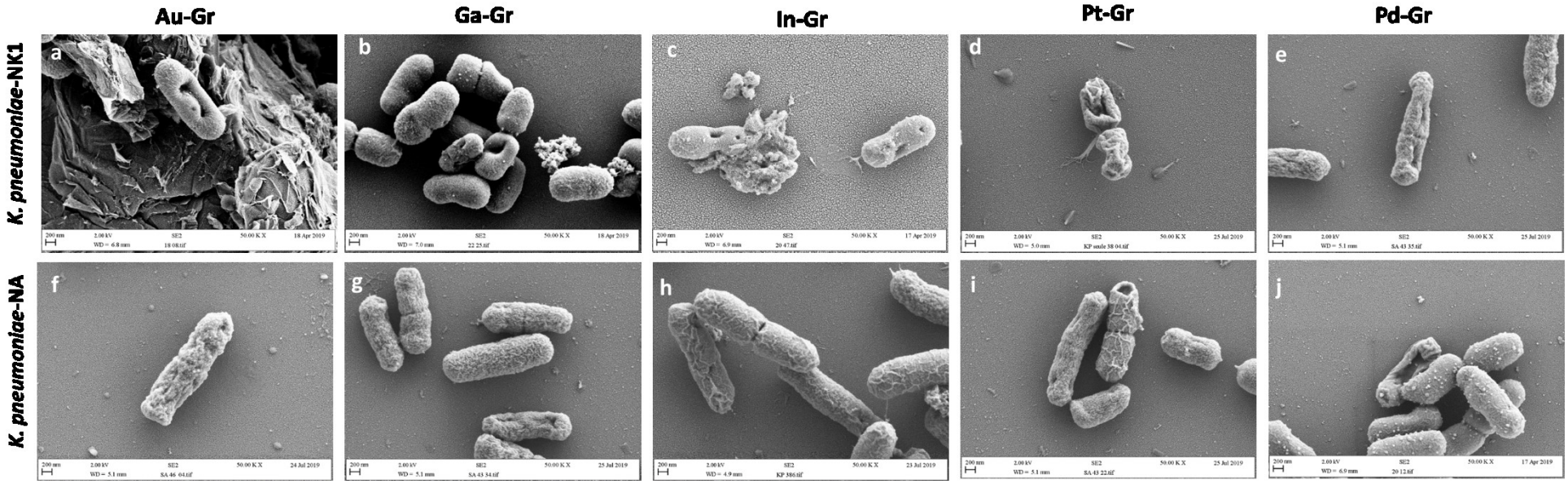

Figure 4.9 SEM images illustrating morphological changes in cell membrane in *K. pneumoniae*-NK1 (a-e) and *K. pneumoniae*-NA (f-j) following their treatment with (a,f) In-Gr, (b,g) Ga-Gr, (c,h) Pt-Gr , (d,i) Au-Gr and (e,j) Pd-Gr.

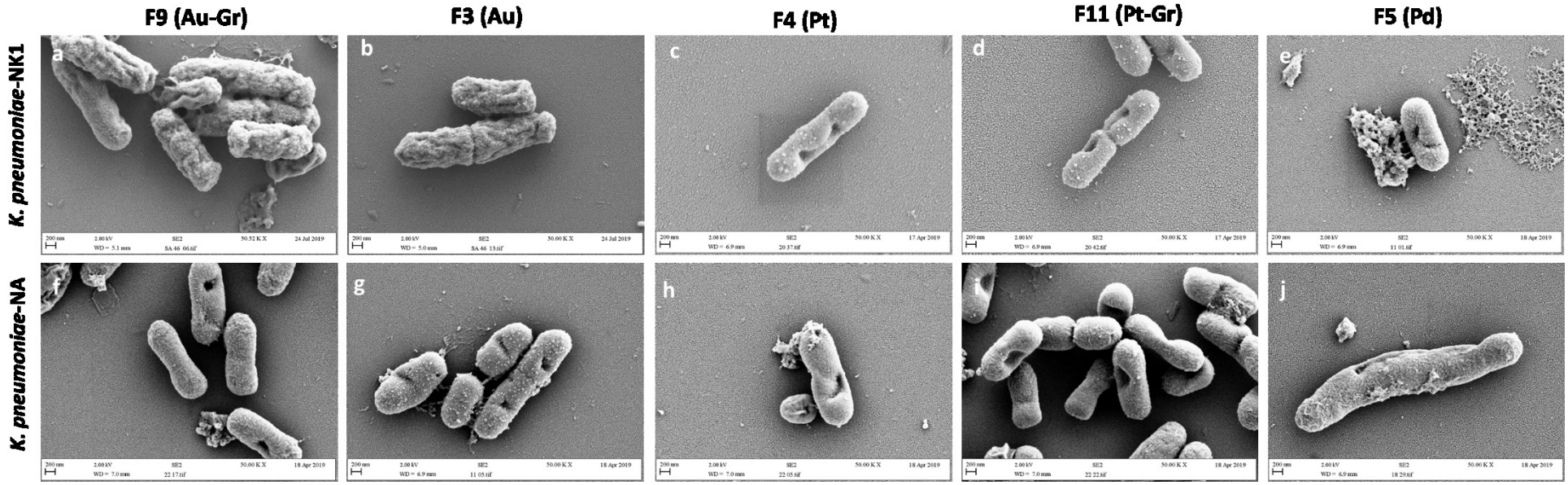

Figure 4.10 SEM images illustrating morphological changes in cell membrane in *K. pneumoniae*-NK1 (a-e) and *K. pneumoniae*-NA (f-j) following their treatment with (a,f) F9 (Au-Gr), (b,g) F3 (Au), (c,h) F4 (Pt), (d,i)F11 (Pt-Gr)and (e,j) F5 (Pd).

The antimicrobial efficacies of CHX and F9 (Au-Gr) were compared against CHX adapted *K. pneumoniae*-NA. SEM confirmed that the treatment with F9 (Au-Gr) formulation (Figure 4.11c) led to considerably greater and morphological changes (deep grooves) in CHX-adapted cells (*K. pneumoniae*-NA) compared to CHX treatment (Figure 4.11b).

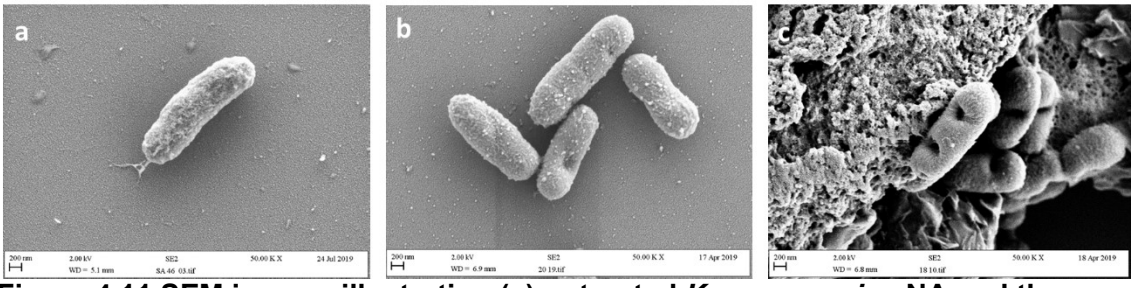

Figure 4.11 SEM images illustrating (a) untreated *K. pneumoniae*-NA and the difference in treatment of *K. pneumoniae*-NA with (b) CHX gluconate and (c) F9 formulation containing Au-Gr.

4.5 Discussion

The high global incidence of *K. pneumoniae* infections has led to an increased awareness of to the hazards of nosocomial infections and this has launched an urge for upgrading infection control and hygienic standards (Abuzaid *et al.*, 2012). At least 17% of *K. pneumoniae* infections in intensive care units are associated with the extensive use of cationic biocides including CHX (Abuzaid *et al.*, 2012). Since 2007, numerous outbreaks have been reported correlated with contaminated CHX solutions (Weber *et al.*, 2007; Kampf, 2016).

4.5.1 Cytotoxicity Assays

In the present study, the cytotoxicity of seven metal ions, graphene and GO was evaluated against skin fibroblasts (WS1 skin cell line). Fibroblasts are cells within the dermis layer of skin. They allow the epithelial cells of the epidermis to effectively join together to form the top layer of the skin (Lynch and Watt, 2018). The MTS readings showed that Ga, Au, Pt, Pd and In were not toxic to the WS1 cells. Metals have been suggested as promising material for biological applications, and their cytotoxicity has been investigated in different forms (ions, alloys) (Penders *et al.*, 2017). For instance, the cytotoxicity of Au nanoparticles toward human dermal fibroblasts was evaluated at different concentrations (0.5 to 100 mg/L) for four days and confirmed that no significant cell viability changes were recorded at any concentration (Penders *et al.*, 2017). This was in agreement with the results whereby gold was shown to be inert to fibroblast cells at 7.8 mg/L. More specifically, there was no indication of any toxic effects or morphological changes in human dermal fibroblasts following their treatment with gold nanoparticles at 500-1000 µg/mL (Penders *et al.*, 2017). Penders *et al*. (2017) also reported that gold cytotoxicity is determined to a large extent by its shape, with Au nanoflowers exhibiting the least cytotoxic cell behaviour toward mammalian cells compared to Au spheres or Au stars.

Gallium and In showed no cytotoxicity in this study at 7.8 mg/L and 26 mg/L. Similarly, Chandler *et al*. (1994) found no significant cytotoxic effects to L-929 fibroblasts for both Ga and In ions when tested at a concentration range

of 10^{-3} to 1 mM. On the contrary, Schedle *et al*. (1995) reported cytotoxic effects of both ions toward L-929 and gingival fibroblasts at the concentration above 10^{-2} mM. The low percentage of viable cells (~40%) revealed by Mo and Sn can be attributed to the fact that both metal ions were diluted in 10% HCl that showed, a similar low vitality rate (40%). On the other hand, the two metal ions were not able to induce cytotoxicity when tested on mouse fibroblasts (Milheiro *et al.*, 2014). The studies investigating the cytotoxicity of Pt and Pd on human skin fibroblasts are scarce. The majority of the reports investigated Pt and Pd as metal alloys or complexes toward mouse fibroblast, mouse embryonic fibroblast cell line, human gingival fibroblasts or monocytes (Wataha *et al.*, 2009; Coskun *et al.*, 2013; Milheiro *et al.*, 2014).

Following the incorporation of graphene and its derivatives into biomedical applications, the toxicity of carbon-based compounds has been debated for the last few years. The results from this work showed that the skin fibroblasts were unaffected, at their tested concentrations, by either graphene or graphene oxide, or the combinations of graphene-based materials with metal ions (In-Gr, Ga-Gr, Ga-GO, Au-Gr, Au-GO, Pt-Gr, Pt-GO, Pd-Gr, Pd-GO and Ru-Gr) (p<0.05). The effect of GO and graphene sheets had previously been explored by Liao *et al*. (2011) who reported that graphene oxide and low densely packed graphene sheets were not damaging to the mammalian fibroblasts. Additionally, data in this thesis were also in agreement with Lasocka *et al*. (2018) who reported no cytotoxicity for graphene on L929 fibroblasts. Lasocka *et al.* (2018) also described an increased cell proliferation and adhesion onto glass upon graphene treatment, suggesting that graphene could be valuable for tissue damage recovery. A discrepancy in the cytotoxicity results of the same metal ions were reported by different studies (Lewinski *et al.*, 2008; Milheiro *et al.*, 2014). It is essential to understand that cell lines are sensitive to changes in their environment and can be easily affected by slight modifications including composition or structure of the tested compound, the surface area of the sample, pH, temperature, and nutrient concentration (Lewinski *et al.*, 2008). Consequently, comparison among the studies was challenging since

different experimental conditions were adapted each time. In addition, it was difficult to find comparable studies using the same cell type (WS-1 cells) and the same metal ions solutions used in this study.

It should be noted that Ag ions were excluded from being tested for cytotoxicity or to be potentially incorporated in the surgical scrub composition for several reasons. Although silver previously exhibited a good antimicrobial activity against three out of the four isolates of *K. pneumoniae*, it was not able to inhibit *K. pneumoniae*-NK1 (MIC = 104 mg/L). Furthermore, increasing evidence has indicated that Ag ions used as topical antimicrobials trigger an oxidative stress response and induce zinc release in human skin fibroblasts (Cortese-Krott *et al.*, 2009). Likewise, MTT assays performed by Milheiro *et al*. (2014) have ranked silver ions as highly cytotoxic against a CCL-1 fibroblast cell line.

4.5.2 Assessment of *K. pneumoniae* Isolate Following Adaptation to CHX

Previous studies have demonstrated that isolates of *K. pneumoniae* are able to adapt to increasing concentrations of CHX, leading to lower susceptibility toward CHX or chlorhexidine-based products (Bock *et al.*, 2016; Wand *et al.*, 2017). It was clear that exposure of *K. pneumoniae*-NA to chlorhexidine in this study was associated with cross-resistance to colistin and cefepime. However, it did not affect its susceptibility towards metal ions. While solid evidence is lacking to prove any link between biocides (such as metal ions) and chlorhexidine resistance, several studies have established the association between chlorhexidine adaptation and cross antimicrobial resistance (Percival *et al.*, 2005; Wand *et al.*, 2017; Hashemi *et al.*, 2019). Cieplik *et al*. (2019) revealed, through whole genome sequencing of chlorhexidine adapted bacterial strains, that the mechanism responsible for cross resistance is due to a mutation in the operon containing *pmrK* (PhoPQ). The upregulation of the target *pmrK* will consequently modify the lipopolysaccharides by replacing the phosphate groups by 4-amino-4-deoxy-L-arabinose. As a result, the net negative charge of lipid A and the bacterial binding affinity to colistin are reduced, respectively (Wand *et al.*,

2017). Additionally, Hashemi *et al*. (2019) was able to show that the colony morphology of *K. pneumoniae* resistant to chlorhexidine changed from a circular smooth shape into rough colonies with undulating margins. This transformation was associated with a higher-mass lipopolysaccharides' shift protecting *K. pneumoniae* from polymixins (colistin).

Fraud *et al.* (2008) showed that chlorhexidine can also induce the MexCD-OprJ pump which contributes to the intrinsic resistance of Gram-negative bacteria (*P. aeruginosa*) towards different classes of antibiotics including macrolides, tetracycline, fluoroquinolone and ß-lactams including cefepime. MexCD-OprJ is typically quiescent in wild-type cells, but is expressed in multidrug resistant *nfxB* mutants (Morita *et al.*, 2003). The overexpression of the *mex*CD-*opr*J is a response to the damage of the bacterial membrane caused by chlorhexidine (Fraud *et al.*, 2008). Furthermore, Nde *et al*. (2009) demonstrated, through global transcriptome analysis, that sub-concentrations of chlorhexidine (4 mg/L) were able to upregulate *mex*C and *mex*D, 14 and 6 times, respectively, following ten minutes exposure time. In particular, it is believed that MexCD-OprJ plays an important role in the dissemination of the multidrug resistance of *P. aeruginosa* in clinical settings, where disinfectants (chlorhexidine gluconate and benzalkonium chloride) are frequently used (Morita *et al.*, 2003).

Due to increased disinfectants and antiseptics (including CHX) resistance often being correlated with increased efflux, the MIC for CHX was retested in the presence of the known efflux pump inhibitor (CCCP) (Wand *et al.*, 2017). *K. pneumoniae*-NA showed a higher susceptibility toward chlorhexidine upon the addition of the CCCP. This is consistent with other studies suggesting that higher susceptibilities towards chlorhexidine might be through an efflux pump that is capable of exporting the chemical outside the bacterial cell (Abuzaid *et al.*, 2012; Mendes *et al.*, 2016; Wand *et al.*, 2017).

The loss of the efficacy of colistin will have significant clinical implications on the treatment of MDR *K. pneumoniae*, specifically the carbapenem-resistant isolates (Hayden *et al.*, 2015). Colistin is usually used as a combination

therapy and is one of the few last resort antibiotics to which carbapenem-resistant *K. pneumoniae* are susceptible (Falagas *et al.*, 2014). Hence, the cross-link between chlorhexidine exposure and colistin resistance would make the eradication and prevention of resistant colonizing *K. pneumoniae* very challenging in the clinical setting (Wand *et al.*, 2017). It should be noted that the concentration of chlorhexidine used in hospitals exceeds to a large extent the MIC values of clinical isolates, and this might be a leading factor contributing to *Klebsiella* and other bacterial pathogens to survive the residual effects of chlorhexidine and develop resistance (Naparstek *et al.*, 2012).

4.5.3 Synergy Testing Between Metal ions and Graphene Composites With Excipients of the Skin Cleanser

Synergy testing revealed no antagonistic effect between any metal ion, graphene or graphene oxide with any component of the skin cleaner. This was the second step to determine the possibility of the incorporation of metal ions into the scrub formulation. Additionally, a synergistic activity was demonstrated between five metal ions (In, Ga, Au, Pt and Pd) and poloxamer 237.

Poloxamer, singularly, has been shown to have an antimicrobial effect (Patel, Patel, *et al.*, 2009). However, its synergistic relationship with metal ions can be attributed to the interaction of oxygen atoms in the polyethylene oxide (PEO) chain with the metal ion. The reduced metal ions by the PEO chain will exhibit an enhanced antimicrobial capacity, which in turn is related to the oxidation capacity (Grumezescu, 2018).

It was also revealed that the graphene interacted synergistically with glycerol. This interaction may be due to graphene exhibiting a solubility parameter very close to that of glycerol (38.62 $MPa^{1/2}$), despite having a low solubility due to its interplanar interactions (Moghaddam *et al.*, 2016; Kumar *et al.*, 2019). This may allow the graphene to form a stable dispersion in glycerol, and enhance its antibacterial properties (Maas, 2016). This can also partially explain the enhanced antimicrobial activity of graphene added to the glycerol combinations. The oxygen containing groups in the

poloxamer chain are also known for their ability to increase the polarity of the sample (graphene), thus decreasing its hydrophobicity (Huang *et al.*, 2019). Hence, a possible explanation might be that poloxamer 237 improved the compatibility of graphene with the rest of the excipients (Huang *et al.*, 2019).

4.5.4 Testing of the Formulations

Fourteen different formulations for skin cleansers were established using different ingredients in slightly varying concentrations. All the formulations had the same base with one fluctuating factor being the composite added. Following the incorporation of metal ions and graphene composites in the base, the physical stability of the whole mixture was not affected, meaning that no creaming or increased viscosity was observed.

Among the 14 formulations tested, those containing Au-Gr (F9), Au (F3), Pt (F4), Pt-Gr (F11), Pd (F5), Au-GO (F10) and Pd-Gr (F13) showed the best antimicrobial activity against both the planktonic and biofilm forms of both isolates, independently of their susceptibility towards CHX. The chemical composition and the synergistic interactions shown between the components may be responsible for the antimicrobial effect against CHX susceptible and adapted *K. pneumoniae* strains.

The inhibitory/bactericidal effect of the different treatments was confirmed using SEM that showed irreversible deformations in the cell membranes (deep pits, groves, cell breakage, complete change in shape, rough surface). Similar morphological changes were reported by previous studies in bacterial cells following their treatments with metal ions or graphene compounds (Chandler *et al.*, 1994; Ruiz *et al.*, 2011; P. Li *et al.*, 2015). The shrinking in size in some bacterial cells might be due to the secretion of intracellular components, while the swelling effect can be due to the change in membrane permeability.

A synergistic effect was demonstrated by the addition of CHX to formulations (F2 (Ga), F3 (Au), F4 (Pt), F7 (Ga-Gr) and F9 (Au-Gr)), resulting in an enhanced antimicrobial activity towards the CHX adapted strain. Hence, the

addition of CHX to the previously discussed formulations might represent one possible solution to increase their antibacterial efficiency. Nevertheless, in light of the increasing rapid evidence of chlorhexidine resistance, it may be prudent, based on this study, to propose the elimination or reduction of the CHX use for the following years until a decrease in adaptation is validated. SEM was a confirmatory procedure to visualize the antimicrobial effect of metal ions, graphene composites and different formulations against the MDR and CHX resistant *K. pneumoniae* isolate. The inhibitory/bactericidal effect of the different treatments was apparent through the pits, groves, cell breakage, complete change in shape, rough surface until cell lysis.

4.6 Conclusion

Studies that investigate the impact of extended use of CHX on bacterial resistance towards antiseptics and cross-resistance to antibiotics are limited. This study proposed six antiseptic formulations containing Au, Pt, Pd, Au-Gr, Pt-Gr and Pd-Gr, respectively that demonstrated an antimicrobial efficacy against the planktonic and biofilm forms of CHX susceptible and adapted *K. pneumoniae* isolates. This study also suggested that metal ions and graphene composites, owing their potent antimicrobial activities and low cytotoxic properties, may be possible antimicrobial substitutes for chlorhexidine that can be integrated in skin cleansers and surgical scrubs formulations.

Chapter 5 Evaluation of Potential Alternatives for the Elimination of Mupirocin Resistant MRSA in Nasal Cavities

5.1 Introduction

5.1.1 Chemical Structure

Mupirocin is an antibacterial agent isolated form the soil bacterium *Pseudomonas fluorescens* NCIMB 10586, and it is produced as a mixture of four acids (pseudomonic acid A, B, C and D) with pseudomonic A being the major component of the mixture (> 90%) (Khoshnood *et al.*, 2019; Tucaliuc *et al.*, 2019). The four pseudomonic acids share the basic structure of monic acid (a C-polyketide-derived substructure) enclosing a pyran ring attached to 9-hydroxynanoic (a short fatty acid side chain) via an ester linkage (Figure 5.1.) (Matthijs *et al.*, 2014). Mupirocin was introduced as a topical antibiotic in the 1980s and accounts today for a total production of 22 tons per year by several manufacturers (Sutherland *et al.*, 1985; Tucaliuc *et al.*, 2019). It is used routinely to treat superficial infections caused by Gram-positive bacteria including *S. aureus* and *Streptococcus pyogenes* (Tucaliuc *et al.*, 2019). Mupirocin presents itself as a white to off-white crystalline powder that is soluble in acetone, chloroform, methanol and ethyl alcohol, but only slightly soluble in water (0.0265mg/mL). This strong acid is pH dependent; it exhibits its best antibacterial activity within a pH range of 4 – 9. In very acidic and basic conditions, an irreversible structural degradation takes place through intramolecular opening of the epoxide ring (Gurney and Thomas, 2011).

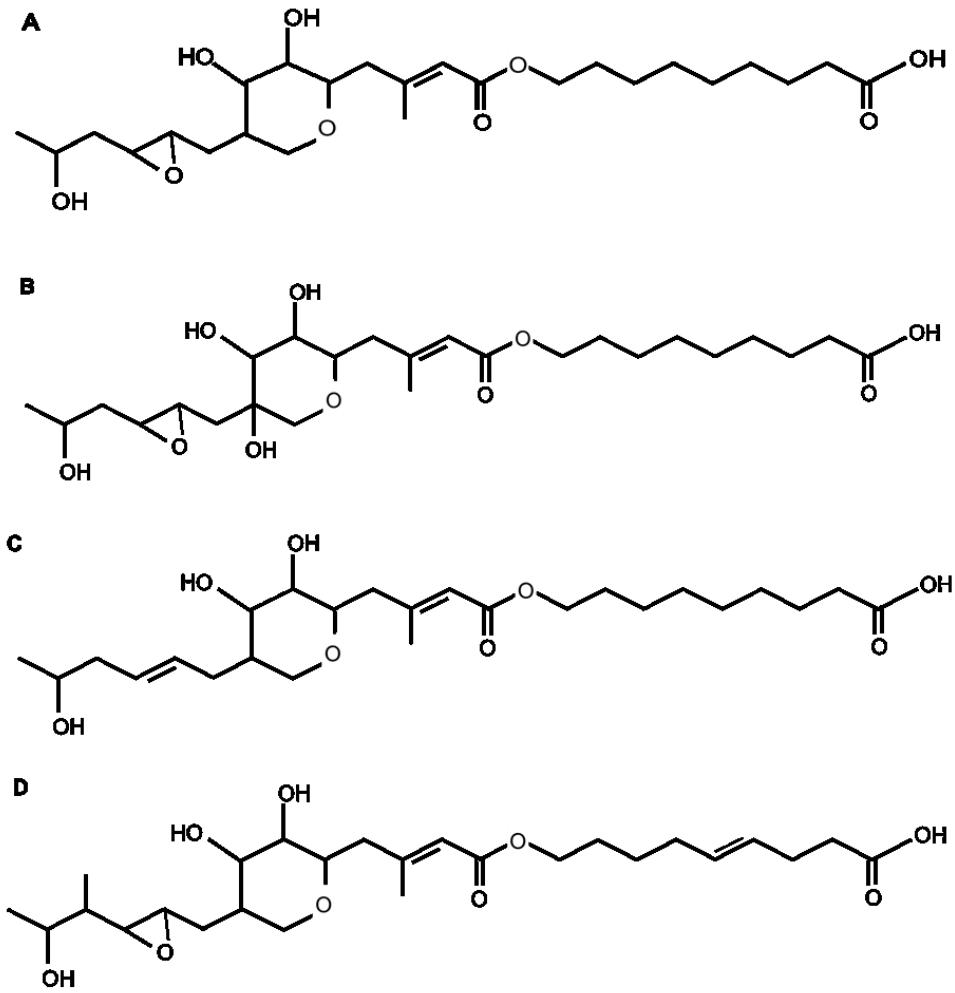

Figure 5.1 Chemical structures of the main components of mupirocin (A) pseudomonic acid A, (B) pseudomonic acid B, (C) pseudomonic acid C and (D) pseudomonic acid D. Figure adapted and reproduced from Tucaliuc *et al*. (2019).

5.1.2 Mechanism of Action

Mupirocin belongs to the monocarboxylic acid antibiotic class, and exhibits a broad antibacterial activity and a limited systemic adsorption. Having a short half-life, the drug is converted within 15-40 minutes into monic acid (the inactive form) which is excreted by the kidneys (Poovelikunnel *et al.*, 2015; Tucaliuc *et al.*, 2019). Due to the structural similarity between the epoxide side chain of mupirocin and the aliphatic side chain of isoleucine, mupirocin can competitively bind to the bacterial isoleucyl t-RNA synthetase. This binding prevents the conversion of isoleucyl t-RNA synthetase into isoleucine-charged transfer molecules, leading to inhibition of protein and

RNA synthesis in bacteria and cell death (Figure 5.2.) (Khoshnood *et al.*, 2019). Mupirocin exhibits low toxicity in humans due to its low affinity for mammalian isoleucyl-transfer-RNA synthetase (Khoshnood *et al.*, 2019). Additionally, the main producer of mupirocin *P. fluorescens*, is not affected by its activity. This is mainly due to the *ileRS2* gene enclosed in the 74-Kb gene cluster that encodes for mupirocin. By displaying eukaryotic features and exhibiting no sensitivity to mupirocin, *ileRS2* is believed to protect the bacterium (Khoshnood *et al.*, 2019). Mupirocin can be either bacteriostatic at concentrations near the bacterial MICs, and bactericidal at higher concentrations (similar to 2% mupirocin found in skin ointments) (Sutherland *et al.*, 1976).

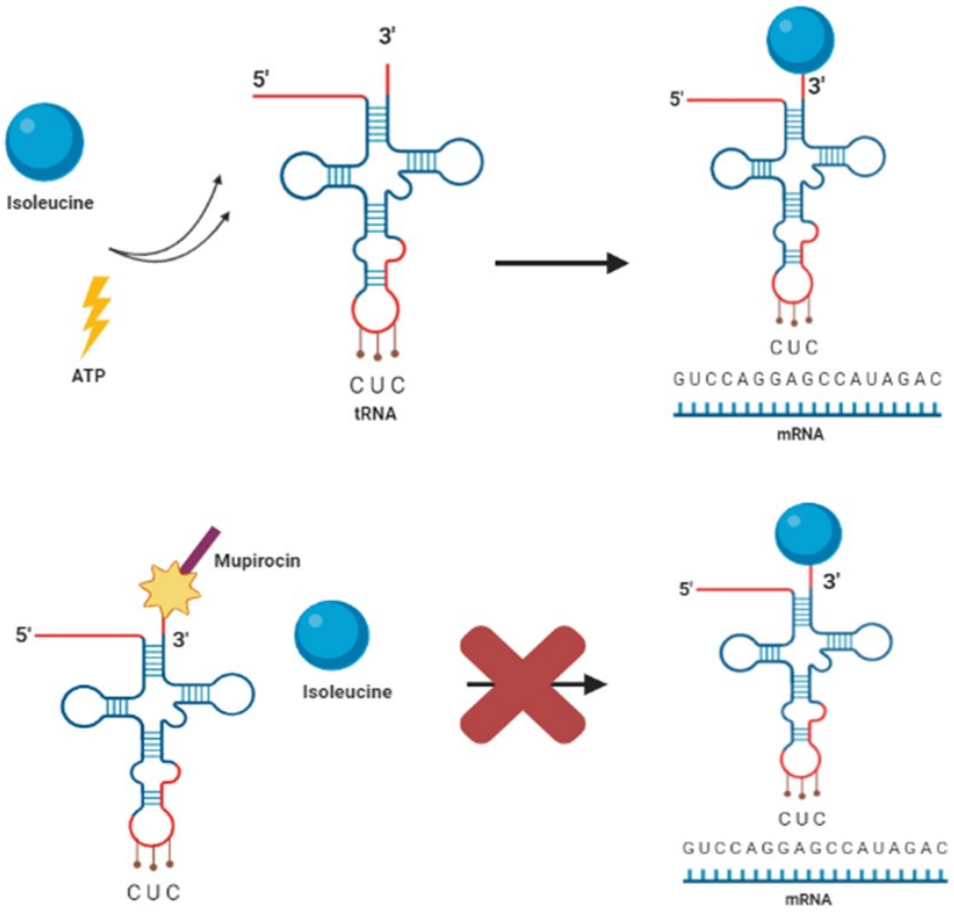

Figure 5.2 The mode of action of mupirocin towards bacterial cells. (A) Isoleucyl t-RNA synthetase is a target enzyme involved in the activation of t-RNA with isoleucine trough an ATP-dependent reaction for protein synthesis. (B) Mupirocin has the ability to bind to the isoleucine specific binding site of isoleucyl-tRNA synthetase through its epoxide chain. This will restrain the aminoacylation of isoleucine t-RNA in *S. aureus* and inhibit the RNA and protein and synthesis. Figure adapted and modified from Drugdetails (2017).

5.1.3 Mupirocin Resistance

Shortly after its application into therapy, resistance towards mupirocin was reported in 1987 at St Thomas hospital (Hughes *et al.*, 2015). Several studies have confirmed that MRSA has developed resistance to mupirocin following its extensive use as a preferred treatment for any MRSA infection (Poovelikunnel *et al.*, 2015; Tucaliuc *et al.*, 2019).

5.1.3.1 Mechanism of Resistance

S. aureus can display one of three types of susceptibility towards mupirocin depending on its MIC. For instance, *S. aureus* is considered susceptible to mupirocin at MIC ≤ 4mg/L, have low-level resistance (LLMR) at MIC of 8 - 64 mg/L, and high-level resistance (HLMR) at MIC ≥ 256 mg/L. Concentrations ranging between 128 to 256 mg/L are not commonly reported, but this range is referred to as low-level resistance (Patel, Gorwitz, *et al.*, 2009; Poovelikunnel *et al.*, 2015; Khoshnood *et al.*, 2019). The chromosomally encoded low-level resistance is primarily due to a point mutation in the *ileS* gene, which in turns, cause a Val-to-Phe change in the mupirocin binding site (Hurdle *et al.*, 2004; Khoshnood *et al.*, 2019). The high-level resistance is mediated by two main mechanisms. The first one is through the acquisition of plasmid mediated *mupA* or *ileS2* genes that contain information for an additional isoleucyl-t-RNA unresponsive to mupirocin (Tucaliuc *et al.*, 2019). The second mechanism is mediated through the *mup*B gene which shares 65% similarity in sequence with the *mup*A gene. A low-level resistance *S. aureus* isolate can also develop high-level resistance through the acquisition of the pSK41-like plasmid (Khoshnood *et al.*, 2019).

5.1.3.2 Epidemiology of Mupirocin Resistance

Resistance rates of *S. aureus*, particularly MRSA, towards mupirocin have emerged increasingly in different parts of the world (Table 5.1) (Udo *et al.*, 2006; Khoshnood *et al.*, 2019). The highest prevalence of mupirocin resistance among *S. aureus* strains was reported in the United States of America at 10.5%, followed by Asia and Europe at 7.3% and 6.6%,

respectively (Dadashi *et al.*, 2020). In the European continent, mupirocin resistance was reported variably by several studies, and was demonstrated to be depended on the pattern of mupirocin use in each country (Khoshnood *et al.*, 2019). For instance, Lee *et al*. (2011) reported that following a 20 year study that analysed MRSA isolates from blood cultures, it was demonstrated that mupirocin resistance is proportional to its use. Lee *et al*. (2011) also showed that low-level mupirocin resistance increased drastically from 0% to 79% in a Swiss tertiary care hospital within only 9 years. On the other hand, France has witnessed an increased resistance rate of 2.2%, of which only 0.8% exhibited high-level resistance (Desroches *et al.*, 2013). Recent surveillance studies investigating the prevalence of mupirocin resistance among MRSA in UK are not very frequent. However, a previous study has reported a prevalence of 42.8% and 28.5% resistance in 1992 in UK (Farmer, Gilbart and Elson, 1992).

Table 5.1 Prevalence of mupirocin resistance among *Staphylococcus* species across European countries

Location	Bacteria	Publication date	MIC (mg/L)	Resistance rate	Reference
United Kingdom	*S. aureus*	1992	8 – 256 ≥ 2048	42.8% (I) 28.5% (H)	Farmer *et al.* (1992)
Poland	*S. aureus*	1999	32 – 128 ≥1024	2.5% (L) 17% (H)	Leski *et al.* (1999)
Spain	MRSA	2006	_	12.8%	Perez-Roth *et al.* (2006)
Belgium	MRSA	2008	8-32 ≥ 512	31.2% 25.6%	Malaviolle *et al.* (2008)
Ireland	MRSA, MSSA *S. epidermidis*, *S. xylosus*	2009	8-32 ≥ 1024	MRSA 3% (H) MSSA 1% (H)	O'Shea *et al.* (2009)
France	MRSA	2013	_	1.4% (L) 0.8% (H)	Desroches *et al.* (2013)
Greece	MRSA	2017	≥ 512	>25% (H)	Doudoulak *et al*. (2017) Papakonstantinou *et al*. (2018)

5.1.4 Clinical Uses

Mupirocin is a polyketide antibiotic found under the brand name Bactroban or Centany. It is registered as an essential medicine on the World Health Organization's list. Bactroban is mainly used to treat impetigo, folliculitis and skin infections caused by *S. aureus* and *Streptococcus* (Hetem and Bonten, 2013). The major therapeutic indication for mupirocin is the eradication of MRSA from nasal carriage, which consequently leads to a significant reduction in *S. aureus* bacteraemia cases among dialysis patients (Boelaert *et al.*, 1993; Poovelikunnel *et al.*, 2015; Khoshnood *et al.*, 2019). In addition to being used for controlling outbreaks in hospitals and nursing homes, mupirocin is also used to prevent recurring infections in patients with community acquired MRSA skin and soft tissue infections (Hetem and Bonten, 2013; Creech *et al.*, 2015; Khoshnood *et al.*, 2019). Mupirocin can be used alone for nasal decolonization or in combination with antiseptics (such as chlorhexidine) as an approach to decolonize MRSA (George *et al.*, 2016). In efforts to reduce the resistance, the treatment should not exceed 10 days with at least 30 days in between treatments (Tucaliuc *et al.*, 2019). Topical antibacterial formulations comprising mupirocin are available as ointments, topical nasal and creams. Bactroban ointment is constituted of a water-soluble polyethylene glycol base and is mainly used for the topical treatment of impetigo caused by *S. aureus*. Bactroban nasal, on the other hand, includes a paraffin-based ointment that is used for intranasal eradication of MRSA (Hatton *et al.*, 2000). A list of excipients found in mupirocin formulations in topical nasal ointments and topical nasal sprays, including their chemical structure and function are detailed in Table 5.2.

Table 5.2 List of excipients in formulations of mupirocin topical nasal ointment and spray.

	Excipient	Chemical structure	Function/use	Reference
Bactroban ointment	**Polyethylene glycol 400** **(PEG 400)**	$C_{2n}\ H_{4n+2}\ O_{n+1}$ (n = 8.2 to 9.1) 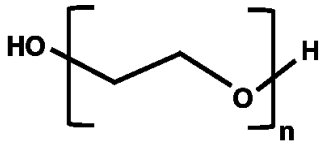	• Emulsion stabilizer (keeps the components from separating into oil and liquid components)	Ooya *et al*. (2003) Ethier *et al.* (2019)
	Polyethylene glycol 3350 **(PEG 3350)**	$C_{2n}\ H_{4n+2}\ O_{n+1}$ (n = 75.7) 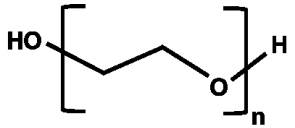	• Humectant	Ethier *et al*. (2019)
Bactroban nasal ointment	**Soft white paraffin (Petrolatum)** 1,1,2-Trimethylbenzeindole	$C_{15}H_{15}N$ 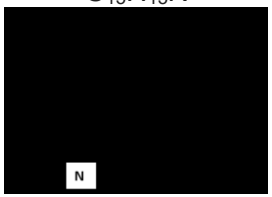	• Emollient/ moisturizer (creates an oil deposit on the skin surface preventing water evaporation)	Loden (2003)
	Softisan 649 Bis-Diglyceryl Polyacyladipate-2		• Lanolin substitute with a high water-binding capacity and good adhesion to the skin • Emollient	Flume *et al.* (2013)
Nasal spray	**Saline**	NaCl	• Decongestant to clear nasal secretions and debris	Hauptman and Ryan (2007) Allen (2019)

5.2 Aim

The aim of this study was to test the possibility of developing nasal topical formulations (ointments and sprays) by integrating metal ions and graphene-based compounds as antimicrobial agents. This also aims at testing the efficacy of these formulations for the treatment of intranasal staphylococcal or MRSA-related skin infections (including impetigo).

5.3 Materials and Methods

5.3.1 Antimicrobial Susceptibility of *S. aureus* to Mupirocin

The susceptibility of the *S. aureus* isolates toward mupirocin was examined using the disc diffusion method (as previously described in section 2.2.2.). Mueller-Hinton agar plates were inoculated with a solution of each bacterial isolate adjusted to 1.5×10^8 CFU/mL, and mupirocin discs (5 µg and 200 µg) (Applichem Gmbh, USA) were placed onto the inoculated agar. Following overnight incubation, the diameters of the zones of inhibition were measured from three different sides and recorded in mm. *S. aureus* isolates showing ZoI ≤ 13 mm with the 5 µg mupirocin disc were considered MUP resistant (Fuchs *et al.*, 1990). Those isolates were subsequently tested with the 200 µg discs to be classified as high level mupirocin resistant (ZoI ≤ 6 mm) or low level mupirocin resistant (ZoI ≥ 7 mm) (McDanel *et al.*, 2013). *S. aureus* ATCC 25923 was used as a control strain.

5.3.2 Synergy Testing

The interaction between the excipients of the Bactroban ointment or the Bactroban nasal (Table 5.2.) with metal ions and graphene composites in different combinations was assessed by calculating the FIC (section 2.2.7.). Metal ions, including Ga (7.8 mg/L), Pt (0.49 mg/L), Pd (20.83 mg/L) and Au (7.8 mg/L) were selected since they exhibited the best inhibitory concentrations against the *S. aureus* isolates and the least cytotoxic effects against skin fibroblasts. Polyethylene glycols (PEG 400 (4%) and PEG 3350 (0.5 g/mL)) were diluted in water, while paraffin (0.76 g/mL) and softisan (0.05 g/mL) were diluted in diethyl ether. Fifty microliters of each tested compound was added to the well. The tested components were added in a 1:1 mixture and were classified as having a synergistic effect if $\sum FIC \leq 0.5$, an additive effect if $0.5 < \sum FIC \leq 1$, an indifferent effect if $1 < \sum FIC \leq 4$ and an antagonistic effect if $\sum FIC > 4$.

5.3.3 Preparation and Testing of the Different Ointment Formulations

5.3.3.1 Nasal Sprays

The conventional fusion method was used for the preparation of the ointment base. Constituents were placed inside glass beakers in a water bath at 70 °C. PEG 3350 (70 g), having a higher molecular weight, was placed in the beaker first and left to melt for few minutes. Hundreds millilitres of PEG 400 was added onto a separate beaker and warmed up. Volumes of PEG 400 and PEG 3350 were added and mixed together as indicated (Table 5.3). The mixture was cooled down to room temperature (or at least below 40 °C) with continuous gentle stirring for 8-10 minutes to form a clear solution. Half of the weighed amount of the base was removed and spread over a clean glass plate. Metal ions (Ga, Au, Pd) or combinations of metal ions and graphene based compounds (Ga-GO, Ga-Gr, Au-GO, Au, Gr, Pd-GO and Pd-Gr) were added to the polyethylene glycol ointment. The cream was folded over the added constituents using a spatula in a side-to-side motion without exertion of any pressure. The rest of the ointment base was blended with the mixture while making sure no granules or streak marks appeared. Ointment mixture was diluted in a 1:9 ratio with saline solution. The different compositions of the topical intranasal spray formulations are listed in Table 5.3. Ointment bases were prepared in accordance with the United States National Formulary (Orr and Greenway, 1986; De Villiers, 2009; USNF, 2013).

Table 5.3 Composition of the topical intranasal spray formulation

	Formulation (100 mL)								
Ingredients	**S1**	**S2**	**S3**	**S4**	**S5**	**S6**	**S7**	**S8**	**S9**
PEG 400	44.5 mL	44.5 mL	39 mL	48 mL	48 mL	46 mL	50 mL	50 mL	50 mL
PEG 3350	44.5 mL	44.5 mL	39 mL	47.5 mL	48 mL	46 mL	47 mL	47.3 mL	45.8 mL
Metal ion	Ga 11 mg	Au 11 mg	Pd 22 mg	Ga 2.25 mg	Au 2 mg	Pd 4 mg	Ga 1.5 mg	Au 1.35 mg	Pd 2.1 mg
Gr/GO	--	--	--	GO 2.25 mg	GO 2 mg	GO 4 mg	GO 1.5 mg	Gr 1.35 mg	Gr 2.1 mg
Saline dilution	1:9	1:9	1:9	1:9	1:9	1:9	1:9	1:9	1:9

5.3.3.2 Nasal Ointment

Ointment formulation was also prepared using the fusion method. Soft white paraffin (100 g) and Softisan 649 (10 g) were melted in separate glass beakers in a water bath set at 70 °C. The volumes of each constituent were added, according to each formulation (Table 5.4), while being stirred gently until congealing. The mixture was then removed from the hot container and allowed to cool down. The rate of cooling was an important element since rapid cooling contributed in increased structure of the formulated product. Next, metal ions (Ga, Au, Pd) or combinations of metal ions and graphene based compounds (Ga-GO, Ga-Gr, Au-GO, Au, Gr, Pd-GO and Pd-Gr) were added. The mixture was folded using a stainless steel spatula and stored in the dark. The different compositions of the topical intranasal spray formulations are listed in Table 5.4. Ointment bases were prepared in accordance with the United States National Formulary (Orr and Greenway, 1986; De Villiers, 2009; USNF, 2013).

Table 5.4 Composition of the topical intranasal ointment formulation

	Formulation (100 mL)								
Ingredients	**O1**	**O2**	**O3**	**O4**	**O5**	**O6**	**O7**	**O8**	**O9**
Paraffin	95 mL	95 mL	94 mL	95 mL	95 mL	95 mL	95 mL	95 mL	95 mL
Softisan 649	3.9 mL	3.9 mL	3.9 mL	4 mL	4.6 mL	4.2 mL	4.7 mL	4.7 mL	4.5 mL
Metal ion	Ga 1.1 mg	Au 1.1 mg	Pd 2.1 mg	Ga 0.5 mg	Au 0.2 mg	Pd 0.4 mg	Ga 0.15 mg	Au 0.15 mg	Pd 0.25 mg
Gr/GO	--	--	--	GO 0.5 mg	GO 0.2 mg	GO 0.4 mg	Gr 0.15 mg	Gr 0.15 mg	Gr 0.25 mg

5.3.4 *In-vitro* Antimicrobial Activity against *S. aureus* Isolates

5.3.4.1 Zone of Inhibition

The *in-vitro* antibacterial activity of the different tested formulations of ointments and sprays was evaluated through their zones of inhibition. TSA

agar plates were prepared following the manufacturer's instructions and stored at 4°C until needed. Bacterial cultures of *S. aureus*-SA1*, S. aureus*-SA2 *and S. aureus*-SA3 were subcultured overnight. One to two colonies of each isolate were suspended in sterile saline and adjusted to 1.5 × 10^8 CFU/mL. The suspension was inoculated onto the TSA agar by streaking 100 µL in three different directions to ensure proper distribution (by rotating the plates around 60 degrees). The plates were dried for 5 min at room temperature. Using a sterile cork borer, holes of 5 mm diameter were punched into the inoculated agar. Each formulation was added to a separate well. The marketed product mupirocin 2% ointment (Advanz Pharma,UK) was tested in parallel as control. The formulation bases containing no metal ions or graphene composites were also tested. Following overnight incubation at 37°C, the diameters of the zone of inhibition were measured and recorded in millimetre (mm). Each formulation was tested in triplicate and results were presented as mean value ± SD.

5.3.4.2 Crystal Violet Biofilm Assay

CVBA assays were conducted to evaluate the antimicrobial efficacy of the tested formulations against *S. aureus* biofilms (section 2.2.8.2). Each formulation was tested individually against a separate biofilm. Results were presented as absorbance at 590 nm. Samples were blanked with acetic acid solutions containing the corresponding formulations.

5.3.5 Scanning Electron Microscopy

Conformational changes in *S. aureus* cells and biofilms treated with different nasal ointment and spray formulations containing metal ions were visualized by SEM imaging (as previously described in section 2.2.9).

5.3.6 Physical Evaluation of Ointment Formulations

5.3.6.1 Organoleptic Inspection

The physical appearance, colour, texture and homogeneity of all tested combinations were examined by visual observation. Homogeneity and texture were inspected by pressing a small amount of the products between

the two fingers (thumb and index). The stiffness, greasiness and the presence of any coarse particles were also assessed through immediate skin feel.

5.3.6.2 Spreadability

The spreadability of the tested formulations was determined by applying 1 g of each formulation between two glass slides placed horizontally. A standard weight of 25 g was exerted for one minute on the upper slide. The spreading diameter was then measured and the spreadability was calculated using the following formula

$$[\ S = \frac{M \times L}{T}\ ] \qquad [4]$$

where S is the Spreadability, M is the total weight (g) applied to the upper slide, L the length (cm) of the slide and T is the time in seconds required for the entire separation of the two slides (Djiobie Tchienou *et al.*, 2018; Gemeda *et al.*, 2018). Spreadability measurements were performed in triplicate.

5.3.6.3 Determination of pH

A suspension of each formulation was prepared by mixing 1 g of the ointment or cream in 25 mL of deionized water. A magnetic stirrer was used to ensure homogeneity. After calibrating the pH meter (Hanna Instruments, UK) with standard buffer solutions (pH 4, 7 and 10), the pH of each formulation was measured three times.

5.3.6.4 Thermal Cycle Testing

Fifteen grams of each formulated product (spray or ointment) was stored at 4-5°C for two days then at 25°C for an additional two days. Another 15 g was stored at 4°C then 50°C for 48 h each. Both procedures were repeated at least 4 times and the stability and appearance of the products were assessed again.

5.3.6.5 Creaming and Coalescence

Twenty grams of each formulation was placed into sterile bijoux and kept at room temperature in the laboratory for 2 months. The physical stability (including pH, colour, physical appearance and texture) and antimicrobial activity of each formulation was re-checked after one week, one month and three months.

5.4 Results

5.4.1 Antimicrobial Susceptibility of *S. aureus* to Mupirocin

The susceptibility of *S. aureus* isolates towards mupirocin was tested using a disc diffusion method. Clear zones of inhibition (larger than 13 mm) were obtained for *S. aureus*-SA2 showing a full sensitivity to mupirocin. *S. aureus*-SA1 (3.66mm) and *S. aureus*-SA3 (no zone) displayed small to no zones of inhibition zones when tested with mupirocin 5 µg indicating their resistance. The 200 µg discs were tested against the resistant isolates to further confirm the level of resistance. Consequently, *S. aureus*-SA1 *S. aureus*-SA3 showed low-level and high-level of mupirocin resistance, respectively (Table 5.3).

Table 5.5 Mean values (± SD) of the zones of inhibition of *S. aureus* isolates by mupirocin (5 µg and 200 µg) discs.

Zol (mm)	Mupirocin 5 µg	Mupirocin 200 µg	Phenotype
***S. aureus*-SA1**	3.66 ± 0.57	10.00 ± 1.00	LLMR
***S. aureus*-SA2**	17 ± 1.00	21.00 ± 1.00	Sensitive
***S. aureus*-SA3**	No zone	4.33 ± 0.57	HLMR

LLMR: Low-level mupirocin resistance, HLMR: High-level mupirocin resistance

5.4.2 Synergy Testing of Different Excipients of the Topical Nasal Ointment and Topical Spray

Metal ions (Ga, Pt, Pd and Au) exhibiting the best inhibitory concentrations against *S. aureus* isolates and the least cytotoxic effects against skin fibroblasts were tested to determine their synergistic effects. The values of

the FIC index were used as a predictor for synergy between metal ions, graphene composites and individual excipients of the topical nasal spray and ointment. PEG 3350 (FIC = 0.11 – 0.4) and PEG 400 (FIC = 0.65 – 0.88) exhibited synergistic and additive effects, respectively, when tested with Ga, Pd and Au, Gr or GO against the three *S. aureus* isolates (Table 5.4). The antimicrobial activity of metal ions was not affected by the addition of paraffin (FIC = 1.75 – 2.12), saline solution (FIC = 1.25 – 2) or softisan 649 (FIC = 1.25 – 2.75) showing an indifferent effect against the three bacterial isolates (Table 5.4). When the excipients were tested in combination with Ga, Pd, Au, GO and Gr, the PEG 400-PEG 3350 combination exhibited a synergistic antimicrobial activity (FIC = 0.11 - 0.46), whilst saline-PEG 400 (FIC = 0.66 - 1), and saline-PEG 3350 (FIC = 0.54 - 1) showed additive effects (p<0.05) (Table 5.5.). The paraffin-saline combination exhibited an indifferent effect (FIC = 1.67 - 3.21). Pt was the only metal ion showing an indifferent activity when tested against the 162 combinations; hence, Pt was excluded from further investigations. The results also revealed that no antagonistic effect was displayed between the four metal ions, graphene, graphene oxide and any tested excipient of nasal topical. The same synergistic patterns were observed with the different tested combinations against the different *S. aureus* isolates. A complete list of FIC values of the different combinations against the three isolates (Tables 5.4. and 5.5). The synergistic values were highlighted in blue and the additive values in green.

Table 5.6 FIC values of excipients of topical nasal spray and ointment, tested individually, with metal ions, graphene and graphene oxide against *S. aureus*-SA1, *S. aureus*-SA2, *S. aureus*-SA3.

	***S. aureus*-SA1**						***S. aureus*-SA2**						***S. aureus*-SA3**					
	Ga	**Pt**	**Pd**	**Au**	**GO**	**Gr**	**Ga**	**Pt**	**Pd**	**Au**	**GO**	**Gr**	**Ga**	**Pt**	**Pd**	**Au**	**GO**	**Gr**
PEG 400	0.77	1.88	0.65	0.88	0.76	0.77	0.65	2.11	0.88	0.66	0.88	0.77	0.65	2.11	0.76	0.66	0.88	0.77
PEG 3350	0.11	2.11	0.21	0.21	0.26	0.30	0.18	2.11	0.38	0.26	0.26	0.33	0.18	2.11	0.26	0.26	0.4	0.33
Paraffin	2.12	3.11	2.00	1.96	1.75	2.09	2.75	2.75	2.00	1.96	2.00	3.06	2.00	2.75	3.06	1.26	2.06	2,75
Softisan 649	2.00	1.66	1.75	2.00	1.06	1.25	1.75	1.75	1.75	2.00	2.00	1.25	2.00	1.75	1.75	1.66	2.00	1.25
Saline	2.00	1.66	2.00	2.00	1.75	1.25	2.00	2.00	1.66	2.00	2.75	1.25	2.00	1.75	1.66	2.00	1.75	1.25

Table 5. 7 FIC values of excipients of topical nasal spray and ointment, tested in different combinations, with metal ions, graphene and graphene oxide against *S. aureus*-SA1, *S. aureus*-SA2, *S. aureus*-SA3.

	***S. aureus*-SA1**						***S. aureus*-SA2**						***S. aureus*-SA3**					
	Ga	**Pt**	**Pd**	**Au**	**GO**	**Gr**	**Ga**	**Pt**	**Pd**	**Au**	**GO**	**Gr**	**Ga**	**Pt**	**Pd**	**Au**	**GO**	**Gr**
PEG400-PEG3350	0.33	2.06	0.36	0.11	0.50	0.50	0.33	2.00	0.26	0.11	0.46	0.46	0.46	2.00	0.36	0.11	0.50	0.50
Saline-PEG 400	0.88	2.33	0.75	0.88	1.00	1.00	0.76	2.06	0.75	0.88	1.00	1.00	0.66	2.06	1.00	0.88	1.00	0.88
Saline-PEG3350	0.67	1.81	0.54	0.83	0.66	0.71	0.56	2.00	0.54	0.88	0.76	1.00	0.67	2.00	0.66	0.83	0.66	0.71
Paraffin-Softisan 649	1.67	2.09	2.50	3.12	3.21	1.96	1.88	2.00	2.50	3.12	3.11	2.00	2.00	2.00	2.66	3.00	2.88	2.00

5.4.3 Antimicrobial Activity of the Formulated Combinations

Nine spray formulations and nine ointment formulations comprising different metal ions or combinations of metal ions with Gr or GO were tested against the planktonic and biofilm forms of three *S. aureus* isolates.

5.4.3.1 Antimicrobial Activity of Ointment and Spray Formulations Using Agar Well Diffusion Assay

Zones of inhibition were recorded to assess and compare the effectiveness of the tested formulations. Amongst all of ointment formulations, O8 (comprising Au-Gr) exhibited the highest antibacterial activity with ZoI of 33 mm, 31.3 mm and 30.6 mm against *S. aureus*-SA1, *S. aureus*-SA2 and *S. aureus*-SA3. O8 was followed by O2 (Au) (25.89 – 28 mm) , O7 (Ga-Gr) (24 - 26.5 mm), O9 (Pd-Gr) (22 – 23 mm), O3 (Pd) (21.6 – 23.33 mm), O1 (Ga) (17.95 – 19.5 mm), O5 (Au-GO) (17.99 – 19.22 mm), O6 (Pd-GO) (16.99 – 18.22 mm) and O4 (Ga-GO) (16.2 – 17.5 mm) (Figure 5.3).

The nasal spray formulations tested against the *S. aureus* isolates showed a similar efficacy pattern to the ointment formulations. The best inhibitory activity was recorded for S8 (Au-Gr) (30 – 31.7 mm), followed by S2 (Au) (24.85 – 28 mm) , S7 (Ga-Gr) (23.5 - 25 mm), S9 (Pd-Gr) (21.22 – 24 mm), S3 (Pd) (21 – 23.11 mm), S1 (Ga) (17.45 – 18.22 mm), S5 (Au-GO) (18 – 19.22 mm), S6 (Pd-GO) (16.22 – 17.5 mm) and S4 (Ga-GO) (15.6 – 16.55 mm) (Figure 5.4).

Thus, the optimum formulations for the ointments and sprays were those containing Au-Gr. Results also showed that each formulation exhibited similar antimicrobial efficacies (ZoIs) against the three distinct *S. aureus* isolates.

When compared to the commercial 2% ointment, the nine tested formulations for the ointments and sprays produced larger ZoIs than when mupirocin alone was tested against *S. aureus*-SA1 and *S. aureus*-SA3. Similarly, five ointment formulations (O8 (Au-Gr), O2 (Au), O7 (Ga-Gr), O9 (Pd-Gr) and O3 (Pd)) and five spray formulations (S8 (Au-Gr), S2 (Au), S7 (Ga-Gr), S9 (Pd-Gr) and S3 (Pd)) showed better efficacy than mupirocin

against the mupirocin sensitive *S. aureus*-SA2. No zones of inhibition were recorded for the formulation bases containing no metal ions or combinations of metal ions and graphene or graphene oxide.). The diameters of zones of inhibition (Zol ± SD) of all formulations are listed in appendix I and J.

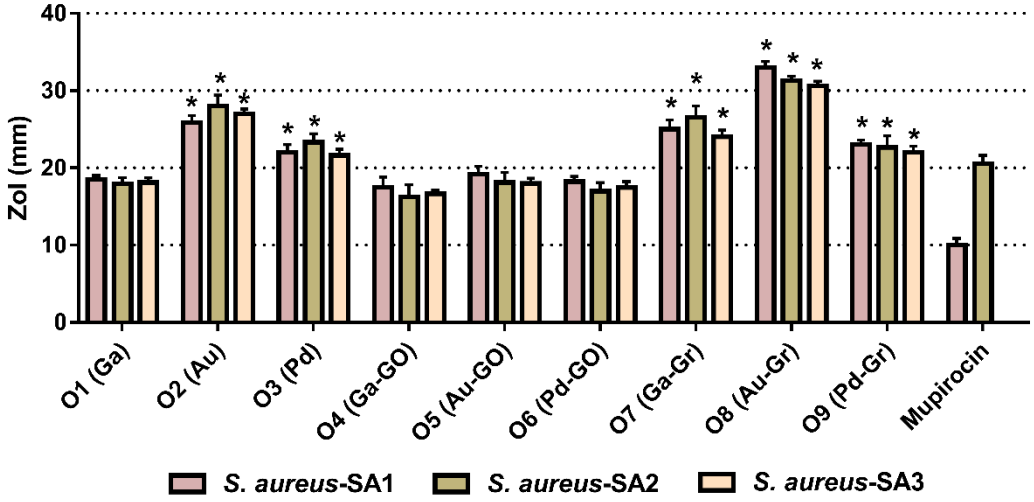

Figure 5.3 Antimicrobial activity (Zol) of nasal ointment formulations containing Ga (O1), Au (O2), Pd (O3), Ga-GO (O4), Au-GO (O5), Pd-GO (O6), Ga-Gr (O7), Au-Gr (O8) and Pd-Gr (O9) against three *S. aureus* isolates. * denotes $p \leq 0.05$ compared to mupirocin.

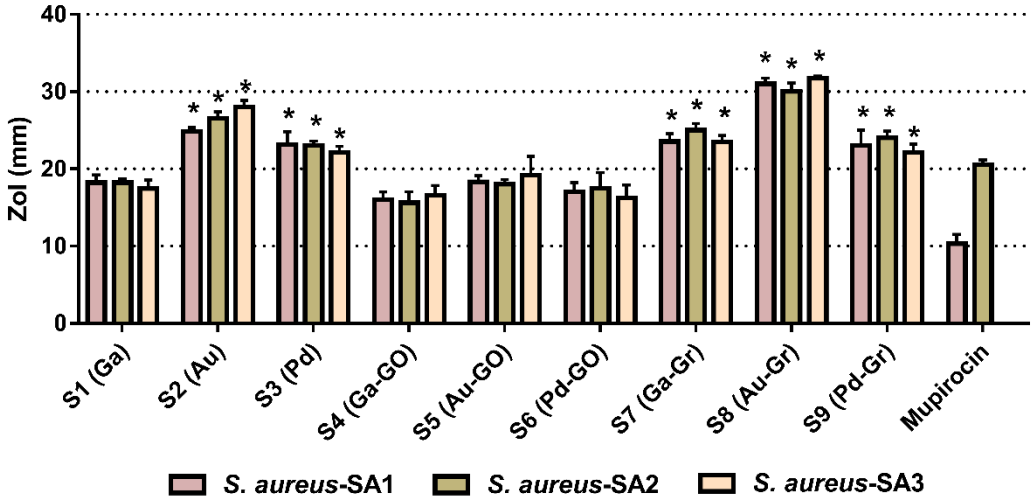

Figure 5.4 Antimicrobial activity (Zol) of nasal spray formulations containing Ga (S1), Au (S2), Pd (S3), Ga-GO (S4), Au-GO (S5), Pd-GO (S6), Ga-Gr (S7), Au-r (S8) and Pd-Gr (S9) against three *S. aureus* isolates. * denotes $p \leq 0.05$ compared to mupirocin.

5.4.3.2 Antibiofilm Activity of Nasal Ointments and Sprays Using Crystal Violet Biofilm Assay

Crystal violet biofilm testing showed that the nine ointment and nine spray formulations inhibited the biofilm of the three *S. aureus* isolates ($p<0.05$). The best antibiofilm activities were recorded for S8 (Au-Gr), O8 (Au-Gr) followed by S2 (Au), O2 (Au) ($p<0.0001$) and S5 (Au-GO) ($p = 0.0002$), O5 (Au-GO) ($p = 0.00016$) (Figures 5.3 and 5.4). The six formulations S8 (Au-Gr), O8 (Au-Gr), S2 (Au), O2 (Au), S5 (Au-GO) and O5 (Au-GO) showed greater antimicrobial activity against the three isolates compared to mupirocin.

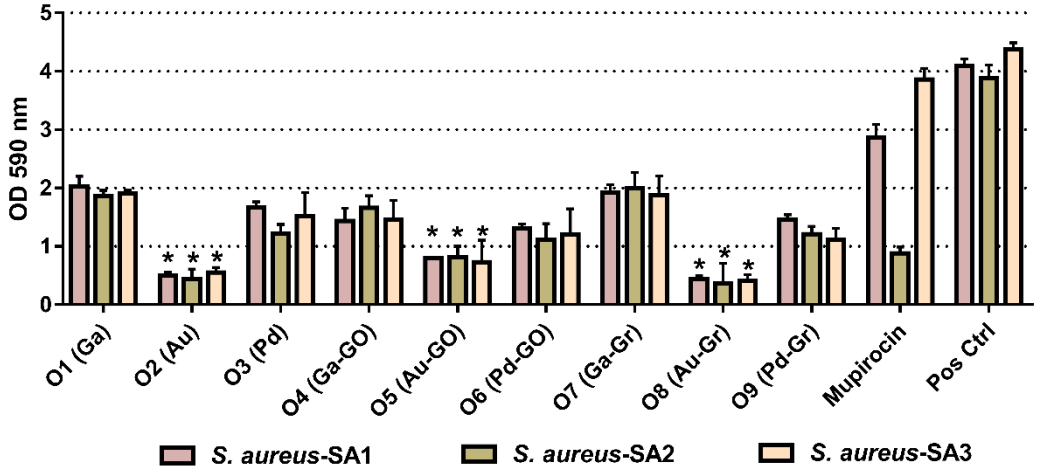

Figure 5.5 Antibiofilm activity as determined by CVBA of nasal ointment formulations containing Ga (S1), Au (S2), Pd (S3), Ga-GO (S4), Au-GO (S5), Pd-GO (S6), Ga-Gr (S7), Au-Gr (S8) and Pd-Gr (S9) against three *S. aureus* isolates. * denotes $p \leq 0.01$ compared to positive control.

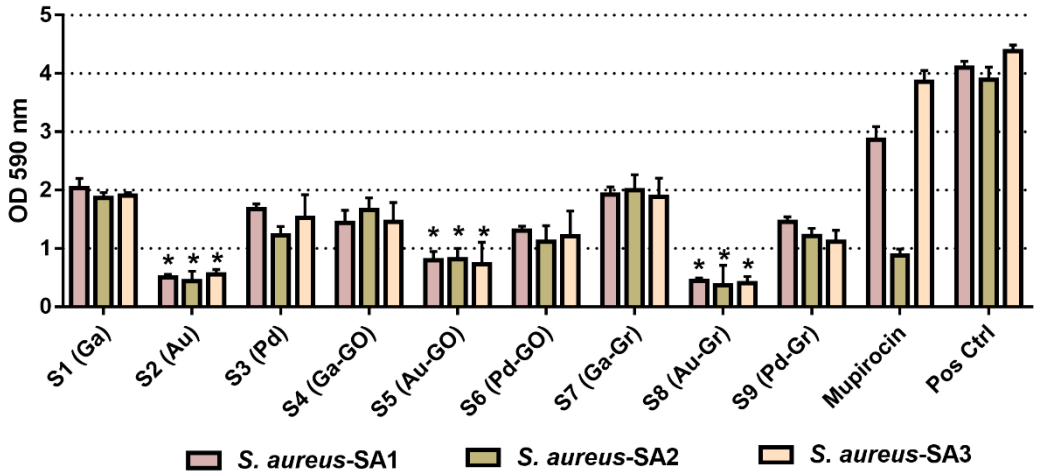

Figure 5.6 Antibiofilm activity as determined by CVBA of nasal spray formulations containing Ga (S1), Au (S2), Pd (S3), Ga-GO (S4), Au-GO (S5), Pd-GO (S6), Ga-Gr (S7), Au-Gr (S8) and Pd-Gr (S9), as determined by CVBA, against three *S. aureus* isolates. * denotes $p \leq 0.01$ compared to positive control.

5.4.4 Scanning Electron Microscopy

The effect of the different formulations on the morphology of *S. aureus* cells treated with different formulations was examined by SEM. The visualization of untreated *S. aureus*-SA1 (Figure 5.7a), *S. aureus*-SA2 (Figure 5.7b) and *S. aureus*-SA3 (Figure 5.7c) showed that bacterial cells existed as single cells (550-800 nm) or as aggregates of loosely packed cells in culture, with intact bacterial membranes.

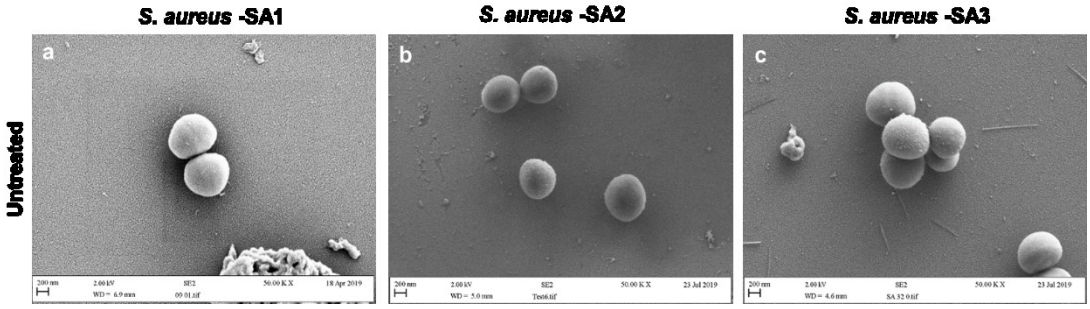

Figure 5.7 SEM images of control untreated cells of (a) *S. aureus*-SA1, (b) *S. aureus*-SA2 and (c) *S. aureus*-SA3.

Prominent changes were observed in the morphology of the treated bacterial cells, compared to their respective controls. *S. aureus* (-SA1, -SA2 and -SA3) cells treated with formulations of sprays and ointments containing Au (O2, S2) or Au-Gr (O8, S8) showed numerous pits and grooves in the bacterial membrane (Figure 5.8). Deep cuts in the middle of the cells were noted (Figure 5.8e, 5.8g and 5.8m). Bacterial cells also showed wrinkled surfaces (Figure 5.8f and 5.8.i).

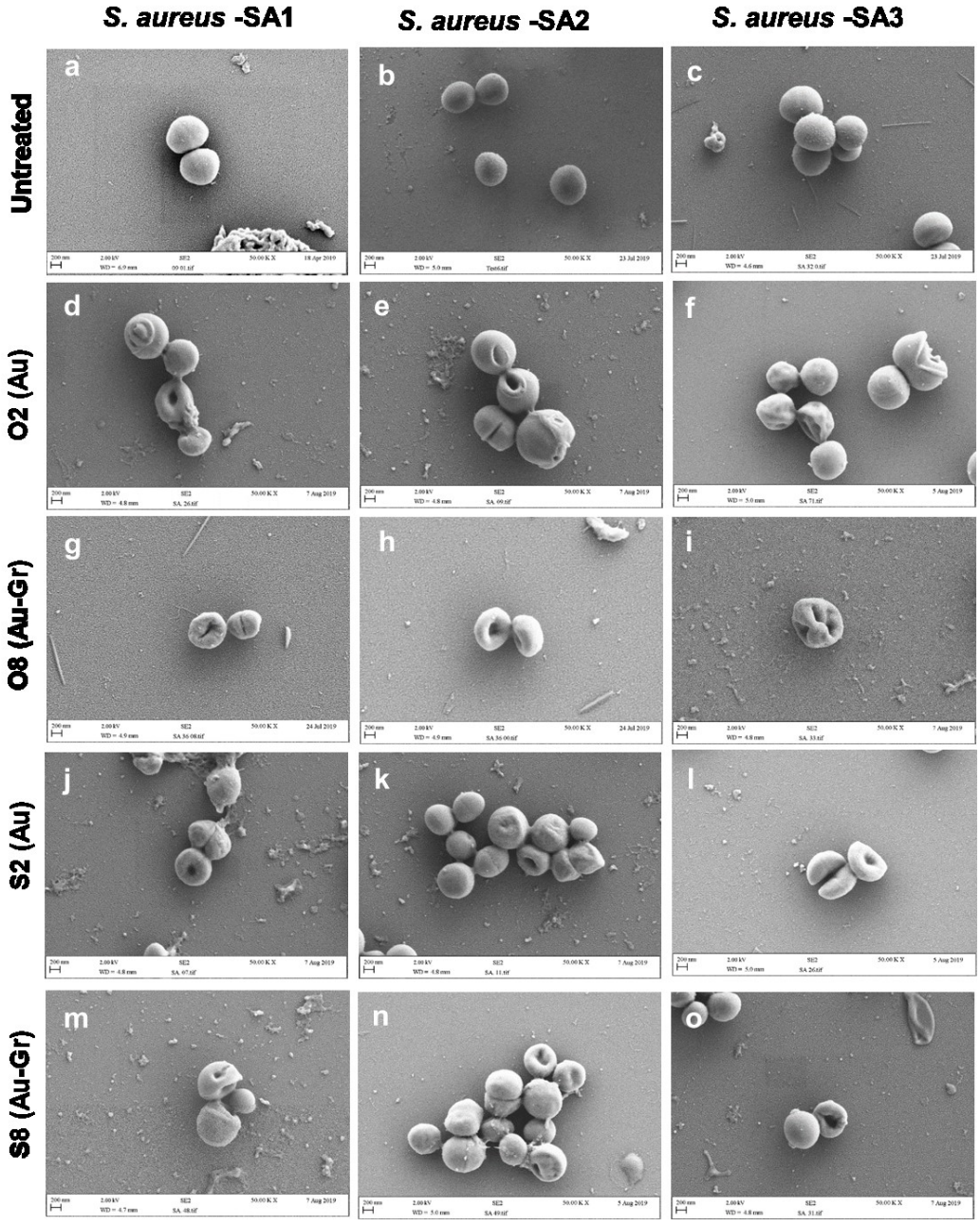

Figure 5.8 SEM images showing the morphological changes in *S. aureus*-SA1, *S. aureus*-SA2 and *S. aureus*-SA3 untreated (a-c) and following the treatment with different ointment formulations (d-i) and spray formulations (j-o) containing Au and Au-Gr.

Structural deformations were also detected in the three *S. aureus* isolates treated with O6 (Pd-GO) ointment. Bacterial cells did not look uniform in size and distribution, with some cells swelling up (~1100 nm) and other cells shrinking (~300-400 nm) (indicated by arrows in Figure 5.9). A leakage of cellular contents was also detected in *S. aureus*-SA1 (Figure 5.9a).

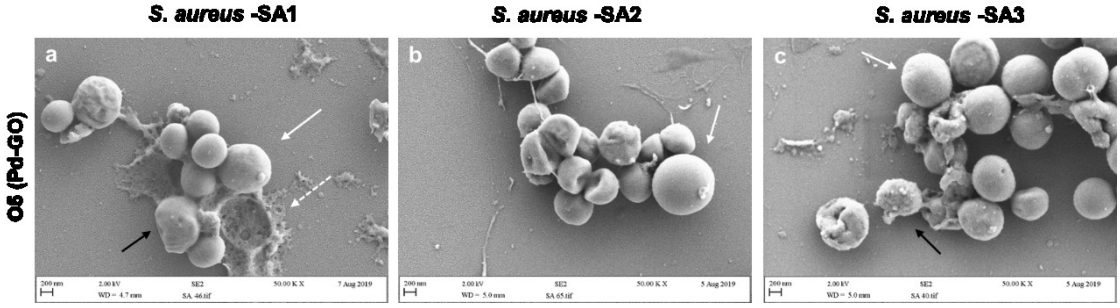

Figure 5.9 SEM images showing the morphological changes in (a) *S. aureus*-SA1, (b) *S. aureus*-SA2 and (c) *S. aureus*-SA3 following the treatment with different O6 (Pd-GO) formulation. White arrows indicate the cells that increased in size while the black arrows indicate the ones that decreased in size. The dotted arrow indicates cellular leakage.

Additional morphological changes were detected in bacterial cells treated with formulations containing Pd, Ga-Gr and Pd-Gr. After being exposed to Ga-Gr, the membranes of *S. aureus* (Figure 5.10 d-f) were damaged and the cellular debris were excreted. *S. aureus* cells also showed an elongation in shape (Figure 5.11. e-f).

Further structural changes included irregular rough surfaces (Figure 5.10d and f), deep grooves (Figure 5.10b and 5.11c and d), distorted edges (Figure 5.10g and i), cell seepage (Figure 5.11h) and folded wrinkled membrane (Figure 5.10c).

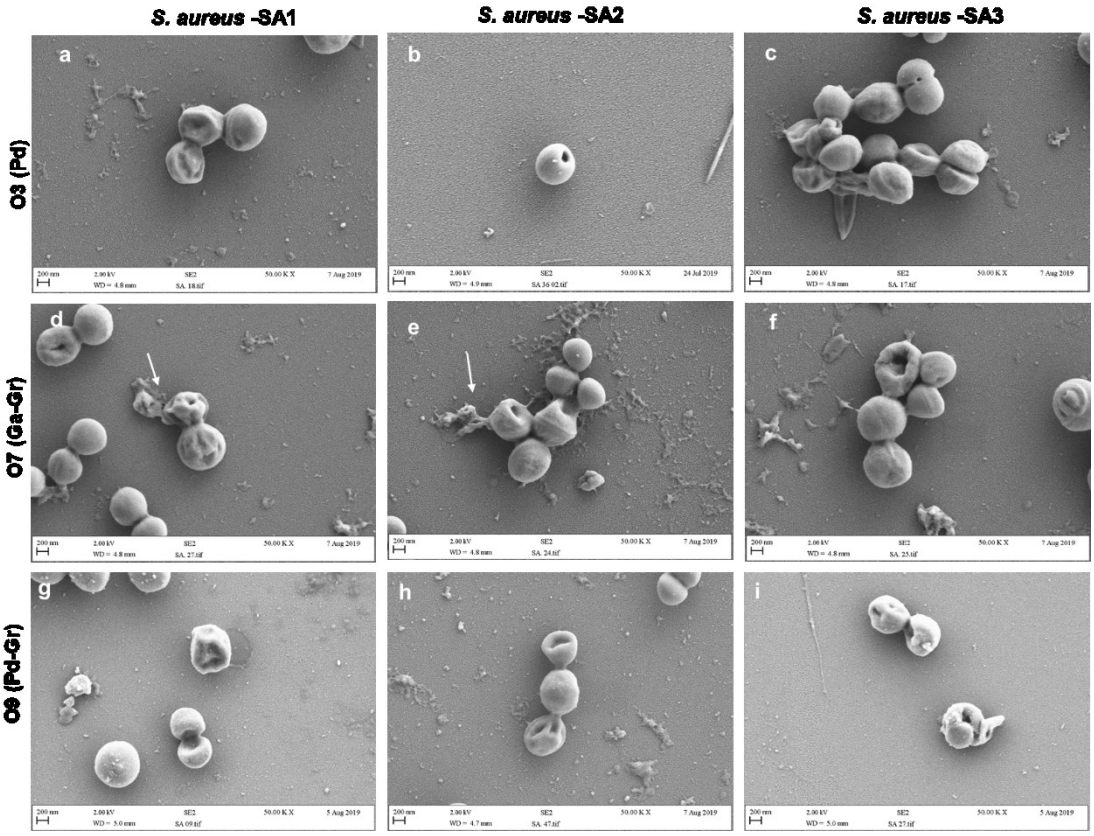

Figure 5.10 SEM images showing the morphological changes in (a) *S. aureus*-SA1, (b) *S. aureus*-SA2 and (c) *S. aureus*-SA3 following the treatment with different O3 (Pd), O7 (Ga-Gr) and 09 (Pd-Gr). Arrows indicate the cellular debris excreted following treatment.

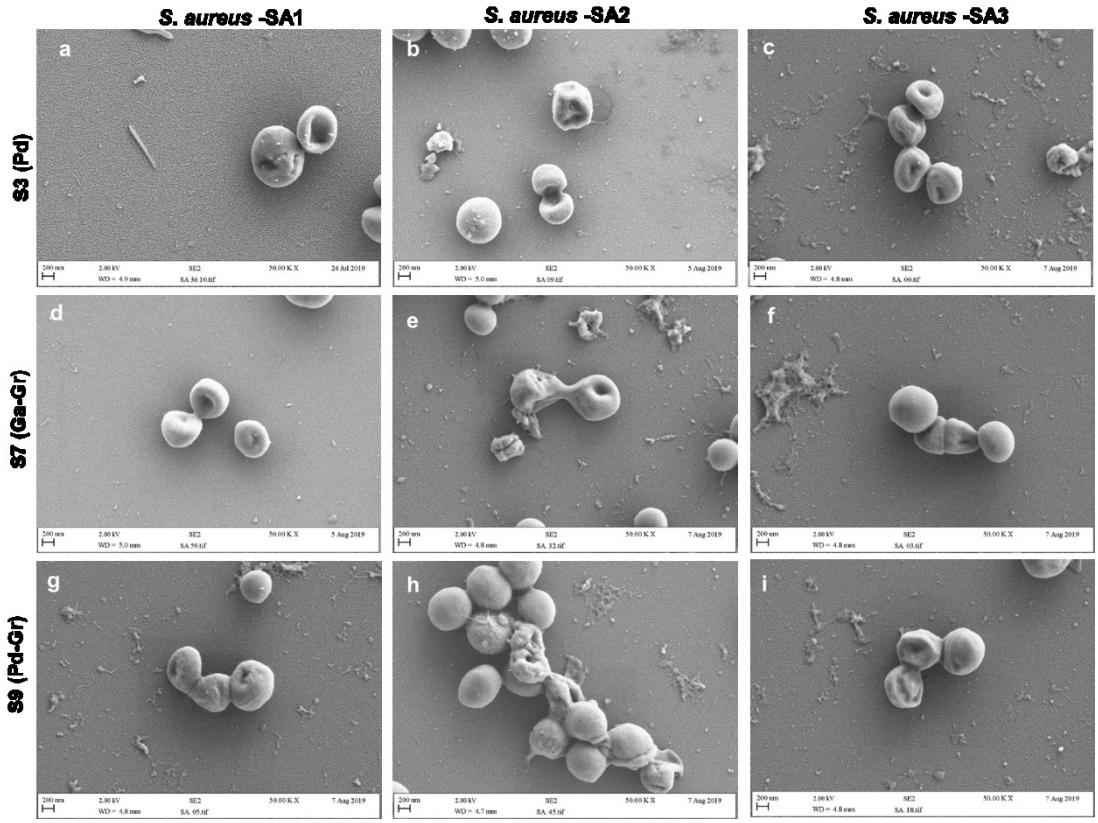

Figure 5.11 SEM images showing the morphological changes in (a) *S. aureus*-SA1, (b) *S. aureus*-SA2 and (c) *S. aureus*-SA3 following the treatment with different S3 (Pd), S7 (Ga-Gr) and S9 (Pd-Gr).

The antimicrobial efficacies of mupirocin and formulation O8 (Au-Gr) were compared against *S. aureus*-SA3. The cellular morphology of *S. aureus*-SA3 (Figure 5.12b) remained intact following the mupirocin treatment, indicating the inefficiency of mupirocin towards this resistant isolate. However, the same bacterial isolate showed numerous holes in its cell membrane following its treatment with O2 (Au) ointment (Figure 5.12c), demonstrating a higher antimicrobial activity.

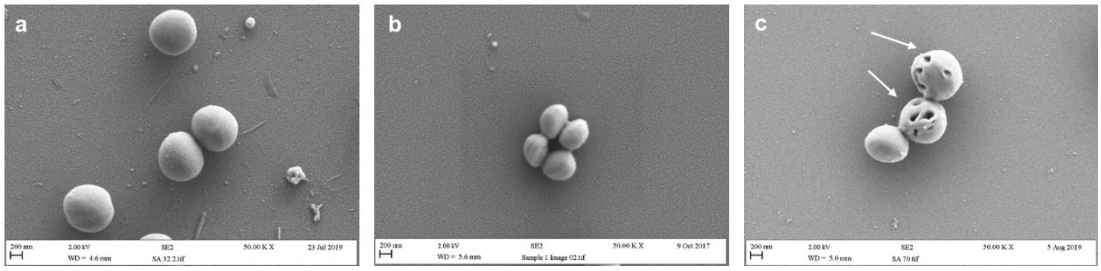

Figure 5.12 SEM images of *S. aureus*-SA3 (a) untreated, (b) treated with mupirocin and (c) treated with O2 (Au) formulation. Arrows indicate the pores created within the membrane following Au treatment.

SEM analysis of biofilms of *S. aureus*-SA3 treated with O2 (Au) formulation showed the production of an extracellular polymeric layer surrounding the cells (Figure 5.13.). In contrast to the control biofilm showing aggregates of cells (Figure 5.13.a), cells in biofilms treated with O2 (Au) appeared as a monolayer of dispersed cells with flattened concave surfaces (Figures 5.13.b and 5.13.c).

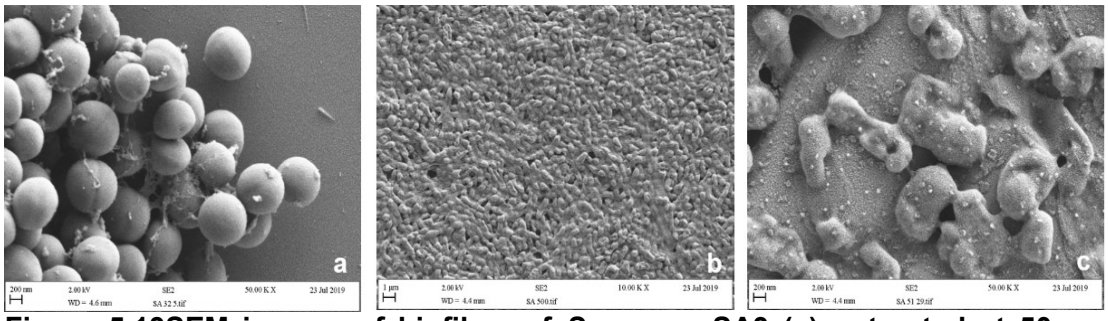

Figure 5.13SEM images of biofilms of *S. aureus*-SA3 (a) untreated at 50x magnification and (b) biofilms treated with O2 formulation at 10x and (c) 50x magnification.

The SEM results showed that the formulated ointments and sprays exhibited strong morphological effects on *S. aureus* bacterial cells including the mupirocin resistant cells.

5.4.5 Physical Evaluation of Topical Formulations for Nasal Ointments and Sprays

5.4.5.1 Organoleptic Characteristics

The organoleptic properties of the different tested formulations were evaluated (Tables 5.8 and 5.9). The results showed that all the ointment formulations except O6 (Pd-GO) exhibited a good appearance, and were homogeneous and stable to creaming and coalescence with no signs of phase separation. O6 (Pd-GO) did not feel homogeneous and formed a white precipitate after testing. The nine tested spray formulations showed a clear fluid appearance. S2 (Au) gave a pale yellowish appearance, while S3 (Pd) looked lightly rusty in colour.

5.4.5.2 Thermal Cycling

The exposure of the different ointment and spray formulations to different varying temperatures (4 °C and 25 °C) over 6 weeks did not change their efficacy against the tested strains. The efficacy of the ointments was also tested in a freezing/thawing cycle (4 °C and 50 °C) and remained unchanged.

5.4.5.3 Formulation pH

pH values of the semi-solid ointments ranged from 5.01 to 8.72, while the pH of the spray formulations ranged from 4.95 to 8.71. The pH values of all the formulations remain unchanged over the 3 months period.

5.4.5.4 Spreadability

The spreadability of a semi-solid ointment formulation is required to determine its ability to cover the skin in an even distribution. Spreadability is an important factor in the precise administration of a specific dose of a tested formulation, which consequently affects majorly a topical therapy. The results revealed that the spreadability values of the tested formulations were comparable each other (14.7-18.4) (Table 5.8). The largest spreading dimeters were shown by formulations including O8 (Au-Gr) (18.4 g.cm/s),

O7 (Ga-Gr) (16.5 g.cm/s) and O2 (Au) (15.9 g.cm/s). O6 (Pd-GO) was the only formulation showing low spreadability (8.8 g.cm/s) compared to other formulations.

Table 5.8 Physicochemical evaluation of nasal ointment formulations

	O1 (Ga)	O2 (Au)	O3 (Pd)	O4 (Ga-GO)	O5 (Au-GO)	O6 (Pd-GO)	O7 (Ga-Gr)	O8 (Au-Gr)	O9 (Pd-Gr)
Texture	Smooth	Smooth	Smooth	Smooth	Smooth	Smooth	Smooth	Smooth	Smooth
Color	White	Pale white	White	White	White	Opaque	White	Pale white	White
Homogeneity	Homogeneous	Homogeneous	Homogeneous	Homogeneous	Homogeneous	Homogeneous	Homogeneous	Homogeneous	Homogeneous
Immediate feel	Light with no grittiness Slightly greasy	Light with no grittiness Slightly greasy	Light with no grittiness Slightly greasy	Light with no grittiness Slightly greasy	Light with no grittiness Slightly greasy	Light with no grittiness Slightly greasy	Light with no grittiness Slightly greasy	Light with no grittiness Slightly greasy	Light with no grittiness Slightly greasy
Phase separation	No	No	No	No	No	No	No	No	No
Fluidity	Viscous	Viscous	Viscous	Viscous	Viscous	Viscous	Viscous	Viscous	Viscous
Spreadability (g×cm/s)	14.7	15.9	15.6	15.1	15.2	8.8	16.5	18.4	15.7
pH	6.01 ± 0.11	6.01 ± 0.03	5.01 ± 0.07	7.21 ± 0.06	6.44 ± 0.10	8.42 ± 0.13	6.88 ± 0.09	5.88 ± 0.14	6.13 ± 0.07
Thermal cycling	Stable	Stable	Stable	Stable	Stable	Stable	Stable	Stable	Stable
Creaming and coalescence	Stable	Stable	Stable	Stable	Stable	Stable	Stable	Stable	Stable

Table 5.9 Physicochemical evaluation of nasal spray formulations

	S1 (Ga)	S2 (Au)	S3 (Pd)	S4 (Ga-GO)	S5 (Au-GO)	S6 (Pd-GO)	S7 (Ga-Gr)	S8 (Au-Gr)	S9 (Pd-Gr)
Physical appearance	Clear	Clear – pale yellowish	Clear - pale rusty	Clear	Clear	Clear	Clear	Clear	Clear
Immediate feel	Greaseless	Greaseless	Greaseless	Greaseless	Greaseless	Greaseless	Greaseless	Greaseless	Greaseless
pH (±SD)	5.65 ± 0.04	5.80 ± 0.13	4.95 ± 0.09	7.11 ± 0.11	6.50 ± 0.02	8.71 ± 0.08	6.33 ± 0.06	6.21 ± 0.06	5.05 ± 0.04
Thermal cycling	Stable	Stable	Stable	Stable	Stable	Stable	Stable	Stable	Stable
Fluidity	Fluid	Fluid	Fluid	Fluid	Fluid	Fluid	Fluid	Fluid	Fluid

5.5 Discussion

Mupirocin is the world's most widely used topical antibiotic for treating MRSA infections (Tucaliuc *et al.*, 2019). A worldwide increase in mupirocin resistance was reported among *S. aureus* during the last few years (Poovelikunnel *et al.*, 2015). This study investigated the antimicrobial activity of metal ions and graphene-based compounds against three clinical *S. aureus* isolates, which were collected from The Whittington Hospital (London), and exhibited high (*S. aureus*-SA3) and low-level mupirocin resistance (*S. aureus*-SA1). The prevalence of mupirocin resistance within UK ranges between 28.5% to 42.8%. However, this rate fluctuates among different regions and even among different healthcare institutions. For instance, mupirocin resistance had been reported only at 0.8% in Yorkshire and Humber but it reached 14% in London (Horner *et al.*, 2017; Xu *et al.*, 2018; Khoshnood *et al.*, 2019). This can be attributed in part to the expanded use of mupirocin following its ease of availability over the counter and its extensive use as a routine treatment for nasal and skin infections (Patel, Gorwitz, *et al.*, 2009).

5.5.1 Synergy Testing of Excipients Combined with Metal ions and Graphene Composites

The synergistic and additive antimicrobial effect exhibited by the addition of metal ions (Pd, Au, Ga) to combinations containing polyethylene glycol compounds (PEG 400 and PEG 3350) can be mainly attributed to the ability of PEG polymers to increase the permeability of bacterial membrane. This may facilitate the entry and accumulation of metal ions inside the cell and consequently enhance their antibacterial activity (Habiba *et al.*, 2015; Marslin *et al.*, 2015). PEG molecules are also known to bind bacterial DNA, assisting at the same time, other metal ions to bind to DNA (Marslin *et al.*, 2015). Other possible factors that may have led to the enhanced antimicrobial activity is that PEG may increase the stability of the metal ions by increasing their compatibility with their biological milieu and reducing their non-specific absorption to other biomolecules (Stiufiuc *et al.*, 2013; Mahmoud *et al.*, 2017; Niţica *et al.*, 2018). Hence, it may be that PEG in

tested formulations acted as a stabilizer due to the coordinative saturation provided by the large number of oxygen atoms in the long PEG chains (Luo *et al.*, 2005; Shameli *et al.*, 2012). It has been reported that PEG is also effective in controlling the shape and size of metal ions, which enhance their effect (Popa *et al.*, 2007; Bin Ahmad *et al.*, 2011; Shameli *et al.*, 2012). PEG polymers have also shown an enhanced antimicrobial effect when combined with graphene-based materials against *S. aureus* since PEG enhances the stability of graphene composites by preventing their aggregation (Habiba *et al.*, 2015; P. Li *et al.*, 2015; Kumar *et al.*, 2019). Furthermore, it has been suggested that the hydrophilicity of PEG polymers will enable graphene and graphene oxide to act on the bacterial membrane (Habiba *et al.*, 2015).

Platinum ions exhibited high inhibitory (0.49 mg/L) and bactericidal (7.8 mg/L) effects against *S. aureus* isolates, hence it has a promising potential to be incorporated in topical formulations. However, Pt exhibited an indifferent effect when tested in combination with PEG 400 or PEG 3350. Work by others has shown that PEG chains demonstrated weak binding to platinum and were not able to act as ion scaffolds (Forbes *et al.*, 2013). Therefore, Pt was excluded from further investigations in this study. Nonetheless, as a suggested possible solution, PEG chains could be coupled with specific alcohol-containing amino acids in order to enhance their binding to Pt ions and hence their antimicrobial effect (Forbes *et al.*, 2013).

5.5.2 Evaluation of the Properties of the Tested Formulations

This study aimed at developing the simplest nasal topical formulations including a short ingredients' list without any redundant elements. It was prudent, during the development process, to preserve the type of emulsifier of each excipient while keeping them within the acceptable ranges, as reported by the Reference List Drug (Chang *et al.*, 2013).

Topical products were assessed for several tests to confirm their efficacy. Texture characteristics of semi solid formulations such as spreadability and viscosity play a significant role in the performance of the ointment (Krishnaiah *et al.*, 2014; Djiobie Tchienou *et al.*, 2018). Polymers of soft

white paraffin and Softisan 649 contributed to giving the tested formulations a silky feeling with a light greasy sensation (De Villiers, 2009; Fiume *et al.*, 2013). It was shown that the nine tested formulations were viscous and spreadable, which are two parameters reflecting on adhesion.

The results revealed that the spreadability values of the formulations tested in this study were comparable to other formulated and commercial products (Garg *et al.*, 2002; Sabale *et al.*, 2011; Chen *et al.*, 2016; Djiobie Tchienou *et al.*, 2018). It should be noted that rheological estimations bear an error margin since each individual applies ointments and creams in a distinct manner (motion, speed, stroke) (Garg *et al.*, 2002). There were no differences in the spreadability values among the nine tested ointment formulations. Differences in spreadability values may generally result from different manufacturing/storage conditions (Kryscio *et al.*, 2008).

The pH measurement of the ointment formulations was challenging because of the lack of standard recommendations for semi-solid non-aqueous bases. The pH of the formulated ointments (pH 5.01 – 8.42) and sprays (pH 4.95 – 8.71), except for O6 (8.42) and S6 (8.71), fell within the optimal pH range for commercially available nasal products (pH 4.5 – 6.5) (Alagusundaram *et al.*, 2010). This is close to the pH of the nasal cavity (pH 5.5 – 6.4) which impacts to a great extent the efficacy of topical drugs (Marx *et al.*, 2016). Therefore, formulations (O6 and S6) containing Pd-GO and displaying a high pH were excluded from further analysis.

Except for the formulation O6 containing (Pd-GO), all eight ointment formulations were smooth, homogenous, stable and consistent. Properties such as physical appearance, texture and colour of products are not critical quality attributes in the product efficacy; however, they have a big impact on the acceptance by the consumer. The spray formulations exhibited a physically clear stable appearance, similar to those noted in the literature (Chang *et al.*, 2013).

5.5.3 Testing of the Efficacy of the Formulations

The findings from agar well diffusion assays showed a strong antimicrobial efficacy of the tested ointment and spray formulations against the three distinct *S. aureus* isolates indicating different antibiograms and different susceptibility patterns towards mupirocin. At least five out of the tested formulations of ointments and five sprays displayed an improved antimicrobial efficacy to the commercial mupirocin (2%) towards the three *S. aureus* isolates in their planktonic and biofilm forms. This may be due to the key differences in the modes of action of mupirocin (inhibition of tRNA), and metal ions (Au, Ga and Pd) and graphene composites (such as triggering ROS production and mechanical lysis). The ZoIs and CVBA of the ointments and spray formulations containing the same active ingredients were comparable to each other demonstrating that they showed similar antimicrobial efficacies. It has been previously reported that the effectiveness of each formulation was highly associated with the nature of bases (hydrocarbon-base or PEG-base) and the affinity of the bioactive compounds (metal ions) towards it (Gemeda *et al.*, 2018). For instance, water-soluble non-ionic polymers of PEG in graphene-based formulations were found to enhance the dispersion of graphene in water aqueous solutions, and hence its efficacy (Takayanagi *et al.*, 2019). This can also partly explain the high antimicrobial efficacy of formulations containing Au-Gr, Ga-Gr and Pd-Gr.

The visualization of the morphology of the post-treated bacterial cells using SEM confirmed the antimicrobial activity of the different formulations, while giving a possible explanation of the antibacterial mechanism of action of the metal ions and graphene composites.

The changes in cellular morphology in treated bacterial cells suggested that the active compounds were able to cause membrane damage and disintegration. The flattened and desiccated appearance of the cells after treatment may have resulted from the leakage of the cytoplasmic contents, while the enlargement of the cells and the swollen edges may be associated with a change in the membrane permeability. It was evident that the integrity

of the cell membranes of the three tested isolates was lost following treatment with ointment or spray formulations, with some bacterial cells looking permanently damaged. The structural changes seen provided a confirmation of the direct interaction between metal ions and graphene composites with the bacterial cell membrane which has been previously demonstrated (Pham *et al.*, 2015; Wang *et al.*, 2017).

Ions of Au, Ga or Pd have not been previously incorporated in topical treatments. However, other metal ions such as Ag ions have been included in some nasal preparations and the results showed that patients did not encounter any side effects associated with the direct intranasal administration of silver (Scott *et al.*, 2017). However, studies indicated that the chronic exposure of silver has been associated with a permanent bluish-grey discoloration of the skin (argyria) or eyes (argyrosis) (Drake and Hazelwood, 2005).

5.5.4 Additional Suggestions or Recommendations for Ointments

In compliance with the standards of the National Formulary (NF) and the United States Pharmacopeia (USP), the formulated ointment products in this study were inexpensive, nonreactive, good emollient and not water-washable so that they can stay in longer contact with the skin (Nikitakis and Lange, 2006; De Villiers, 2009). However, topical ointment preparations have a high potential for microbial contamination. The quality of pharmaceutical preparations is under considerable threat of bacterial or fungal contamination during the preparation or after the first consumption (Esposito *et al.*, 2003; Hugbo *et al.*, 2005). Bacterial enzymes can lead to the breakdown or alteration of the active ingredients and hence variation in the treatment efficacy (Morgan, 1985; Nawas and Alkofahi, 1994; Hugbo *et al.*, 2005). Therefore, preservatives such as methylparaben, imidurea and hydantoin are usually added to the formulations to inhibit bacterial growth, but there is an increasing evidence of sensitization, allergic contact dermatitis and carcinogenesis caused by the use of such chemicals (Chang *et al.*, 2013). This study opted to exclude preservatives from all ointment formulations. Consequently, it is suggested that ointments can be packed in

a single-use tubes (with half the amount used in each nostril). Alternatively, ointment tubes can contain a collapsible bag or a movable piston to compensate for the ejected semi-solid volume, while eliminating the risk of sucking air into the tube (Djupesland, 2013).

This study also opted at excluding the fragrance component since that at least 1% of the population are allergic to fragrance chemicals (U.S. AAD, 1998). This is in compliance to the SUPAC-SS guidance that indicates that the deletion of an ingredient used for aromatic purposes would not affect the activity of the tested formulation (FDA, 1997).

5.6 Conclusion

Metal ions, graphene and graphene oxide were successfully incorporated into topical formulations of sprays and ointments for the eradication of MRSA. Out of the nine formulations, ointments and sprays containing Au and Au-Gr exhibited the greatest antimicrobial activity against the planktonic and biofilm forms of mupirocin sensitive and resistant MRSA. The four formulations showed a superior antimicrobial activity when compared to the respective mupirocin commercial drug. The formulated products showed good pH, spreadability, viscosity and stability when tested up to a 3-month period. Consequently, the formulated ointments could be promising alternatives for current intranasal treatment.

Chapter 6 Conclusions and Future Work

6.1 Conclusions

This thesis sought to contribute towards the development of topical formulations for the management of bacterial infections caused by three MDR ESKAPE pathogens (*P. aeruginosa*, *K. pneumoniae* and *S. aureus*). The basis of this work focused on assessing the antimicrobial activity of eighteen metal ion solutions and graphene-based compounds (graphene and graphene oxide).

The results confirmed that Pt, Pd, Sn, Mo and Au inhibited, at low concentrations, the planktonic bacterial cells of *P. aeruginosa* (2 isolates), *K. pneumoniae* (4 isolates) and *S. aureus* (4 isolates), irrespective of their antibiotic susceptibility patterns. Additionally, combinations of graphene or graphene oxide to specific metal ions (Mo-Gr, Mo-GO, Au-GO, Au-Gr, Pt-GO, Ga-Gr and Ga-GO) showed an enhanced antimicrobial action toward the bacterial isolates, compared to metal ions, graphene or graphene oxide tested alone. The results also confirmed the antibiofilm activity of these combinations that resulted in an 80% reduction in the metabolic activity of the biofilm cells of the same isolates.

This study highlighted the controversial consistent use of silver as an antimicrobial following the uprising resistance concerns. Following the excessive use of silver as an antimicrobial surface coating material and as an additive in numerous consumer products, this study was one of the few that refrained from using silver and copper, and suggested new antimicrobial alternatives.

Metal ions and graphene derivatives incorporated into formulations of surgical cleansers did not exhibit any antagonistic interaction with the different excipients of the surgical scrub. Five formulations (Au-Gr, Au, Pt, Pt-Gr and Pd), out of the fourteen formulations tested, displayed the best inhibitory effect against both the planktonic and biofilm forms of CHX susceptible and CHX adapted *K. pneumoniae* strains.

In view of the escalating concerns of mupirocin resistance, this study also sought to continue exploring the potential of integrating these metal ions in intranasal topical formulations as a substitution for mupirocin. Active

materials of metal ions and combinations of metal ions and graphene were added to PEG-based and hydrocarbon-based ointment bases. An ointment formulation comprising 11 mg/L of Au was proven to have high inhibitory efficacy against mupirocin resistant *S. aureus*.

In conclusion, this study has contributed to the literature in the subsequent aspects:

- Confirmed the high promising potential of metal ions and Gr composites to be part of intranasal topical formulations or disinfectant formulas that can be used in healthcare settings.
- Suggested new inexpensive alternative antimicrobials that can be produced on a low cost and large scale as substitutes for the currently used antibiotics.

  The price of mupirocin nasal (30 mL), also named as bactroban or centany, ranges between £4.86 to £6.58. The drug is recommended to be applied 2-3 times per day for 5-7 days to ensure proper eradication of MRSA. A rough cost analysis for formulations of ointment (O2) and spray (S2) containing Au is shown below:

Ointment O2		
Ingredients	**Formulation (100 mL)**	**Price (£)**
Paraffin	95.00 mL	0.051
Softisan 649	3.90 mL	0.600
Au ions	1.10 mg	0.033
	Total price	0.684

Spray S2		
Ingredients	**Formulation (100 mL)**	**Price (£)**
PEG 3350	4.45 mL	0.350
PEG 400	4.45 mL	0.026
Au ions	1.10 mg	0.440
saline	9.00 mL	0.200
	Total price	1.016

  Therefore, a volume of 30 mL of O2 and S2 formulations would cost £0.2 and £0.3, respectively, excluding the packaging and manufacturing costs. Therefore, the alternative formulations would still be at least 3 times less expensive than mupirocin.

6.2 Limitations and Future Work

The bacterial samples tested in this study were collected from one clinical centre, hence, this was not representative of the *P. aeruginosa*, *K. pneumoniae* or *S. aureus* populations across the UK. Furthermore, the *S. aureus* strains were not isolated from patients suffering from infections or rhinosinusitis. It is recommended to reproduce the assays to test a larger number of heterogeneous clinical isolates.

Limitations of PEG-Based Spray Formulations Containing Metal Ions

Nasal sprays in various forms deposit the drug in the nasal cavities, with a high probability of reaching the anterior nares, at a high speed of 1 - 5 m/s. Since metal ions (Au, Ga and Pa) are particles with an aerodynamic diameter of picometer (pm) size, there is a probability that these particles might reach the lower airways after inhalation.

Further preclinical and clinical investigations are necessary to determine the efficacy, stability and safety of using the formulated products. Several parameters should be assessed including:

- Viscosity which has a high impact on the drug release from the ointment formulations.
- *In-vitro* drug release from topicals to determine the permeation/flux pattern across synthetic membranes.
- Shelf-life and stability of the products over a course of 2 years.
- Antifungal activity of the formulations.

Whilst *in-vitro* cytotoxicity assays undertaken were valuable in assessing the cytotoxic behaviour of metal ions and graphene compounds, these cannot account for the antimicrobial efficacy or safety of the compounds *in-vivo*. Therefore, it is also recommended to perform:

- Dose escalation studies for cell cytotoxicity assays to establish therapeutic ranges for each compound or combination (MTS assays should be carried out at concentrations higher than the tested MICs).
- *In-vitro* skin sensitization assays.

- *In-vitro* assays to compare the effectiveness of the formulations to traditional mupirocin using a wounded porcine skin biofilm model.
- Chemical toxicology assays using *in-vitro* (culture of human airway and alveolar epithelial cells) and *in-vivo* suitable animal (rats) models.
- *In-vivo* assays on animal models to test the safety (Genotoxicity) and efficacy (pharmacology) of the formulations *in-vivo*.
- *In-vivo* assays on healthy volunteers who are not suspected to have any allergic contact dermatitis.
- Randomized crossover control clinical trials to compare topical commercial mupirocin ointments to the formulated products in the treatment of patients with acute or chronic rhinosinusitis.
- Whole genome sequencing of the bacterial isolated to help build a wider picture on the modes of action of the tested compounds especially for the mupirocin and CHX resistant strains.

  The above-mentioned parameters will increase the chance of success of the tested formulations (cleansers, ointments and sprays) in pharmaceutical development.

While research to date on metal-based antibacterial formulations has considerable promise, concerns regarding possible bacterial resistance are still escalating. It should be noted that bacterial adaptation to changing availability of metal ions by altering gene expression and the development of metal resistance are relatively slow processes and can take up to many years (Chandragsu *et al.*, 2018). Furthermore, biotechnology approaches including genomics and proteomics can provide biomarkers for resistance traits. Ultimately, this can lead to the sustainable use of metal antimicrobials through focused and personalized application approaches, particularly where MBAs are not used if resistance markers are present.

Therefore, while waiting for more lengthy and costly experiments (*in-vitro* and *in-vivo*) requiring a detailed comprehension of the toxicity of MBAs and graphene-based compounds, the tested metal-based formulations can represent a possible solution for disinfectants.

Chapter 7 References

Abuzaid, A., Hamouda, A. and Amyes, S. G. B. (2012) ‘Klebsiella pneumoniae susceptibility to biocides and its association with cepA, qacΔE and qacE efflux pump genes and antibiotic resistance’, *Journal of Hospital Infection*, pp. 87–91.

Bin Ahmad, M., Tay, M. Y., Shameli, K., Hussein, M. Z. and Lim, J. J. (2011) ‘Green synthesis and characterization of silver/chitosan/polyethylene glycol nanocomposites without any reducing agent’, *International Journal of Molecular Sciences*, 12(8) pp. 4872–4884.

Akhavan, O. and Ghaderi, E. (2010) ‘Toxicity of graphene and graphene oxide nanowalls against bacteria’, *ACS Nano*, 4(10) pp. 5731–5736.

Al-Jumaili, A., Alancherry, S., Bazaka, K. and Jacob, M. V. (2017) ‘Review on the antimicrobial properties of Carbon nanostructures’, *Materials*, 10(9) pp. 1–26.

Alagusundaram, M., Chengaiah, B., Gnanaprakash, K., Ramkanth, S., Madhusudhana, C., Chetty, C. M. and Dhachinamoorthi, D. (2010) ‘Nasal drug delivery: An overview’, *Indian Journal of Research in Pharmaceutical Science*, 1(4) pp. 454–465.

Alexander, J. W. (2009) ‘History of medical silver use’, *Surgical Infections*, 10(3) pp. 289–292.

Allen, L. (2019) ‘Mupirocin 1% in normal saline nasal suspension’, *U.S. Pharmacist*, April pp. 47–48. Available at: https://www.uspharmacist.com/article/mupirocin-1-in-normal-saline-nasal-suspension.

Allen, M. J., Tung, V. C. and Kaner, R. B. (2010) ‘Honeycomb carbon: A review of graphene’, *Chemical Reviews*, 110(1) pp. 132–145.

Altimira, F., Yẫez, C., Bravo, G., González, M., Rojas, L. A. and Seeger, M. (2012) ‘Characterization of copper-resistant bacteria and bacterial communities from copper-polluted agricultural soils of central Chile’, *BMC Microbiology*, 12(193) pp. 1–12.

Anderl, J. N., Franklin, M. J. and Stewart, P. S. (2000) ‘Role of antibiotic

penetration limitation in Klebsiella pneumoniae biofilm resistance to ampicillin and ciprofloxacin', *Antimicrobial Agents and Chemotherapy*, 44(7) pp. 1818–1824.

Anjem, A. and Imlay, J. A. (2012) 'Mononuclear Iron Enzymes Are Primary Targets of Hydrogen Peroxide Stress', *The journal of biological chemistry*, 287(19) pp. 15544–15556.

Asakura, K. A., Satoh, H. S., Chiba, M. C., Okamoto, M. O., Serizawa, K. S., Nakano, M. N. and Omae, K. O. (2009) 'Genotoxicity Studies of Heavy Metals : Lead , Bismuth , Indium , Silver and Antimony', *Journal of Occupational Health*, 51 pp. 498–512.

Ayres, P. G. (2004) 'Alexis Millardet : France ' s forgotten mycologist', *Mycologist*. Manchester Metropolitan University, 18(February) pp. 23–26.

Ayukekbong, J. A., Ntemgwa, M. and Atabe, A. N. (2017) 'The threat of antimicrobial resistance in developing countries : causes and control strategies', *Antimicrobial Resistance and Infection Control*. Antimicrobial Resistance & Infection Control, 47(6) pp. 1–8.

Azman, N. H. N., Mamat, S., Ngee, L. H. and Sulaiman, Y. (2018) 'Graphene-based ternary composites for supercapacitors', *International Journal of Energy Research*, 42(February) pp. 2104–2116.

Banin, Ehud, Lozinski, A., Brady, K. M., Berenshtein, E., Butterfield, P. W., Moshe, M., Chevion, M., Greenberg, E. P. and Banin, Eyal (2008) 'The potential of desferrioxamine-gallium as an anti-Pseudomonas therapeutic agent', *PNAS*, 105(43) pp. 16761–16766.

Barapatre, A., Aadil, K. R. and Jha, H. (2016) 'Synergistic antibacterial and antibiofilm activity of silver nanoparticles biosynthesized by lignin-degrading fungus', *Bioresources and Bioprocessing*. Springer Berlin Heidelberg, 3(8) pp. 1–13.

Barber, M. (1961) 'Methicillin-Resistant Staphylococcus aureus', *Journal of clinical pathology*, 14 pp. 385–393.

Barbolina, I., Woods, C. R., Lozano, N., Kostarelos, K., Novoselov, K. S.

and Roberts, I. S. (2016) ‘Purity of graphene oxide determines its antibacterial activity’, *2D Materials*. IOP Publishing, 3(2) pp. 1–12.

Bassetti, M., Vena, A., Croxatto, A., Righi, E. and Guery, B. (2018) ‘How to manage Pseudomonas aeruginosa infections’, *Drugs in Context*, 7 pp. 1–18.

Becker, L. C., Bergfeld, W. F., Belsito, D. V., Hill, R. A., Klaassen, C. D., Liebler, D., Marks, J. G., Shank, R. C., Slaga, T. J., Snyder, P. W. and Andersen, F. A. (2014) *Safety Assessment of Trimoniums as Used in Cosmetics*, *Cosmetic Ingredient Review*.

Bednarek, R., Nasreddin, A. and Ramsey, M. (2020) *Skin (Integument) Antiseptics*. StatPearls. Available at: https://www.ncbi.nlm.nih.gov/books/NBK507853/.

Beier, R., Anderson, P., Hume, M., Poole, T., Duke, S., Crippen, T., Sheffield, C., Cladwell, D., Byrd, J., Anderson, R. and Nisbet, D. (2011) ‘Characterization of Salmonella enterica isolates from turkeys in commercial processing plants for resistance to antibiotics, disinfectants, and a growth promoter’, *Foodborne Pathogens and Disease*, 8(5) pp. 593–600.

Birnie, C. R. and Malamud, D. (2000) ‘Antimicrobial Evaluation of N -Alkyl Betaines and N -Alkyl- N , N -Dimethylamine Oxides with Variations in Chain Length’, *Antimicrobial Agents and Chemotherapy*, 44(9) pp. 2514–2517.

Bjarnsholt, T. (2013) *The role of bacterial biofilms in chronic infections.*, *APMIS*.

Blair, J. M. A., Webber, M. A., Baylay, A. J., Ogbolu, D. O. and Piddock, L. J. V. (2015) ‘Molecular mechanisms of antibiotic resistance’, *Nature Reviews Microbiology*. Nature Publishing Group, 13(1) pp. 42–51.

Blodgett, R. and Pietrusko, R. (1986) ‘Long-term efficacy and safety of auranofin: A review of clinical experience’, *Scand. J. Rhenmatol. Suppl*, 63 pp. 67–78.

Bock, L. J., Wand, M. E. and Sutton, J. M. (2016) ‘Varying activity of chlorhexidine-based disinfectants against Klebsiella pneumoniae clinical isolates and adapted strains’, *Journal of Hospital Infection*. Elsevier Ltd, 93(1) pp. 42–48.

Boelaert, J. R., Daneels, R. F., Schurgers, M. L., Matthys, E. G., De Baere, Y. A., Gheyle, D. W., Van Landuyt, H. W., Gordts, B. Z., Godard, C. A. and Herwaldt, L. A. (1993) ‘Nasal mupirocin ointment decreases the incidence of staphylococcus aureus bacteraemias in haemodialysis patients’, *Nephrology Dialysis Transplantation*, 8(3) pp. 235–239.

Bonchi, C., Imperi, F., Minanadri, F., Visca, P. and Frangipani, E. (2014) ‘Review Article gallium-based drugs for antibacterial therapy’, *BioFactors*, 40(6) pp. 303–312.

Boonkaew, B., Kempf, M., Kimble, R., Supaphol, P. and Cuttle, L. (2014) ‘Antimicrobial efficacy of a novel silver hydrogel dressing compared to two common silver burn wound dressings: Acticoat™ and PolyMem Silver’, *Burns*. Elsevier Ltd and International Society of Burns Injuries, 40(1) pp. 89–96.

Borkow, G., Zhou, S. S., Page, T. and Gabbay, J. (2010) ‘A novel anti-influenza copper oxide containing respiratory face mask’, *PLoS ONE*, 5(6) p. e11295.

Borkow, G. and Gabbay, J. (2009) ‘Copper, An Ancient Remedy Returning to Fight Microbial, Fungal and Viral Infections’, *Current Chemical Biology*, 3(3) pp. 272–278.

Botelho, M. G. (2000) ‘Fractional inhibitory concentration index of combinations of antibacterial agents against cariogenic organisms’, *Journal of Dentistry*, 28(8) pp. 565–570.

Bridge, T. A. M., White, C. and Gadd, G. M. (1999) ‘Extracellular metal binding activity of the sulphate’, *Microbiology*, 145 pp. 2987–2995.

Burnett, C. (2015) *Safety Assessment of Inorganic Hydroxides as Used in Cosmetics Status : Release Date : Panel Meeting Date : Draft Report for*

Panel Review.

Calva, J. (1996) 'Antibiotic use in a periurban community in Mexico: A household and drugstore survey', *Social Science and Medicine*, 42(8) pp. 1121–1128.

Campbell, E. A., Korzheva, N., Mustaev, A., Murakami, K., Nair, S., Goldfarb, A. and Darst, S. A. (2001) 'Structural mechanism for rifampicin inhibition of bacterial RNA polymerase', *Cell*, 104(6) pp. 901–912.

Cassini, A. *et al.* (2019) 'Attributable deaths and disability-adjusted life-years caused by infections with antibiotic-resistant bacteria in the EU and the European Economic Area in 2015: a population-level modelling analysis', *The Lancet Infectious Diseases*, 19(1) pp. 56–66.

Chambers, H. F. and Deleo, F. R. (2009) 'Waves of resistance: Staphylococcus aureus in the antibiotic era', *Nature Reviews Microbiology*, 7(9) pp. 629–641.

Chandler, J. E., Messer, H. H. and Ellender, G. (1994) 'Cytotoxicity of Gallium and Indium Ions Compared with Mercuric Ion', *Journal of Dental Research*, 73(9) pp. 1554–1559.

Chandragsu, P., Rensing, C. and Helmann, J. D. (2018) 'Metal Homeostasis and Resistance in Bacteria', *Physiology & behavior*, 176(1) pp. 139–148.

Chang, R., Raw, A., Lionberger, R. and Yu, L. (2013) 'Generic Development of Topical Dermatologic Products : Formulation Development , Process Development , and Testing of Topical Dermatologic Products', *The American Association of Pharmaceutical Scientists Journal*, 15(1) pp. 41–52.

Chen, M. X., Alexander, K. S. and Baki, G. (2016) 'Formulation and Evaluation of Antibacterial Creams and Gels Containing Metal Ions for Topical Application', *Journal of Pharmaceuticals*. Hindawi Publishing Corporation, 2016.

Cheung, H., Wong, M. M., Cheung, S., Liang, L. Y., Lam, Y. and Chiu, S.

(2012) ‘Differential Actions of Chlorhexidine on the Cell Wall of Bacillus subtilis and Escherichia coli’, *PLOS ONE*, 7(5) p. e36659.

Chopra, I. and Roberts, M. (2001) ‘Tetracycline Antibiotics: Mode of Action, Applications, Molecular Biology, and Epidemiology of Bacterial Resistance’, *Microbiology and Molecular Biology Reviews*, 65(2) pp. 232–260.

Christensen, G. D., Simpson, W. A., Younger, J. J., Baddour, L. M., Barrett, F. F., Melton, D. M. and Beachey, E. H. (1985) ‘Adherence of coagulase-negative staphylococci to plastic tissue culture plates: A quantitative model for the adherence of staphylococci to medical devices’, *Journal of Clinical Microbiology*, 22(6) pp. 996–1006.

Cieplik, F., Jakubovics, N. S., Buchalla, W., Maisch, T., Hellwig, E., Al-ahmad, A. and Devine, D. A. (2019) ‘Resistance Toward Chlorhexidine in Oral Bacteria – Is There Cause for Concern ?’, *Frontiers in Microbiology*, 10(587).

Ciriolo, M. R., Civitareale, P., Teresa, M. C., Martino, A. De, Galiazzo, F. and Rotilios, G. (1994) ‘Purification and Characterization of Ag , Zn-Superoxide Dismutase from Saccharomyces cerevisiae Exposed to Silver *’, *The Journal of Biological Chemistry*, 269(41) pp. 25783–25787.

Clifton, L. A., Skoda, M. W. A., Brun, A. P. Le, Ciesielski, F., Kuzmenko, I., Holt, S. A. and Lakey, J. H. (2015) ‘E ff ect of Divalent Cation Removal on the Structure of Gram-Negative Bacterial Outer Membrane Models’, *Langnuir*, 31 pp. 404–412.

Cochran, W. L., Suh, S., Mcfeters, G. A. and Stewart, P. S. (2000) ‘Role of RpoS and AlgT in Pseudomonas aeruginosa biofilm resistance to hydrogen peroxide and monochloramine’, *Journal of Applied Microbiolgy*, 88 pp. 546–553.

Cornaglia, G., Lonnroth, A., Struelens, M. and Conference, P. in the (2004) *Report from the European Conference on the Role of Research in Combating Antibiotic Resistance , 2003*. Verona.

Cortese-Krott, M. M., Münchow, M., Pirev, E., Heßner, F., Bozkurt, A., Uciechowski, P., Pallua, N., Kröncke, K. D. and Suschek, C. V. (2009) 'Silver ions induce oxidative stress and intracellular zinc release in human skin fibroblasts', *Free Radical Biology and Medicine*, 47(11) pp. 1570–1577.

Coskun, M. D., Ari, F., Oral, A. Y., Sarimahmut, M., Kutlu, H. M., Yilmaz, V. T. and Ulukaya, E. (2013) 'Promising anti-growth effects of palladium(II) saccharinate complex of terpyridine by inducing apoptosis on transformed fibroblasts in vitro', *Bioorganic and Medicinal Chemistry*. Elsevier Ltd, 21(15) pp. 4698–4705.

Cowley, B. A. and Woodward, B. (2011) 'A Healthy Future : Platinum in Medical Applications', *Platinum Metals Reviews*, 55(2) pp. 98–107.

Cox, G. and Wright, G. D. (2013) 'Intrinsic antibiotic resistance: Mechanisms, origins, challenges and solutions', *International Journal of Medical Microbiology*. Elsevier GmbH., 303(6–7) pp. 287–292.

Creech, C. B., Al-Zubeidi, D. N. and Fritz, S. A. (2015) 'Prevention of Recurrent Staphylococcal Skin Infections', *Infectious Disease Clinics of North America*, 29(3) pp. 429–464.

Crossman, L. C. *et al.* (2008) 'The complete genome, comparative and functional analysis of Stenotrophomonas maltophilia reveals an organism heavily shielded by drug resistance determinants', *Genome Biology*, 9(4) p. R74.

Crouzet, M., Le Senechal, C., Brözel, V. S., Costaglioli, P., Barthe, C., Bonneu, M., Garbay, B. and Vilain, S. (2014) 'Exploring early steps in biofilm formation: Set-up of an experimental system for molecular studies', *BMC Microbiology*, 14 pp. 1–12.

Dadashi, M., Hajikhani, B., Darban-Sarokhalil, D., van Belkum, A. and Goudarzi, M. (2020) 'Mupirocin Resistance in Staphylococcus aureus: A Systematic Review and Meta-Analysis', *Journal of Global Antimicrobial Resistance*. Taibah University, 20 pp. 238–247.

Dallavalle, M., Calvaresi, M., Bottoni, A., Melle-Franco, M. and Zerbetto, F. (2015) ‘Graphene can wreak havoc with cell membranes’, *ACS Applied Materials and Interfaces*, 7(7) pp. 4406–4414.

Dasari, S. T., Zhnag, Y. and Yu, H. (2015) ‘Antibacterial Activity and Cytotoxicity of Gold (I) and (III) Ions and Gold Nanoparticles’, *Biochemistry & Pharmacology: Open Access*, 4(6) pp. 287–327.

Dastjerdi, R. and Montazer, M. (2010) ‘A review on the application of inorganic nano-structured materials in the modification of textiles: Focus on anti-microbial properties’, *Colloids and Surfaces B: Biointerfaces*. Elsevier B.V., 79(1) pp. 5–18.

Davies, J. and Davies, D. (2010) ‘Origins and evolution of antibiotic resistance.’, *Microbiología (Madrid, Spain)*, 74(3) pp. 417–433.

Dcosta, V. M., King, C. E., Kalan, L., Morar, M., Sung, W. W. L., Schwarz, C., Froese, D., Zazula, G., Calmels, F., Debruyne, R., Golding, G. B., Poinar, H. N. and Wright, G. D. (2011) ‘Antibiotic resistance is ancient’, *Nature*. Nature Publishing Group, 477 pp. 457–461.

Delmar, J. A., Su, C.-C. and Yu, E. W. (2014) ‘Bacterial Multidrug Efflux Transporters’, *Annual Review of Biophysics*, 43(1) pp. 93–117.

Demerec, M. (1948) ‘Origin of Bacterial Resistance to Antibiotics’, in *Symposium on Antibiotics at the Chicago meeting*, pp. 63–74.

Desroches, M. *et al.* (2013) ‘Prevalence of mupirocin resistance among invasive coagulase-negative staphylococci and methicillin-resistan Staphylococcus aureus (MRSA) in France: Emergence of a mupirocin-resistant MRSA clone harbouring mupA’, *Journal of Antimicrobial Chemotherapy*, 68(8) pp. 1714–1717.

Dizaj, S. M., Mennati, A., Jafari, S., Khezri, K. and Adibkia, K. (2015) ‘Antimicrobial activity of carbon-based nanoparticles’, *Advanced Pharmaceutical Bulletin*, 5(1) pp. 19–23.

Djiobie Tchienou, G. E., Tsatsop Tsague, R. K., Mbam Pega, T. F., Bama, V., Bamseck, A., Dongmo Sokeng, S. and Ngassoum, M. B. (2018) ‘Multi-

response optimization in the formulation of a topical cream from natural ingredients', *Cosmetics*, 5(1) pp. 1–14.

Djupesland, P. G. (2013) 'Nasal drug delivery devices : characteristics and performance in a clinical perspective — a review', *Drug Delivery and Translational Research*, 3 pp. 42–62.

Doudoulakakis, A., Spiliopoulou, I., Spyridis, N., Giormezis, N., Kopsidas, J., Militsopoulou, M., Lebessi, E. and Tsolia, M. (2017) 'Emergence of a staphylococcus aureus clone resistant to mupirocin and fusidic acid carrying exotoxin genes and causing mainly skin infections', *Journal of Clinical Microbiology*, 55(8) pp. 2529–2537.

Drake, P. L. and Hazelwood, K. J. (2005) 'Exposure-related health effects of silver and silver compounds: A review', *Annals of Occupational Hygiene*, 49(7) pp. 575–585.

Dreyer, D. R., Park, S., Bielawski, W. and Ruoff, R. S. (2010) 'The chemistry of graphene oxide', *Chemical Society Reviews*, 39 pp. 228–240.

Driscoll, J. A., Brody, S. L. and Kollef, M. H. (2007) 'The Epidemiology , Pathogenesis and Treatment of Pseudomonas aeruginosa Infections', *Drugs*, 67(3) pp. 351–368.

Drlica, K., Malik, M., Kerns, R. J. and Zhao, X. (2008) 'Quinolone-mediated bacterial death', *Antimicrobial Agents and Chemotherapy*, 52(2) pp. 385–392.

Drugdetails (2017) *Mupirocin*. Available at: https://drugsdetails.com/mupirocin/ (Accessed: 31 December 2019).

Duffus, J. H. (2002) '"Heavy Metal" - A Meaningless Term?', *Pure Applied Chemistry*, 74(5) pp. 793–807.

ECDC (2018) *Surveillance of antimicrobial resistance in Europe*, *Surveillance of antimicrobial resistance in Europe*. Stockholm.

El-mahallawy, H. A., Shawky, S. and El-wakil, M. (2016) 'Bacteremia due to ESKAPE pathogens : An emerging problem in cancer patients', *Journal of the Egyptian National Cancer Institute*. National Cancer Institute, Cairo

University, 28(3) pp. 157–162.

Eliopoulos, G. M. and Eliopoulos, C. T. (1988) ‘Abtibiotic combinations: Should they be tested?’, *Clinical Microbiology Reviews*, 1(2) pp. 139–156.

EMBL-EBI (2019) *The European Bioinformatics Institute*, *ChEBI Chlorhexidine*.

Esposito, E., Bortolotti, F., Nastruzzi, C., Menegatti, E. and Cortesi, R. (2003) ‘Diffusion of preservatives from topical dosage forms: A comparative study’, *Journal of Cosmetic Science*, 54(3) pp. 239–250.

Ethier, A., Bansal, P., Baxtar, J., Langley, N., Richardson, N. and Patel, A. M. (2019) *The Role of Excipients in the Microstructure of Topical Semisolid Drug Products*. Springer, Cham.

EUCAST: European Committee on Antimicrobial Susceptibility Testing (2019) ‘Clinical breakpoints’, pp. 0–99. Available at: http://www.eucast.org.

EUCAST (2000) *Terminology relating to methods for the determination of susceptibility of bacteria to antimicrobial agents*, *Clinical Microbiology and Infection*.

EUCAST, E. C. on A. S. T. (2019) ‘Antimicrobial susceptibility testing EUCAST disk diffusion method - Version 7.0’, *European Society of Clinical Microbiology and Infectious Deseases*, 0(January) pp. 1–21. Available at: www.eucast.org.

Ewald, A., Glückermann, S. K., Thull, R. and Gbureck, U. (2006) ‘Antimicrobial titanium/silver PVD coatings on titanium’, *BioMedical Engineering Online*, 5(3) pp. 1–10.

Fair, R. J. and Tor, Y. (2014) ‘Perspectives in Medicinal Chemistry Antibiotics and Bacterial Resistance in the 21st Century’, *Perspectives in Medicinal Chemistry*, 6 pp. 25–64.

Falagas, M. E., Lourida, P., Poulikakos, P., Rafailidis, P. I. and Tansarli, S. (2014) ‘Antibiotic Treatment of Infections Due to Carbapenem-Resistant Enterobacteriaceae : Systematic Evaluation of the Available Evidence’, *Antimicrobial ACC*, 58(2) pp. 654–663.

Farmer, T. H., Gilbart, J. and Elson, S. W. (1992) ‘Biochemical basis of mupirocin resistance in strains of staphylococcus aureus’, *Journal of Antimicrobial Chemotherapy*, 30(5) pp. 587–596.

Faúndez, G., Troncoso, M., Navarrete, P. and Figueroa, G. (2004) ‘Antimicrobial activity of copper surfaces against suspensions of Salmonella enterica and Campylobacter jejuni’, *BMC Microbiology*, 4(May) pp. 1–7.

FDA (1997) *Guidance for Industry Guidance for Industry Nonsterile Semisolid Dosage Forms*.

Feng, Q. L., Wu, J., Chen, G. Q., Cui, F. Z., Kim, T. N. and Kim, J. O. (2000) ‘A mechanistic study of the antibacterial effect of silver ions on Escherichia coli and Staphylococcus aureus’, 4636(3) pp. 662–668.

Feng, Y., Sun, W. Z., Wang, X. S. and Zhou, Q. X. (2019) ‘Selective Photoinactivation of Methicillin-Resistant Staphylococcus aureus by Highly Positively Charged RuII Complexes’, *Chemistry - A European Journal*, 25(61) pp. 13879–13884.

Finney, L. A. and Halloran, T. V. O. (2003) ‘Transition Metal Speciation in the Cell : Insights from the Chemistry of Metal Ion Receptors’, *Science*, 300(May) pp. 931–937.

Fiume, M. M., Bergfeld, W. F., Belsito, D. V., Hill, R. A., Klaassen, C. D., Liebler, D. C., Marks, J. G., Shank, R. C., Slaga, T. J., Snyder, P. W. and Andersen, F. A. (2013) ‘Safety Assessment of Bis-Diglyceryl Polyacyladipate-2 and Bis-Diglyceryl Polyacyladipate-1 as Used in Cosmetics’, *International Journal of Toxicology*, 32(Supplement 3) pp. 56S-64S.

Floss, H. G. and Yu, T. W. (2005) ‘Rifamycin - Mode of action, resistance, and biosynthesis’, *Chemical Reviews*, 105(2) pp. 621–632.

Fock, K. M., Graham, D. Y. and Malfertheiner, P. (2013) ‘Helicobacter pylori research: Historical insights and future directions’, *Nature Reviews Gastroenterology and Hepatology*. Nature Publishing Group, 10(8) pp.

495–500.

Forbes, L. M., Sattayasamitsathit, S., Xu, P. F., O'Mahony, A., Samek, I. A., Kaufmann, K., Wang, J. and Cha, J. N. (2013) 'Improved oxygen reduction reaction activities with amino acid R group functionalized PEG at platinum surfaces', *Journal of Materials Chemistry A*, 1(35) pp. 10267–10273.

Fortini, D., Fashae, K., García-Fernández, A., Villa, L. and Carattoli, A. (2011) 'Plasmid-mediated quinolone resistance and β-lactamases in Escherichia coli from healthy animals from Nigeria', *Journal of Antimicrobial Chemotherapy*, 66(6) pp. 1269–1272.

Fraud, S., Campigotto, A. J., Chen, Z. and Poole, K. (2008) 'MexCD-OprJ multidrug efflux system of Pseudomonas aeruginosa: Involvement in chlorhexidine resistance and induction by membrane-damaging agents dependent upon the AlgU stress response sigma factor', *Antimicrobial Agents and Chemotherapy*, 52(12) pp. 4478–4482.

Frei, A. (2020) 'Metal complexes, an untapped source of antibiotic potential?', *Antibiotics*, 9(2).

Frei, A. *et al.* (2020) 'Metal complexes as a promising source for new antibiotics', *Chemical Science*. Royal Society of Chemistry, 11(10) pp. 2627–2639.

Fuchs, P. C., Jones, R. N. and Barry, A. L. (1990) 'Interpretive criteria for disk diffusion susceptibility testing of mupirocin, a topical antibiotic', *Journal of Clinical Microbiology*, 28(3) pp. 608–609.

Fux, C. A., Shirtliff, M., Stoodley, P. and Costerton, J. W. (2005) 'Can laboratory reference strains mirror " real-world " pathogenesis ?', *Trends in Microbiology*, 13(2) pp. 59–63.

Le Gall, T., Lemercier, G., Chevreux, S., Tücking, K. S., Ravel, J., Thétiot, F., Jonas, U., Schönherr, H. and Montier, T. (2018) 'Ruthenium(II) Polypyridyl Complexes as Photosensitizers for Antibacterial Photodynamic Therapy: A Structure–Activity Study on Clinical Bacterial Strains',

ChemMedChem, 13(20) pp. 2229–2239.

Galloway, W. R. J. D., Isidro-Llobet, A. and Spring, D. R. (2010) 'Diversity-oriented synthesis as a tool for the discovery of novel biologically active small molecules', *Nature Communications*. Nature Publishing Group, 1(6) pp. 1–13.

Gao, N., Chen, Y. and Jiang, J. (2013) 'Ag @ Fe 2 O 3 - GO Nanocomposites Prepared by a Phase Transfer Method with Long-Term Antibacterial Property', *ACS Applied Materials & Interfaces*, 5 pp. 11307–11314.

Garg, A., Aggarwal, D., Garg, S. and Singla, A. K. (2002) 'Spreading of semisolid formulations: An update', *Pharmaceutical Technology North America*, 26(9) pp. 84–105.

Gebreyohannes, G., Nyerere, A., Bii, C. and Sbhatu, D. B. (2019) 'Challenges of intervention, treatment, and antibiotic resistance of biofilm-forming microorganisms', *Heliyon*. Elsevier Ltd, 5(8) p. e02192.

Geim, A. K. and Novoselov, K. S. (2007) 'The rise of graphene', *Nature Materials*, 6 pp. 183–191.

Gemeda, N., Tadele, A., Lemma, H., Girma, B., Addis, G., Tesfaye, B., Abebe, A., Gemechu, W., Yirsaw, K., Teka, F., Haile, C., Amano, A., Woldkidan, S., Geleta, B. and Debella, A. (2018) 'Development,characterization, and evaluation of novel broad-spectrum antimicrobial topical formulations from cymbopogon martini (Roxb.) W. Watson essential oil', *Evidence-based Complementary and Alternative Medicine*. Hindawi, 2018 pp. 1–16.

George, S., Leasure, A. R. and Horstmanshof, D. (2016) 'Effectiveness of Decolonization With Chlorhexidine and Mupirocin in Reducing Surgical Site Infections A Systematic Review', *Dimensions of Critical Care Nursing*, 35(4).

Ghosh, C., Sarkar, P., Issa, R. and Haldar, J. (2019) 'Alternatives to Conventional Antibiotics in the Era of Antimicrobial Resistance', *Trends in*

Microbiology. Elsevier Ltd, 27(4) pp. 323–338.

Gilbart, J., Perry, C. R. and Slocombe, B. (1993) 'High-level mupirocin resistance in Staphylococcus aureus: Evidence for two distinct isoleucyl-tRNA synthetases', *Antimicrobial Agents and Chemotherapy*, 37(1) pp. 32–38.

Gilbert, P. and Moore, L. E. (2005) 'Cationic antiseptics : diversity of action under a common epithet', *Journal of Applied Microbiolgy*, 99 pp. 703–715.

Gollavelli, G. and Ling, Y. C. (2012) 'Multi-functional graphene as an invitro and invivo imaging probe', *Biomaterials*, 33(8) pp. 2532–2545.

Gould, K. (2016) 'Antibiotics: From prehistory to the present day', *Journal of Antimicrobial Chemotherapy*, 71(3) pp. 572–575.

Gould, S. W. J., Cuschieri, P., Rollason, J., Hilton, A. C., Easmon, S. and Fielder, M. D. (2010) 'The need for continued monitoring of antibiotic resistance patterns in clinical isolates of Staphylococcus aureus from London and Malta', *Annals of Clinical Microbiology and Antimicrobials*, 9(20) pp. 1–7.

Grumezescu, A. (2018) *Lipid nanocarriers for drug targeting*. 1st editio. Elsevier.

Guo, W., Shan, K., Xu, B. and Li, J. (2015) 'Determining the resistance of carbapenemresistant Klebsiella pneumoniae to common disinfectants and elucidating the underlying resistance mechanisms', *Pathogens and Global Health*, 109(4) pp. 184–192.

Gurney, R. and Thomas, C. M. (2011) 'Mupirocin: Biosynthesis, special features and applications of an antibiotic from a Gram-negative bacterium', *Applied Microbiology and Biotechnology*, 90(1) pp. 11–21.

Gurunathan, S., Han, J. W., Abdal Dayem, A., Eppakayala, V. and Kim, J. H. (2012) 'Oxidative stress-mediated antibacterial activity of graphene oxide and reduced graphene oxide in Pseudomonas aeruginosa', *International Journal of Nanomedicine*, 7 pp. 5901–5914.

Gutnick, D. L. and Bach, H. (2000) 'Engineering bacterial biopolymers for

the biosorption of heavy metals; new products and novel formulations', *Applied Microbiology and Biotechnology*, 54(4) pp. 451–460.

Habiba, K., Bracho-rincon, D. P., Gonzalez-feliciano, J. A., Villalobos-santos, J. C., Makarov, V. I., Ortiz, D., Avalos, J. A., Gonzalez, C. I., Weiner, B. R. and Morell, G. (2015) 'Synergistic antibacterial activity of PEGylated silver – graphene quantum dots nanocomposites', *Applied Materials Today*. Elsevier Ltd, 1 pp. 80–87.

Haefeli, C., Franklint, C., Hardy, K., Biogen, S. A. and Acacias, R. (1984) 'Plasmid-Determined Silver Resistance in Pseudomonas stutzeri Isolated from a Silver Mine C __', *JOurnal of Bacteriology*, 158(1) pp. 389–392.

Hancock, R. E. W. (1981) 'Aminoglycoside uptake and mode of action-with special reference to streptomycin and gentamicin: II. Effects of aminoglycosides on cells', *Journal of Antimicrobial Chemotherapy*, 8(6) pp. 429–445.

Hancock, R. E. W. and Brinkman, F. S. L. (2002) ' Function of Pseudomonas Porins in Uptake and Efflux ', *Annual Review of Microbiology*, 56(1) pp. 17–38.

Harrison, J., Ceri, H. and Turner, R. (2007) 'Multimetal resistance and tolerance in microbial biofilms', *Nature Reviews*. Nture Publishing Group, 5 pp. 928–938.

Harrison, J. J., Turner, R. J., Joo, D. A., Stan, M. A., Chan, C. S., Allan, N. D., Vrionis, H. A., Olson, M. E. and Ceri, H. (2008) 'Copper and quaternary ammonium ations Exert Synergistic Bactericidal and antibiofilm activity against Pseudomonas aeruginosa', *Antimicrobial Agents and Chemotherapy*, 52(8) pp. 2870–2881.

Harrison, J. J., Tremaroli, V., Stan, M. A., Chan, C. S., Vacchi-suzzi, C., Heyne, B. J., Parsek, M. R., Ceri, H. and Turner, R. J. (2009) 'Chromosomal antioxidant genes have metal ion-specific roles as determinants of bacterial metal tolerance', *Envirnmental Microbiology*, 11(10) pp. 2491–2509.

Hashemi, M. M., Holden, B. S., Coburn, J., Taylor, M. F., Weber, S., Hilton, B., Zaugg, A. L., Mcewan, C., Carson, R., Andersen, J. L., Price, J. C., Deng, S. and Savage, P. B. (2019) 'Proteomic Analysis of Resistance of Gram-Negative Bacteria to Chlorhexidine and Impacts on Susceptibility to Colistin , Antimicrobial Peptides , and Ceragenins', *Frontiers in Microbiology*, 10(February) pp. 1–13.

Hatton, A. G., Scott, H. and Hilton, J. E. (2000) 'Calcium mupirocin non-aqueous nasal spray for otitis media or for recurrent acure bacterial sinusitis'. UK. Available at: https://patentimages.storage.googleapis.com/28/a8/f9/27f04482a81173/US6156792.pdf.

Hauptman, G. and Ryan, M. W. (2007) 'The effect of saline solutions on nasal patency and mucociliary clearance in rhinosinusitis patients', *Otolaryngology - Head and Neck Surgey*, 137 pp. 815–821.

Hayden, M. K., Lin, M. Y., Lolans, K., Weiner, S., Blom, D., Moore, N. M., Fogg, L., Henry, D., Lyles, R., Thurlow, C., Sikka, M., Hines, D. and Weinstein, R. A. (2015) 'Prevention of Colonization and Infection by Klebsiella pneumoniae Carbapenemase – Producing Enterobacteriaceae in Long-term Acute-Care Hospitals', *CID*, 60 pp. 1153–1161.

Helbig, K., Bleuel, C., Krauss, G. J. and Nies, D. H. (2008) 'Glutathione and transition-metal homeostasis in Escherichia coli', *Journal of bacteriology*, 190(15) pp. 5431–5438.

Hemani, M. L. and Lepor, H. (2009) 'Skin Preparation for the Prevention of Surgical Site Infection : Which Agent Is Best ?', *Reviews in Urology*, 11(4) pp. 190–195.

Henry, R. J. (1943) 'The Mode of Action of Sulfonamides', *Journal of the American Chemical Society*, 66(3) pp. 459–464.

Hetem, D. J. and Bonten, M. J. M. (2013) 'Clinical relevance of mupirocin resistance in Staphylococcus aureus', *Journal of Hospital Infection*. Elsevier Ltd, 85(4) pp. 249–256.

Higgins, C. S., Murtough, S. M., Williamson, E., Hiom, S. J., Payne, D. J., Russell, A. D. and Walsh, T. R. (2001) ‘ORIGINAL AR TICLE Resistance to antibiotics and biocides among non-fermenting Gram-negative bacteria’, *Clinical Microbiology and Infection*. European Society of Clinical Infectious Diseases, 7(6) pp. 308–315.

Hijazi, S., Visaggio, D., Pirolo, M. and Frangipani, E. (2018) ‘Antimicrobial Activity of Gallium Compounds on ESKAPE Pathogens’, *Frontiers in cEllular and Infection Microbiology*, 8(September) pp. 1–11.

Ho, T.-L. (1975) ‘The hard and soft acid bases (HSAB) principle and organic chemistry’, *Chemical Reviews*, 75(1) pp. 1–20.

Hobby, G. and Chaffee, E. (1942) ‘Observations on the mechanism of action of penicillin’, *Proc. Soc. Exp. Biol. Med.*, 50 pp. 281–285.

Hobman, J. (2017) ‘Antimicrobial metal-ion resistance and its impact on co-selection of anibiotic resistance’, *Culture*, 37(1) pp. 1–7.

Hobman, J. L. and Crossman, L. C. (2015) ‘Bacterial antimicrobial metal ion resistance’, *Journal of Medical Microbiology*, 64 pp. 471–497.

Hong, R., Kang, T. Y., Michels, C. A. and Gadura, N. (2012) ‘Membrane Lipid Peroxidation in Copper Alloy-Mediated Contact Killing of Escherichia coli’, *Applied and Environmental Microbiology*, (1) pp. 1776–1784.

Horner, C., Utsi, L., Coole, L. and Denton, M. (2017) ‘Epidemiology and microbiological characterization of clinical isolates of Staphylococcus aureus in a single healthcare region of the UK, 2015’, *Epidemiology and Infection*, 145(2) pp. 386–396.

Horner, C., Mawer, D. and Wilcox, M. (2012) ‘Reduced susceptibility to chlorhexidine in staphylococci : is it increasing and does it matter ?’, *Journal of Antimicrobial Chemotherapy*, 67(July) pp. 2547–2559.

Hoyle, B. D., Alcantara, J. and Costerton, J. W. (1992) ‘Pseudomonas aeruginosa biofilm as a diffusion barrier to piperacillin’, *Antimicrobial Agents and Chemotherapy*, 36(9) pp. 2054–2056.

Hu, W., Peng, C., Luo, W., Lv, M., Li, X., Li, D., Huang, Q. and Fan, C.

(2010) ‘Graphene-based antibacterial paper’, *ACS Nano*, 4(7) pp. 4317–4323.

Huang, K., Yu, H., Xie, M., Liu, S. and Wu, F. (2019) ‘Effects of poly(ethylene glycol)-grafted graphene on the electrical properties of poly(lactic acid) nanocomposites’, *RSC Advances*. Royal Society of Chemistry, 9(19) pp. 10599–10605.

Hugbo, P. G., Onyekweli, A. O. and Igwe, I. (2005) ‘Microbial contamination and preservative capacity of some brands of cosmetic creams’, *Tropical Journal of Pharmaceutical Research*, 2(2) pp. 229–234.

Hughes, J., Stabler, R., Gaunt, M., Karadag, T., Desai, N. and Betley, J. (2015) ‘resistance of MRSA isolates in south-east London Clonal variation in high- and low-level phenotypic and genotypic mupirocin resistance of MRSA isolates in south-east London’, *Journal of an*, 70(August) pp. 3191–3199.

Hurdle, J. G., Neill, A. J. O., Ingham, E., Fishwick, C. and Chopra, I. (2004) ‘Analysis of Mupirocin Resistance and Fitness in Staphylococcus aureus by Molecular Genetic and Structural Modeling Techniques’, *Antimicrobial Agents and Chemotherapy*, 48(11) pp. 4366–4376.

Hussain, N., Gogoi, A., Sarma, R. K. and Sharma, P. (2014) ‘Reduced Graphene Oxide Nanosheets Decorated with Au Nanoparticles as an Effective Bactericide : Investigation of Biocompatibility and Leakage of Sugars and Proteins’, *ChemPlusChem*, 79 pp. 1774–1784.

Ianeva, O. D. (2009) ‘Mechanisms of bacteria resistance to heavy metals’, *Mikrobiolohichnyĭ zhurnal*, 71(6) pp. 54–65.

Ilbay, Z., Hasimoglu, A., Ozdemir, O., Ates, F. and Sahin, S. (2017) ‘Highly efficient recovery of biophenols onto graphene oxide nanosheets : Valorisation of a biomass Highly ef fi cient recovery of biophenols onto graphene oxide nanosheets : Valorisation of a biomass’, *Journal of Moleculr Liquids*, 246(September) pp. 208–214.

Jamal, M., Ahmad, W., Andleeb, S., Jalil, F., Imran, M., Nawaz, M. A.,

Hussain, T., Ali, M., Rafiq, M. and Kamil, M. A. (2018) ‘Bacterial biofilm and associated infections’, *Journal of the Chinese Medical Association*. Elsevier Ltd, 81(1) pp. 7–11.

Jenkins, S. G. and Schuetz, A. N. (2012) ‘Current concepts in laboratory testing to guide antimicrobial therapy’, *Mayo Clinic Proceedings*. Elsevier Inc., 87(3) pp. 290–308.

Ji, H., Sun, H. and Qu, X. (2016) ‘Antibacterial applications of graphene-based nanomaterials: Recent achievements and challenges’, *Advanced Drug Delivery Reviews*. Elsevier B.V., 105 pp. 176–189.

Jia, Z., Shi, Y., Xiong, P., Zhou, W., Cheng, Y., Zheng, Y., Xi, T. and Wei, S. (2016) ‘From Solution to Biointerface: Graphene Self-Assemblies of Varying Lateral Sizes and Surface Properties for Biofilm Control and Osteodifferentiation’, *ACS Applied Materials and Interfaces*, 8(27) pp. 17151–17165.

Jiang, J., Pi, J. and Cai, J. (2018) ‘The Advancing of Zinc Oxide Nanoparticles for Biomedical Applications’, *Bioinorganic Chemistry and Applications*, 2018(5) pp. 1–18.

John, N., Somaraj, M. and Tharayil, N. J. (2018) ‘Synthesis , Characterization and Anti – Bacterial Activities of SnO 2 Nanoparticles Using Biological Molecule’, in *IOP Conference Series: Materials Science and Engieering*.

Jones, C. G. (1997) ‘Chlorhexidine : is it still the gold standard ?’, *Peridontology*, 15 pp. 55–62.

Kahne, D., Leimkuhler, C., Lu, W. and Walsh, C. (2005) ‘Glycopeptide and lipoglycopeptide antibiotics’, *Chemical Reviews*, 105(2) pp. 425–448.

Kampf, G. (2016) ‘Acquired resistance to chlorhexidine - is it time to establish an “ antiseptic stewardship ” initiative ?’, *Journal of Hospital Infection*. Elsevier Ltd, 94(3) pp. 213–227.

Kampf, G. (2018) ‘Biocidal Agents Used for Disinfection Can Enhance Antibiotic Resistance in Gram-Negative Species’, *Antibiotics*, 7(110) pp. 1–

24.

Kaneko, Y., Thoendel, M., Olakanmi, O., Britigan, B. E. and Singh, P. K. (2007) ‘The transition metal gallium disrupts Pseudomonas aeruginosa iron metabolism and has antimicrobial and antibiofilm activity’, *The journal of clinical investigation*, 117(4) pp. 877–888.

Kantikosum, K., Chongpison, Y., Chottawornsak, N. and Asawanonda, P. (2019) ‘The efficacy of glycolic acid, salicylic acid, gluconolactone, and licochalcone a combined with 0.1% adapalene vs adapalene monotherapy in mild-to-moderate acne vulgaris: A double-blinded within-person comparative study’, *Clinical, Cosmetic and Investigational Dermatology*, 12 pp. 151–161.

Karlowsky, J. A., Hoban, D. J., Hackel, M. A., Lob, S. H. and Sahm, D. F. (2017) ‘Resistance among Gram-negative ESKAPE pathogens isolated from hospitalized patients with intra-abdominal and urinary tract infections in Latin American countries: SMART 2013–2015’, *The Brazilian Journal of Infectious Diseases*. Elsevier Editora Ltda, 21(3) pp. 343–348.

Karpiński, T. M. and Szkaradkiewicz, A. K. (2015) ‘Chlorhexidine - Pharmaco-biological activity and application’, *European Review for Medical and Pharmacological Sciences*, 19(7) pp. 1321–1326.

Katas, H., Lim, C. S., Nor Azlan, A. Y. H., Buang, F. and Mh Busra, M. F. (2019) ‘Antibacterial activity of biosynthesized gold nanoparticles using biomolecules from Lignosus rhinocerotis and chitosan’, *Saudi Pharmaceutical Journal*. King Saud University, 27(2) pp. 283–292.

Kavitha, T., Gopalan, I. A., Lee, K. and Park, S. (2012) ‘Glucose sensing , photocatalytic and antibacterial properties of graphene – ZnO nanoparticle hybrids’, *Carbon*. Elsevier Ltd, 50(8) pp. 2994–3000.

Kazy, S. K., Sar, P., Singh, S. P., Sen, A. K. and D’Souza, S. F. (2002) ‘Extracellular polysaccharides of a copper-sensitive and a copper-resistant Pseudomonas aeruginosa strain: Synthesis, chemical nature and copper binding’, *World Journal of Microbiology and Biotechnology*, 18(6) pp. 583–588.

Keynan, Y. and Rubinstein, E. (2007) ‘The changing face of Klebsiella pneumoniae infections in the community’, *International Journal of Antmicrobial Agents*, 30 pp. 385–389.

Khoshnood, S., Heidary, M., Asadi, A. and Soleimani, S. (2019) ‘Biomedicine & Pharmacotherapy A review on mechanism of action , resistance , synergism , and clinical implications of mupirocin against Staphylococcus aureus’, *Biomedicine & Pharmacotherapy*. Elsevier, 109(October 2018) pp. 1809–1818.

Kikuvi, G. M., Ombui, J. N. and Mitema, E. S. (2010) ‘Serotypes and antimicrobial resistance profiles of Salmonella isolates from pigs at slaughter in Kenya’, *Journal of Infection in Developing Countries*, 4(4) pp. 243–248.

Kohanski, M. A., Dwyer, D. J., Hayete, B., Lawrence, C. A. and Collins, J. J. (2007) ‘A Common Mechanism of Cellular Death Induced by Bactericidal Antibiotics’, *Cell*, 130(5) pp. 797–810.

Kohanski, M. A., Dwyer, D. J. and Collins, J. J. (2010) ‘How antibiotics kill bacteria: From targets to networks’, *Nature Reviews Microbiology*, 8(6) pp. 423–435.

Koller, M., Javid, S. M., Sengstick, C., Tschulik, K., Schlidhauer, T. A. and Ludwig, A. (2017) ‘Antibacterial activity of microstructured sacrificial anode thin films by combination of silver with platinum group elements (platinum, palladium, iridium)’, *Materials Science and Engineering C*, 74(9) pp. 536–541.

Korber, D. R., James, G. A. and Costerton, J. W. (1994) ‘Evaluation of fleroxacin activity against established pseudomonas fluorescens biofilms’, *Applied and Environmental Microbiology*, 60(5) pp. 1663–1669.

Kostakioti, M., Hadjifrangiskou, M. and Hultgren, S. J. (2013) ‘Bacterial Biofilms : Development , Dispersal , and Therapeutic Strategies in the Dawn of the Bacterial Biofilms : Development , Dispersal , and Therapeutic Strategies in the Dawn of the Postantibiotic Era’, *Cold Spring Harbor Perspectives in Medicine*, 3 p. a010306.

Krishnaiah, Y. S. R., Xu, X., Rahman, Z., Yang, Y., Katragadda, U., Lionberger, R., Peters, J. R., Uhl, K. and Khan, M. A. (2014) 'Development of performance matrix for generic product equivalence of acyclovir topical creams', *International Journal of Pharmaceutics*. Elsevier B.V., 475(1–2) pp. 110–122.

Krishnamoorthy, K., Veerapandian, M., Zhang, L. and Yun, K. (2012) 'Antibacterial E ffi ciency of Graphene Nanosheets against Pathogenic Bacteria via Lipid Peroxidation', *The journal of Physical Chemistry*, 116 pp. 17280–17287.

Kryscio, D. R., Sathe, P. M., Lionberger, R., Yu, L., Bell, M. A., Jay, M. and Hilt, J. Z. (2008) 'Spreadability measurements to assess structural equivalence (Q3) of topical formulations - A technical note', *AAPS PharmSciTech*, 9(1) pp. 84–86.

Kumar, P., Huo, P., Zhang, R. and Liu, B. (2019) 'Antibacterial properties of graphene-based nanomaterials', *Nanomaterials*, 9(5) pp. 1–32.

Lachiewicz, A. M., Hauck, C. G., Weber, D. J., Cairns, B. A. and Van Duin, D. (2017) 'Bacterial Infections after Burn Injuries: Impact of Multidrug Resistance', *Clinical Infectious Diseases*, 65(12) pp. 2130–2136.

Lambert, P. A. (2005) 'Bacterial resistance to antibiotics: Modified target sites', *Advanced Drug Delivery Reviews*, 57(10) pp. 1471–1485.

Lasocka, I., Szulc-Dąbrowska, L., Skibniewski, M., Skibniewska, E., Strupinski, W., Pasternak, I., Kmieć, H. and Kowalczyk, P. (2018) 'Biocompatibility of pristine graphene monolayer: Scaffold for fibroblasts', *Toxicology in Vitro*, 48(February) pp. 276–285.

Latifi, N. A. and Karimi, H. (2017) 'Correlation of Occurrence of Infection in Burn Patients Corrélation Entre La Flore Cutanée Et Celle Responsable D ' Infections Chez Les Brûlés', *Annals of Burns and Fire Disasters*, (September) pp. 172–176.

Lee, A. S., Macedo-Vinas, M., François, P., Renzi, G., Vernaz, N., Schrenzel, J., Pittet, D. and Harbarth, S. (2011) 'Trends in mupirocin

resistance in meticillin-resistant Staphylococcus aureus and mupirocin consumption at a tertiary care hospital', *Journal of Hospital Infection*. the Healthcare Infection Society, 77(4) pp. 360–362.

Lemire, J. A., Harrison, J. J. and Turner, R. J. (2013) 'Antimicrobial activity of metals: Mechanisms, molecular targets and applications', *Nature Reviews Microbiology*. Nature Publishing Group, 11(6) pp. 371–384.

Łęski, T. A., Gniadkowski, M., Skoczyńska, A., Stefaniuk, E., Trzciński, K. and Hryniewicz, W. (1999) 'Outbreak of mupirocin-resistant Staphylococci in a hospital in Warsaw, Poland, due to plasmid transmission and clonal spread of several strains', *Journal of Clinical Microbiology*, 37(9) pp. 2781–2788.

Levy, S. B. (2002) 'Active efflux , a common mechanism for biocide and antibiotic resistance', *Journal of Applied Microbiology Symposium Supplement*, 92 pp. 65–71.

Lewinski, N., Colvin, V. and Drezek, R. (2008) 'Cytotoxicity of nanopartides', *Small*, 4(1) pp. 26–49.

Lewis, K. (2007) 'Persister cells, dormancy and infectious disease', *Nature Reviews Microbiology*, 5(1) pp. 48–56.

Li, F., Mulyana, Y., Feterl, M., Warner, J. M., Collins, J. G. and Keene, F. R. (2011) 'The antimicrobial activity of inert oligonuclear polypyridylruthenium(ii) complexes against pathogenic bacteria, including MRSA', *Dalton Transactions*, 40(18) pp. 5032–5038.

Li, F., Feterl, M., Warner, J. M., Keene, F. R. and Grant Collins, J. (2013) 'Dinuclear polypyridylruthenium(II) complexes: Flow cytometry studies of their accumulation in bacteria and the effect on the bacterial membrane', *Journal of Antimicrobial Chemotherapy*, 68(12) pp. 2825–2833.

Li, F., Collins, J. G. and Keene, F. R. (2015) 'Ruthenium complexes as antimicrobial agents', *Chemical Society Reviews*. Royal Society of Chemistry, 44(8) pp. 2529–2542.

Li, J., Wang, G., Zhu, H., Zhang, M., Zheng, X., Di, Z., Liu, X. and Wang,

X. (2014) ‘Antibacterial activity of large-area monolayer graphene film manipulated by charge transfer’, *Scientific Reports*, 4(1) pp. 1–8.

Li, P., Sun, S., Dong, A., Hao, Y., Shi, S., Sun, Z., Gao, G. and Chen, Y. (2015) ‘Developing of a novel antibacterial agent by functionalization of graphene oxide with guanidine polymer with enhanced antibacterial activity’, *Applied Surface Science*. Elsevier B.V., 355 pp. 446–452.

Li, W., Atkinson, G., Thakor, N., Allas, U., Lu, C.-C., Chan, K.-Y., Tenson, T., Schulten, K., Wilson, K. S., Hauryliuk, V. and Frank, J. (2013) ‘Mechanism of Tetracycline Resistance by Ribosomal Protection Protein Tet(O)’, *Nat Commun*, 176(8) pp. 1–17.

Liao, K. H., Lin, Y. S., MacOsko, C. W. and Haynes, C. L. (2011) ‘Cytotoxicity of graphene oxide and graphene in human erythrocytes and skin fibroblasts’, *ACS Applied Materials and Interfaces*, 3(7) pp. 2607–2615.

Lin, Y. E., Stout, J. E. and Yu, V. L. (2011) ‘ Controlling Legionella in Hospital Drinking Water: An Evidence-Based Review of Disinfection Methods ’, *Infection Control & Hospital Epidemiology*, 32(2) pp. 166–173.

Linklater, D. P., Baulin, V. A., Juodkazis, S. and Ivanova, E. P. (2018) ‘Mechano-bactericidal mechanism of graphene nanomaterials’, *Interface Focus*, 8(3) pp. 1–9.

Lipsitch, M. and Samore, M. H. (2002) ‘Antimicrobial Use and Antimicrobial Resistance : A Population Perspective’, *Perspectives*, 8(4) pp. 347–354.

Liu, S., Zeng, T. H., Hofmann, M., Burcombe, E., Wei, J. and Jiang, R. (2011) ‘Antibacterial Activity of Graphite , Graphite Oxide , Graphene Oxide , and Reduced Graphene Oxide : Membrane and Oxidative Stress’, *ACS Nano*, 9(9) pp. 6971–6980.

Liu, S., Hu, M., Zeng, T. H., Wu, R., Jiang, R., Wei, J., Wang, L., Kong, J. and Chen, Y. (2012) ‘Lateral Dimension-Dependent Antibacterial Activity of Graphene Oxide Sheets’, *ACS Publications*, 28 pp. 12364–12372.

Liu, X., Sen, S., Liu, J., Kulaots, I., Geohegan, D., Kane, A., Puretzky, A.

A., Rouleau, C. M., More, K. L., Palmore, G. T. R. and Hurt, R. H. (2011) 'Antioxidant deactivation on graphenic nanocarbon surfaces', *Small*, 7(19) pp. 2775–2785.

Loden, M. (2003) 'Role of Topical Emollients and Moisturizers in the Treatment of Dry Skin Barrier Disorders', *American Journal of Clinical Dermatology*, 4(11) pp. 771–788. Available at: https://link.springer.com/content/pdf/10.2165%2F00128071-200304110-00005.pdf.

Lok, C., Ho, C., Chen, R., He, Q., Yu, W., Sun, H., Tam, P. K., Chiu, J. and Che, C. (2006) 'Proteomic Analysis of the Mode of Antibacterial Action of Silver Nanoparticles', *Journal of proteome*, 5 pp. 916–924.

López, J. L., Esparza, M. R., Pérez, G. R. R. and González, M. E. (2019) 'Catalytic and antibacterial properties of gold nanoparticles synthesized by a green approach for bioremediation applications', *3 Biotech*. Springer International Publishing, 9(4) pp. 1–9.

Lu, K., Zhao, G. and Wang, X. (2012) 'A brief review of graphene-based material synthesis and its application in environmental pollution management', *Chinese Science Bulletin*, 57(11) pp. 1223–1234.

Luo, C., Zhang, Y., Zeng, X., Zeng, Y. and Wang, Y. (2005) 'The role of poly(ethylene glycol) in the formation of silver nanoparticles', *Journal of Colloid and Interface Science*, 288(2) pp. 444–448.

Lynch, M. D. and Watt, F. M. (2018) 'Fibroblast heterogeneity: implications for human disease', *Journal of Clinical Investigation*, 128(1) pp. 26–35.

Maas, M. (2016) 'Carbon nanomaterials as antibacterial colloids', *Materials*, 9(8) pp. 1–19.

Magiorakos, A., Srinivasan, A., Carey, R., Carmeli, Y., Falagas, M., Giske, C., Harbarth, S., Hindler, J., Kahlmeter, G., Olsson-Lilijequist, B., Paterson, D. L., Rice, L. B., Stelling, J., Struelens, M. J., Vatopoulos, A., Weber, J. T. and Monnet, D. L. (2012) *Multidrug-resistant, extensively drug-resistant and pandrug-resistant bacteria: An international expert proposal for interim*

standard definitions for acquired resistance, *Clinical Microbiology and Infection*. European Society of Clinical Infectious Diseases.

Mah, T.-F. C. and O'Toole, G. A. (2001) 'Mechanisms of biofilm resistance to antimicrobial agents', *Trends in Microbiology*, 9(1) pp. 34–39.

Mahmoud, N. N., Alkilany, A. M., Khalil, E. A. and Al-Bakri, A. G. (2017) 'Antibacterial activity of gold nanorods against Staphylococcus aureus and Propionibacterium acnes : misinterpretations and artifacts', *International Journal of Nanomdicine*, 12 pp. 7311–7322.

Malaviolle, X., Nonhoff, C., Denis, O., Rottiers, S. and Struelens, M. J. (2008) 'Evaluation of disc diffusion methods and Vitek 2 automated system for testing susceptibility to mupirocin in Staphylococcus aureus', *Journal of Antimicrobial Chemotherapy*, 62(5) pp. 1018–1023.

Manson, J. M., Hancock, L. E. and Gilmore, M. S. (2010) 'Mechanism of chromosomal transfer of Enterococcus faecalis pathogenicity island, capsule, antimicrobial resistance, and other traits', *Proceedings of the National Academy of Sciences of the United States of America*, 107(27) pp. 12269–12274.

Maris, P. (1991) 'Resistance of 700 Gram-negative bacterial strains to antispetics and antibiotics', *Annales de recherches veterinaires. Annals of veterinary research*, 22(1) p. 11.

Marslin, G., Mary, A., Kumar, V., Khandelwal, M., Balakumar, K., Sheeba, C. J. and Franklin, G. (2015) 'PEGylated ofloxacin nanoparticles render strong antibacterial activity against many clinically important human pathogens', *Colloids and Surfaces B: Biointerfaces*. Elsevier B.V., 132 pp. 62–70.

Martínez, L. and Baquero, F. (2002) 'Intercations amng strategies associated with bacterial infection: pathogenicity, epidemicity, and antibiotic resistance', *Clinical Microbiology Reviews*, 15(4) pp. 647–679.

Marx, D., Williams, G. and Birkhoff, M. (2016) 'Intranasal Drug Administration - An Attractive Delivery Route for Some Drugs', in *Drug*

Discovery and Development - From Molecules to Medicine tration. Radolfzell: INTECH, p. 13.

Matthijs, S., Vander, C., Cornu, B., Ye, L., Cornelis, P., Thomas, C. M. and Ongena, M. (2014) 'Antimicrobial properties of Pseudomonas strains producing the antibiotic mupirocin', *Research in Microbiologoy*. Elsevier Masson SAS, 165(8) pp. 695–704.

McDanel, J. S., Murphy, C. R., Diekema, D. J., Quan, V., Kim, D. S., Peterson, E. M., Evans, K. D., Tan, G. L., Hayden, M. K. and Huang, S. S. (2013) 'Chlorhexidine and mupirocin susceptibilities of methicillin-resistant Staphylococcus aureus from colonized nursing home residents', *Antimicrobial Agents and Chemotherapy*, 57(1) pp. 552–558.

McDonnell, G. and Russell, D. (1999) 'Antiseptics and Disinfectants : Activity , Action , and Resistance', *Clinical Microbiology Reviews*, 12(1) pp. 147–179.

McMurry, L., Petrucci, R. E. and Levy, S. B. (1980) 'Active efflux of tetracycline encoded by four genetically different tetracyline resistance determinants in Escherichia coli', *Proceedings of the National Academy of Sciences of the United States of America*, 77(7 II) pp. 3974–3977.

McQuillan, J. S., Groenaga Infante, H., Stokes, E. and Shaw, A. M. (2012) 'Silver nanoparticle enhanced silver ion stress response in Escherichia coli K12', *Nanotoxicology*, 6(8) pp. 857–866.

Mehtar, S., Wiid, I. and Todorov, S. D. (2008) 'The antimicrobial activity of copper and copper alloys against nosocomial pathogens and Mycobacterium tuberculosis isolated from healthcare facilities in the Western Cape: an in-vitro study', *Journal of Hospital Infection*, 68(1) pp. 45–51.

Mendes, E. T., Ranzani, O. T., Marchi, A. P., Da Silva, M. T., Filho, J. U. A., Alves, T., Guimarães, T., Levin, A. S. and Costa, S. F. (2016) 'Chlorhexidine bathing for the prevention of colonization and infection with multidrug-resistant microorganisms in a hematopoietic stem cell transplantation unit over a 9-year period: Impact on chlorhexidine

susceptibility', *Medicine (United States)*, 95(46) pp. 1–8.

Meritt, J. H., Kadouri, D. E. and O'toole, G. A. (2015) 'HHS Public Access, Growing and Analyzing Static Biofilms Judith', *Current Protocols in Microbiology*, pp. 1–29.

Michael, C. A., Dominey-howes, D., Labbate, M., Maria, C. and Elisabeth, J. (2014) 'The antimicrobial resistance crisis : causes , consequences , and management', *Frontiers in Public Health*, 2(September) pp. 1–8.

Milheiro, A., Nozaki, K., Kleverlaan, C. J., Muris, J., Miura, H. and Feilzer, A. J. (2014) 'In vitro cytotoxicity of metallic ions released from dental alloys', *Odontology*, 104(2) pp. 136–142.

Mittapally, S., Taranum, R. and Parveen, S. (2018) 'Journal of Drug Delivery and Therapeutics Metal ions as antibacterial agents', *Journal of Drug Delivery and Therapeutics*, 8(6-s) pp. 411–419.

Moghaddam, M. B., Goharshadi, E. K. and Moosavi, F. (2016) 'Structural and transport properties and solubility parameter of graphene/glycerol nanofluids: A molecular dynamics simulation study', *Journal of Molecular Liquids*. Elsevier B.V., 222 pp. 82–87.

Monych, N. K., Gugala, N. and Turner, R. J. (2019) 'Metal-Based Antimicrobials', in *Antimicrobial Materials for Biomedical Applications*, pp. 252–276.

Moradigaravand, D., Martin, V., Peacock, S. J. and Parkhill, J. (2017) 'crossm Evolution and Epidemiology of', *American Society for Microbiology*, 8(1) pp. 1–13.

De Moraes, A. C. M., Lima, B. A., de Faria, A. F., Brocchi, M. and Alves, O. L. (2015) 'Graphene oxide-silver nanocomposite as a promising biocidal agent against methicillin- resistant Staphylococcus aureus', *Interantional Journal of Nanomedicine*, 10 pp. 6847–6961.

Morgan, J. R. (1985) 'Microbial Contamination of Creams', in Marks, R. (ed.) *Topics in Topicals*. Springer, Dordrecht, pp. 61–67.

Morita, Y., Murata, T., Mima, T., Shiota, S., Kuroda, T., Mizushima, T.,

Gotoh, N., Nishino, T. and Tsuchiya, T. (2003) ‘Induction of mexCD-oprJ operon for a multidrug efflux pump by disinfectants in wild-type Pseudomonas aeruginosa PAO1’, *Journal of Antimicrobial Chemotherapy*, 51(4) pp. 991–994.

Mukhtar, T. A. and Wright, G. D. (2005) ‘Streptogramins, oxazolidinones, and other inhibitors of bacterial protein synthesis’, *Chemical Reviews*, 105(2) pp. 529–542.

Munita, J. M., Arias, C. A., Unit, A. R. and Santiago, A. De (2016) ‘HHS Public Access Mechanisms of Antibiotic Resistance’, *Microbiology Spectrum*, 4(2) pp. 1–37.

Naparstek, L., Carmeli, Y., Chmelnitsky, I., Banin, E. and Navon-Venezia, S. (2012) ‘Reduced susceptibility to chlorhexidine among extremely-drug-resistant strains of Klebsiella pneumoniae’, *Journal of Hospital Infection*. Elsevier Ltd, 81(1) pp. 15–19.

National Center for Biotechnology (2019) *Pubchem Database*, *Isopropyl alcohol*. Available at: https://pubchem.ncbi.nlm.nih.gov/compound/Isopropyl-alcohol (Accessed: 6 December 2019).

National Center for Biotechnology Information (2019a) *Pubchem Database*, *Chlorhexidine*. Available at: https://pubchem.ncbi.nlm.nih.gov/compound/Chlorhexidine#section=Structures (Accessed: 6 December 2019).

National Center for Biotechnology Information (2019b) *PubChem Database*, *Lauramine oxide*. Available at: https://pubchem.ncbi.nlm.nih.gov/compound/Lauramine-oxide (Accessed: 6 December 2019).

National Center for Biotechnology Information (2019c) *PubChem Database*, *Ponceau 4R*.

Navon-Venezia, S., Kondratyeva, K. and Carattoli, A. (2017) ‘Klebsiella pneumoniae: A major worldwide source and shuttle for antibiotic

resistance', *FEMS Microbiology Reviews*, 41(3) pp. 252–275.

Nawas, T. and Alkofahi, A. (1994) 'Microbial contamination and preservative efficacy of topical creams', *Journal of Clinical Pharmacy and Therapeutics*, 19(1) pp. 41–46.

Nde, C. W., Jang, H. J., Toghrol, F. and Bentley, W. E. (2009) 'Global transcriptomic response of Pseudomonas aeruginosa to chlorhexidine diacetate', *Environmental Science and Technology*, 43(21) pp. 8406–8415.

Neto, V. de O. S. (2019) *Nanomaterials Applications for Environmental Matrices*. 1st editio, *Nanomaterials Applications for Environmental Matrices*. 1st editio. Edited by R. Nascimento et al. Elsevier.

Nichols, W. W., Dorrington, S. M., Slack, M. P. E. and Walmsley, H. L. (1988) 'Inhibition of tobramycin diffusion by binding to alginate', *Antimicrobial Agents and Chemotherapy*, 32(4) pp. 518–523.

Nieboer, E. and Richardson, D. H. S. (1980) 'The replacement of the nondescript term "heavy metal" by a biologically and chemically significant classification of metal ions', *Envirnemtal Pollution*, 1(Series B) pp. 3–26.

Nikaido, H. (1994) 'Prevention of drug access to bacterial targets: Permeability barriers and active efflux', *Science*, 264 pp. 382–388.

Nikitakis, J. and Lange, B. (2006) *International Cosmetic Ingredient Dictionary and Handbook*. Sixteenth. Edited by J. Nikitakis and B. Lange. Personal Care Products Counci.

Niţica, S., Moldovan, A. I., Toma, V., Moldovan, C. S., Berindan-Neagoe, I., Ştiufiuc, G., Lucaciu, C. M. and Ştiufiuc, R. (2018) 'PEGgylated gold nanoparticles with interesting plasmonic properties synthesized using an original, rapid, and easy-to-implement procedure', *Journal of Nanomaterials*, 2018 pp. 1–7.

Norrby, R., Nord, C. E. and Finch, R. (2005) 'Lack of development of new antimicrobial drugs : a potential serious threat to public health', *Lancet Infectious Diseases*, 5 pp. 115–119.

Noyce, J. O., Michels, H. and Keevil, C. W. (2006) 'Potential use of copper

surfaces to reduce survival of epidemic meticillin-resistant Staphylococcus aureus in the healthcare environment', *Journal of Hospital Infection*, 63(3) pp. 289–297.

O'Shea, S., Cotter, L., Creagh, S., Lydon, S. and Lucey, B. (2009) 'Mupirocin resistance among staphylococci: Trends in the southern region of Ireland', *Journal of Antimicrobial Chemotherapy*, 64(3) pp. 649–650.

Obst, S., Kastowsky, M. and Bradaczek, H. (1997) 'Molecular dynamics simulations of six different fully hydrated monomeric conformers of Escherichia coli re-lipopolysaccharide in the presence and absence of Ca2+', *Biophysical Journal*, 72(3) pp. 1031–1046.

Ooya, T., Lee, J. and Park, K. (2003) 'Effects of ethylene glycol-based graft , star-shaped, and dendritic polymers on solubilization and controlled release of paclitaxel', *Journal of Controlled Release*, 93 pp. 121–127.

Orr, N. A. and Greenway, M. J. (1986) 'Topical pharmaceutical composition comprising pseudomonic acid or a salt or ester thereof and a corticosteroid.' Great Britain: Beecham Group. Available at: https://patentimages.storage.googleapis.com/82/53/da/d52a9e478c6d8b/EP0231621A2.pdf.

Othman, N., Babakir-Mina, M., Noori, C. K. and Rashid, P. Y. (2014) 'Pseudomonas aeruginosa infection in burn patients in Sulaimaniyah, Iraq: risk factors and antibiotic resistance rates', *Journal of Infection in Developing Countries*, 8(11) pp. 1498–1502.

Ouyang, Yu, Cai, X., Shi, Q., Liu, L., Wan, D., Tan, S. and Ouyang, Yousheng (2013) 'Poly-l-lysine-modified reduced graphene oxide stabilizes the copper nanoparticles with higher water-solubility and long-term additively antibacterial activity', *Colloids and Surfaces B: Biointerfaces*. Elsevier B.V., 107 pp. 107–114.

Páez, P. L., Bazán, C. M., Bongiovanni, M. E., Toneatto, J., Albesa, I., Becerra, M. C. and Argüello, G. A. (2013) 'Oxidative stress and antimicrobial activity of chromium(iii) and ruthenium(II) complexes on staphylococcus aureus and Escherichia coli', *BioMed Research*

International, 2013.

Pages, J.-M., James, C. E. and Winterhalter, M. (2008) ‘Pages.PDF’, *Nature Reviews Microbiology*, 6(12) pp. 893–903.

Pal, S., Tak, Y. K. and Song, J. M. (2007) ‘Does the antibacterial activity of silver nanoparticles depend on the shape of the nanoparticle? A study of the gram-negative bacterium Escherichia coli’, *Applied and Environmental Microbiology*, 73(6) pp. 1712–1720.

Pankey, G. A. and Sabath, L. D. (2004) ‘Clinical Relevance of Bacteriostatic versus Bactericidal Activity in the Treatment of Gram-Positive Bacterial Infections’, *Clinical Infectious Diseases*, 39(5) pp. 755–756.

Papakonstantinou, P. E., Samonis, G., Andrianaki, A. M., Christofaki, M., Dimopoulou, D., Papadakis, J., Gikas, A. and Kofteridis, D. P. (2018) ‘Epidemiology, microbiological and clinical features, treatment, and outcomes of infective endocarditis in crete, Greece’, *Infection and Chemotherapy*, 50(1) pp. 21–28.

Patel, Gorwitz, R. J. and Jernigan, J. A. (2009) ‘Mupirocin Resistance’, *Antimicrobial Resistance*, 49(49) pp. 935–941.

Patel, Patel, R. P. and Patel, M. M. (2009) ‘Poloxamers: A pharmaceutical excipients with therapeutic behaviors’, *International Journal of PharmTech Research*, 1(2) pp. 299–303.

Pearson, R. G. (1963) ‘Hard and Soft Acids and Bases’, *Journal of The American Chemical Society*, 265 pp. 3533–3539.

Penders, J., Stolzoff, M., Hickey, D. J., Andersson, M. and Webster, T. J. (2017) ‘Shape-dependent antibacterial effects of non-cytotoxic gold nanoparticles’, *International Journal of Nanomedicine*, 12 pp. 2457–2468.

Percival, S. L., Bowler, P. G. and Russell, D. (2005) ‘Bacterial resistance to silver in wound care’, *Journal of Hospital Infection*, 60 pp. 1–7.

Pereira, Y., Lagniel, G., Godat, E., Baudouin-cornu, P., Junot, C. and Labarre, J. (2008) ‘Chromate Causes Sulfur Starvation in Yeast’,

Toxicological Sciences, 106(2) pp. 400–412.

Pérez-Roth, E., López-Aguilar, C., Alcoba-Florez, J. and Méndez-Álvarez, S. (2006) 'High-level mupirocin resistance within methicillin-resistant Staphylococcus aureus pandemic lineages', *Antimicrobial Agents and Chemotherapy*, 50(9) pp. 3207–3211.

Perreault, F., Fonesa de Faria, A., Nejati, S. and Elimelech, M. (2015) 'Antimicrobial Properties of Graphene Oxide Nanosheets : Why Size Matters', *ACS NANO*, 9(7) pp. 7226–7236.

Pham, V. T. H., Truong, V. K., Quinn, M. D. J., Notley, S. M., Guo, Y., Baulin, V. A., Al Kobaisi, M., Crawford, R. J. and Ivanova, E. P. (2015) 'Graphene Induces Formation of Pores That Kill Spherical and Rod-Shaped Bacteria', *ACS Nano*, 9(8) pp. 8458–8467.

Podolsky, S. H. (2018) 'The evolving response to antibiotic resistance (1945–2018)', *Palgrave Communications*. Springer US, 4(124) pp. 1–8.

Pogue, J. M., Kaye, K. S., Cohen, D. A. and Marchaim, D. (2015) 'Appropriate antimicrobial therapy in the era of multidrug-resistant human pathogens', *Clinical Microbiology and Infection*. Elsevier Ltd, 21(4) pp. 302–312.

Pontel, L. B. and Soncini, F. C. (2009) 'Alternative periplasmic copper-resistance mechanisms in Gram negative bacteria', *Molecular Microbiology*, 73(2) pp. 212–225.

Poovelikunnel, T., Gethin, G. and Humphreys, H. (2015) 'Mupirocin resistance : clinical implications and potential alternatives for the eradication of MRSA', *Journal of Antimicrobial Chemotherapy*, 70(July) pp. 2681–2692.

Popa, M., Pradell, T., Crespo, D. and Calderón-Moreno, J. M. (2007) 'Stable silver colloidal dispersions using short chain polyethylene glycol', *Colloids and Surfaces A: Physicochemical and Engineering Aspects*, 303(3) pp. 184–190.

Projan, S. J. (2003) 'Why is big Pharma getting out of antibacterial drug

discovery ?', *Current Opinion in Microbiology*, 6 pp. 427–430.

Qasim, M., Udomluck, N., Chang, J., Park, H. and Kim, K. (2018) 'Antimicrobial activity of silver nanoparticles encapsulated in poly-N-isopropylacrylamide-based polymeric nanoparticles', *International Journal of Nanomedicine*, 13 pp. 235–249.

Quinn, J. P., Dudek, E. J., Divincenzo, C. A., Lucks, D. A. and Lerner, S. A. (1986) 'Emergence of Resistance to Imipenem During Therapy for Pseudomonas aeruginosa Infections', *The journal of infectious diseases*, 154(2) pp. 289–294.

Ramirez, M. and Tolmasky, M. (2010) 'Stroke care delivery at North Shore Hospital, Waitemata District Health Board 2014', *New Zealand Medical Journal*, 13(6) pp. 151–171.

Renwick, M. J., Brogan, D. M. and Mossialos, E. (2016) 'A systematic review and critical assessment of incentive strategies for discovery and development of novel antibiotics', *The Journal of Antibiotics*. Nature Publishing Group, 69 pp. 73–88.

Rîmbu, C., Danac, R. and Pui, A. (2014) 'Antibacterial Activity of Pd (II) Complexes with Salicylaldehyde-Amino Acids Schiff Bases Ligands', *Chemical and Pharmaceutical Bulletin*, 62(1) pp. 12–15.

Rodloff, A., Bauer, T., Ewig, S., Kujath, P. and Müller, E. (2008) 'Übersichtsarbeit: Sensibel, intermediär und resistent - Wirkintensität von antibiotika', *Deutsches Arzteblatt*, 105(39) pp. 657–662.

Rose, H., Baldwin, A., Dowson, C. G. and Mahenthiralingam, E. (2009) 'Biocide susceptibility of the Burkholderia cepacia complex', *Journal of Antimicrobial Chemotherapy*, 63(3) pp. 502–510.

Round, J. L., Connell, R. M. O. and Mazmanian, S. K. (2010) 'Coordination of tolerogenic immune responses by the commensal microbiota', *Journal of Autoimmunity*. Elsevier Ltd, 34(3) pp. J220–J225.

Rowan, M. P., Cancio, L. C., Elster, E. A., Burmeister, D. M., Rose, L. F., Natesan, S., Chan, R. K., Christy, R. J. and Chung, K. K. (2015) 'Burn

wound healing and treatment: Review and advancements', *Critical Care*. Critical Care, 19(1) pp. 1–12.

Roy, A., Bulut, O., Some, S., Mandal, A. K. and Yilmaz, M. D. (2019) 'Green synthesis of silver nanoparticles: biomolecule-nanoparticle organizations targeting antimicrobial activity', *RSC advances*. Royal Society of Chemistry, 9 pp. 2673–2702.

Ruiz, O. N., Fernando, K. A. S., Wang, B., Brown, N. A., Luo, P. G., McNamara, N. D., Vangsness, M., Sun, Y. P. and Bunker, C. E. (2011) 'Graphene oxide: a nonspecific enhancer of cellular growth', *ACS Nano*, 5(10) pp. 8100–8107.

Rupp, M. E., Fitzgerald, T., Marion, N., Helget, V., Puumala, S., Anderson, J. R. and Fey, P. D. (2004) 'Effect of silver-coated urinary catheters: Efficacy, cost-effectiveness, and antimicrobial resistance', *American Journal of Infection Control*, 32(8) pp. 445–450.

Sabale, V., Kunjwani, H. and Sabale, P. (2011) 'Formulation and in vitro evaluation of the topical antiageing preparation of the fruit of Benincasa hispida', *Journal of Ayurveda and Integrative Medicine*, 2(3) pp. 124–128.

Saikia, I., Sonowal, S., Pal, M., Boruah, P. K., Das, M. R. and Tamuly, C. (2016) 'Biosynthesis of gold decorated reduced graphene oxide and its biological activities', *Materials Letters*. Elsevier, 178 pp. 239–242.

Saiman, L. (2007) 'Clinical utility of synergy testing for multidrug-resistant Pseudomonas aeruginosa isolated from patients with cystic fibrosis: "the motion for"', *Paediatric Respiratory Reviews*, 8(3) pp. 249–255.

Saleem, H. G. M., Seers, C. A., Sabri, A. N. and Reynolds, E. C. (2016) 'Dental plaque bacteria with reduced susceptibility to chlorhexidine are multidrug resistant', *BMC Microbiology*. BMC Microbiology, 16(1) pp. 1–9.

Saleh, N., Awada, S., Zaiter, L. and Dib, W. (2015) 'Evaluation of antibiotic prescription in the Lebanese community: a pilot study', *Infection ecology & epidemiology*, 5 pp. 1–10.

Sanchez, V., Jachak, A., Hurt, R. and Kane, A. (2012) 'Biological

Interactions of Graphene-Family Nanomaterials', *Chem Res Toxicol.*, 25(1) pp. 15–34.

Santajit, S. and Indrawattana, N. (2016) 'Mechanisms of Antimicrobial Resistance in ESKAPE Pathogens', *BioMed Research International*. Hindawi Publishing Corporation, 2016(5) pp. 1–8.

Santo, C. E., Morais, P. V. and Grass, G. (2010) 'Isolation and characterization of bacteria resistant to metallic copper surfaces', *Applied and Environmental Microbiology*, 76(5) pp. 1341–1348.

Sauer, K., Cullen, M. C., Rickard, A. H., Zeef, L. A. H., Davies, D. G. and Gilbert, P. (2004) 'Characterization of Nutrient-Induced Dispersion in Pseudomonas aeruginosa PAO1 Biofilm', *Journal of Bacteriology*, 186(21) pp. 7312–7326.

Savin, M., Bierbaum, G., Hammerl, A., Heinemann, C., Parcina, M. and Sib, E. (2020) 'crossm Process Water from German Poultry Slaughterhouses', *Applied and Environmental Microbiology*, 86(8) pp. 1–18.

Schedle, A., Ellinger, A., Samorapoompichit, P., Rausch-Fan, X. H., Franz, A., Boltz-Nitulescu, G., Füreder, W., Sperr, W. R., Valent, P., Sperr, W. and Slavicek, R. (1995) 'Response of L-929 Fibroblasts, Human Gingival Fibroblasts, and Human Tissue Mast Cells to Various Metal Cations', *Journal of Dental Research*, 74(8) pp. 1513–1520.

Schwarz, S., Kehrenberg, C., Doublet, B. and Cloeckaert, A. (2004) 'Molecular basis of bacterial resistance to chloramphenicol and florfenicol', *FEMS Microbiology Reviews*, 28(5) pp. 519–542.

Scott, J. R., Krishnan, R., Rotenberg, B. W. and Sowerby, L. J. (2017) 'The effectiveness of topical colloidal silver in recalcitrant chronic rhinosinusitis : a randomized crossover control trial', *Journal of Otolaryngology Head and Neck Surgery*. Journal of Otolaryngology - Head & Neck Surgery, 64(46) pp. 1–6.

Seabra, A. B., Paula, A. J., De Lima, R., Alves, O. L. and Durán, N. (2014)

‘Nanotoxicity of graphene and graphene oxide’, *Chemical Research in Toxicology*, 27(2) pp. 159–168.

Sengupta, S., Chattopadhyay, M. K. and Grossart, H. (2013) ‘The multifaceted roles of antibiotics and antibiotic resistance in nature’, *Frontiers in Microbiology*, 4(March) pp. 1–13.

Shameli, K., Ahmad, M. Bin, Jazayeri, S. D., Sedaghat, S., Shabanzadeh, P., Jahangirian, H., Mahdavi, M. and Abdollahi, Y. (2012) ‘Synthesis and characterization of polyethylene glycol mediated silver nanoparticles by the green method’, *International Journal of Molecular Sciences*, 13(6) pp. 6639–6650.

Sharma, D., Misba, L. and Khan, A. U. (2019) ‘Antibiotics versus biofilm : an emerging battleground in microbial communities’, *Antimicrobial Resistance and Infection Control*. Antimicrobial Resistance & Infection Control, 8 pp. 1–10.

da Silva, W. J., Seneviratne, J., Parahitiyawa, N., Rosa, E. A. R., Samaranayake, L. P. and del Bel Cury, A. A. (2008) ‘Improvement of XTT assay performance for studies involving Candida albicans biofilms’, *Brazilian Dental Journal*, 19(4) pp. 364–369.

Silver, S. and Phung, L. T. (1996) ‘BACTERIAL HEAVY METAL RESISTANCE: New Surprises’, *Annual Review of Microbiology*, 50(1) pp. 753–789.

Sims, J. M. (1998) ‘On the Treatment of Vesico-Vaginal Fistula’, *International Urogynecology Journal*, 9 pp. 236–248.

Singh, B. R. (2014) ‘Antibacterial Activity of Glycerol, Lactose, Maltose, Mannitol, Raffinose and Xylose’, *Noto-are*, (July 2014) pp. 1–3. Available at: http://www.notoare.com/17223318.

Slate, A. J., Karaky, N. and Whitehead, K. A. (2019) ‘Antimicrobial Properties of Modified Graphene and other Advanced 2D Material Coated Surfaces’, in *2D Materials: Characterization, Production and Applications*. CRC Press.

Smith, K., Gemmell, C. G. and Hunter, I. S. (2008) ‘The association between biocide tolerance and the presence or absence of qac genes among hospital-acquired and community-acquired MRSA isolates’, *Journal of Antimicrobial Chemotherapy*, 61(1) pp. 78–84.

Souli, M., Galani, I., Plachouras, D., Panagea, T., Armaganidis, A., Petrikkos, G. and Giamarellou, H. (2013) ‘Antimicrobial activity of copper surfaces against carbapenemase-producing contemporary Gram-negative clinical isolates’, *Journal of Antimicrobial Chemotherapy*, 68(4) pp. 852–857.

Southam, H. M., Butler, J. A., Chapman, J. A. and Poole, R. K. (2017) ‘The Microbiology of Ruthenium Complexes’, in *Advances in Microbial Physiology*. 1st edn. Elsevier Ltd., pp. 1–96.

Spellberg, B. and Gilbert, D. N. (2014) ‘The Future of Antibiotics and Resistance : A Tribute to a Career of Leadership by John Bartlett’, *Clinical Infectious Diseases*, 59(Suppl 2) pp. 71–75.

Stadtman, E. R. and Levine, R. L. (2003) ‘Free radical-mediated oxidation of free amino acids and amino acid residues in proteins’, *Amino Acids*, 25 pp. 207–218.

Stapleton, P. D. and Taylor, P. W. (2002) ‘Methicillin resistance in Staphylococcus aureus: mechanisms and modulation’, *Science Progress Journal*, 85(Pt 1) pp. 57–72.

Stewart, E. J., Åslund, F. and Beckwith, J. (1998) ‘Disulfide bond formation in the Escherichia coli cytoplasm : an in vivo role reversal for the thioredoxins’, *the EMBO Journal*, 17(19) pp. 5543–5550.

Stewart, P. S. (1996) ‘Theoretical aspects of antibiotic diffusion into microbial biofilms’, *Antimicrobial Agents and Chemotherapy*, 40(11) pp. 2517–2522.

Stewart, P. S. (2002) ‘Mechanisms of antibiotic resistance in bacterial biofilms’, *International Journal of Medical Microbiology*, 292 pp. 107–113.

Stiufiuc, R., Iacovita, C., Nicoara, R., Stiufiuc, G., Florea, A., Achim, M.

and Lucaciu, C. M. (2013) ‘One-step synthesis of PEGylated gold nanoparticles with tunable surface charge’, *Journal of Nanomaterials*, 2013.

Stout, E. and McKessor, A. (2012) ‘Glycerin-Based Hydrogel for Infection Control’, *WHS Wound Healing Society*, 1(1) pp. 48–51.

Suci, P. A., Mittelman, M. W., Yu, F. P. and Geesey, G. G. (1994) ‘Investigation of ciprofloxacin penetration into Pseudomonas aeruginosa biofilms’, *Antimicrobial Agents and Chemotherapy*, 38(9) pp. 2125–2133.

Sumner, E. R., Shanmuganathan, A., Sideri, T. C., Willetts, S. A., Houghton, J. E., Avery, S. V and Avery, S. V (2005) ‘Oxidative protein damage causes chromium toxicity in yeast’, *Microbiology*, 151 pp. 1939–1948.

Sutherland, R., Comber, K. R., Mizen, L. W., Slocombe, B. and Clayton, J. P. (1976) ‘Pseudomonic acid, an antibiotic produced by Pseudomonas Fluorescens’, in *Proceedings of the 16th Iterscience Conference on Antimicrobial Agents and Chemotherapy, Chicago*.

Sutherland, R., Boon, R. J., Griffin, K. E., Masters, P. J., Slocombe, B. and White, A. R. (1985) ‘Antibacterial activity of mupirocin (pseudomonic acid), a new antibiotic for topical use’, *Antimicrobial Agents and Chemotherapy*, 27(4) pp. 495–498.

Suwantarat, N., Carroll, K. C., Tekle, T., Ross, T., Maragakis, L. L., Cosgrove, S. E. and Milstone, A. M. (2014) ‘High Prevalence of Reduced Chlorhexidine Susceptibility in Organisms Causing Central Line – Associated Bloodstream Infections’, *Infection control and hospital epidemiology*, 35(9) pp. 1183–1186.

Szunerits, S. and Boukherroub, R. (2016) ‘Antibacterial activity of graphene-based materials’, *Journal of Materials Chemistry*. Royal Society of Chemistry, 4 pp. 6892–6912.

Takayanagi, T., Becchaku, Y., Tomiyama, Y., Kurashina, M. and Mizuguchi, H. (2019) ‘Polyethylene glycols for the dispersion development

of graphene in an aqueous surfactant solution studied by affinity capillary electrophoresis', *Analytical Sciences*, 35(3) pp. 307–313.

Taneja, N., Sethi, S., Tahlan, A. K. and Kumar, Y. (2019) 'Introductory Chapter: Stepping into the Post-antibiotic Era - Challenges and Solutions', in *Antimicrobial Resistance - A Global threat*. Chandigarh: IntechOpen, pp. 1–11.

Tchounwou, P. B., Yedjou, C. G., Patlolla, A. K. and Sutton, D. J. (2012) 'Molecular, clinical and environmental toxicicology Volume 3: Environmental Toxicology', *Molecular, Clinical and Environmental Toxicology*, 101 pp. 133–164.

Tenson, T., Lovmar, M. and Ehrenberg, M. (2003) 'The mechanism of action of macrolides, lincosamides and streptogramin B reveals the nascent peptide exit path in the ribosome', *Journal of Molecular Biology*, 330(5) pp. 1005–1014.

The CIR Expert Panel (2014) *Safety Assessment of PEGylated Alkyl Glycerides as Used in Cosmetics*. Washingtion DC.

Thomas, C. M. and Nielsen, K. M. (2005) 'Mechanisms of, and barriers to, horizontal gene transfer between bacteria', *Nature Reviews Microbiology*, 3(9) pp. 711–721.

Tipper, D. and Strominger, J. (1965) 'Mechanism of action of penicllins: a prposal based on their structural similarity to acyl-D-alanyl-D-alanine', in *Proceedings of the National Academy of Sciences of the United States of America*, pp. 1133–1141.

Tong, S. Y. C., Davis, J. S., Eichenberger, E., Holland, T. L. and Fowler, V. G. (2015) 'Staphylococcus aureus Infections : Epidemiology , Pathophysiology , Clinical Manifestations , and Management', *Clinical Microbiology Reviews*, 28(3) pp. 603–661.

Touati, D. (2000) 'Iron and Oxidative Stress in Bacteria', *Archives of Biochemistry and Biophysics*, 373(1) pp. 1–6.

Towse, A., Hoyle, C. K., Goodall, J., Hirsch, M., Mestre-ferrandiz, J. and

Rex, J. H. (2017) ‘Time for a change in how new antibiotics are reimbursed : Development of an insurance framework for funding new antibiotics based on a policy of risk mitigation’, *Health policy*. Elsevier Ireland Ltd, 121(10) pp. 1025–1030.

Tu, Y., Lv, M., Xiu, P., Huynh, T., Zhang, M., Castelli, M., Liu, Z., Huang, Q., Fan, C., Fang, H. and Zhou, R. (2013) ‘Destructive extraction of phospholipids from Escherichia coli membranes by graphene nanosheets’, *Nature Nanotechnology*. Nature Publishing Group, 8(8) pp. 594–601.

Tucaliuc, A., Cristina, A. and Galaction, A. I. (2019) ‘Mupirocin : applications and production’, *Biotechnology Letters*. Springer Netherlands, 41(4) pp. 495–502.

Turner, R. J. (2017) ‘Metal-based antimicrobial strategies’, *Microbial biotechnology*, 10(5) pp. 1062–1065.

U.S. AAD (1998) *The Chemical Identity of Fragrances*. Available at: https://server.aad.org/Forms/Policies/Uploads/PS/PS-Chemical Identity of Fragrances.pdf.

Udo, E. E., Al-Sweih, N., Mokaddas, E., Johny, M., Dhar, R., Gomaa, H. H., Al-Obaid, I. and Rotimi, V. O. (2006) ‘Antibacterial resistance and their genetic location in MRSA isolated in Kuwait hospitals, 1994-2004’, *BMC Infectious Diseases*, 6 pp. 1–8.

Usluer, G., Ozgunes, I. and Leblebicioglu, H. (2005) ‘A multicenter point-prevalence study : antimicrobial prescription frequencies in hospitalized patients in turkey’, *BioMed Central*, 4(16) pp. 1–5.

USNF (2013) *USP35 NF30, 2012: U. S. Pharmacopoeia National Formulary*. 9th edn. Rockville: United States Pharmacopeial. Available at: https://www.uspnf.com/official-text/proposal-statuscommentary/usp-35-nf-30 (Accessed: 12 December 2020).

Vaara, M. (1992) ‘the Permeability of the Outer Membrane’, *Microbiological Reviews*, 56(3) pp. 395–411.

Vaidya, M. Y., Mcbain, A. J., Butler, J. A., Banks, C. E. and Whitehead, K.

A. (2017) ‘Antimicrobial Efficacy and Synergy of Metal Ions against Enterococcus Planktonic and Biofilm Phenotypes’, *Scientific Reports*. Springer US, 7(June) pp. 1–9.

Ventola, L. (2015) ‘The Antibiotic Resistance Crisis’, *Pharmacology and Therapeutics*, 40(4) pp. 277–283.

Vijayakumar, R. and Sandle, T. (2019) ‘A review on biocide reduced susceptibility due to plasmid-borne antiseptic-resistant genes—special notes on pharmaceutical environmental isolates’, *Journal of Applied Microbiology*, 126(4) pp. 1011–1022.

De Villiers, M. M. (2009) ‘Ointment bases.’, in Thompson, J. E. (ed.) *A practical Guide to Contemporary Pharmacy Practice*. 3rd edn. Lippincott Williams & Wilkins, pp. 277–290.

Vincent, M., Hartemann, P. and Engels-deutsch, M. (2016) ‘Antimicrobial applications of copper’, *International Journal of Hygiene and Environmental Health*. Elsevier GmbH., 219(7) pp. 585–591.

Wand, M. E., Bock, L. J., Bonney, L. C. and Sutton, J. M. (2017) ‘Mechanisms of increased resistance to chlorhexidine and cross-resistance to colistin following exposure of Klebsiella pneumoniae clinical isolates to chlorhexidine’, *Antimicrobial agents and chemotherapy*, 61(1) pp. 1–12.

Wang, K., Ruan, J., Song, H., Zhang, J., Wo, Y., Guo, S. and Cui, D. (2011) ‘Biocompatibility of Graphene Oxide’, *Nanoscale Research Letters*. Springer Open Ltd, 6(1) pp. 1–8.

Wang, L., Hu, C. and Shao, L. (2017) ‘The antimicrobial activity of nanoparticles : present situation and prospects for the future’, *International Journal of Nanomedicine*, 12 pp. 1227–1249.

Wang, Y., Cao, A., Jiang, Y., Zhang, X., Liu, J. and Liu, Y. (2014) ‘Superior Antibacterial Activity of Zinc Oxide/Graphene Oxide Composites Originating from High Zinc Concentration Localized around Bacteria’, *ACS Applied Materials and Interfaces*, 6 pp. 2791–2798.

Wassenaar, T., Ussery, D., Nielsen, L. and Ingmer, H. (2015) ‘ Review and

phylogenetic analysis of qac genes that reduce susceptibility to quaternary ammonium compounds in Staphylococcus species ', *European Journal of Microbiology and Immunology*, 5(1) pp. 44–61.

Wataha, J. C., Hobbs, D. T., Lockwood, P. E., Davis, R. R., Elvington, M. C., Lewis, J. B. and Messer, R. L. W. (2009) 'Peroxotitanates for biodelivery of metals', *Journal of Biomedical Materials Research - Part B Applied Biomaterials*, 91(2) pp. 489–496.

Webber, M. A. and Piddock, L. J. V. (2003) 'The importance of efflux pumps in bacterial antibiotic resistance', *Journal of Antimicrobial Chemotherapy*, 51(1) pp. 9–11.

Weber, D. J., Rutala, W. A. and Sickbert-Bennett, E. E. (2007) 'Outbreaks associated with contaminated antiseptics and disinfectants', *Antimicrobial Agents and Chemotherapy*, 51(12) pp. 4217–4224.

Weitzul, S. and Taylor, R. S. (2005) *Surgical Stainless Steel Learn more about Surgical Stainless Steel Suturing Technique and Other Closure Materials Biomaterials for Dental Implants*.

Wertheim, H. F. L., Melles, D. C., Vos, M. C., Van Leeuwen, W., Van Belkum, A., Verbrugh, H. A. and Nouwen, J. L. (2005) 'The role of nasal carriage in Staphylococcus aureus infections', *Lancet Infectious Diseases*, 5(12) pp. 751–762.

Westman, E. L., Canova, M. J., Radhi, I. J., Koteva, K., Kireeva, I., Waglechner, N. and Wright, G. D. (2012) 'Bacterial inactivation of the anticancer drug doxorubicin', *Chemistry and Biology*. Elsevier Ltd, 19(10) pp. 1255–1264.

WHO (2014) *Antimicrobial resistance: Global report on surveillance*. Available at: https://apps.who.int/iris/bitstream/handle/10665/112642/9789241564748_eng.pdf?sequence=1.

WHO (2015) *19th WHO Model List of Essential Medicines (April 2015) Explanatory notes*.

WHO (2016) ‘WHO Surgical Site Infection Prevention Guidelines Web Appendix 10’, *Guidelines*, (15) pp. 1–18.

WHO (2017) *Global priority list of antibiotic-resistant bacteria to guide research, discovery, and development of new antibiotics*.

Wilks, S. A., Michels, H. and Keevil, C. W. (2005) ‘The survival of Escherichia coli O157 on a range of metal surfaces’, *International Journal of Food Microbiology*, 105(3) pp. 445–454.

Wong, W. R., Oliver, A. G. and Linington, R. G. (2012) ‘Development of antibiotic activity profile screening for the classification and discovery of natural product antibiotics’, *Chemistry and Biology Resource*. Elsevier Ltd, 19(11) pp. 1483–1495.

Wood, T. K., Knabel, S. J. and Kwan, B. W. (2013) ‘Bacterial persister cell formation and dormancy’, *Applied and Environmental Microbiology*, 79(23) pp. 7116–7121.

Wood, T. K., Song, S. and Yamasaki, R. (2019) ‘Ribosome dependence of persister cell formation and resuscitation’, *Journal of Microbiology*, 57(3) pp. 213–219.

Workentine, M. L., Harrison, J. J., Stenroos, P. U., Ceri, H. and Turner, R. J. (2008) ‘Pseudomonas fluorescens ’ view of the periodic table’, *Envirnmental Microbiology*, 10(1) pp. 238–250.

Wyszogrodzka, G., Marszałek, B., Gil, B. and Dorozyński, P. (2016) ‘Metal-organic frameworks: Mechanisms of antibacterial action and potential applications’, *Drug Discovery Today*, 21(6) pp. 1009–1018.

Xu, K. D., Franklin, M. J., Park, C. H., McFeters, G. A. and Stewart, P. S. (2001) ‘Gene expression and protein levels of the stationary phase sigma factor, RpoS, in continuously-fed Pseudomonas aeruginosa biofilms’, *FEMS Microbiology Letters*, 199(1) pp. 67–71.

Xu, Z., Liang, Y., Lin, S., Chen, D., Li, B., Li, L. and Deng, Y. (2016) ‘Crystal Violet and XTT Assays on Staphylococcus aureus Biofilm Quantification’, *Current Microbiology*. Springer US, 73(4) pp. 474–482.

Xu, Z., Shah, H. N., Misra, R., Chen, J., Zhang, W., Liu, Y., Cutler, R. R. and Mkrtchyan, H. V. (2018) 'The prevalence, antibiotic resistance and mecA characterization of coagulase negative staphylococci recovered from non-healthcare settings in London, UK', *Antimicrobial Resistance and Infection Control*. Antimicrobial Resistance & Infection Control, 7(73) pp. 1–10.

Yaganza, E., Rioux, D., Simard, M., Arul, J. and Tweddell, R. J. (2004) 'Caused by Treatment with Aluminum Chloride and Sodium Metabisulfite', *Applied and Environmental Microbiology*, 70(11) pp. 6800–6808.

Yamada, K. J. and Kielian, T. (2019) 'Biofilm-Leukocyte Cross-Talk: Impact on Immune Polarization and Immunometabolism', *Journal of Innate Immunity*, 11(3) pp. 280–288.

Yamanaka, M., Hara, K. and Kudo, J. (2005) 'Bactericidal Actions of a Silver Ion Solution on Escherichia coli , Studied by Energy-Filtering Transmission Electron Microscopy and Proteomic Analysis', *Applied and Environmental Microbiology*, 71(11) pp. 7589–7593.

Yougbare, S., Chang, T. K., Tan, S. H., Kuo, J. C., Hsu, P. H., Su, C. Y. and Kuo, T. R. (2019) 'Antimicrobial gold nanoclusters: Recent developments and future perspectives', *International Journal of Molecular Sciences*, 20(12) pp. 1–17.

Yu, D., Pi, B., Chen, Y., Wang, Y., Ruan, Z., Otto, M. and Yu, Y. (2014) 'Characterization of the staphylococcal cassette chromosome composite island of Staphylococcus haemolyticus SH32, a methicillin-resistant clinical isolate from China', *PLoS ONE*, 9(1) pp. 1–6.

Zavascki, A. P., Goldani, L. Z., Li, J. and Nation, R. L. (2007) 'Polymyxin B for the treatment of multidrug-resistant pathogens: A critical review', *Journal of Antimicrobial Chemotherapy*, 60(6) pp. 1206–1215.

Zhang, Y.-M. and Rock, C. O. (2008) 'Membrane lipid homeostasis in bacteria', *Nature Reviews*, 6(2) pp. 222–233.

Zhen, X., Lundborg, C. S., Sun, X., Hu, X. and Dong, H. (2019) 'Economic

burden of antibiotic resistance in ESKAPE organisms : a systematic review', *Antimicrobial reisstance and infection control*. Antimicrobial Resistance & Infection Control, 8(137).

Zhou, R. and Gao, H. (2014) 'Cytotoxicity of graphene: Recent advances and future perspective', *Nanomedicine and Nanobiotechnology*, 6(5) pp. 452–474.

Zhu, J., Wang, J., Hou, J., Zhang, Y., Liu, J. and Van dr Bruggen, B. (2017) 'Graphene-based antimicrobial polymeric membranes: a review', *Journal of Materials Chemistry*. Royal Society of Chemistry, 5 pp. 6776–6793.

Appendix

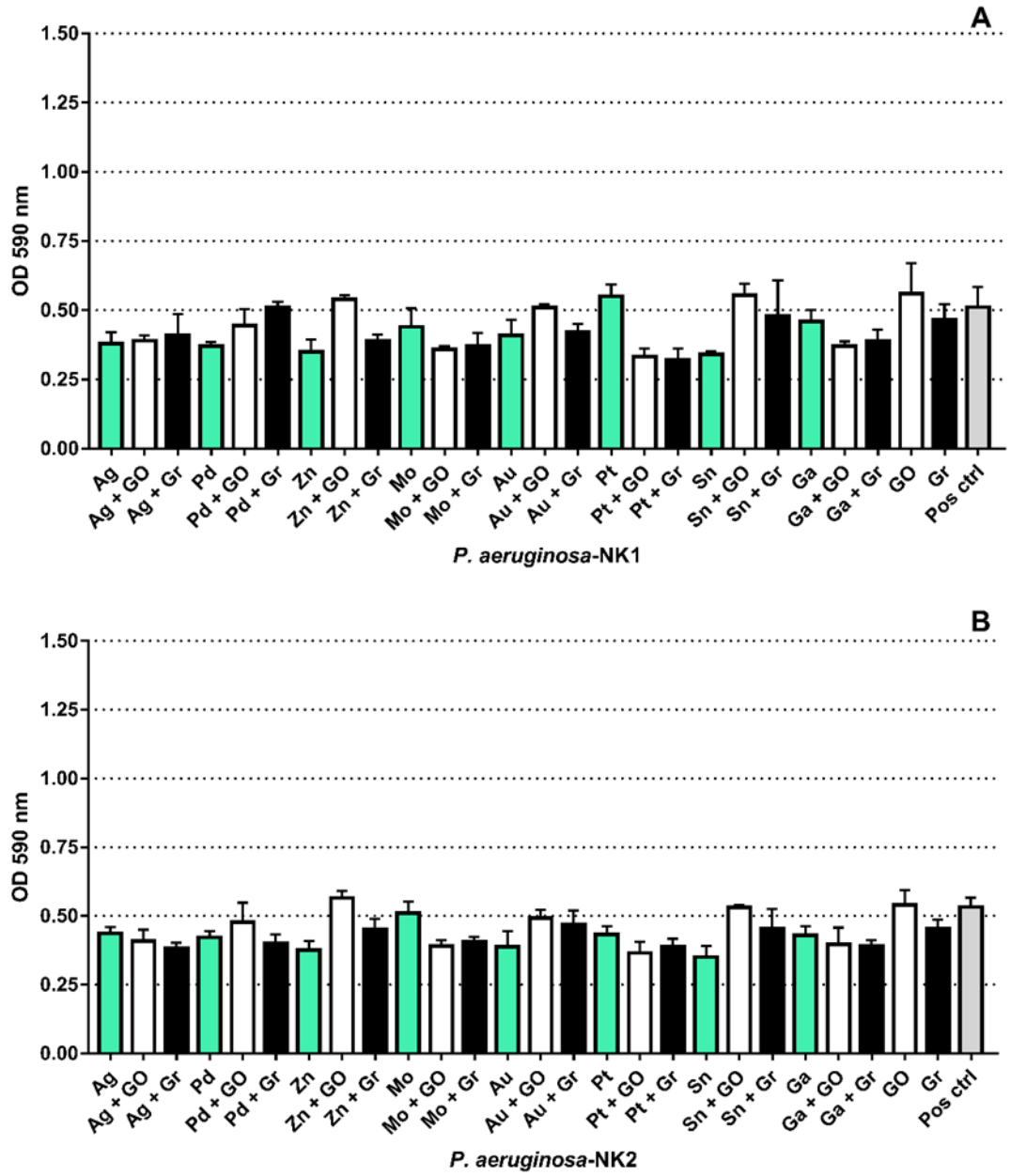

Appendix A. The antimicrobial effect of metal ions and graphene-based compounds as determined by CVBA at 1×MIC on pre-formed biofilms of (A) *P. aeruginosa*-NK1 and (B) *P. aeruginosa*-NK2 after 24 h treatment.

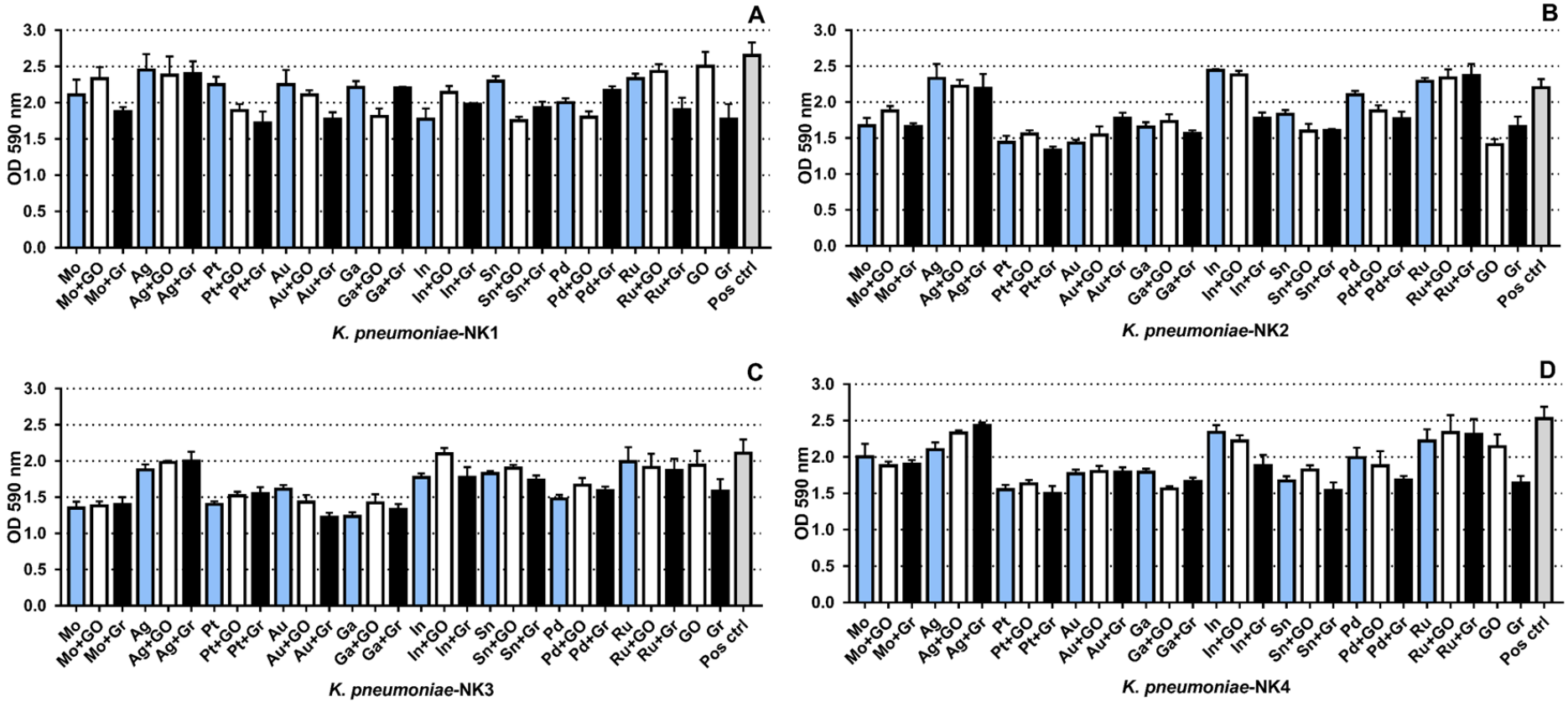

Appendix B. The antimicrobial effect of metal ions and graphene-based compounds as determined by CVBA on pre-formed biofilms at 1 ×MIC of (A) *K. pneumoniae*-NK1, (B) *K. pneumoniae*-NK2, (C) *K. pneumoniae*-NK3 and (D) *K. pneumoniae*-NK4 after 24 h treatment.

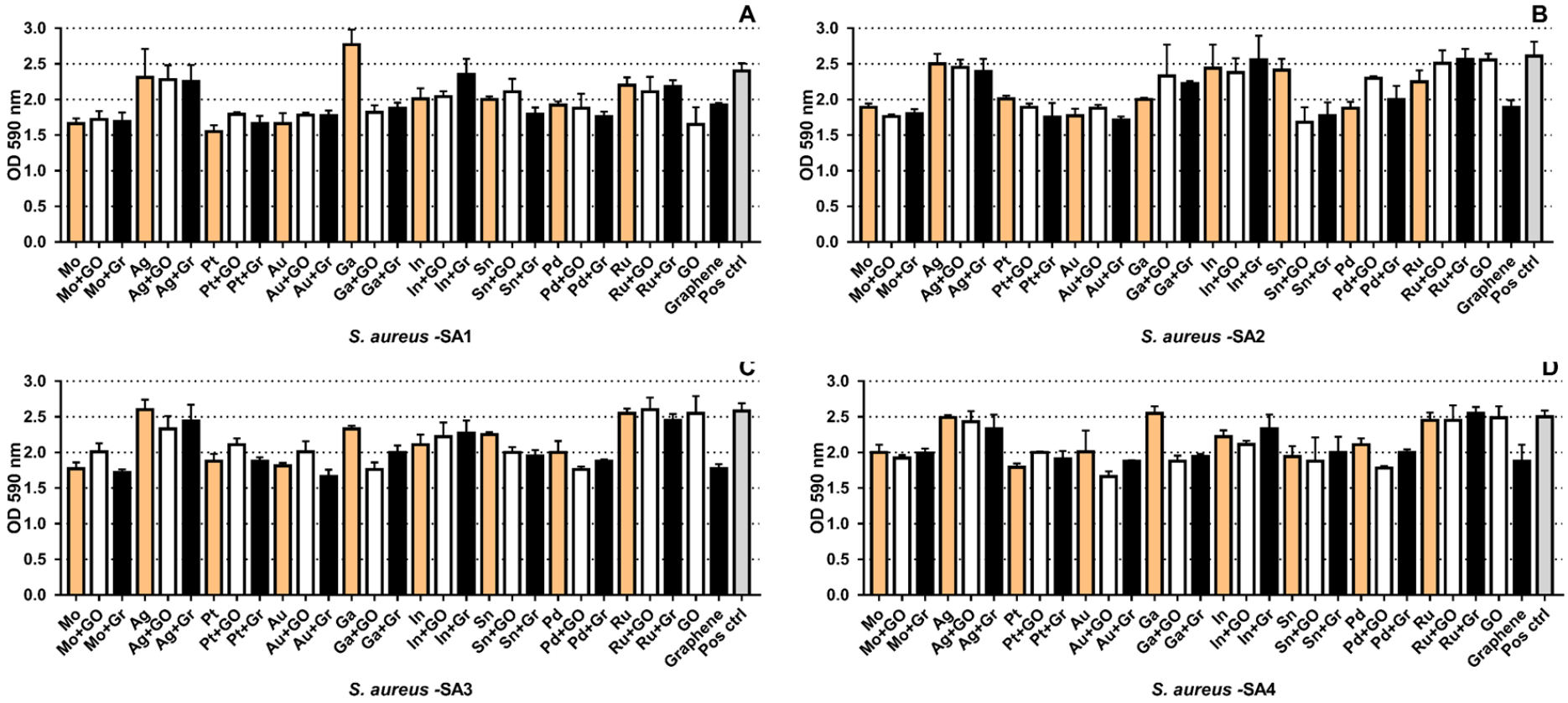

Appendix C. The antimicrobial effect of metal ions and graphene-based compounds as determined by CVBA at 1×MIC on pre-formed biofilms of (A) *S. aureus*-SA1, (B) *S. aureus*-SA2, (C) *S. aureus*-SA3 and (D) *S. aureus*-SA4 after 24 h treatment.

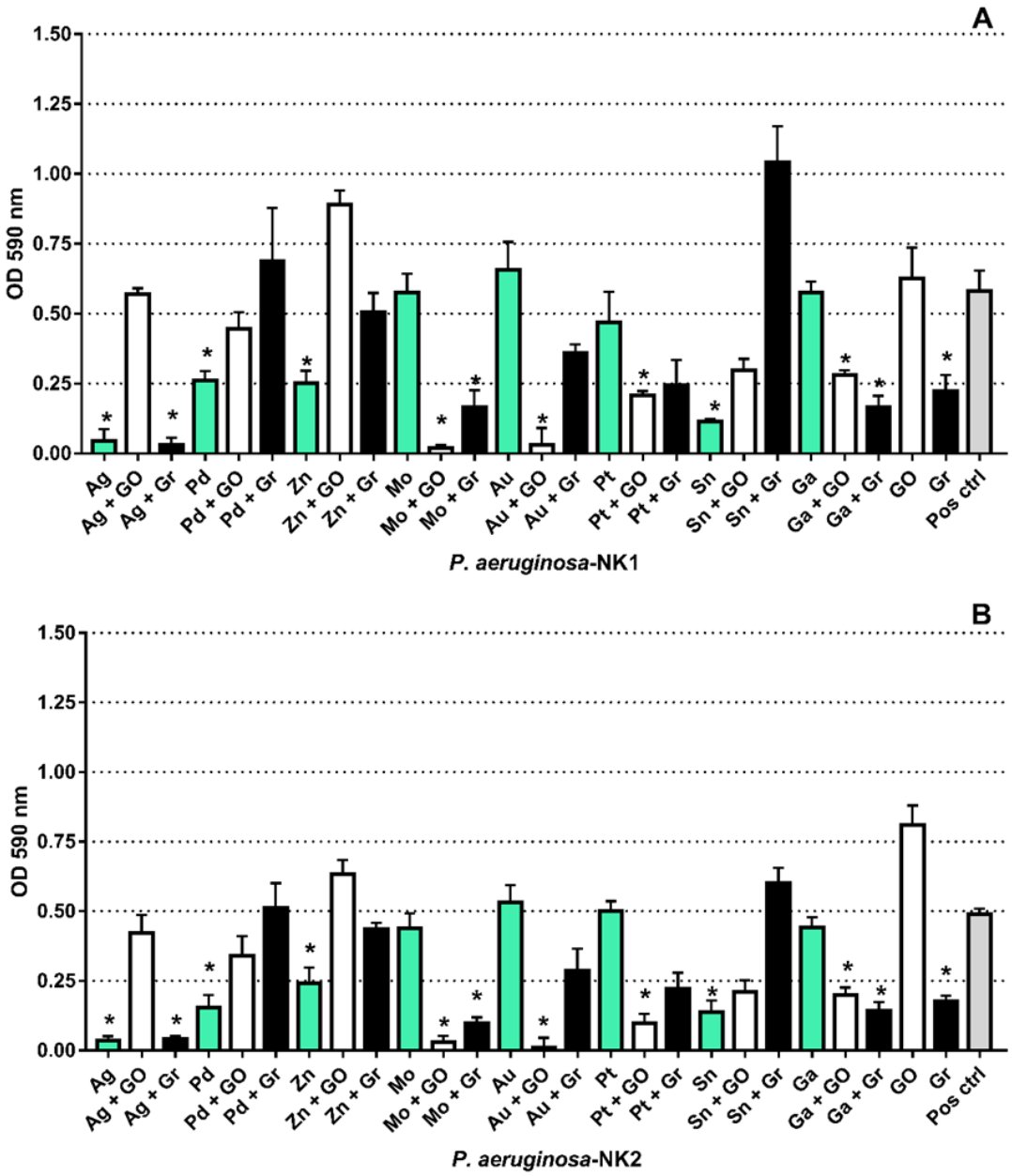

Appendix D. The antimicrobial effect of metal ions and graphene-based compounds as determined by CVBA at 4× MIC on pre-formed biofilms of (A) *P. aeruginosa*-NK1 and (B) *P. aeruginosa*-NK2 after 24 h treatment. * denotes $p \leq 0.05$ compared to control.

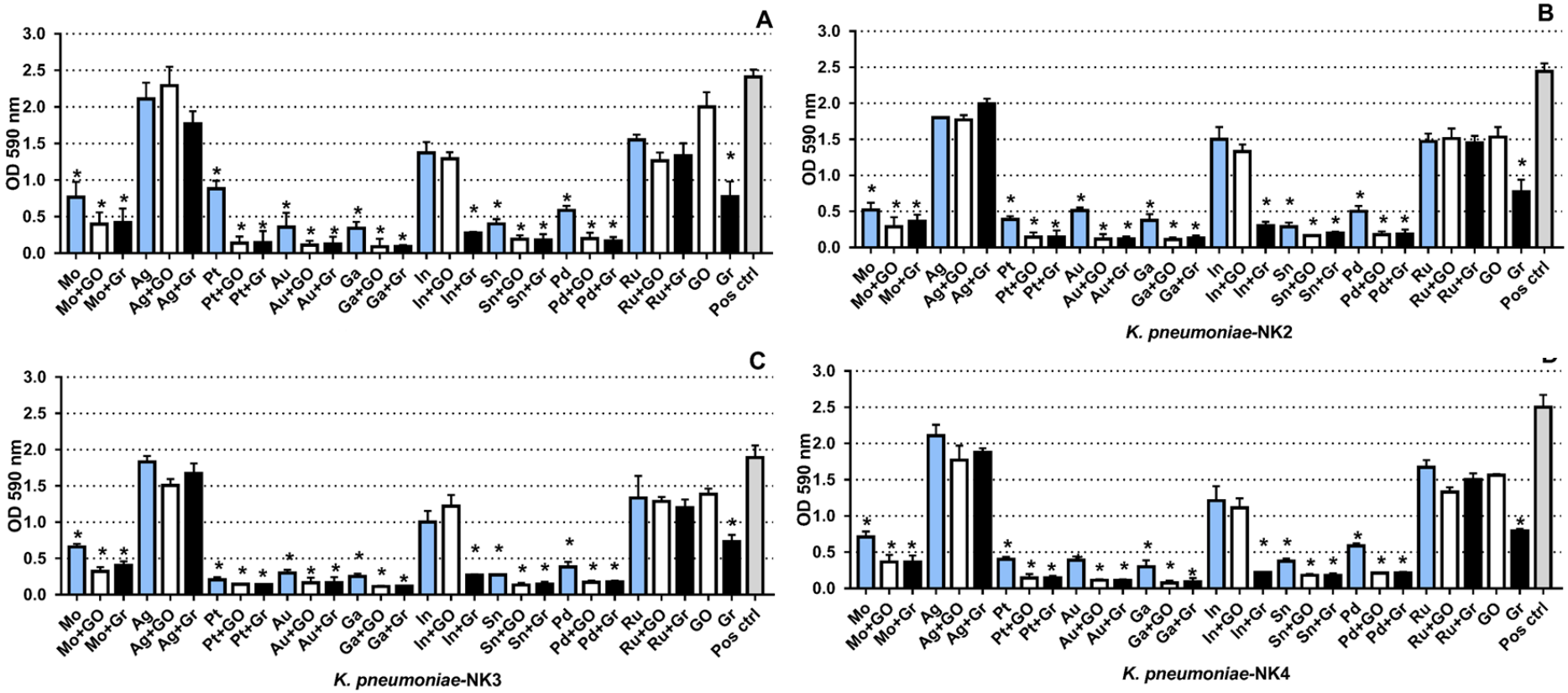

Appendix E. The antimicrobial effect of metal ions and graphene-based compounds as determined by CVBA at 4 ×MIC on pre-formed biofilms of (A) *K. pneumoniae*-NK1, (B) *K. pneumoniae*-NK2, (C) *K. pneumoniae*-NK3 and (D) *K. pneumoniae*-NK4 after 24 h treatment. The absorbance values (±SD) are directly proportional to the amount of biofilm that remained intact post exposure. . * denotes $p \leq 0.05$ compared to control.

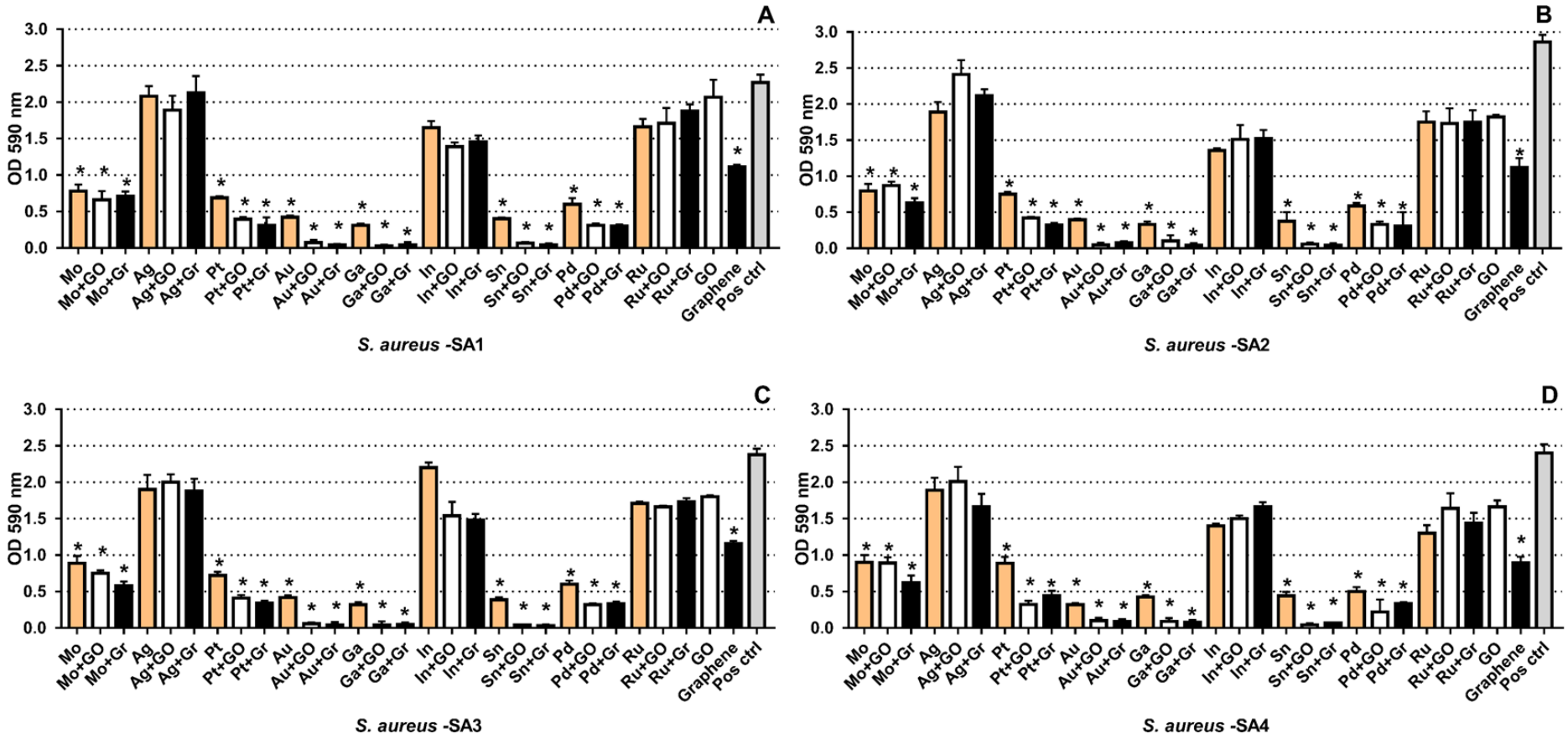

Appendix F. The antimicrobial effect of metal ions and graphene-based compounds as determined by CVBA at 4 × MIC on pre-formed biofilms of (A) *S. aureus*-SA1, (B) *S. aureus*-SA2, (C) *S. aureus*-SA3 and (D) *S. aureus*-SA4 after 24 h treatment. The absorbance values (±SD) are directly proportional to the amount of biofilm that remained intact post exposure. . * denotes $p \leq 0.05$ compared to control.

Appendix G. Zones of inhibition (Zol ± SD) (mm) of the different skin cleanser formulations (F1 to F14) containing different metal ions and graphene composites against *K. pneumoniae*-NK1 and *K. pneumoniae*-NA.

	***K. pneumoniae*- NK1**	***K. pneumoniae*- NA**
F1 (In)	15.01 ± 1.30	17.50 ± 2.00
F2 (Ga)	17.00 ± 2.13	18.20 ± 0.99
F3 (Au)	23.02 ± 1.40	21.50 ± 1.10
F4 (Pt)	21.00 ± 2.30	21.01 ± 1.77
F5 (Pd)	20.00 ± 2.09	20.00 ± 1.70
F6 (In-Gr)	16.02 ± 1.60	14.75 ± 1.00
F7 (Ga-Gr)	18.01 ± 0.20	19.25 ± 2.20
F8 (Ga-GO)	15.00 ± 0.90	16.50 ± 1.60
F9 (Au-Gr)	25.00 ± 1.09	23.75 ± 2.00
F10 (Au-GO)	19.66 ± 0.50	20.04 ± 0.44
F11 (Pt-Gr)	20.00 ± 1.00	19.50 ± 0.88
F12 (Pt-GO)	14.02 ± 2.00	15.00 ± 1.50
F13 (Pd-Gr)	19.00 ± 0.69	20.03 ± 0.77
F14 (Pd-GO)	14.10 ± 0.77	16.00 ± 1.10
CHX gluconate	19.03 ± 1.20	4.02 ± 0.55
Gentamicin	19.00 ± 0.70	18.00 ± 1.00

Appendix H. Zones of inhibition (ZoI ± SD) (mm) of the different skin cleanser formulations (F1 to F14) in the absence or presence of CHX against *K. pneumoniae*-NA.

	Formulations alone	Formulations with CHX
F1 (In)	17.50 ± 2.00	18.22 ± 1.20
F2 (Ga)	18.20 ± 0.99	21.88 ± 1.70
F3 (Au)	21.50 ± 1.10	24.80 ± 1.10
F4 (Pt)	20.25 ± 1.77	23.55 ± 0.80
F5 (Pd)	20.00 ± 1.70	21.00 ± 0.55
F6 (In-Gr)	14.75 ± 1.00	16.00 ± 1.50
F7 (Ga-Gr)	19.25 ± 2.20	24.00 ± 0.77
F8 (Ga-GO)	16.50 ± 1.60	16.00 ± 1.65
F9 (Au-Gr)	23.75 ± 20	28.00 ± 1.34
F10 (Au-GO)	18.50 ± 0.44	16.00 ± 1.20
F11 (Pt-Gr)	21.00 ± 0.88	17.00 ± 2.00
F12 (Pt-GO)	15.00 ± 1.50	15.30 ± 1.66
F13 (Pd-Gr)	20.03 ± 0.77	19.00 ± 0.88
F14 (Pd-GO)	16.00 ± 1.10	18.00 ± 2.88

Appendix I. Zones of inhibition (Zol ± SD) (mm) of the different ointment formulations (O1 to O9) containing different metal ions and graphene composites against *S. aureus*-SA1, *S. aureus*-SA2, *S. aureus*-SA3.

	***S. aureus*-SA1**	***S. aureus*-SA2**	***S. aureus*-SA3**
O1 (Ga)	18.50 ± 0.50	17.95 ± 0.80	18.11 ± 0.60
O2 (Au)	25.89 ± 0.90	28.00 ± 1.40	27.00 ± 0.60
O3 (Pd)	22.00 ± 1.00	23.33 ± 1.10	21.60 ± 0.80
O4 (Ga-GO)	17.50 ± 1.30	16.20 ± 1.60	16.66 ± 0.50
O5 (Au-GO)	19.22 ± 1.00	18.11 ± 1.30	17.99 ± 0.66
O6 (Pd-GO)	18.22 ± 0.66	16.99 ± 1.10	17.45 ± 0.77
O7 (Ga-Gr)	25.00 ± 1.20	26.50 ± 1.50	24.00 ± 0.88
O8 (Au-Gr)	33.00 ± 0.77	31.30 ± 0.57	30.60 ± 0.60
O9 (Pd-Gr)	23.00 ± 0.60	22.66 ± 1.50	22.00 ±0.80
Mupirocin	10.02 ± 0.88	20.5 ± 1.10	00.00 ± 0.00

Appendix J. Zones of inhibition (ZoI ± SD) (mm) of the different spray formulations (S1 to S9) containing different metal ions and graphene composites against *S. aureus*-SA1, *S. aureus*-SA2, *S. aureus*-SA3.

	***S. aureus*-SA1**	***S. aureus*-SA2**	***S. aureus*-SA3**
S1 (Ga)	18.20 ± 1.05	18.22 ± 0.5	17.45 ± 1.10
S2 (Au)	24.85 ± 0.50	26.50 ± 0.88	28.00 ± 0.88
S3 (Pd)	23.11 ± 1.70	23.00 ± 0.6	22.12 ± 0.79
S4 (Ga-GO)	16.00 ± 1.00	15.60 ± 1.44	16.55 ± 1.30
S5 (Au-GO)	18.33 ± 0.77	18.00 ± 0.61	19.22 ± 2.40
S6 (Pd-GO)	17.00 ± 1.20	17.50 ± 2	16.22 ± 1.70
S7 (Ga-Gr)	23.55 ± 1.01	25.00 ± 0.88	23.50 ± 0.80
S8 (Au-Gr)	31.00 ± 0.75	30.00 ± 1.1	31.70 ± 0.30
S9 (Pd-Gr)	23.00 ± 2.00	24.00 ±0.88	22.11 ± 1.12
Mupirocin	10.33 ± 1.20	20.51 ± 0.66	00.00 ± 00.00